



MINISTRY OF EDUCATION
OF BELARUS
POLOTSK STATE UNIVERSITY



EUROPEAN
& NATIONAL
DIMENSION
IN RESEARCH

TECHNOLOGY

Electronic collected materials
of XIII Junior Researchers' Conference
(Novopolotsk, 17 - 21, 2021)

Novopolotsk

2021

MINISTRY OF EDUCATION OF BELARUS

Polotsk State University

EUROPEAN AND NATIONAL DIMENSION IN RESEARCH

TECHNOLOGY

Electronic collected materials of XIII Junior Researchers' Conference
(Novopolotsk, May 17 – 21, 2021)

24

Обновляется 1 раз в год

Novopolotsk
Polotsk State University
2021

PUBLISHING BOARD:

Dr. Yury Holubeu (chairperson);
Ms. Volha Zhuravskaya (vice-chairperson);
Dr. Katsiaryna Lushneuskaya;
Ms. Rita Rusina

РЕДАКЦИОННАЯ КОЛЛЕГИЯ:

к.т.н., доц. Ю. П. Голубев (председатель);
О.В. Журавская (зам. председателя);
к.филол.н., доц. Е.В. Лушневская;
Р.С. Русина

EUROPEAN AND NATIONAL DIMENSION IN RESEARCH. TECHNOLOGY = ЕВРОПЕЙСКИЙ И НАЦИОНАЛЬНЫЙ КОНТЕКСТЫ В НАУЧНЫХ ИССЛЕДОВАНИЯХ. ТЕХНОГОЛИЯ : Electronic collected materials of XIII Junior Researchers' Conference, Novopolotsk, May 17–21, 2021 / Polotsk State University ; ed. Yu. Holubeu [et al.]. – Novopolotsk : PSU, 2021. – 1 CD-ROM.

Издается с 2017 года (в печатном виде – с 2009 г.).

Сборник включен в Государственный регистр информационного ресурса. Регистрационное свидетельство № 3981711557 от 17.04.2017 г.

Первые два печатных издания вышли под заглавием «Материалы конференции молодых ученых», третье – «Европейский и национальный контексты в научных исследованиях» в 3 томах: «Гуманитарные науки», «Экономика» и «Технология».

В настоящем электронном сборнике «Европейский и национальный контексты в научных исследованиях. Технология» представлены работы молодых ученых по геодезии и картографии, химической технологии и машиностроению, информационным технологиям, строительству и радиотехнике.

Предназначены для работников образования, науки и производства. Будут полезны студентам, магистрантам и аспирантам университетов.

The first two conferences were issued under the heading “Materials of junior researchers’ conference”, the third – “European and national dimension in research” in 3 parts: “Humanities”, “Economics”, “Technology”.

In this Electronic collected materials “European and national dimension in research. Technology” works in the fields of geodesy, chemical technology, mechanical engineering, information technology, civil engineering, and radio-engineering are presented.

It is intended for trainers, researchers and professionals. It can be useful for university graduate and post-graduate students.

211440, ул. Блохина, 29, г. Новополоцк,
Тел. 8 (0214) 50-57-09, e-mail: inter.office.psu@gmail.com

Технический редактор Прадидова Анастасия Андреевна
Компьютерная верстка Прадидовой Анастасии Андреевны
Компьютерный дизайн обложки Мухоморовой Марии Сергеевны

ARCHITECTURE AND CIVIL ENGINEERING

UDC 69.059.4

NON-DESTRUCTIVE TESTING (NDT) OF CONCRETE STRENGTH: METHODS, PARTICULAR QUALITIES

L. SINIAUSKAYA, A. KOLTUNOV

Polotsk State University, Belarus

This paper reviews the most common non-destructive testing (NDT) methods of concrete strength as utilized by the structural engineering industry. The factors that influence the success of NDT methods are discussed and ways to mediate their influence are recommended. Reference is made to standard guidelines for the application and interpretation of the discussed NDT methods. Perceptions of NDT inadequacy were attributable to lack of understanding construction materials and NDT methods themselves. The intent of this paper is to address these concerns by describing the most common successful methods of NDT as applied to concrete structures.

Introduction. It is often necessary to test concrete structures after the concrete has hardened to determine whether the structure is suitable for its designed use. Ideally such testing should be done without damaging the concrete. According to the standard guideline of the ministry of architecture and construction of the republic of Belarus «Control and assessment of concrete strength»: control and assessment of the strength of concrete must be carried out directly in the structures (in situ) with non-destructive testing (NDT) devices with the involvement of specialists from an accredited laboratory [1]. NDT methods have materialized as a response to the need for structural damage detection and prevention. The extensive use of NDT is driven by economics and safety [2].

Research part. NDT methods. Surface hardness methods (ГОСТ 22690-2015, СТБ 2264-2012) [3,4]. The two categories that define concrete surface hardness techniques are indentation methods and rebound methods. These methods attempt to exploit empirical correlations between strength properties of concrete and surface hardness as measured by indentation or rebound. The most commonly used surface hardness procedure is the standard rebound hammer test. **Penetration resistance methods** [3,4]. Penetration resistance methods are invasive NDT procedures that explore the strength properties of concrete using previously established correlations. These methods involve driving probes into concrete samples using a uniform force. Measuring the probe's depth of penetration provides an indication of concrete compressive strength by referring to correlations. **Pull-out resistance methods** [3,4]. Pull-out resistance methods measure the force required to extract standard embedded inserts from the concrete surface. Using established correlations, the force required to remove the inserts provides an estimate of concrete strength properties. The two types of inserts, cast-in and fixed-in-place, define the two types of pull-out methods. **Pull-off resistance method** [3,4]. The pull-off test is an in-situ strength assessment of concrete which measures the tensile force required to pull a disc bonded to the concrete surface with an epoxy or polyester resin or registering the force required to shear a section of concrete on the rib of the structure. **Ultrasonic pulse velocity method** (ГОСТ 17624-2012) [5]. Ultrasonic pulse velocity methods involve propagating ultrasonic waves in solids while measuring the time taken for the waves to propagate between a sending and receiving point.

Testing. In the study of NDT methods for controlling the strength of concrete, the most famous and frequently used ones were considered, such as surface hardness methods, pull-out resistance methods and ultrasonic pulse velocity method. The concrete cubes 100x100 from one batch were tested: a concrete surface of the upper edges of the surface with beads and depressions, the side faces and the bottom did not have significant defects (Fig. 1).

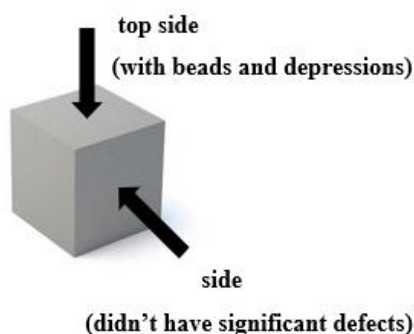


Fig. 1. – Prototype (cube 100x100)

After the experiments, the cubes were tested using a press to determine their true compressive strength and concrete class (C 25/30). In this case, the tests were carried out on all sides of the cubes without cleaning. After testing on an uncleaned surface, the samples were cleaned and the tests were repeated. In addition, foundation structures were tested on site (Fig. 2).

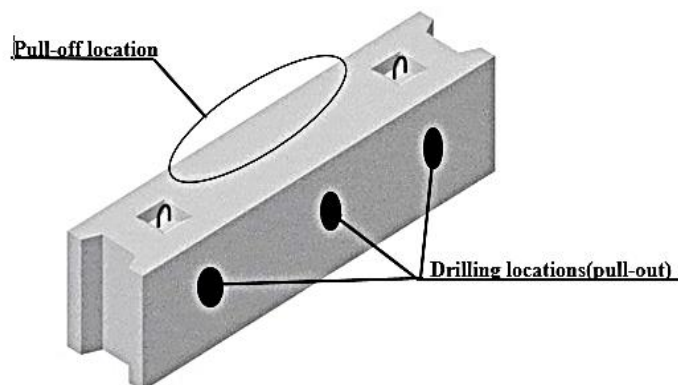


Fig. 2. – Prototype (foundation structure, tested in situ/laboratory)

Results. From a series of tests carried out, it can be concluded that the most accurate methods of non-destructive testing (NDT) of concrete strength are the pull-out/off resistance methods. Methods such as ultrasonic and surface hardness methods allow roughly assessing the strength of concrete (Fig. 3,4,5).

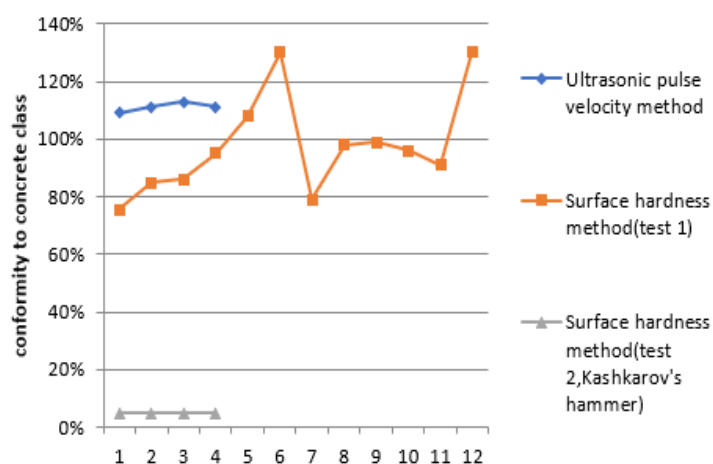


Fig. 3. – Cubes (100x100) test

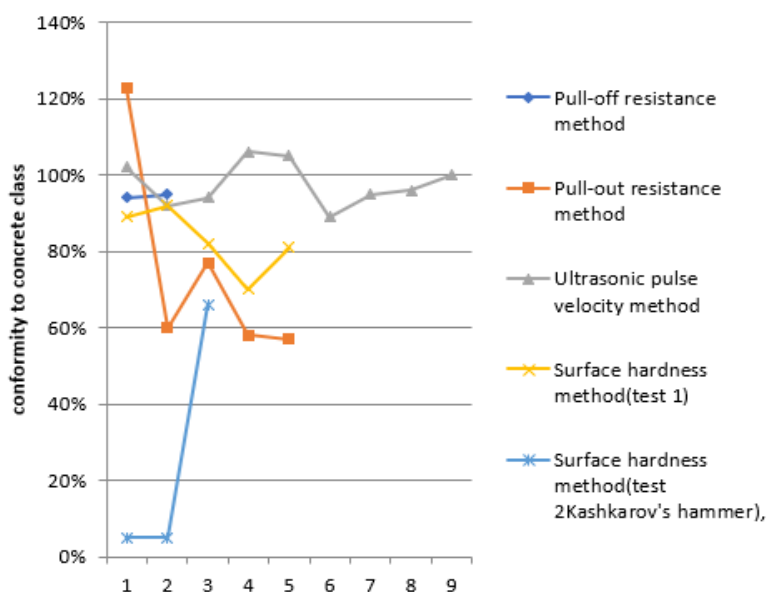


Fig. 4. – Foundation structures, tested in laboratory

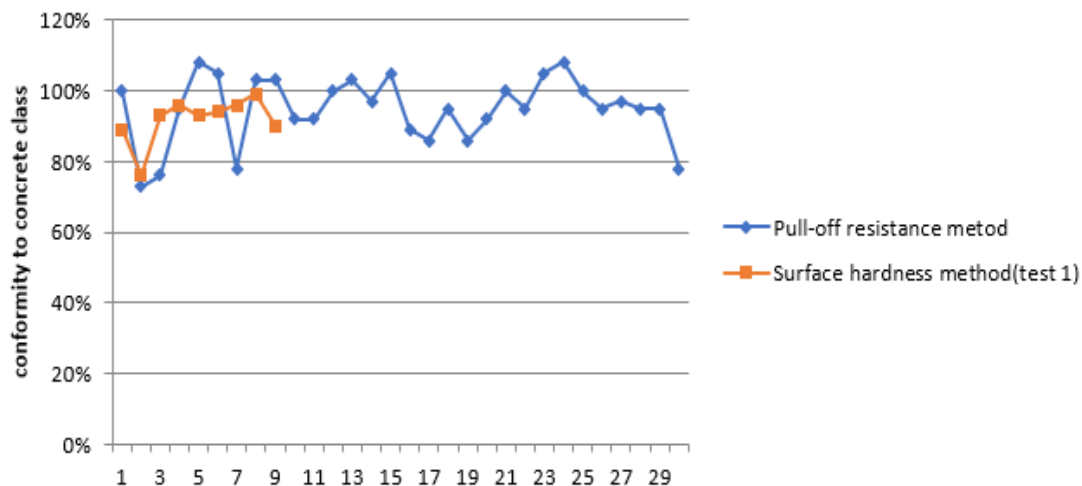


Fig. 5. – Foundation structures, tested in situ

Comparison of the actual and permissible errors of the methods of NDT of concrete strength are presented in Table 1.

Table 1. – Comparison of the actual and permissible errors of methods of NDT of concrete

Methods of NDT	Actual error	Allowable error
Ultrasonic pulse velocity method	2-15%	+/- 2%
Surface hardness methods (test 1)	10-30%	+/-8%
Surface hardness methods (test 2 Kashkarov's hammer)	50-100%	+/-12%
Pull-out/off resistance methods	5-15%	+/- 2%

Non-destructive testing (NDT) of concrete strength requires a comprehensive analysis of the factors that determine the strength of concrete to improve the accuracy, reliability and information content of standardized methods for controlling the strength of concrete in structures.

The table 2 shows the main parameters affecting the strength of concrete, which were identified analytically and experimentally.

Table 2. – Main parameters affecting concrete strength indicators during testing

Construction parameters	Technological parameters
Type of construction	The composition of the concrete mixture (water-cement ratio, type and quality of aggregate, presence of additives) Concrete age Concrete hardening conditions (temperature, humidity, etc.) Compaction methods
Type of construction surface(roughness)	
Test site (laboratory/in situ)	

Conclusion. 5 methods of non-destructive testing of concrete strength were considered. From a series of tests carried out, it can be concluded that the most accurate methods of non-destructive testing (NDT) of concrete strength are pull-out/off resistance methods. Methods such as ultrasonic and surface hardness methods allow only a rough estimate of the strength of concrete.

The factors contributing to the variability of NDT methods as applied to concrete are aggregate properties, cement type, water- cement ratio, admixtures and age of concrete, as well as the type of construction, construction surface, test site. It was found that the majority of NDT methods rely on comparing tested parameters with established correlations. Empirical relationships provided by manufacturers were found to often provide unsatisfactory results. Where applicable, it is recommended to conduct test-specific correlation procedures for the NDT of concrete. It can be noted that the experience of the person conducting the test has a significant impact on the results.

Advances in sensors, development of new materials, and miniaturization of devices are all paving the way for new NDT methods. Data fusion techniques are being developed to integrate several NDT methods in the aim of enabling effective data-acquisition, processing, and interpretation of test parameters in relation to material integrity.

REFERENCES

1. Письмо министерства архитектуры и строительства РБ от 11 сентября 2015 года № 02-1-05/10168. «О проведении контроля и оценки прочности бетона» (Электронный ресурс). – 2015 – Режим доступа: <http://mas.gov.by/uploads/documents/beton.PDF>. – Дата доступа: 13.04.2021.
2. Guidebook on non-destructive testing of concrete structures. INTERNATIONAL ATOMIC ENERGY AGENCY, VIENNA, 2002. – 220 с.
3. ГОСТ 22690-2015. Бетоны. Определение прочности механическими методами неразрушающего контроля. Москва, 2016.
4. СТБ 2264-2012. Испытание бетона. Неразрушающий контроль прочности. РУП "Стройтехнорм", 2012.
5. ГОСТ 17624-2012. Бетоны. Ультразвуковой метод определения прочности. Москва, 2014.

UDC 666.973.2

CONTINUOUS MONITORING OF THE OPERATING TEMPERATURE OF WOOD CONCRETE USING A SMART-SYSTEM

ZHENG ZHIXU, YUAN JINBIN, A. YAGUBKIN
Polotsk State University, Belarus

Wood concrete is one of the bio-stable and hardly combustible materials. The material provides the necessary air exchange and regulates the humidity in the premises. The experiment showed comparable heat retention results for mineral wool, expanded polystyrene and wood concrete. Foil was found to be significantly less effective.

Introduction. Currently rural houses are built with bricks or reinforced concrete panels. In order to reduce the cost, walls in modern houses are made of gas silicate blocks or of panels with insulation and sheathing made of wood or siding. However, each of these types of wall materials has its own disadvantages. So, in houses built with reinforced concrete panels, because of insufficient humidity in the premises, asthmatic diseases are exacerbated among residents. In houses with walls made of cellular gas silicate blocks, mold and fungus on the walls can be observed, what may cause allergic diseases. In addition, the materials must be environmentally friendly and have a low cost price. In a market economy, the developer must have a choice - wall materials must meet new modern requirements for creating a favourable microclimate in residential premises.

In view of the above, it should be recognized that at present an excellent wood-based material - wood concrete - is undeservedly forgotten. Wood concrete is one of the bio-stable and hardly combustible materials, it has high heat-insulating and sound-insulating properties, it is well finished with cement mortar, sawn and nailed. The material holds fasteners firmly, has high sound absorption and improved crack resistance. This allows to reduce the risks of building sinking when the maximum safe loads are exceeded. The material provides the necessary air exchange and regulates the humidity in the premises [1-6].

Task formulation. Improvement of the energy efficiency of residential buildings, resulted from the energy crisis, required a significant change of regulatory requirements for the heat transfer resistance of the building envelopes and the development of a set of energy-saving measures.

At the moment, issues related to the use of screen insulation in modern building envelopes are not well understood. At the same time, the lack of methodology for calculating such heat-shielding systems and technical solutions for the insulation of building envelopes hinders the use of the above materials in construction.

The goal of the study was to compare popular thermal insulation materials with wood concrete using continuous temperature control sensors.

Methods of research. Digital temperature sensors were used to monitor the temperature readings.

Main characteristics of digital temperature sensor ds18b20: - range of measured temperature from -55 to + 125 ° C; - measurement error in the range from -10 to + 85 ° C is 0.5 ° C.

The connection diagram of the ds18b20 sensor to the microcontroller (for example, Arduino) is shown in Fig. 1.

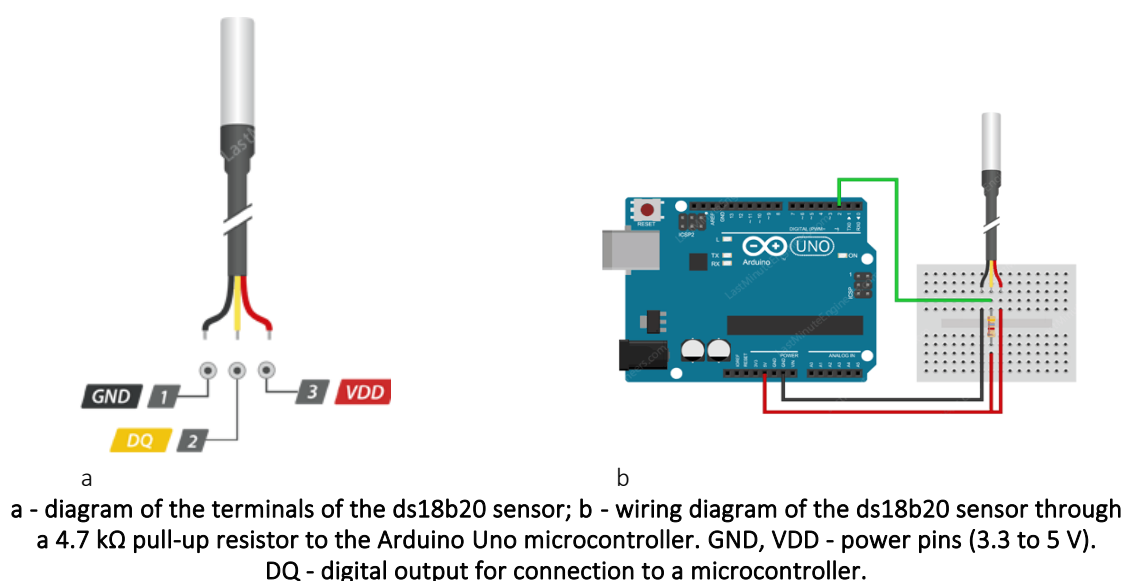


Fig. 1. – Connecting the ds18b20 sensor to the Arduino Uno microcontroller

Based on the analysis of existing heat-insulating materials, we carried out laboratory studies in which the following were used as heat-insulating materials: mineral wool, penoplex, expanded polystyrene, aluminium foil, wood concrete.

Architecture and Civil Engineering

A sample (with sensors inside) was placed on the setup, a lamp inside the sample was turned on and heated the space (Fig. 2.). The temperature readings were recorded by sensors and provided information to the specialized program Arduino Uno. The automated processing of the obtained experimental data was carried out using the Microsoft Office Excel software package.

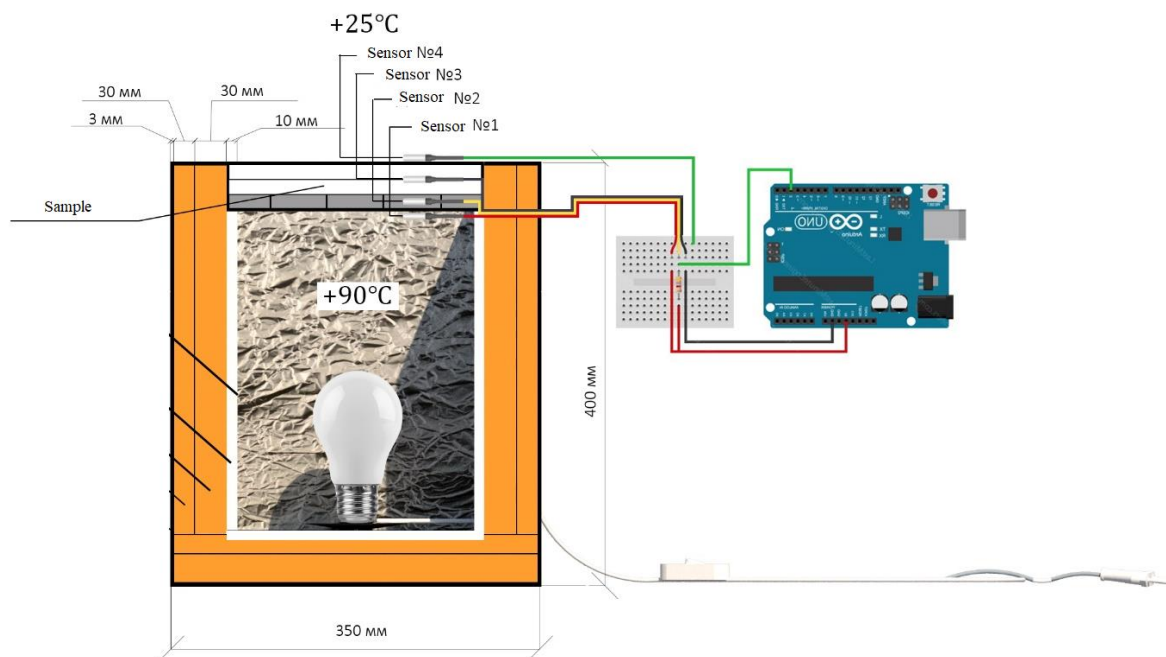


Fig. 2. – Sectional view of the pilot plant

Results, discussions and outlooks. A prototype was placed on the top of the pilot plant. The pilot plant was heated to create a temperature difference of $+90^{\circ}\text{C}$ and $+25^{\circ}\text{C}$, after heating the incandescent lamp was turned off and the temperature readings as well as the rate at which the heat from the pilot plant went outside were monitored (Fig. 3).

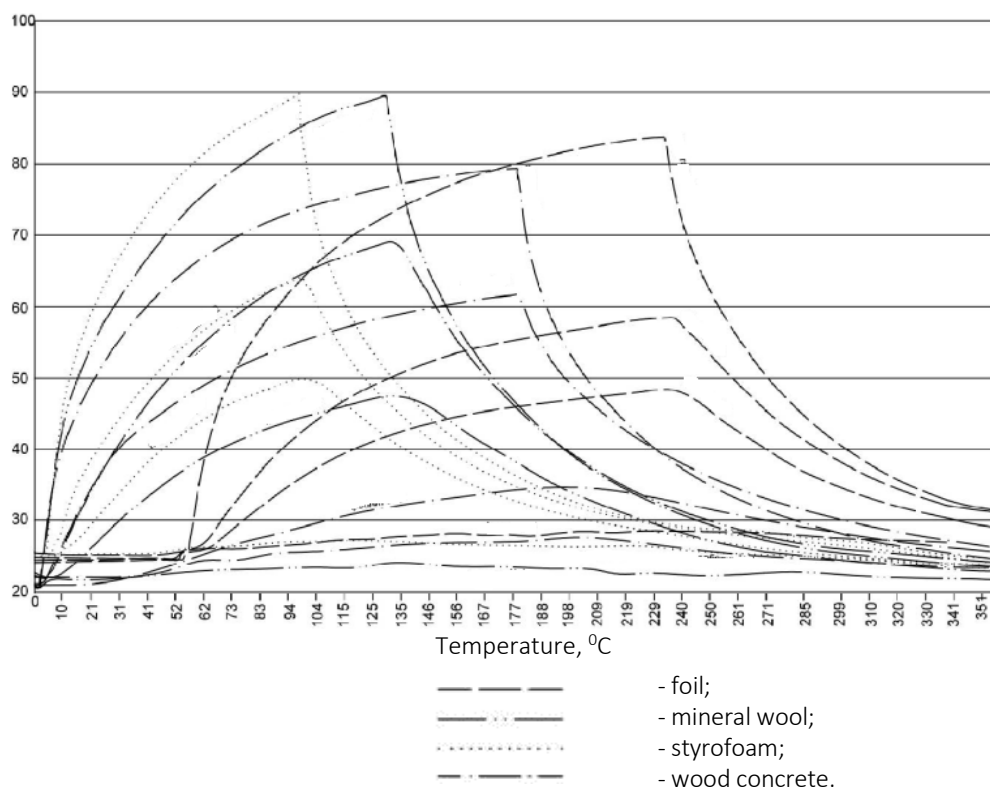


Fig. 3. – Graph with sensor readings (Temperature, $^{\circ}\text{C}$ – Time, min)

The experiment showed comparable heat retention results for mineral wool, expanded polystyrene and wood concrete. Foil was found to be significantly less effective.

Conclusion. Having finished laboratory tests the authors are going to carry out full-scale tests in existing buildings, what will allow to continuously monitor the temperature and maintain an optimal thermal regime as well as save energy for heating.

REFERENCES

1. Wilson, J. D. Modeling the effects of biological tissue on RF propagation from a wrist-worn device / J. D. Wilson, J. A. Blanco, S. Mazar, M. Bly // 36th Annual International Conference of the IEEE Engineering in Medicine and Biology Society. doi:10.1109/embc.2014.6944290. – 2014. – p. 3146-3149.
2. Li, M. Mechanical characterization of concrete containing wood shavings as aggregates / M. Li, M. Khelifa, M. El Ganaoui // International Journal of Sustainable Built Environment. – 2017. – №6. – p. 587-596.
3. Coatanlem, P. Lightweight wood chipping concrete durability / P. Coatanlem, R. Jauberthie, F. Rendell // Construction and Building Materials. – 2006. – №20. – p. 776-781.
4. Chowdhury, S. The incorporation of wood waste ash as a partial cement replacement material for making structural grade concrete: An overview / S. Chowdhury, M. Mishra, O. Suganya // Ain Shams Engineering Journal. – 2015. – №6. – p. 429-437.
5. Bouguerra, A. Effect of microstructure on the mechanical and thermal properties of lightweight concrete prepared from clay, cement, and wood aggregates / A. Bouguerra, A. Ledhem, F. de Barquin, R.M. Dheilly, M. Quéneudec // Cement and Concrete Research. – 1998. – Vol. 28. - №8. – p. 1179-1190.
6. Koohestani, B. Experimental investigation of mechanical and microstructural properties of cemented paste backfill containing maple-wood filler / B. Koohestani, A. Koubaa, T. Belem, B. Bussière, H. Bouzahzah // Construction and Building Materials. – 2016. – №121. – p. 222-228.

IMPROVEMENT OF INTERIOR LIGHT ENVIRONMENT IN APARTMENTS OF LARGE-PANEL BUILDINGS OF OLD TYPICAL SERIES

D. ZMITROVICH, D. ZHUKAU
Polotsk State University, Belarus

The article considers issues connected to natural lighting in rooms. The problem of lack of natural light in an apartment of a typical building of the M111-90 series in Belarus is described and ways of its solution are presented.

Natural lighting significantly affects the physical and psycho-emotional state of people. Lack and overabundance of direct and diffuse sunlight negatively affects a person. Person's comfortable vital activity requires the optimal level and quality of natural illumination in premises. This can be achieved, among other things, due to the interior design that is competent in terms of lighting technology.

Natural lighting is the result of natural processes and depends on the geographical data of the area, season, time of day and the state of the atmosphere [2]. Lighting should be uniform, intense and not glare [1].

The penetration of natural light into the room is carried out primarily due to such light openings as windows, roof windows, balcony doors, stained glass windows and skylights, as well as reflective surfaces of the ceiling, walls, floor and other elements in the interior. Diffuse light can be created by light which is being reflected from various surfaces in the interior.

Luxmeters or photometers are used to measure the level of illumination in rooms.

According to the location of the sensor, luxmeters are divided into monoblocks and devices with remote sensors. For simple measurements, a simple monoblock luxmeter is suitable. To determine several parameters of illumination, it is necessary to use devices with advanced functionality. A specialized luxmeter with light filters is able to determine more accurately the values of the intensity of light emanating from sources with variations in its shades. Devices with remote sensors are able to determine the level of illumination more accurately than monoblocks, so this measurement reduces the influence of third-party factors. For household needs, a person can use a smartphone as a light meter. To do this, a person can install the appropriate computer program and first check the measurement results with the results of specialized devices in order to determine the error in the smartphone for correct operation with it.

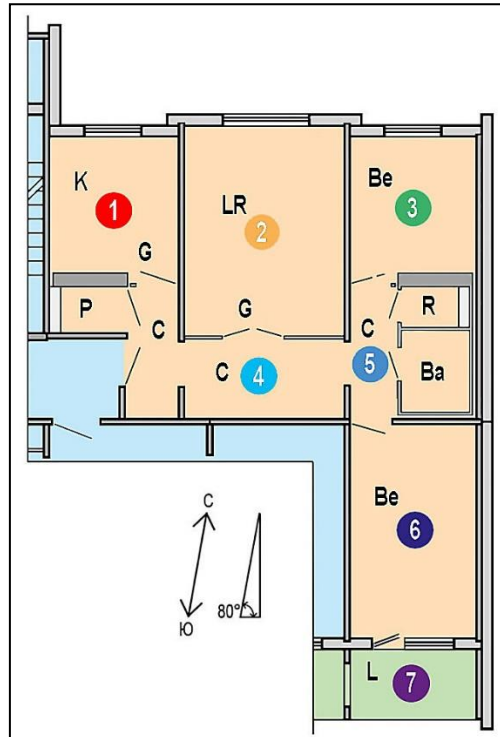
The problem of lack of natural light in rooms exists, in particular, in residential buildings of the M111-90 series, a large number of which were built in Belarus in the 1980s and 1990s. Exactly one of these buildings located in Minsk is considered in this work.

With Smart Luxmeter ver. 1.0.0 installed from the Play Store on the Xiaomi Redmi 4X smartphone, natural light was measured in the premises of the edge apartment located on the 9th floor of a 12-storey building (fig. 1). The illumination level was measured three times under different weather conditions at different times of the day (table 1).

Table 1. – Illumination measurement results

Measurement location	Room name	Illumination, lx		
		1st dimension	2nd dimension	3rd dimension
1	Kitchen	56	12	16
2	Living room	56	12	12
3	Bedroom	62	16	16
4	Corridor	4 (2)	0	0
5	Corridor	8 (0)	4	4
6	Bedroom	72	8	8
7	Loggia	1530	276	388

The corridor receives especially little daylight. If we also take into account that side lighting of rooms means a sharp decrease in illumination with distance from windows and balcony doors, we can conclude, that the apartments under consideration and similar in illumination need a significant improvement in their light environment. Moreover, such an improvement can be carried out within the framework of a general reconstruction or even a major overhaul of buildings of the type under consideration.

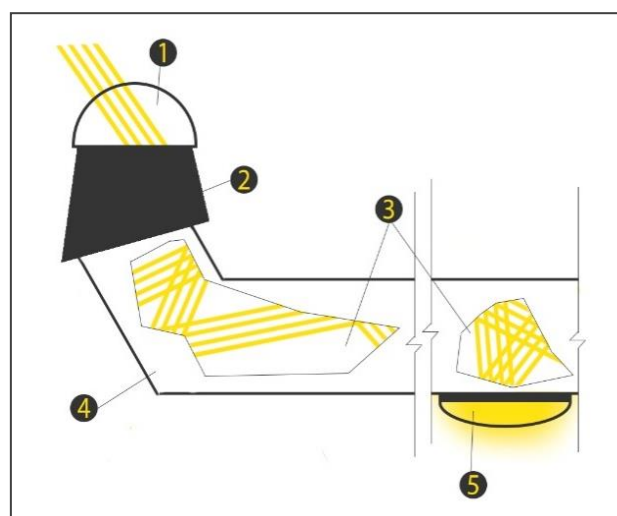


Ba – bathroom; LR – living room; P – pantry; C – corridor; K – kitchen; L – loggia;
GD – glass door; R – restroom; 1–7 – light measurement locations

Figure 1. – Scheme of the plan of a 3-room apartment of a building series M111-90

There are innovative methods of improving the light environment of premises using light guides, light wells, reflective installations. The reflective system installed on the outer wall of the building in cloudy weather redirects the reflected scattered daylight from the street through the reorientation element into the room, inside which the incoming light is reflected from the ceiling and is evenly distributed throughout the room.

Light wells are a type of light guides. The light well has a reflective inner surface [3]. The light guide lens captures sunlight with a transparent dome, after which the light enters the mirror tube, reflects from its walls and is scattered in the room with a light diffuser (fig. 2). Light wells are becoming more and more popular and technologically advanced. For example, some of them transmit up to 98% of the sunlight captured from the street into the room [4].



1 – light-collecting dome; 2 – roof connection element;
3 – reflective tube cover; 4 – light guide tube; 5 – light diffuser

Figure 2. – Light well construction

Light wells allow solving problems of insulation of premises in the absence of an architectural opportunity to raise the illumination level to optimal values. The disadvantage of this design is that the system can partially cover the window opening, thereby reducing its light-transmitting area.

To solve the problem of lack of natural light in the considered apartment of the building of the M111-90 series, the following scenario is proposed: the installation of two light guides and one reflective system. The integration of two light guides into the volume of the apartment is carried out through the eastern load-bearing wall and the loggia, which faces south. The first of these light guides has two diffusing elements and runs along the corridor, adjacent to the ceiling. The second light guide has one light outlet into the room, which is located in the central part of the ceiling of the room adjacent to the loggia. The reflective installation is fixed on the window of a large room (living room) in such a way that the main stream of light, reflected from the system, hits the ceiling and is evenly scattered throughout the room.

Thus, in order to improve the light environment, namely the level of natural light in apartments that need it, innovative methods can be used to improve the light performance. As a result of the implementation of the described scenario, the light comfort in the apartment is significantly improved in terms of the flow of sunlight into apartments premises.

REFERENCES

1. ЭкоСфера [Electronic resource] / Освещение – Access mode: <http://ekosf.ru/poleznoe-alias/articles/34-izmenenie-keo-ekolajt> – Access date: 05.02.2020.
2. Соловьев, А. К. Физика среды. Учебник / А. К. Соловьев. – Москва: Издательство АСВ, 2008. – 334 с.
3. Энергосвет [Electronic resource] / Научное обоснование новых технологий устройства солнечного освещения в зданиях – Access mode: http://www.energsovet.ru/bul_stat.php?idd=440 – Access date: 05.04.2021.
4. Энергосвет [Electronic resource] / Технология передачи естественного (солнечного) света по световым каналам – Access mode: <http://www.energsovet.ru/entech.php?idd=111> – Access date: 05.02.2021.

UDC 624.04:72.01

THE HISTORY OF ARCHITECTURE DEVELOPMENT, FORMS OF BUILDING CONSTRUCTIONS
AND THE ESTABLISHMENT OF COMPUTING METHODS IN THE FIRST HALF OF THE 20TH CENTURY

M. TARASAVA, T. TARASAVA, L. TOURICHEV
Polotsk State University, Belarus

The work of an architect is impossible without the engineering calculations as well as construction methods can't provide the aesthetic needs of a person by themselves only. The significant bond between architecture and engineering was formed at the beginning of the 20th century. The following article describes this relationship.

Scientific research aims to identify the correlation between forms of building constructions and their computing methods and architecture from the end of the 19th century to the beginning of the 20th century. The hypothesis of the research is the assumption that it was during this period that the consistent link of the engineer and architect's occupations was formed despite the established division of these two areas.

The main objective of architecture is the design of the inhabited space. Building constructions is a tool for solving this task as soon as it carries out the following assignments: 1) expression of the architect's concept; 2) load-bearing structure of the building; 3) utilitarian function. One of the main problems of architecture planning is the expression of the architect's concept through the construction. This can be managed with the tectonics principals which are the following: 1) the artistic expression; 2) the reflection of the statics; 3) the effective usage of building materials [1].

The history of the building's construction can be divided into two periods. The first one defines the computing methods as the experiment. During the second period the technology, construction machinery, and equipment were based on scientific research (since the 19th century) [1].

The connection between structural analysis calculations in the 19th and the 20th centuries should be taken into account mainly because of the reinforced concrete discovery by J.L. Lambot in 1849. The engineers faced a significant challenge on the way of the reinforced concrete research being that it wasn't possible to apply old computing methods to the newest material. The tensions between the permitted stress calculations and the reinforced concrete's actual behavior appeared. The searches of the new computing methods resulted in the following additional requirements: 1. The reduction factor was added to the calculation. Now every cross-section unit of the armature was replaced by n units of the concrete cross-section. 2. The tensile strength of concrete was neglected [2].

In 1904 the calculation analysis of the pedestrian bridge in Vienna made by A.F. Loeit was the important conclusion in the research of the reinforced concrete. It resulted in calculations of bending reinforced concrete elements at the elastic stage being unacceptable [2].

The architecture of the 20th century shows a range of new architectural styles (for example, constructivism, functionalism, etc.), types of buildings (skyscrapers, etc.), design solutions, and the usage of new and improved materials and structures. The connections between engineering and architecture will be examined on the example of the USA architecture in the 20th century.

The specific feature of the building's construction in the USA at the beginning of the 20th century is its great extent. The technology level was higher than in other countries. Here the mounting methods were combined with machinery, for example, derrick cranes and tower cranes facilitated the lifting of the large constructive elements. At the beginning of the 20th century, old frames were replaced with lightened frames with joints in the bearing units. The skyscrapers spread widely. The framework took its place as the main constructive system. One of the first examples of the new building type was a ten-story Home Insurance Building (1883-1885) made by W. Le Baron Jenney, where the cast-iron columns and posts alongside Bessemer steel frames [3]. The Bessemer steel is steel manufactured as a result of the Bessemer process. The key principle of the process is the removal of impurities from the iron by oxidation with air being blown through the molten iron [4]. Home Insurance Building is the first example of such a wide usage of iron constructions and the beginning of the steel construction spread across the USA [3].

The skyscrapers' design began from the inside, from the small unit to the building in its entirety. The unit was a typical office inscribed into the rational plan of the level of the building. Even if space wasn't divided but rather was a solid structure, it depended on the measurement of the span and the window opening's distribution on the building surface [3].

The features of the typical skyscraper of this period best represented in the Woolworth Building. 55-storey in height, it was built in 1913 by architect C. Gilbert and structural engineers G. Aus and K. Berle. The building's construction faced its main engineering problems which were the bearing of the horizontal load of the wind and the vertical load of the weight of the building itself. The steel columns of the building are composite joined by rivets and have a cross-section of a never-before-seen width. For the bearing of the wind load engineers used all of the known joints such as diagonals in the plane of the floors, bracing on the main elements' crossings, etc [3].

The USA wasn't immune to the usage of the reinforced concrete patented in 1867. The research of this material began here as well. By the end of the 19th century in general terms, the theory of the permitted stress calculation of the reinforced concrete was formed based on the computing methods of the strengths of the elastic materials. For the calculations, one should assume that support reactions of the capital are distributed by the triangle, and the calculated span of the panel is the distance between the centers of gravity of these triangles. The whole bending moment calculation is given in equation 1.

$$M = \frac{1}{8} \cdot W \cdot L \cdot \left(1 - \frac{2c}{3L}\right) \cdot \left(1 - \frac{2c}{3L}\right) \quad (1)$$

W is the whole load on the floor unit, L is the width of the column spacing, c is the size of the capital. This equation was derived by G.R. Nichols in 1914 [5]. The beamless floor is shown in the figure 1.

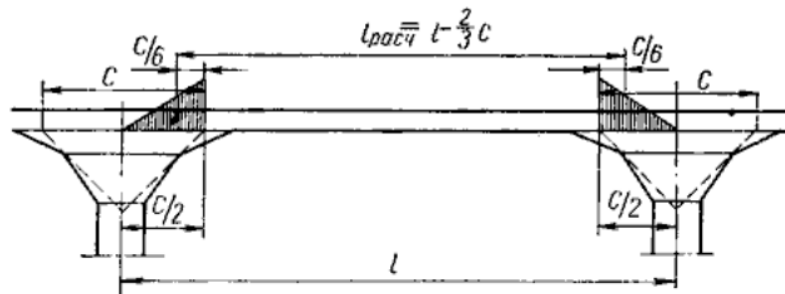
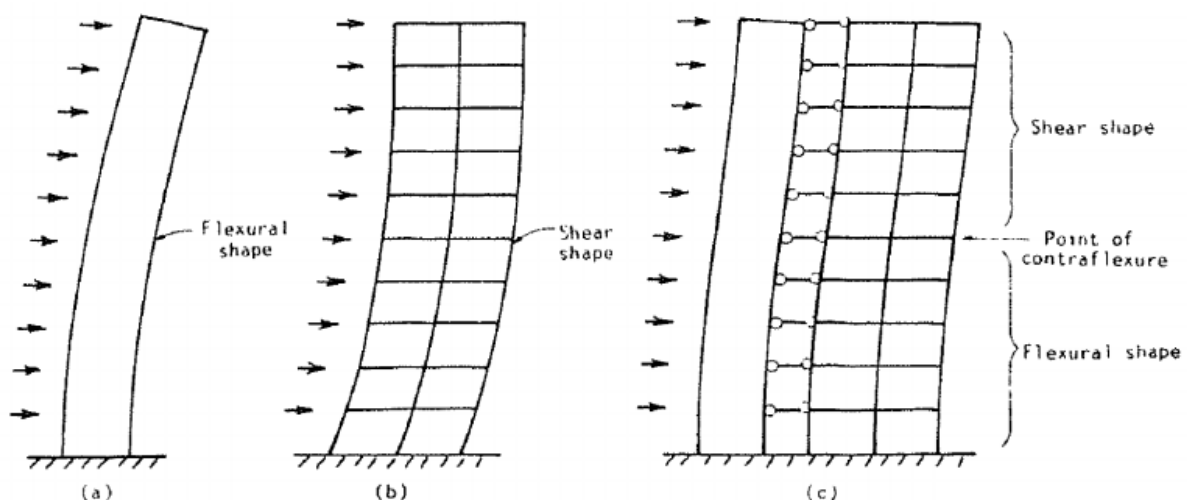


Fig.1. – Beamless floor

The high-rise buildings bear static loads as well as dynamic loads. Depends on the building's construction these indicators can vary. When calculating the static loads the reaction forces, bending moments, deflections, forces between composite elements, and the distribution of the forces between concrete cores are taken into account. For dynamic loads, resonant frequencies and accelerations are being considered. One of the main tasks when designing high-rise buildings is their ability to absorb the horizontal forces and to transmit the resulting moment into the foundation. The building behavior under the lateral loading can be seen as a cantilever fixed at the ground. If the wind is assumed to have a uniform distribution the base moment increases quadratically with the height. However, the real shape of the wind pressure is increasing with the height, which gives an even greater base moment [6].

A building needs to be stabilized for horizontal load and several different structural systems can be chosen in order to achieve this. A framed tube system and a bundled tube system were designed in the first half of the 20th century, others (a tube in tube system, a diagonalized system, etc.) appeared and began to improve later. Every one of these systems is a variation of the traditional rigidly jointed structural frame. The basic design for these systems has been to place as much of the load-carrying material as possible around the building external fringe to maximize its flexural rigidity. Advantage can be taken by locating the vertical members and, with the compressive stresses from self-weight, suppress the lateral load tensile stresses [6]. The deformation shapes of a tall building is shown in the figure 2.



a) Bending deflection, b) Shear deflection and c) Total deflection

Fig.2. – Deformation shapes of a tall building

One of the most impressive examples of the architectural and engineering excellence of this period is the Empire State Building. The building's construction ended in 1931. It has 102 stories and held the place of the highest building in the world. The building's overall height is 448 meters. This includes the antenna at the top of the building. The main construction system is the steel frame [7].

The technology of the construction is the following [7]:

A substantial concrete base was laid as a foundation in order to be able to withstand the weight of the steel framework of the building. All the steel sections were prefabricated and transported to the construction site. The sections were manufactured to exact sizes to within 2mm tolerance and prepared so that they could either be bolted together or joined with rivets. It took three days for the sections to be manufactured, transported, and positioned in the framework as part of the building's structure. Once the steel framework was fixed it was then finished with an outer skin of stone [7].

In order to join the parts of the building, two techniques were used. The first one is that the laborers walked up and down the structure as it was put together. Their job was to fix the separate sections together, using large nuts and bolts. The second technique is the usage of hot rivets. It was first used in the shipbuilding industry as a method of joining large steel plates. The steel rivet is heated until the plain end is red hot. Then it is passed through the holes of the two sections. When hot the rivet is soft and can be shaped using a rivet gun which rounds the plain end so that it is permanently fixed in the position [7].

To conclude, the beginning of the 20th century is a reflection of the strong bond between architecture and engineering. It would be impossible to implement the challenging ideas of the architects without construction engineers, the appearance of the new materials and construction systems, and its computing methods. The same goes for the ideas of the architects. Without them, there would be no place for the research of building materials and constructions.

REFERENCES

1. Взаимосвязь строительного материала, конструкции и архитектурной формы [Электронный ресурс] // Infopedia.su [сайт]. – 2016. – Режим доступа: <https://infopedia.su/2xaa81.html>. – Дата доступа: 13.04.2021.
2. Лопатто А.Э. Из истории развития строительных конструкций: L,M,Q,N / А.Э. Лопатто. – Киев: Будивельник, 1990. – 160 с.
3. Всеобщая история архитектуры: в 12 т. / Государственный комитет по гражданскому строительству и архитектуре при Госстрое СССР, Научно-исследовательский институт теории, истории и перспективных проблем советской архитектуры. — Ленинград; Москва: Издательство литературы по строительству, 1966—1977. — Т.10: Архитектура XIX — начала XX вв. / Под редакцией С. О. Хан-Магомедова (ответственный редактор), П. Н. Максимова, Ю. Ю. Савицкого. - Лени — 1972. — 592 с., ил.
4. Bessemer process [Electronical resource] // Wikipedia [website]. – 2021. – Mode of access: https://en.wikipedia.org/wiki/Bessemer_process. – Date of access: 13.04.2021.
5. Безбалочное перекрытие [Электронный ресурс] // Studwood.ru [сайт]. – 2021. – Режим доступа: <https://studwood.ru/2070621/nedvizhimost/istoriya>. – Дата доступа: 13.04.2021.
6. Hallebrand E. Structural design of high-rise buildings / Hallebrand E., Jakobsson W. – Lund : Faculty of Engineering LTH, Lund University, Media-Tryck, 2016.
7. The Empire State Building [Electronical resource] // Technologystudent.com [website]. – 2009. – Mode of access: <https://technologystudent.com/culture1/empire1.htm>. – Date of access: 13.04.2021.

METHODS FOR TESTING FORMULATIONS FOR A CONSTRUCTION 3D PRINTER

V. KHVATYNETS, L. PARFENOVA
Polotsk State University, Belarus

The article describes the application of 3D printing in construction. The main factors hindering the wide-spread development of these technologies are noted. The main technological characteristics of the mixture affecting the possibility of using it in a construction 3D printer are given. Possible ways of achieving the required parameters for the mixture are given.

3D printing is developing at a rapid pace and every year new areas are mastering it and construction is no exception [1]. For several decades, there have been construction 3D printers that differ in their dimensions, printing technology or place of application (fig. 1).

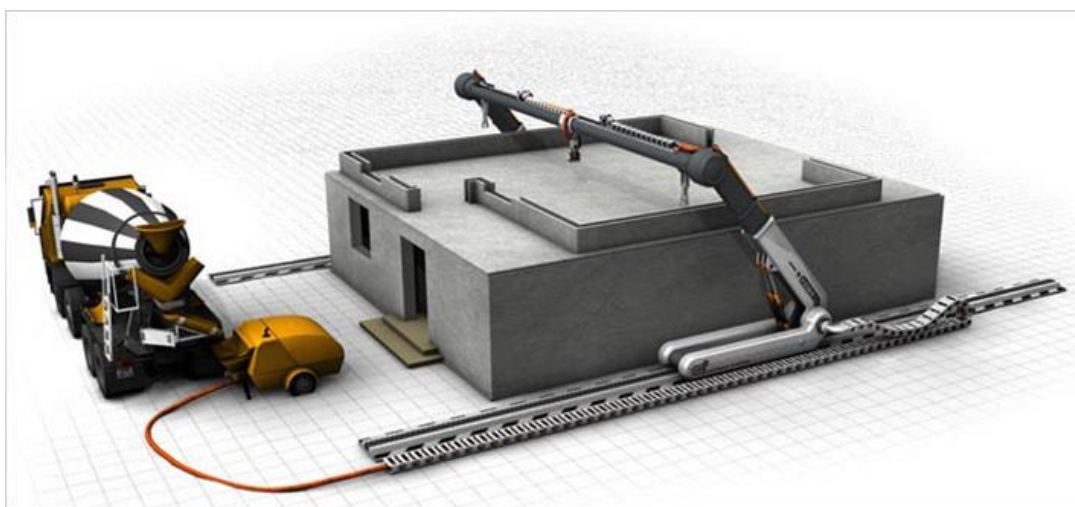


Fig. 1. – Construction 3D printer

However, if the creation of construction printers is not very difficult, and their designs are constantly being improved, then there are constraints. One problem is insufficient quantity of print mix. There are various formulations to suit different printer designs, however, they all include local materials or waste. Based on this, the purchase of such a mixture and its transportation becomes high in cost and makes the construction process using a 3D printer financially unreasonable.

Based on this, for the successful use of printers, it is required to develop a composition based on local materials and production waste, which will not only remove the cost of purchasing foreign material, but also contribute to reducing the cost of construction. In this regard, the question arises, what properties should a solution for a construction 3D printer correspond to.

In the publication, the authors note that the main technological characteristics of concrete mixes for 3D printing are: mobility, extrudability, shape stability, setting time and shrinkage [2].

The mobility index should ensure that the slurry will be easily pumped through the conveying system and will easily pass through the extruder. Fine mineral additives can fill voids and lubricate the mortar. Research has shown that crushed ash increases mobility, but adding too much of it increases friction between particles and increases viscosity, which has the opposite effect.

Extrudability indicates the ability of a solution to be continuously delivered through pipes and through a printer nozzle. Achieving good extrudability is possible when using round aggregates, as well as with a significant volume of cement to fill the voids. It was found that the optimal ratio of fine aggregate to cement is 1.28, and that of fine aggregate to sand is 2.0.

Shape stability refers to the ability of a printed material to maintain its shape after printing under its own weight and pressure from the top layers. The high rate is achieved due to the high content of sand and fine aggregates. It is noted that the viscosity modifier can provide a set of more than half the strength for 28 days, already one day after printing. Also, the test results showed that the addition of 0.05% lithium hydroxide can shorten the curing start time to 9 minutes.

To ensure a continuous printing process, it is required that the material has a significant setting time, while the onset of hardening should not increase. Studies have shown that the setting time increases when replacing 30% of the cement with blast furnace slag. The main additives that affect the setting time are accelerators and hardening retarders. It is noted that alkaline accelerators are more effective than alkali-free ones. It is described that the introduction of alkali-free accelerators from 2% to 7% by weight of cement reduces the setting time of the cement paste from 360 to 150 minutes.

Shrinkage is one of the main characteristics, since the dimensional accuracy of the layer and shape stability depend on it. Concrete material for 3D printing requires a significant water content to provide the required mobility and extrudability. As a result, shrinkage deformations occur during hydration. It should be noted that structures created using 3D printing always have a larger surface area than structures cast in formwork, which also leads to evaporation of free water and deformations. Shrinkage control is carried out by introducing mineral additives. The data obtained show that replacing cement with 80% ash leads to a decrease in slump by 66.7%. Using 5% and 15% silica reduced sediment by 29% and 35%, respectively.

D. Soltan and co-author also call the extrudability, print window, compressive strength and strength between layers the main parameters of a solution for a construction 3D printer [3]. The authors note that such indicators as extrudability, extensibility and interlayer bonding depend on workability, and manufacturability can be equated with flowability.

The relationship between extrudability and extensibility is inversely opposite. Thus, by increasing the rate of extrudability, the possibility of building up layers is reduced and vice versa. This complicates the task of finding the optimal balance for the solution.

Another criterion for evaluating a mixture for 3D printing is the adhesion of layers of concrete mixture. The authors of [4] note that the bond strength between layers depends on many parameters, which include: viscosity, setting time, contact area between layers. It has been found that a rectangular nozzle gives a larger contact area than a circular one, hence the adhesion between the layers is better.

Thus, summing up, it can be noted that there are the main technological characteristics affecting the quality of sweep, these are: mobility, extrudability, shape stability, setting time and shrinkage. The balance between some indicators is quite difficult to maintain, which requires the addition of various modifiers affecting specific characteristics to sweep away. If all the required criteria are met, it can be argued that the resulting mixture will be suitable for printing on a construction 3D printer.

REFERENCES

1. Хватынец, В. А. Современный уровень развития строительных 3D-принтеров / В.А. Хватынец, Л.М. Парфёнова // Архитектурно-строительный комплекс: проблемы, перспективы, инновации. – 28-29 ноября 2019. – Электронный сборник статей II международной научной конференции. - С. 327-331.
2. Guowei M.A. A critical review of preparation design and workability measurement of concrete material for largescale 3D printing / M.A. Guowei, Li WANG // Frontiers of Structural and Civil Engineering – 2017. – С. 1-19.
3. Soltan D.G. A self-reinforced cementitious composite for building-scale 3D printing / D.G. Soltan, V.C. Li // Cement and Concrete Composites – 2018.
4. Suvash C.P. Fresh and hardened properties of 3D printable cementitious materials for building and construction / C.P. Suvash, D.T. Yi Wei, P. Biranchi, J.T. Ming // Archives of civil and mechanical engineering – 2018. – С. 311-319.

FIBER CONCRETE IS A MODERN BUILDING MATERIAL

O. PODOBED, U. KHVATYNETS
Polotsk State University, Belarus

The article deals with a modern building material - fiber-reinforced concrete. Different types of fibers and their influence on the characteristics of the resulting concrete are described. The technology of creation is considered and its distinctive features are described. The list of possible directions of use of fiber-reinforced concrete is given.

The field of construction in our time is developing quite rapidly and more and more new, unique building materials appear. One of which is fiber-reinforced concrete (fig. 1).



Fig. 1. – Fiber concrete

A distinctive feature of fiber-reinforced concrete is the content of dispersed fibers or fiber in the structure, which gives the material high strength [1].

Fiber in its composition is presented in two variations:

The first type is steel wire. For this type of fiber, the fibers are represented by pieces of wire with a length of up to 50 mm, wave or straight shape. The manufacturing technology depends on the required wire diameter (electrical or mechanical). Fiber-reinforced concrete using steel fiber has extremely high strength and wear resistance. The high weight and tendency to corrosion of this material are its significant disadvantages.

The second type is synthetic fiber. In turn, synthetic fiber, depending on the required characteristics, is made from various materials: fiberglass, basalt, carbon, cellulose and polypropylene.

Fiberglass fibers are made from inorganic glass by melting and pulling the glass mass. The properties of such fiber-reinforced concrete vary depending on the length, thickness and strength of the fibers. Fiber concrete, using this type of fiber, turns out to be quite plastic. Among the minuses, one can single out instability to an alkaline environment.

Basalt fiber is produced by melting the basalt mineral. Basalt threads have high strength, are acid and alkali resistant, and also do not burn.

Carbon fiber is produced by high-temperature treatment of carbon. Fiber concrete with carbon fibers is resistant to corrosion and mechanical stress, acids and alkalis, as well as to high temperatures. It is the most resilient among all types of fiber-reinforced concrete. The only limiting factor in its manufacture is its high cost.

Cellulose fiber is resistant to acids, fire and water. The use of these fibers slows down shrinkage and promotes the removal of moisture to the surface from the lower layers of the screed.

Polypropylene fiber is obtained by cutting and twisting a propylene film. Such fiber-reinforced concrete is resistant to chemical attack and shock loads. It has a number of disadvantages, such as instability to high temperatures, as well as to compressive and tensile loads.

A feature of fiber-reinforced concrete is also the method of its manufacture. The bottom line is that fiber is injected into the cement mortar. Specific routes of administration depend on the fiber material. This is followed by the stage of mixing the fiber with the solution. The main part of the production of fiber-reinforced concrete is accurate proportioning and good mixing.

Fiber-reinforced concrete with synthetic fibers requires a special mixing technology. In this case, mixing should be done by spraying a mixture of fiberglass and concrete. If the preparation technology is not followed, the solution will clump and cease to be homogeneous, which will lead to a decrease in the final strength of the concrete.

The main positive properties of fiber-reinforced concrete include the following [2]:

- high strength;
- frost resistance;
- resistance to moisture;
- resistance to chips and cracks;
- resistance to chemical attack.

Fiber concrete with the addition of steel fibers is widely used in the production of high-strength structures. Foundations, bridge decks, bridge piers, bank protection strips, road surfaces, tunnels, platinum and runways. Fiber concrete has also found a place in the decorative design of high-strength facades, roofs, fences, etc.

The study showed that fiber-reinforced concrete is widely used in various fields due to its positive properties. For the manufacture of fiber-reinforced concrete, various fibers can be used, the choice of which determines the further characteristics of the material obtained. In addition, it is required to strictly adhere to the production technology in order to eliminate the inhomogeneity of the solution.

REFERENCES

1. Что такое фибробетон: плюсы и минусы, где применяется [Электронный ресурс] // URL: <https://1beton.info/vidy/fibrobeton/chto-takoe-fibrobeton-plyusy-i-minusy-gde-primenyaetsya> (дата обращения 12.04.2021).
2. Фибробетон: нюансы использования и варианты применения материала в строительстве [Электронный ресурс] // <https://homius.ru/primenenie-fibrobetona.html> (дата обращения 12.04.2021).
3. Хватынец, В.А. Создание высокопрочных оснований за счёт дисперсного армирования цементной матрицы / В.А. Хватынец, Е.А. Трамбицкий, Д.Н. Шабанов // Вестник Полоцкого государственного университета. Серия F. Строительство. Прикладные науки – 2018 – С. 56-59.
4. Хватынец, В.А. Эффективные параметры фибрового армирования бетонов / В.А. Хватынец, Л.М. Парфёнова // Актуальные проблемы архитектуры Белорусского Подвinya и сопредельных регионов – 2018 – С. 266-269.
5. Хватынец В.А. Тенденции в области совершенствования конструкций при проектировании и строительстве автомобильных дорог / В.А. Хватынец, Л.М. Парфёнова, Д.Н. Шабанов // Современные направления в проектировании, строительстве, ремонте и содержании транспортных сооружений: материалы II Международной студенческой конференции, Минск, 2018 – С. 51-55.

MODULAR CONSTRUCTION DURING A PANDEMIC

I. BORODEYKO, U. KHVATYNETS

Polotsk State University, Belarus

The article analyzes the experience of building hospitals during a pandemic, and on the basis of this, a proposal is formulated to create modules that are most efficiently used in construction. The use of these types of modules will reduce the time of their production, and as a result, reduce the construction time of the entire facility.

Modular construction is one of the classic ways of constructing buildings, but recently, modules have been modernized, adjusted to different needs and become more versatile [1-2]. Thanks to this, the scope of application of modular construction is expanding. One of the most relevant directions in recent years is the construction of hospitals.

During the construction of hospitals during a pandemic, one of the main indicators is the speed of construction [3]. When constructing modular buildings, the speed of construction directly depends on the speed of manufacturing modules at the factory.

To increase the rate of productivity of manufacturing plants, it is proposed to reduce the variety of types of module sizes used for the construction of hospitals. An analysis was carried out to identify the most used modules, as well as a study of the structural diagram of pre-fabricated hospital buildings.

The most effective is a corridor structural scheme, in which a corridor runs along the entire building, and rooms are located on one or two sides. In this regard, the use of the following modules was proposed.

Modules used for corridor rooms (fig. 1). It is proposed to use four main types of the module. Two of which on one side have doors for entering other rooms, and on the other side - window openings. The use of such modules is implied when the premises are located only on one side of the corridor. The second type has doorways on both sides, respectively, when the premises are located on both sides of the corridor. All corridor modules have door openings at their ends for a through passage. The length of the modules will be of two types 3000mm and 6000mm, respectively, designed to interface with one or two modules for infected patients. The height of all modules is 2800mm.

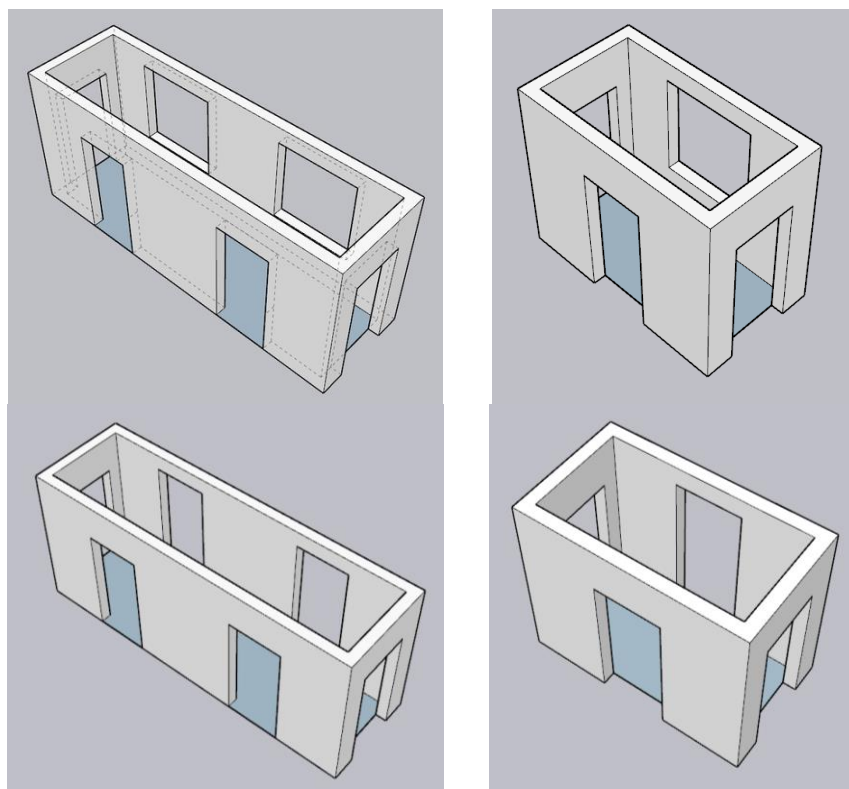


Fig. 1. – Modules for corridor rooms

The second main type of modules will be to accommodate infected patients, equipment, and staff accommodation (fig. 2). Such modules are subdivided into corner and private. The width of a private is 3000mm, and the

length is 3000mm, 4500mm and 6000mm, depending on the required number of beds and according to technological characteristics for the placement of hospital equipment. The dimensions of the corner module are 3000x3000mm and 1500x1500mm.

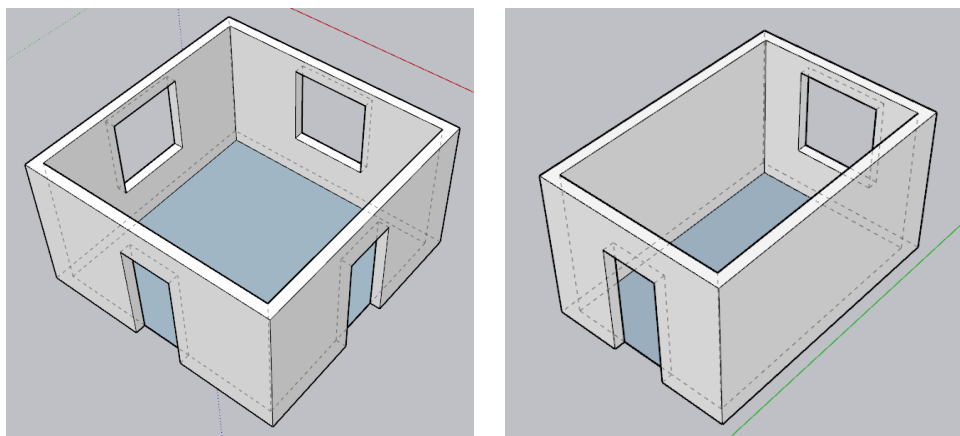


Fig. 2. – Modules for accommodating the infected

The interfaces are typical and depend on the material from which the module itself is made.

It should be noted that we are talking about one-story construction, which is the most common in the construction of hospitals during a pandemic. One of the advantages is that in the future, if necessary, the modules can be transported to another place and be used for the construction of a completely different object for its intended purpose. Such a reduced typing of modules will increase the pace of construction and will allow to create a larger number of hospitals in the shortest possible time.

Modular construction is distinguished by its speed of construction of buildings, which is one of the most important criteria for the construction of hospitals during a pandemic. Based on the analysis carried out, our own variants of the modules have been developed and modeled, which are most suitable for the construction of hospitals.

REFERENCES

1. Бородейко, И. В. Зарубежный опыт проектирования модульных зданий / И. В. Бородейко // Международное сотрудничество: опыт, проблемы и перспективы. – 30 сентября 2020. – Сборник материалов международной научно-практической конференции. - С. 6-9.
2. Бородейко, И. В. Формообразование модульных зданий и их объёмно-планировочные решения / И. В. Бородейко // Результативность и эффективность внедрения современных методологий в научные исследования и разработки. – 16 октября 2020. – Сборник материалов международной научно-практической конференции. - С. 6-8.
3. Бородейко, И. В. Оптимальный метод строительства в период пандемии / И. В. Бородейко // Результативность и эффективность внедрения современных методологий в научные исследования и разработки. – 16 октября 2020. – Сборник материалов международной научно-практической конференции. - С. 8-11.
4. Бородейко, И. В. Особенности модульных зданий / И. В. Бородейко // Результативность и эффективность внедрения современных методологий в научные исследования и разработки. – 16 октября 2020. – Сборник материалов международной научно-практической конференции. - С. 14-16.
5. Бородейко, И. В. Типы используемых модулей в современном строительстве / И. В. Бородейко // Результативность и эффективность внедрения современных методологий в научные исследования и разработки. – 16 октября 2020. – Сборник материалов международной научно-практической конференции. - С. 11-14.

ANALYSIS OF THE DEVELOPMENT LEVEL OF FIBER CONCRETE AND ITS PROSPECTS

Y. SHALEIKA, U. KHVATYNETS
Polotsk State University, Belarus

The article analyzes the publications of authors who have made a great contribution to the development and study of fiber-reinforced concrete. The analysis carried out gives a clear definition of the concept of fiber-reinforced concrete and describes the main types of fibers used. Other measures are being considered to achieve high compressive strength and flexural tensile strengths.

From the article by S.I.Suhova, fiber-reinforced concrete is concrete in which special inclusions, called fibers, are distributed throughout the structure [1]. Fiber-reinforced concrete is many times greater than the strength characteristics of conventional concrete. Reinforced concrete is divided into several types. The most commonly used materials are steel, synthetic materials and fiberglass. The main indicators of the properties of fiber-reinforced concrete are: compressive strength, axial tensile strength, flexural tensile strength, frost resistance, water resistance, impact strength, toughness. The most important of these are tensile strength and impact strength 3-5 times higher than that of conventional concrete. The most rational areas of application of fiber-reinforced concrete: highways, pavement re-laying, industrial floors, railway sleepers, pipelines, beams, steps. For the manufacture of fibers, fibers with a wire diameter of 0.2 mm to 1.0 mm are used. The used fiber, cut from a thin cold-rolled sheet, has a thickness of 0.3 to 1.0 mm, a width of 0.4x0.6 mm and a length of 30 to 40 mm. The strength of this fiber is from 480 to 600 MPa. The cheapest and most chemically resistant fiber is made from synthetic fibers. However, this type of fiber has a low modulus of elasticity and high ultimate deformability. Synthetic fiber is used in construction, often in fine-grained concrete due to its accelerated strength development.

After analyzing the article by SV Klyuev, it was found that there are many varieties of fiber-reinforced concrete products that have a wide range of applications [2]. From the point of view of saving materials, fiber-reinforced concrete with the addition of polypropylene fibers is used for highways due to the reduction in the thickness of the coating. This is primarily due to the fact that this material has shown its strength, lightness and high viscosity. When assessing the quality and studying the physical and mechanical properties of aggregates, it was found that the dispersed reinforcement of the cement matrix with polypropylene fiber, which has a high chemical resistance to an alkaline medium, increases the compressive strength to 13%, and the flexural strength to 38%. Therefore, the use of polypropylene fiber is more effective in increasing the flexural tensile strength of fine-grained concrete.

In the article by R.V. Lesovik, it is said that steel-fiber concrete is mainly used abroad in three directions, such as aerodrome coatings, sprayed concrete and monolithic tunnels, bank protection and berthing structures [3]. Steel-fiber concrete is widely used for repair work, industrial buildings, flooring, and thin-walled load-bearing structures. The advantages of using this material in the construction of busy industrial buildings, warehouses with a high specific static and dynamic load: reducing the thickness of the floors, partial replacement of traditional reinforcement, high wear resistance, impact strength, and reduced labor intensity. This material is good for the construction of aerodrome pavements as it provides a thickness reduction of 40-50% without loss of bearing properties. When steel fiber is added to fine-grained concrete, the compressive strength increases by 28% and the modulus of elasticity by 27%.

However, an increase in the strength of fine-grained concrete is associated only with the use of fiber, but only with the use of complex measures in production.

Auto publications, S.V. Klyuev argues that due to large-sized equipment and storage of materials in industrial buildings and structures, there is a need for development in the field of concrete for heavy-duty floors [4]. For this purpose, for fine-grained concrete with increased operational characteristics, high-density packing of aggregate is used, such as screening of granite crushing and hyperplasticizer, as well as fiber reinforcement. Thanks to the research, it became clear that the developed composition of fine-grained concrete with high-density aggregate packing on a composite binder exceeds the strength of concrete without a high-density aggregate by 3 times. Due to the high-quality packing of aggregate particles and structure. For heavily loaded floors, fiber-reinforced concrete with aggregate from granite screening and sand with a size modulus of 1.2 a are used as a binder TMC-100, VNV-100 and Portland cement CEM I 42.5N. When using a plasticizer, concrete is obtained with a high-density aggregate packing. Using a composite binder, hyperplasticizer Muraplast FK 68, metal wave-like fiber, compositions of finely dispersed fiber-reinforced concrete were obtained on screening granite crushing with a compressive strength of 118.8 MPa, and a bending strength of 14.1 MPa.

The analysis of publications has shown that fiber-reinforced concrete is a modern building material with a fairly wide range of applications. The fibers can be various materials by their nature, as well as various production wastes. In addition, in order to achieve the best result of strength readings, a number of measures should be used, associated not only with the correct selection of fiber and its characteristics, but also with the selection of an aggregate to create a dense matrix of the resulting material.

REFERENCES

1. Сухова, С.И. Фибробетон / С.И. Сухова. – Наука ЮУрГУ: материалы 67-й научной конференции. 2015. – 1636-1640 с.
2. Ключев, С.В. Мелкозернистый фибробетон с использованием полипропиленового волокна для покрытия автомобильных дорог / С.В. Ключев., Е.Н. Авилова – Вестник БГТУ им. В.Г. Шухова, №1. 2013. – 37-40 с.
3. Лесовик, Р.В. Мелкозернистый фибробетон на основе техногенного песка / Р.В. Лесовик., К.С. Ракитченко, С.А. Казлитин – Сухие строительные смеси, №3. 2014. – 24-25 с.
4. Ключев, С.В. Монолитный фибробетон для полов промышленных зданий / С.В. Ключев., А.В. Нетребенко, А.В. Дураченко, Е.К. Пикалова – Сборник научных трудов Sworld 19(1). 2014. – 29-32 с.
5. Хватынец, В.А. Создание высокопрочных оснований за счёт дисперсного армирования цементной матрицы / В.А. Хватынец, Е.А. Трамбицкий, Д.Н. Шабанов // Вестник Полоцкого государственного университета. Серия F. Строительство. Прикладные науки – 2018 – С. 56-59.
6. Хватынец, В.А. Эффективные параметры фибрового армирования бетонов / В.А. Хватынец, Л.М. Парфёнова // Актуальные проблемы архитектуры Белорусского Подвинья и сопредельных регионов – 2018 – С. 266-269.

APPLICATIONS OF SMART BUILDING TECHNOLOGIES IN THE COVID-19 ENVIRONMENT

E. KURGANOV, I. SHANIUKEVICH

Belarusian National Technical University, Minsk, Belarus

The article is devoted to the ways of application of smart building technologies in the COVID-19 environment, which will help prevent the spread of infectious diseases and improve the efficiency of property management.

COVID-19 has caused massive upheaval around the world. Many people have started working from home to prevent the spread of the virus. However, as people return to their workplaces, property owners need to prepare for this, including controlling and limiting the spread of infectious diseases. The use of smart building technologies can help solve the problems of adjustment to the conditions created by COVID-19.

Companies feel the impact of the global spread of COVID-19 in different ways, depending on the type of property and location. Currently, property owners are concerned about preserving the value of real estate [1], ensuring the safety of people during a period of infection with the virus [2] and reducing the cost of cleaning measures.

One of the long-term consequences of COVID-19 has been the need for more flexible systems. Property owners have focused on finding technologies that will help re-open the property while respecting certain restrictions. In this regard, smart building technologies are becoming an increasingly important element of the building. Take, for example, an office building. Thousands of people enter and leave such a building every day. The use of smart cameras equipped with video analytics can help maintain optimal occupancy in a building, distance people from each other and ensure that masks are worn. The data provided by these devices can help the security service and property owners more effectively guide visitors in lobbies, stairwells, and escalators.

An example of successful implementation of smart technologies is the hotel business and healthcare. In the hotel business, the installation of "smart" lighting in the rooms, as well as the provision of contactless room keys using QR codes on smartphones, has become widespread.

In the health sector, with the increasing spread of infectious diseases, the priority tasks of hospitals have become to reduce the risks of infection, improve the air quality in the premises of the building and eliminate problems with the supply of medicines. An intelligent hospital can solve all these problems much better than a traditional one. For example, a mobile application can be integrated into a hospital management system, allowing doctors to simplify interaction with drug suppliers, know about the state of health around the clock, and individualize medical care for each patient. The leading providers of mobile healthcare applications are AirStrip, Air-strip/Cardiology, Epic Systems, and MyChart, which provide secure two-way messaging and interactivity between the patient and the doctor based on data collected in the hospital information database [3].

However, with the introduction of intelligent systems in buildings, the quality of cleaning during the spread of viral infection is an important issue. Based on smart construction technologies, it is possible to achieve control over places with a large crowd of people by combining information about employment and job reservations. This information will allow to determine the frequently used spaces and the time of intensive flow of people. It should also consider using QR codes in the building to track the time and frequency of cleaning through the mobile app. This technology is used at the University of Stirling [4].

The pandemic has also increased the need for improved air quality. To solve the problem, it's possible to create an air filtration system. This system will use data from indoor air quality sensors and analytical data on the presence of people. Besides to improving air ventilation, organizations should pay attention to HVAC (heating, ventilation and air conditioning). To improve the efficiency of these systems, it should use an automatic fault detection and diagnosis system. In addition, air quality sensors should be used, which collect information about CO₂ and volatile organic compounds.

To prevent the risk of the spread of COVID-19, it is necessary to constantly monitor the interaction of employees in the office. The solution to this problem may be to track the health status of people and their recent contacts with each other using smartphones. An example of such a technology is the joint development of Apple and Google. When the function is activated on the smartphone, the disease status is entered: positive or negative. Upon receiving a positive test, the user changes his status and a notification about the need for a medical examination is sent to the smartphones of people with whom they have recently been in contact. In addition, using the latest technology, it is possible to check for infection in large crowds of people at a relatively low cost. An example of such technology is CoTest, which can be used to test up to 40 people on COVID-19 with results obtained in 30 minutes. Significantly reducing the burden on centralized testing services, CoTest quickly and accurately provides results on the health status of employees to health authorities [5].

Due to non-compliance with COVID-19 guidelines in team workplaces, organizations need to rethink the concept of the workplace. In the short term, it should pay attention to the use of sensors to measure the employment of the workplace (for example, presence and light sensors), as well as programs to track the movement of employees around the office. For example, TEECOM has created a Room Search app for its headquarters in Auckland, New Zealand, which is one way to manage a workplace based on measuring room occupancy [6].

Nevertheless, smart buildings have their drawbacks. To improve the well-being and safety of people, they collect huge amounts of information, which increases the level of service, reduces the cost of operating the building and helps reduce the spread of COVID-19. However, the collection of people's data may also violate the personal data protection and privacy rules. Barclays Bank faced this in early 2020 [7]. In accordance with the EU General Data Protection Regulation (GDPR) [8] the processing of personal data requires an appropriate legal framework. To ease privacy and data protection concerns, smart building technology is built with privacy in mind to ensure it complies with GDPR requirements and national data protection laws.

Along with the issue of personal data protection, one of the important issues is the allocation of costs for the modernization of buildings when implementing smart building technologies. Even if the investment costs are initially covered by the property owners, they are likely to pass them on to tenants and residents who may find this unacceptable. However, realizing that the use of smart technologies leads to lower utility costs and helps prevent the spread of infectious diseases, authors believe that the initiative to introduce smart technologies in buildings should receive the support of society, including with a certain possibility of a financial initiative.

The above-mentioned issues are just some of those that smart building technologies can solve. COVID-19 has accelerated the adoption of smart building technologies and associated plug-in equipment. This is mainly due to the new conditions that have emerged as a result of the emergence of a viral infection and the ability of intelligent technologies to ensure that the necessary rules are followed and enforced, as well as to improve the efficiency of construction and property management. At the same time, smart building technologies have solutions to such problems as:

1. Ensuring the safety of people at a time of high risk of COVID-19 infection.
2. Changing attitudes towards the quality of cleaning in buildings.
3. Improved air quality and more efficient ventilation in buildings to minimize virus survival.
4. Monitoring the interaction of employees in the office in order to minimize the risks of spreading a viral infection.
5. Changing the design of the workplace if individual and team workspaces are too densely populated for requirements or recommendations against COVID-19.

Investment in smart building technologies is expected to rise in the near future, which will not only better prepare for future outbreaks of viral infection, but also increase the comfort of being in the premises and the level of maintenance of buildings.

REFERENCES

1. Reassessing Real Estate Investments During the Coronavirus Pandemic [Electronic resource]. – Mode of access: <https://www.wellsfargo.com/the-private-bank/insights/reassessing-ream-during-covid/>. – Date of access: 27.02.2021.
2. Coronavirus disease (COVID-19): Health and safety in the workplace [Electronic resource]. – Mode of access: <https://www.who.int/news-room/q-a-detail/coronavirus-disease-covid-19-health-and-safety-in-the-workplace>. – Date of access: 27.02.2021.
3. Top 10 Healthcare Mobile Apps Among Hospital, Health Systems [Electronic resource]. – Mode of access: <https://mhealthintelligence.com/news/top-10-healthcare-mobile-apps-among-hospital-health-systems>. – Date of access: 22.02.2021.
4. Check in to buildings, locations and teaching rooms [Electronic resource]. – Mode of access: <https://www.stir.ac.uk/coronavirus/changes-at-stirling/making-campus-safer/scan-in-to-buildings-on-arrival/>. – Date of access: 17.02.2021.
5. CoTest [Electronic resource]. – Mode of access: <https://www.ttp.com/cotest>. – Date of access: 25.02.2021.
6. Occupancy Measurement Enables Digital Workplace Management [Electronic resource]. – Mode of access: <https://teecom.com/occupancy-measurement-drives-digital-workplace-management-during-and-beyond-covid-19/>. – Date of access: 19.02.2021.
7. Barclays scraps "Big Brother" staff tracking system [Electronic resource]. – Mode of access: <https://www.bbc.com/news/business-51570401>. – Date of access: 08.02.2021.
8. Regulation (EU) 2016/679 of the European Parliament and of the council [Electronic resource]. – Mode of access: <https://eur-lex.europa.eu/eli/reg/2016/679/oj>. – Date of access: 10.02.2021.

DEVELOPMENT OF "GREEN" CONSTRUCTION IN BELARUS AND CHINA

D. ZHAVORONOK, ZHAN XINXIN, L. PARFENOVA

Polotsk State University, Belarus

A brief analysis of international green building standards is presented. The main approaches to the development of "green" construction in Belarus and China are presented. It is noted that in order to stimulate "green" construction, the issues of preferential tariffs for environmentally friendly materials and technological systems, tax incentives for organizations that build and own "green" buildings should be resolved, "green" standards have been developed.

Relevance of the topic. The guarantee of sustainable development is a significant aspect for the investment and construction complex. One of the main criteria for the activity of the investment and construction complex is the guarantee of the quality of construction products throughout the entire life cycle - from construction to demolition of a building. Requirements for modern buildings to ensure safety and create favorable conditions for human life, limit the negative impact of construction activities on the environment and ensure the protection and rational use of all types of natural resources make such quality indicators as energy efficiency, energy intensity and environmental friendliness of the building paramount. These parameters are the components of the concept of "green" construction.

Green building standardization. In world practice, there are a number of generally recognized "green" standards. The main ones are the English BREEAM standard, American LEED, German DGNB, French HQE. The fundamental concept of each is the goal of minimizing the negative impact on nature, which is caused by the construction and operation of the facility, and at the same time providing a comfortable atmosphere for subsequent operation.

The BREEAM (Environmental Assessment Method) standard was created in the UK in 1990. The essence of the BREEAM standard is to assign a building one of five levels of rating: satisfactory, good, very good, excellent, excellent. Assignment occurs through the integral assessment of such indicators as: water, materials, energy, land use, waste disposal.

The strength of the BREEAM in USE standard is that it is divided into three parts. The first part is the Part 1 Asset Performance. It is largely based on an assessment of the physical characteristics of the structure: the area of translucent structures (affects the availability of daylight and energy savings), the level of illumination, the ability to control temperature and air supply, the boilers used, ventilation machines and their efficiency, transport accessibility, water consumption, waste management infrastructure, land use, pollution, etc.

The second part - Building management (Part 2 Building management). To a greater extent, it concerns building management based on an assessment of the management company's approaches: to documenting procedures, training, forming and implementing policies, taking measurements, providing a comfortable environment for users (fresh air supply levels, monitoring CO₂, NO_x), controlling the content of volatile organic matter in the air, acoustic assessment, legionella control, energy efficiency and water management, as well as materials, landscape, pollution, etc.

The third part - Management of tenants (Part 3 Occupier Management). To a greater extent, it develops the issues of the second part, therefore, only joint certification of the third and second parts is possible (while the second part can be certified separately).

Advantages of the BREEAM assessment system - the assessment system is applicable to various types of buildings, the criteria are "tuned" to British law and, accordingly, British values, including high quality construction, and compliance with the declared project at the operational stage, an individual approach to one or another objects, the possibility of individual assessment programs, a clear scheme of adaptation to foreign norms. The disadvantages of the "BREEAM" assessment system are very strict requirements, high cost of obtaining approvals, the standard is tied to building and engineering norms and approaches of Great Britain [1,2].

The LEED standard (The Leadership in Energy & Environmental Design) was created in the USA in 1998 and is applicable for new construction projects, global renovation projects, interior renovation of buildings, projects for the creation of commercial interiors. The LEED grading system is based on the assignment of points to the object. Points are awarded based on the criteria of industrial development (26 possible points), water efficiency (10), energy and atmosphere (14), internal environmental quality (15), innovation and development process (5), availability of an accredited LEED professional (1) and availability regional advantage (4 possible points). In accordance with the points scored, there are 4 levels of compliance with standards assigned to objects by rating systems. LEED certification levels: 40–49 points mean Certified, 50–59 points Silver, 60–79 points Gold and 80 and above Platinum [1].

The German DGNB system, in turn, at the design stage, allows making decisions that will provide maximum savings in the operation of the facility. The mission of HQE is to create a high quality environment. In terms of the frequency of using standards for assessing "green" construction, BREEAM ranks first, LEED comes second, followed by the German DGNB standard, followed by France and its HQE standard [2].

Development of "green" construction in the Republic of Belarus. In the Republic of Belarus, one of the plans for the upcoming five-year period is the development and implementation of national standards for "green" construction and the development of voluntary certification of construction according to such standards. It is planned to approach the implementation of these directions in an integrated manner, already at the stage of developing urban planning documentation, the functions of the territory will be determined, parks, squares will be created, requirements for the norms of greening areas will be formed [3].

At the moment in the Republic of Belarus "green building" is developing with the support of the state and international organizations. Within the framework of the international technical assistance project GEF-UNDP-Ministry of Natural Resources "Belarus: support for" green "urban development in small and medium-sized cities of Belarus" for 2016-2021. the principles of strategic territorial planning have been tested and successfully implemented, combining socio-economic directions of development and the vision of spatial development of the territory; methods for a comprehensive technical and economic assessment of the effectiveness of various measures were worked out, the possibilities of attracting "green" instruments for financing infrastructure projects and the implementation of sustainable procurement were considered, and pilot initiatives were implemented in the field of energy efficiency (Novogrudok) and sustainable urban mobility (Novopolotsk and St. Polotsk), focused on achieving a comprehensive energy, economic, environmental and social effect. During the implementation of the project, a direct reduction in greenhouse gas emissions during the life cycle of pilot initiatives in the amount of 77.8 thousand tons of CO₂ equivalent is expected by increasing the efficiency of urban transport in Polotsk and Novopolotsk, as well as 13.3 thousand tons CO₂ equivalent from energy efficiency improvements in Novogrudok. The indirect reduction of emissions cumulatively over a 10-year period after the completion of the project will be from 25.2 thousand tons to 231 thousand tons of CO₂ equivalent [4].

In order to develop "green" construction, the Decree of the President of the Republic of Belarus of September 4, 2019 No. 327 "On improving the energy efficiency of multi-apartment residential buildings" was adopted, which is one of the first regulatory legal acts that provide citizens with support in their desire to reduce heat consumption, increase energy efficiency residential building, thereby increasing the comfort of living. An example of a "green" building in Belarus is the Omega Tower business center at 57 Dzerzhinsky Street in Minsk, which became the first certified "green" building in Belarus according to the international BREEAM standard.

As the main ideological line of the Concept of the National Strategy for Sustainable Development of the Republic of Belarus for the period up to 2035, the strategy of inclusive sustainable "green" growth in all spheres of society is defined. The main vector for the implementation of this strategy is defined as the "green" economy, which ensures economic growth in conditions of preservation of natural capital, which allows to identify new potential sources of economic growth, without creating an "unstable" load on the quantity and quality of natural resources. To achieve this goal, priority directions and tasks have been identified in the field of ensuring an environmentally safe living environment, preserving and rational use of natural potential, biological and landscape diversity, effective use of waste and their environmentally friendly disposal, greening of industrial production.

Development of "green" construction in China. In China, the development of green buildings is also following in the footsteps of the world. In 1986, China issued the industry standard JGJ26-86 "Civil building energy-saving design standards (heating residential building part)", set a target of 30% energy conservation, which is Also China's First Building Energy-Saving Standards. In the 1990s, China issued the Notice of the State Council on The Approval of the State Building Materials Bureau and other departments on speeding up the innovation of wall materials and the promotion of energy-saving building opinions, the People's Republic of China Energy Conservation Law and other energy-saving-related policies and regulations.

In the 21st century, China began to promote green buildings throughout its life cycle. In 2001, China's first scientific research project on green buildings was completed. In 2004, China held the first China International Symposium on Intelligent and Green Building Technology, expressing the Chinese government's determination and ability to act on green buildings. In 2006, China's Ministry of Housing and Construction issued GB/T50378 Green Building Evaluation Standards. Green buildings at this stage are defined as buildings that maximize resource conservation (energy saving, land saving, water saving, material saving), protecting the environment, reducing pollution, providing people with healthy, suitable and efficient use of space, and living in harmony with nature over a lifetime.

The second generation of green buildings in the 11th and 12th Five-Year Plan period has been rapid development, from scratch, from less to more, from some cities to the overall development of the whole country. Some cities or regions have been led by the government to enforce green building standards, or in the construction

Architecture and Civil Engineering

drawing audit to include green buildings in the special audit requirements. According to the requirements of the 13th Five-Year Plan for Building Energy Conservation and Green Building Development issued by the Ministry of Housing and Construction in 2017, the development of green buildings in China has entered the accelerator of "incremental quality" between 2016 and 2020. Planning requirements by 2020, the proportion of urban green buildings in China accounted for more than 50% of new buildings, new green construction area of more than 2 billion square meters. It is required that the proportion of green buildings with two-star logo above the project exceeds 80%, and the proportion of green building projects that obtain the running logo exceeds 30%.

In recent years, many parts of China frequent haze, secondary water supply caused by the drinking water quality of households is not up to standard, complex decoration caused by indoor formaldehyde and TVOC exceeding the standard, as well as the aging of residents, have put forward new requirements for the development of a new generation of green buildings.

In the industry, from the point of view of building users, the new people-oriented model has gradually become a new consensus for the development of green buildings. In 2019, China conducted its third iteration of green building standards, releasing the 2019 edition of gb-50378 Green Building Evaluation Standards. The new version of the green building standards and the new era of people's needs for a better life, reflecting the "people-centered" basic concept, in the original focus on building and environmental relations, "four sections and one environmental protection" on the basis of the dimension of expansion, the addition of safety and durability, energy conservation, healthy livability, full-age friendly and other aspects of technical content, reconstructed "safe and durable, healthy and comfortable, convenient life, resource conservation, environmental livability" five indicators system, defined China's third generation of green buildings.

It can be found that a new generation of green buildings has gradually incorporated the content of sponge cities and healthy buildings, healthy building concepts and green ecology, designed to enhance the experience and sense of access of building users to green buildings, the real combination of people-oriented and sustainable building development [5].

In the PRC, the priority tasks of the Chinese leadership are the formation of innovative models and methods of economic growth, an increase in the standard of living of the population, a decrease in the anthropogenic load on the environment and respect for nature. The concept of China's ecological civilization began to form after the adoption of the "Program for Sustainable Development of China at the Beginning of the 21st Century" in 2003. It received the greatest theoretical and practical development since 2012, when it was formulated a complex task of building "ecological civilization" and "beautiful China" as an integral part of the further economic, cultural and social sustainable development of the Chinese nation [7].

Xie Zhenhua, Special Representative of China for Climate Change, Deputy Chairman of the Committee on Population, Resources and Environment of the CPPCC (People's Political Consultative Council of the People's Republic of China), writes: recycling and reuse, environmental protection, harmony between nature and humans, and the development of a unified regulatory environment in the relevant areas. In a narrow sense, "green development" is the protection and protection of the environment, in particular the elimination of the consequences of pollution, the restoration of the environment, and the increase in production capacity for the production of eco-products" [8].

Conclusion. Analyzing the prospects for the development of "green" construction, experts stress that the "greening" of the Belarusian construction industry will: improve the environment, increase energy security, increase the level of investment attractiveness of the country [9].

Studies in the field of green economy regulation in the context of sustainable development [2] have shown that in order to stimulate green construction it is necessary to increase the degree of economic and physical accessibility of environmental materials and technological systems. To achieve these goals, it is proposed to use the following tactics:

- set preferential tariffs for the import of materials and systems (especially in the absence of national production);
- at the stages of design and construction of buildings and structures for state needs, ensure compliance with "green" standards;
- to establish the possibility of subsidizing, at the expense of budgetary resources, part of the costs (including interest rates on bank loans: for construction - for enterprises, mortgage - for the population) investors of green buildings;
- to provide tax incentives for organizations that build and own "green" buildings.

It is noted [2, 9] that a significant resource of the state policy for the development of "green" construction and the economy in general is the assistance of scientific and educational programs in this area, including international ones. Universities and research centers are proposed to be involved in development by increasing public and private funding, which can provide a significant effect due to innovative thinking and the desire for "green" entrepreneurship among young people.

REFERENCES

1. Gelmanova, Z.S., Amirkhanova, M.A., Georgiadi, I.V. "Green" construction as an effective tool for ensuring sustainable development of territories [Electronic resource] / Z.S. Gelmanova, M.A. Amirkhanova, I.V. Georgiadi // Scientific Review. Economic sciences. - 2016. - No. 1. - S. 12-14. - Mode of access: <https://science-economy.ru/ru/article/view?id=764>. - Date of access: 10.02.2021.
2. Khalil Musab Rushadi Ahmad Scientific and methodological support of state policy for regulating the green economy in the context of sustainable development: dis ... cand. econom. Sciences: 08.00.05 / Khalil Musab Rushadi Ahmad. - Kursk, 2020.- 182 p. [Electronic resource]. - Mode of access: <https://www.dissercat.com/content/nauchno-metodicheskoe-obespechenie-gosudarstvennoi-politiki-regulirovaniya-zelenoi-ekonomiki>. - Date of access: 10.02.2021.
3. National standards for green building are planned to be developed and implemented in Belarus [Electronic resource] // Belarusian telephone agency BELTA: official site. - Mode of access: <https://www.belta.by/economics/view/natsionalnye-standarty-zelenogo-stroitelstva-planirujut-razrabotat-i-vnedrit-v-belarusi-426388-2021/>. - Date of access: 03/17/2021.
4. Plans for "green" urban development and streets with "smart" light - what has been done under the UNDP-GEF project [Electronic resource] // Belarus Today: official site. - Mode of access: <https://sb-by.turbopages.org/sb.by/s/articles/plany-zelenogo-gradostroitelstva-i-ulitsy-s-umnym-svetom-cto-sdelano-po-proektu-proongef.html>. - Date of access: 10.02.2021.
5. Li Guikun Path The development of green buildings in China [Electronic resource] / Li Guikun // Sinoceanland-Design. - 2021. - Mode of access: https://mp.weixin.qq.com/s/jsoO7dppkYFSVmiyd_tupQ. - Date of access: 04.19.2021.
6. Yingxin Zhua, Ling Song. Jerome Damiensa State of the art of green building standards and labelling system development in China / Yingxin Zhua, Ling Song. Jerome Damiensa [Electronic resource] // International Journal of Sustainable Building Technology and Urban Development. - 2013. - Vol. 4. - No. 3. - pp. 178-184. - Mode of access: <http://dx.doi.org/10.1080/2093761X.2013.837216/>. - Date of access: 04.19.2021.
7. Balchindorzhieva, O.B. The problem of building a green economy in China / O.B. Balchindorzhieva // Eurasianism and the World. - 2019. - No. 1. - P. 37-41.
8. Xie Zhenhua Path of "green development" / Xie Zhenhua // China. - 2018. - No. 10 (156). - S. 24-25.
9. Balamut, T.V. Green construction - investment in the future [Electronic resource] / T.V. Balamut // Ecology at the enterprise. - 2016. - No. 10 (64). - Mode of access: <https://ecologia.by/number/2016/10/>.

INVESTIGATION OF THE INFLUENCE OF A SPECIFIED WATER FLOW RATE IN THE HOT WATER SUPPLY SYSTEMS OF MULTI-APARTMENT RESIDENTIAL BUILDINGS ON THE MATERIAL CHARACTERISTIC OF A PIPELINE NETWORK

V. YAKAULEVA, E. DOROFEEV, A. NIYAKOUSKI

Polotsk State University, Belarus

The article deals with the influence of the amount of water consumption by one consumer per hour of maximum water consumption in the hot water supply system of multi-apartment residential buildings on the diameters of pipelines of a water supply network. It is shown that with an increase in the values of this flow rate, the material characteristic of the hot water pipeline network monotonically increases what leads to an increase in capital costs. However, this effect is negligible. The conclusions made in this article can be used for discrete optimization of the diameters of the pipelines of centralized hot water supply systems of multi-apartment residential buildings.

Capital expenditures for the construction of centralized hot water supply systems for multi-apartment residential buildings are directly dependent on the pipeline section diameters selected during the design process. In their turn the diameters depend on the water volume that is pumped through the pipelines per unit of time. Determining water consumption in the design process is a difficult task if the goal is to perform a discrete optimization of the costs of construction and operation of a hot water system. The situation is aggravated by the fact that there is no unambiguous interpretation of this issue in the technical regulatory legal acts that regulate design.

Obviously, an increase in water consumption leads to an increase in the diameter of the pipelines. In this case, the area of their cross-section increases in proportion to the increment of the squared diameter. This allows us to expect that the total pressure loss in the system will decrease or at least not increase.

In accordance with the new construction standards of the Republic of Belarus, when performing the hydraulic calculation of pipelines of hot water supply systems, it is necessary to take the values of the estimated water consumption based on the actual data of water consumption for at least the two-year preceding period. In the absence of such data on the projected object and similar objects, the hydraulic calculation should be performed according to the method based on the probability of simultaneous operation of devices for supplying water to consumers [1].

To compare the standard and actual water consumption by one consumer per hour of maximum water consumption, field studies were performed on a group of multi-apartment residential buildings in Novopolotsk (the Republic of Belarus), the results of which are presented in Table 1.

Table 1. – Water consumption per hour of maximum water consumption per inhabitant, $q_{hr,u}^h$, l/hour

Object	Number of consumers, persons	Jan.	Feb.	Mar.	Apr.	May	June	Sep.	Oct.	Nov.	Dec.
1	206	9,3	8,9	9,1	10,0	9,4	9,1	10,3	10,1	9,3	9,8
2	113	7,6	5,1	8,2	9,3	9,5	7,3	7,3	8,5	8,0	7,3
3	197	8,6	12,4	8,4	10,6	8,6	10,5	8,9	8,9	9,4	9,0
4	189	9,5	7,6	9,8	9,0	11,0	9,4	10,3	8,6	9,2	9,7

As a result, the average actual value of water consumption by one consumer per hour of maximum water consumption was 9.1 l/hour, while the standard value is 10.0 l/hour [1, 2].

To determine the degree of influence of the amount of water consumption by one consumer per hour of the maximum water consumption, $q_{hr,u}^h$, in the hot water supply system of multi-apartment residential buildings on the diameters of the pipelines of the water supply network, a hydraulic calculation of the pipeline network was performed for three variants of such flow, l/h: 8, 10 and 12. A 100-apartment residential building with 200 water faucets was accepted as the design object. The hydraulic calculation was performed with the help of a technique based on the probability of simultaneous operation of the equipment for supplying water to consumers [2]. When designing the pipeline network, polypropylene pipes were used. The choice of diameters was made based on the speed of water movement through the pipes (up to 1.5 m/s). The calculated diameter values were rounded to the nearest standard values specified in the polypropylene pipes catalogues. For the selected pipe diameters, pressure losses were determined in all sections of the network, and pressure losses were correlated in all directions of water

movement. For the purpose of simplification, only the hydraulic calculation of the hot water pipelines was performed, since the diameters of the other circulation lines practically do not depend on the amount of water consumption by one consumer per hour of maximum water consumption. As a result of the calculations performed, the diameters of the pipelines were determined, which in different sections of the network for all three variants of water consumption by one consumer per hour of maximum water consumption ranged from 25 to 60 mm.

The estimation of material costs was carried out by determining the material characteristic of the pipeline network, which was calculated using the formula:

$$M = \sum_{i=1}^{i=N} d_i \cdot l_i, \text{ m}^2, \quad (1)$$

i – the network section number; N – is the total number of all sections in the network; d_i and l_i – the diameter of the section and the length of the network section, respectively, m.

It is established that the change in the accepted water consumption by one consumer per hour of the maximum water consumption per inhabitant from 8 to 12 liters / hour leads to a monotonous increase in the material characteristic of the network (fig.1).

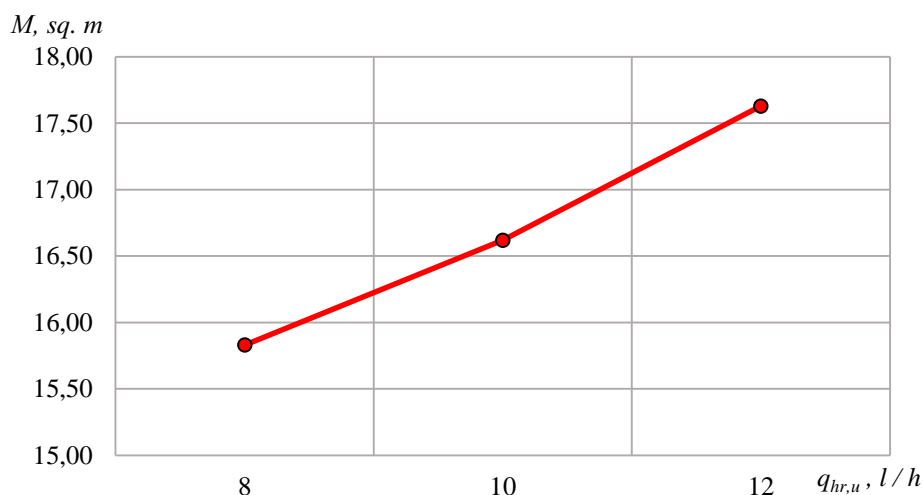


Fig.1. – Dependence of the material characteristic of the network on the water consumption by one consumer per hour of maximum consumption

Conclusions. It is established that the material characteristic of the pipelines of the hot water supply system increases with the increase in the calculated water consumption by one consumer per hour of the maximum water consumption from 8 to 12 liters, which leads to an increase in capital costs during construction. The relative limits of such a change for the considered design example are determined.

REFERENCES

1. СН 4.01.03-2019. Системы внутреннего водоснабжения и канализации зданий. Строительные нормы Республики Беларусь. Мн. : Минстройархитектуры РБ, 2020. – 38с.
2. ТКП 45-4.01-52-2007. Системы внутреннего водоснабжения зданий. Строительные нормы проектирования. Мн. : Минстройархитектуры РБ, 2014. – 50с.

TECHNOLOGY, MACHINE-BUILDING

UDK 665.662.5

PROPERTIES AND THERMO-OXIDATIVE STABILITY OF THE DEWAXED RESIDUAL PRODUCT OF THE VACUUM GAS OIL HYDROCRACKING PROCESS

A. ELISEEVA, S. VALEEVA, A. ERMAK
Polotsk State University, Belarus

The actual problem of oil oxidizability after hydrogenation and cleaning processes is considered. The separation capacity of various adsorbents is analyzed. The group composition of oils and its effect on stability are analyzed. The main theories of oxidizability, mechanisms and causes are also considered. The thermal stability of the dewaxed residual product of vacuum gas oil hydrocracking after purification and with the introduction of an inhibitor was analyzed.

Introduction. The use of hydrogenation processes in the production of base oils makes it possible to obtain high-quality hydrocracking commercial oils with improved technical characteristics compared to traditional mineral oils. Hydrocracking base oils have a high viscosity index, better injectivity to additives, and are more environmentally friendly [1,2].

However, deep cleaning has a very important drawback: oils are characterized by low resistance to auto-oxidation by air oxygen during storage, which leads to a change in their color and chemical composition, increased corrosion activity, and sediment formation [3].

During hydrocracking, raw materials undergo a complex of complex chemical transformations that lead to a significant change in their group composition, including the redistribution of various groups of hydrocarbons into fractions. In this regard, we can expect that the fraction isolated from the hydrocracking residue by vacuum distillation, will vary not only by boiling temperatures, but the content of different groups of hydrocarbons, and therefore, have different physical and chemical properties, which further affect the properties of the produced oils and their operating characteristics [4].

This article discusses the main properties of the dewaxed residual product of the hydrocracking process of vacuum gasoils, the group composition, the distribution patterns of hydrocarbons and their thermal and oxidative stability, and the effect of inhibitors on oxidizability.

Research part. It is known that the stability of different groups of hydrocarbons differs from each other. The main components of petroleum oils are hydrocarbons that simultaneously contain naphthene-paraffin, paraffin-aromatic, or paraffin-nafteno-aromatic structural elements. In addition to hydrocarbons, oils also contain a variety of heteroorganic compounds containing sulfur, oxygen, nitrogen, and various metals. All this makes it very difficult to study the dependence of the operating properties of oils, including stability against oxidation.

According to one of the first studies, it can be said that aromatic hydrocarbons that do not have side chains have the greatest stability to oxidation. As the number of cycles increases, the stability against oxidation decreases. Hydrocarbons containing both aromatic and naphthenic cycles are less stable than aromatic ones.

Naphthenic-aromatic hydrocarbons are actively oxidized with the formation of a number of products, including resins. Naphthenic and paraffinic hydrocarbons of oils are less stable than aromatic ones during a significant oxidation time and form mainly acids and hydroxyacids.

The stability of the mixture of saturated and aromatic hydrocarbons is not additive. It is mainly determined by the amount and especially the structure of the aromatic hydrocarbons contained in them. When 1-10% aromatic hydrocarbons without side chains or with short side chains, as well as hydrocarbons containing phenyl radicals, are introduced into the fraction of saturated hydrocarbons, the oxidation of the mixture is sharply inhibited. Fractions of aromatic hydrocarbons with long side chains are effective only at a concentration of more than 20% by weight. [4].

Thus, aromatic and naphthenic-aromatic hydrocarbons in optimal concentrations are natural oxidation inhibitors. The reason for this action is the formation of phenols, quinolines, quinones and resinous products, which also act as inhibitors.

In this work, the initial dewaxed hydrocracking residue was purified using various adsorbents: granular active clay and ASCG grade silica gel.

The nature and size of the adsorbent pore surface are crucial factors determining the adsorption efficiency. The size of the adsorbed molecules is also important. Coarse-pored and fine-pored adsorbents, all other things being equal, equally adsorb surfactants consisting of small molecules, and in different ways – substances whose molecules have large sizes. If the size of the molecules of the adsorbed substances exceeds the pore size of the adsorbent, the efficiency of the adsorption process decreases. As a rule, coarse-pored adsorbents are used for oil adsorption purification [5].

It was found that granulated active clay has a greater separating ability in relation to the components of the group composition of the hydrocracking oil under study than silica gel of the ASKG brands. This is due to the increased pore size of the active clay and higher acidity, due to which the active clay exhibits an increased polarizing ability.

The main changes in the characteristics after cleaning the initial dewaxed hydrocracking residue with active clay in an inert medium are shown in Table.

Table. – Sample properties

Indicator	Value for the sample		Changing
	before cleaning	after cleaning	
Refractive index n_D^{20}	1,4652	1,4644	-0,0008
Color according to ASTM D1500 (STB 1796)	1,5	less than 0,5	–
– Density at 20°C, kg / m ³	843,3	841,6	-1,7
– Density at 15°C, kg / m ³	846,6	844,9	-1,7
– Solidification temperature, °C	minus 15	minus 15	0
– Iodine number, gI ₂ / 100 g	0,70	0,20	-0,5
– Acid number mg KOH/g	0,65	0,31	0,34
Kinematic viscosity at:			
– 40 °C, mm ² /s	23,52	23,44	-0,08
– 100 °C, mm ² /s	4,71	4,70	-0,01
Viscosity index	120	120	0
Group composition (wt%):			
– naphthenic-paraffinic hydrocarbons	98,3	99,74	1,44
– aromatic hydrocarbons	0,75	0,17	-0,58
– resins	0,95	0,09	-0,86

The hydrocracking residue is characterized by a low total content of aromatic hydrocarbons. The residual product of the hydrocracking process contains mainly aromatic compounds of group I with an interval of refractive index change at 20 °C from 1,49 to 1,53 [6]. In the remainder of the Unicracking process, aromatic hydrocarbons are mainly represented by more stable monocyclic compounds, i.e. benzene derivatives. This pattern can be traced by analyzing the spectra.

Also, it is impossible not to take into account the effect of sulfur compounds on the oxidizability of oils. The oils contain approximately equal amounts of sulfides and residual sulfur compounds. Organic sulfides are more easily oxidized than hydrocarbons, and with a low content in oils, it slows down oxidation.

In addition to the above components, the oxidation of oils is affected by resinous-asphaltene substances. Petroleum resins in concentrations of up to 1% stabilize the oil, with a further increase in the concentration, their effectiveness decreases, and sometimes the oil's oxidizability increases. This phenomenon may be related to the formation of asphaltenes [7].

To study the thermal and oxidative stability of oils, it is necessary to consider the oxidation mechanism directly in more detail. Modern ideas about the mechanism of hydrocarbon oxidation processes are based on the peroxide theory of autooxidation by A. N. Bach and K. Engler and the theory of chain reactions developed by N. N. Semenov and his school.

According to the peroxide theory, the first oxidation products are peroxides and hydroperoxides. According to these propositions, oxygen activation occurs as a result of breaking one bond between atoms in an oxygen molecule, which requires less energy than complete dissociation of the oxygen molecule. The active oxygen molecule easily combines with combustible substances without breaking down into atoms.

The energy of breaking the —O—O bond in peroxides and hydroperoxides is much lower than in the oxygen molecule, so they are very reactive and poorly stable. When heated and exposed to mechanical forces, they easily disintegrate to form new substances or radicals. The radicals formed during the decomposition of peroxides are the active centers of oxidation reactions [8].

In paraffinic and naphthenic hydrocarbons, the tertiary CH group is most easily oxidized. The quaternary carbon group does not oxidize itself and prevents the oxidation of those closest to it C-H groups (even tertiary ones).

However, the peroxide theory of oxidation is not able to explain the existence of the induction period. This was explained by the doctrine of chain reactions.

According to N. N. Semenov, a branched chain process generates active particles in a substance - free radicals, the number of which increases rapidly in time due to branching of the chain.

This oxidation process can be divided into three periods: the first is the induction period. During this period, no visible changes are observed, and compounds that change the characteristics of oils do not accumulate. After the end of the induction period, active interaction with oxygen begins, oxidation is initiated, and the formation of primary oxidation products – hydroperoxides-occurs. Decomposition and oxidation of hydroperoxides leads to the appearance of acidic and neutral oxidation products.

The next stage is the formation of precipitation. Depending on the base of the oil, different products can be formed and in different proportions [7].

The accumulation of R-O-O-H hydroperoxide in the system, which is the main intermediate product of oxidation, causes auto-acceleration of the process, since it decomposes with the formation of free radicals. After the formation of hydroperoxides, products of deep oxidation appear. Numerous experimental data indicate that alcohols, ketones, aldehydes, and carboxylic acids are the final decomposition products of hydroperoxides. In addition, peroxides can enter into condensation reactions with carbonyl compounds to form oxy-alkyl peroxides that break down into acid, aldehyde and hydrogen.

Among other factors that accelerate the process of oil oxidation, the role of the oil contact surface with air or oxygen should be noted. The larger this surface area, the correspondingly more intense the oxidation. The oxidation rate also depends on the rate of oxygen diffusion into the oil. Also surface metals have obvious catalytic actions. Most actively accelerate the oxidation process of chalk, lead and their alloys, manganese, chromium; a little less – iron and tin. Organic salts of copper, iron, manganese, silver, and cobalt cause heavy precipitation during oil oxidation.

The easiest way to increase the oxidation resistance of oils is to add anti-oxidation additives. Let's consider their effectiveness in comparison with samples without an inhibitor.

The research was conducted in accordance with GOST 20354-74. Methods for determining evaporation in cups.

Object of research: dewaxed residual product of the hydrocracking process after adsorption purification.

As can be seen from the results obtained (Fig. 1), the lowest deviation from the initial sample is the depreciation curve with a temperature control time of 30 minutes. A further increase in time leads to intensive oxidation and, as a consequence, a decrease in transmission coefficients. Compared to the original oil sample, the transmittance at lengths of 400 and 450 nm from 59,4/98,2 approached very low values of 0/0,4. The change in these indicators for a sample that was thermostated for 30 minutes is more abrupt than for samples of 60 and 240 minutes. This may be due to the accumulation of oxidation products in the medium, which act as natural inhibitors.

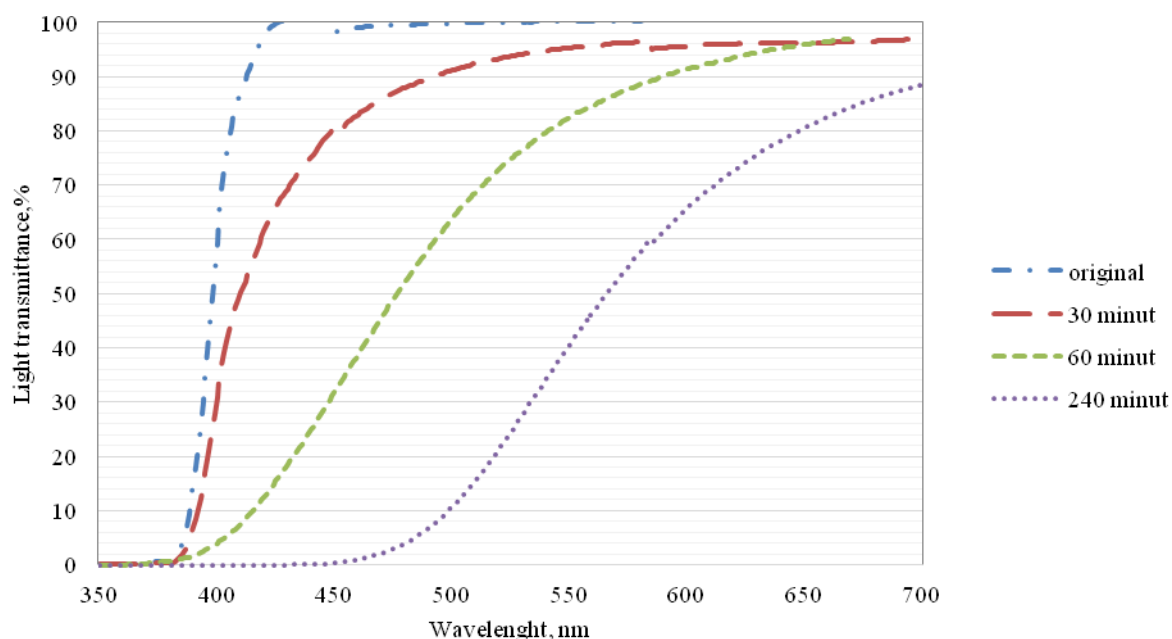


Figure 1. - Dependence of the transmission coefficient on the wavelength and temperature control time of samples

Next, we consider the effect of the duration of heat treatment on the properties of the purified dewaxed residual product of the hydrocracking process of vacuum gas oils in the presence of 0,5% by weight an inhibitor (Fig.2).

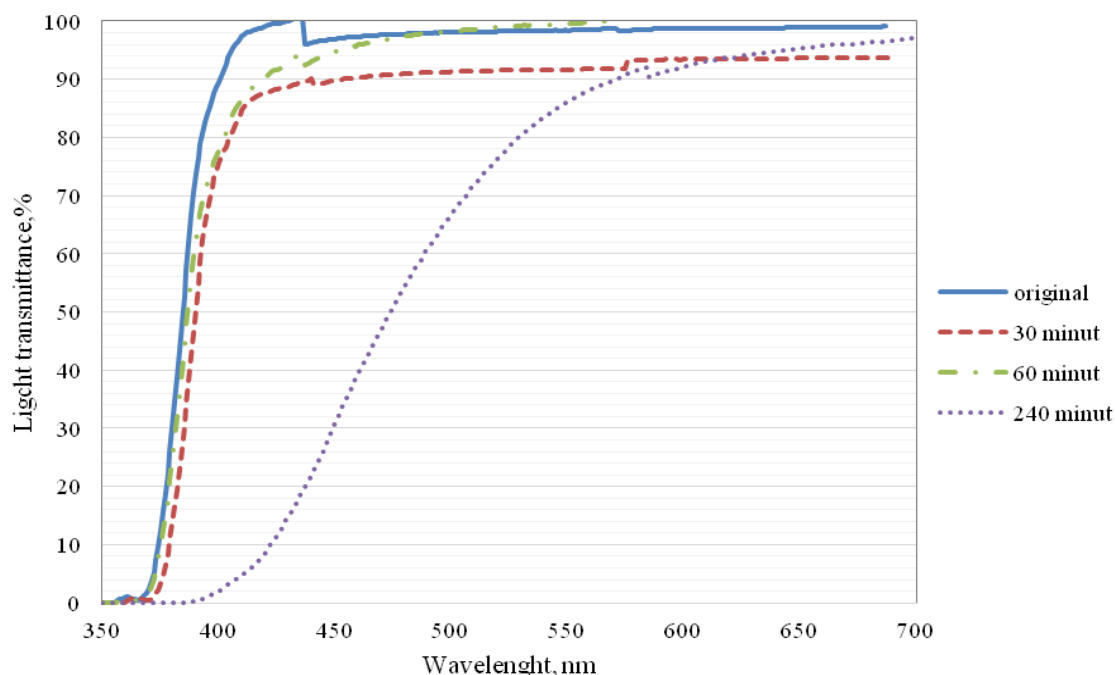


Figure 2. - Dependence of the transmission coefficient on the wavelength and temperature control time of samples

After analyzing the results, we see that the curves of the oil samples, which are thermostated for 30 and 60 minutes, have small deviations from the original sample. If we compare the results of the samples with the inhibitor and without-noticeable improvements in the thermal-oxidative stability in terms of light transmittance and color indicators.

Conclusion. Based on the analysis of the results of the group composition from the hydrocracking residue, it can be concluded that the total content of aromatic hydrocarbons is low. The residual product of the hydrocracking process contains mainly aromatic compounds of group I, represented mainly by benzene derivatives. According to the peroxide theory and the chain reaction theory, oxidation develops due to the formation of peroxide compounds and free reactive radicals. The oxidation process is provoked by such factors as: increased temperature, light radiation, catalyzing metals in the composition of the contacting surfaces. The conditional process It can be divided into three stages: induction period, initiation period and stabilization period. The main task is to increase the first period, increase stability during operation in conditions of suspended rigidity. This can be done by adding oxidation inhibitors. According to the results of studies, the introduction of an anti-oxidative additive improves the stability of samples in comparison with oils without it.

REFERENCES

1. Petro-Canada Lubricants Handbook 2017. Industry-leading products for improved business performance. Petro-Canada Lubricants Inc. Mississauga, Ontario, Canada. 2017. p. 228.
2. Technology and marketing of hydrocracking base oils. / Automotive oils and lubricants. Масла ConocoPhillips Oils [Electronic resource]. - Access mode: <http://masla55.ru/3> - Access date: 26.03.2021.
3. Ermak, A. A., Grishin, P. F. "Oxidative stability of hydrocracking base oils and ways to increase it" / Bulletin of Polotsk State University. Series B. Industry. Applied sciences. -2021.
4. Ermak A. A., Buraya I. V., Pokrovskaya S. V., and others, Properties and perspective directions of processing the residual product of the "Unicracking" process, Vestnik Polotsk State University. Series B. Industry. Applied sciences. -2015. - №11. - p. 115-120.
5. Shashkin, P. I. Regeneration of spent petroleum oils, 2nd ed./ P. I. Shashkin, I. V. Bray, Moscow: Khimiya Publ., 1970, 303 p.
6. Polyakova L. P., Jafarov S. I., Adigezalova V. A., Movsumzade E. M. Chemical composition and properties of oils from different horizons of the Naftalan field. Ufa: Reactiv Publ., 2001, 124 p. (in Russian).
7. Bratkov A. A., Seregin E. Gorenkov A. F. et al. Chemmotology of rocket and jet fuels.- Moscow: A. A. Bratkova. M P.,: Khimiya Publ., 1987, 304 p. (in Russian).
8. Berko A.V. Method of control of motor oils according to the parameters of thermal-oxidative stability and tribotechnical characteristics. Dis. cand. of technical sciences.- Tomsk.: 2015-164 p.

REDUCTION OF LOSSES OF HYDROCARBONS IN THE TANK FARM OF THE FILLING STATION «SOLNECHNOGORSKAYA» PAO «TRANSNEFT» (RUSSIA) (OVERVIEW)

D. FEDORENKOVA, I. BURAYA
Polotsk State University, Belarus

Combating the loss of petroleum products is one of the most important areas of resource conservation, playing a leading role in the development of the economy and ecology. The generalization of literature data on the main types and sources of hydrocarbon losses in the tank farm is presented. Methods for reducing losses of hydrocarbons are considered. The indicators characteristic for various stages of the reservoir operation process are analyzed. The calculation of technological losses during storage of petroleum products is carried out depending on the temperature and pressure conditions of the environment, density, technological conditions of filling and emptying the tanks.

Introduction. Reducing the loss of oil and oil products is one of the important ways in saving fuel and energy resources, which plays a significant role in the development of the organization's economy. An essential task in the operation of tank farms is maintaining the quantity and quality of oil products. For this, it is necessary to ensure maximum sealing of all processes of unloading, filling and storage.

Research part. The filling station "Solnechnogorskaya" was commissioned in 1977, it is a structural subdivision of Joint-Stock Company "Transneft Upper Volga".

The main functions of the Solnechnogorskaya FS are the storage of oil products in tanks, the delivery of petroleum products to consumers by filling them into tank trucks, ensuring the safety of petroleum products, both in terms of quantitative and qualitative indicators.

The tank farm of the Solnechnogorskaya FS includes 5 tanks with a capacity of 5000 m³ for storing motor gasoline and 3 tanks with a capacity of 5000 m³ for storing diesel fuel. All tanks are steel, vertical and cylindrical. The annual capacity of the «Solnechnogorskaya» filling station is 450 m³.

In the process of delivering oil products to the storage site, there are operations of filling and emptying the tanks of the warehouse of the filling station, as well as the stationary storage of oil products, as a result of which large losses from evaporation are allowed. This causes economic damage to the enterprise and significant air pollution occurs. Therefore, reservoirs for storing hydrocarbons are equipped with means to reduce losses.

It is necessary to select a means of reducing losses specifically for each reservoir. To determine the effectiveness of the use of loss reduction means, it is necessary to compare the amount of evaporated oil product from the reservoir without established means of loss reduction with a similar value in the reservoirs on which the loss reduction means are installed.

Based on the literature review, the loss of oil products can be classified according to two approaches, which have some similarities and some differences.

First, we will consider the first group of classification. It includes quantitative, qualitative-quantitative and qualitative losses.

Quantitative losses occur as a result of leaks, overflows, incomplete draining of transport tanks and reservoirs. These losses become possible in the event of leakage of the walls and bottoms of tanks, malfunctioning valves, non-observance of the technology of operations and malfunctioning of instrumentation [1, 2, 3, 4].

Qualitative and quantitative losses occur during the evaporation of oil products. Due to evaporation from petroleum products, light hydrocarbons are lost, which are valuable components. Losses of light fractions reduce the quality of petroleum products. This applies to the greatest extent to gasolines, to a lesser extent to diesel fuels [3].

In gasoline, due to the loss of light fractions, the octane number and the pressure of saturated vapors decrease, the temperature of the initial and final boiling points of various fractions increases, which worsens the starting qualities of gasoline, increases fuel consumption and engine wear.

With losses from "small breaths", part of the liquid oil product, evaporating, turns into a gaseous state, thereby reducing the volume occupied by the oil product, and increasing the volume of the GS reservoir.

Losses at "big breaths" mean that while pumping out the product from the container, the released volume of the GS is filled with atmospheric air. In this case, the partial vapor pressure of the oil product in the GS decreases, and the evaporation of the oil product begins until the GS saturation.

The next time the tank is filled, the air-vapor mixture in the GS is displaced from the tank.

Losses from "big breaths" depend on the frequency of injection and pumping out and are proportional to the volume of oil injected into the reservoir [4].

Next are quality losses. A decrease in the quality of petroleum products as a result of compounding occurs during sequential pumping through one pipeline of petroleum products of different properties, as well as when filling tanks containing residues of petroleum products of a different type. In this case, it is possible to transfer part of the oil product to a lower grade.

For petroleum products that change quality quickly, the minimum storage time is recommended. The recommended storage periods for oil products have been increased in the middle and northern zones, in semi-underground and underground reservoirs, due to lower storage temperatures.

Losses of light fractions from evaporation from tanks are divided as follows [5]: from "big breaths" - 80.2%; from ventilation of GP - 19.05%; from "small breaths" - 0.8%.

The second approach to the classification of oil or oil product losses includes: natural, operational, accidental losses.

Losses from evaporation belong to natural losses, which depend on natural and climatic conditions, the physicochemical properties of the oil product and the design of the technological equipment of tanks of oil depots and warehouses.

These losses at the modern level of technical equipment of facilities intended for the storage of petroleum products are practically not amenable to complete liquidation, however, they can be significantly reduced as a result of the implementation of appropriate technical and organizational measures [6,4].

Operational losses resulting from malfunctions or improper operation of oil storage equipment include losses from spills, leaks, incomplete discharge, pollution and watering of oil products [6,4,7,8].

This type of loss can be completely eliminated provided that the necessary measures are observed:

- technically competent organization of storage of petroleum products;
- timely and high-quality performance of periodic maintenance and preventive maintenance of tanks;
- clear planning and correct implementation of loading and unloading operations.

Methods for reducing the loss of oil products from evaporation can be divided into 5 groups [9, 10, 11]:

Group 1 - reducing the volume of the GS reservoir. From the analysis of the loss equation, it follows that the smaller the GS volume, the lower the losses, and at $V_1 = V_2 = 0$ in the reservoir, theoretically, there should be no evaporation losses.

This condition is implemented in tanks with floating roofs or pontoons, which allow to reduce losses from "large breaths" and "reverse exhalation": by 70-75% with an annual turnover rate of up to 60 times a year; by 80-85% with an annual turnover rate of over 60 times a year, and from "small breaths" - by 70%.

Group 2 - overpressure storage.

According to the loss equation, if the design of the reservoir is designed to operate under excess pressure, then losses from "small breaths" and partly from "large breaths" can be completely eliminated in such a reservoir.

Group 3 - a decrease in the amplitude of the temperature fluctuation of the GS.

To create conditions for isothermal storage of oil products or to significantly reduce fluctuations in the temperature of the gas space and the surface of the oil product, thermal insulation of tanks is used, they are cooled in summer with water and painted white, as well as underground storage.

Group 4 - capturing vapors of petroleum products displaced from the tank.

For this, gas equalizing piping is used, which are separate pipelines or a system of pipelines connecting the gas spaces of tanks or transport tanks. The use of a gas equalizing piping allows to reduce losses from "big breaths".

Group 5 - organizational and technical measures.

Correct organization of the operation of tanks is one of the most important means of reducing the loss of oil products.

The main reason for technological losses of valuable raw materials and harmful emissions into the environment during storage in tanks is the volatility of light hydrocarbon fractions. When storing liquids in tanks, emissions of vapors and gases into the atmosphere occur periodically at certain intervals associated with the injection and pumping of liquid and daily fluctuations in the ambient temperature. When the tanks are connected to the atmosphere, emissions occur when the vapor-air mixture is displaced from the gas space through the ventilation pipes or breathing valves. The level of air pollution is an important indicator of the negative impact on the environment.

Prevention of such situations involves: legal, organizational, economic, engineering and technical, environmental protection, sanitary and epidemiological and social measures that ensure observation and control of the state of the environment and potentially dangerous objects, forecasting and prevention of sources of emergency situations, preparation for these situations [13].

Most of the methods for assessing and analyzing properties and quality are standardized and for their intended purpose. They are subdivided into acceptance, control, full, arbitration and special.

Technology, Machine-building

Losses of oil products from "big breaths" over a long (week, month, quarter, season of the year) period of time are usually defined as:

$$G_{бД} = \left[V_{\text{H}} - V_{\text{r}} \cdot \left(\frac{P_2 - P_1}{P_2 - P_{Y_{\text{зак}}}} \right) \right] \cdot \frac{P_{Y_{\text{зак}}}}{P_2} \cdot \rho_Y$$

Where:

V_{H} -volume of the injected oil product;

V_{r} -volume of the gas space of the reservoir before injection;

P_2 - absolute pressure of the overpressure valves;

P_1 -the absolute pressure of the vacuum valves;

$P_{Y_{\text{зак}}}$ -average partial vapor pressure of petroleum product;

ρ_Y -the density of the oil product.

In accordance with the guidelines for determining the technological losses of hydrocarbons from "small breaths", the calculation is made according to the formula:

$$G_{\text{МД}} = \sigma \cdot V_{\text{n}} \cdot \ln \left[\frac{(P_{\text{A}} - P_{\text{KB}} - P_{\text{min}}) \cdot T_{\text{r,max}}}{(P_{\text{A}} + P_{\text{KD}} - P_{\text{max}}) \cdot T_{\text{r,min}}} \right]$$

Where:

σ -- the average mass content of vapors of petroleum products in the steam-air mixture;

V_{n} - volume of the vapor phase;

P_{A} --barometric pressure;

P_{KB} - absolute pressure of the vacuum valves;

P_{KD} - absolute pressure of the breathing valves;

$P_{\text{min}}, P_{\text{max}}$ - minimum and maximum partial pressure;

$T_{\text{r,max}}, T_{\text{r,min}}$ - the maximum and minimum temperature of the GS.

Based on the necessary data, the following indicators were determined:

- fractional composition according to GOST 2177-99 (method A)
- density at 20 °C according to MVI 2302-13M-2007
- saturated vapor pressure according to GOST EN 13016-1-2013 with the addition of p. 8.4 GOST 32513-2013.

And it was also determined the type of tank; injection performance; maximum and minimum filling height; downtime; average air temperature; vacuum valve data; pressure valve data; atmosphere pressure.

Having performed tests and calculations according to these formulas, the total losses of hydrocarbons in motor gasoline and diesel fuel in the tank farm of the filling station "Solnechnogorskaya" are equal to 55 thousand m³ / year.

Reducing the loss of hydrocarbons during the evaporation of motor gasoline can be achieved by introducing gas equalization systems (GES) into the tank farm scheme. GES is called a gas piping, to which a gas collector is connected, where the vapor-air mixture is displaced when the reservoir is filled, and from where it is re-supplied to the GS of the reservoir when it is emptied.

To reduce the loss of hydrocarbons during the evaporation of diesel fuel, pontoons are installed. A pontoon is a rigid floating roof that is placed in a tank with a fixed roof in order to reduce the rate of saturation of the tank's GS with vapors. Tanks with a fixed roof, supplemented by a pontoon, significantly reduce evaporation losses of light fractions.

Conclusion. This paper addresses the issues causing the losses of petroleum products, as well as measures to reduce the loss of petroleum products.

Basically, the loss of petroleum products occurs due to the unsatisfactory technical condition of storage, transportation, pumping facilities, non-observance of the rules for their operation. The problems associated with losses, to varying degrees, affect all links in the functioning of the oil product supply system and are important indicators of the technical improvement of all operations.

REFERENCES

1. Бунчук В.А. Транспорт и хранение нефти, нефтепродуктов и газа. - М.: Недра, 1977.
2. Абузова Ф. Ф., И. С. Бронштейн и др. Борьба с потерями нефти и нефтепродуктов при их транспортировке и хранении //М.: недра. – 1981. – Т. 260.
3. В.И. Черников. Сооружение и эксплуатация нефтебаз. Издание второе, переработанное и дополненное. – Государственное научнотехническое издательство нефтяной и горно-топливной литературы, М.: 1955г.
4. П.И. Тугунов, В.Ф. Новосёлов, А.А. Коршак, А.М. Шаммазов. Типовые расчеты при проектировании и эксплуатации нефтебаз и нефтепроводов. Учебное пособие для ВУЗов. – Уфа: ООО «ДизайнПолиграфСервис», 2002.

5. Лоповок С.С. Моделирование процесса заполнения резервуара нефтепродуктами. Тезисы докладов 68-й международной молодежной научной конференции «Нефть и газ – 2014», секция «Проектирование, сооружение и эксплуатация систем трубопроводного транспорта», 14–16 апреля, 2014 г.
6. Коршак С.А. Совершенствование методов расчета потерь бензинов от испарения из резервуаров типов РВС и РВСП. Диссертация к.т.н. 25.00.19. – М.: РГБ, 2003.
7. А. А. Коршак, Г. Е. Коробков, Е. М. Муфтахов. Нефтебазы и АЗС: Учебное пособие –Уфа: ООО «Дизайн-ПолиграфСервис», 2006.
8. Н.Н. Константинов. Борьба с потерями от испарения нефти и нефтепродуктов. – Государственное научно-техническое издательство нефтяной и горно-топливной литературы. М.: 1961.
9. Бабичев Д.А. Оценка напряженно-деформированного состояния конструктивных элементов сооружений переменного объема для хранения нефти и нефтепродуктов: Диссертация к.т.н. 02.13 Тюмень, 2008.
10. Министерство энергетики Российской Федерации. Приказ от 13 августа 2009г. №365 об утверждении норм естественной убыли нефти при хранении.
11. РД 153-39.4-078-01 Правила технической эксплуатации резервуаров магистральных нефтепроводов и нефтебаз.
12. Официальный сайт НПО «Санеф» [Электронный ресурс]. – Режим доступа: <http://nposanef.ru/catalog/patrubki> (дата обращения 05.12.2020).
13. ГОСТ Р 22.3.03-94 Безопасность в ЧС. Защита населения. Основные положения.

RESEARCH ON CHEMICAL PRESERVATION OF TIMBER OF HISTORICAL MONUMENTS
FROM EXTERNAL INFLUENCES

F. TALIBLI, M. NASIROV

Western Caspian University, Baku, Azerbaijan

The tree is sensitive to the effects of abiotic factors (non-biological origin), such as fire, sunlight, water, oxygen and others, as well as damage to biological pests, bacteria, fungi, insects, birds, etc. The longevity of less resistant wood species is increased by the use of chemical protection such as fungicides and insecticides. Often, flame retardants and other preservatives are also used to improve the quality of wood.

Introduction. On the one hand, it is the right choice of wood in favor of more durable wood species. However, you cannot underestimate the structural protection of wood, which is the creation of ideal conditions to suppress the influence of abiotic and biotic pests. Chemical protection of wood is also irreplaceable, and it is treated with substances with a biocidal, hydrophobic or fire-resistant effect. Modern technologies also provide wood protection modification, which performs thermal and enzymatic treatment of substances directly in wood cells in order to increase resistance to biological pests and increase hydrophobization. Some defenses are also biocontrolled when microscopic fungi or bacteria are planted on the wood, which prevents the subsequent attack of dangerous wood-destroying organisms.

The authors consider it expedient to abandon the classification of chemical means of protection, which is usually set forth in educational and reference literature on wood protection. It seems more logical to characterize simple inorganic and organic compounds that are part of multicomponent drugs used in industry and then give the formulation of these drugs. This approach enables a researcher to develop new drugs based on the provisions of GOST 30495-2006. Chemical means and methods of wood protection should be used when all constructional and structural possibilities of wood protection have been exhausted or are constructively impossible. Chemical protection of wood is achieved by coating or impregnating wood with chemical protection agents.

The use of wood preservatives always means the use of biocides, since when chemical protection is applied, organisms that attack and destroy wood are destroyed or scared away. Microorganisms are also used as such substances, including viruses and fungi of the corresponding action and purpose.

Wood preservatives are preparations that mainly consist of active substances (biocides), binders (for fixing), emulsifiers, pigments, solvents and other auxiliary substances. Chromium compounds in wood preservatives serve primarily to fix the active ingredients on the wood, thereby effectively reducing washout. There are many chemical treatments to protect wood. A distinction is made between deep processing - pressure impregnation and immersion (inclusion method) - and surface processing methods. When impregnated under pressure, full penetration of chemical protection agents into the sapwood of the wood is achieved (complete protection). With the immersion method (long-term immersion), the tree species must be completely submerged for a long period of time (from 24 hours to several days). The penetration depth must be greater than 10 mm, otherwise it is only edge protection. Depending on the type of wood, this method achieves a penetration depth of several microns to several millimeters. Most heartwoods are difficult to penetrate due to their anatomy. However, it is important that low-hardy sapwood is usually deeply permeable and thus protected.

Wood used in direct contact with the ground, such as a palisade (hedge), is a good illustration that early fungal attack can only be prevented by using naturally resistant tree species or by preventive chemical protection. This can be done in the usual way by pressure impregnation in a boiler. As a protection against blue stains in pine sapwood, the penetration depth must be greater than 1.5 mm (control according to EN 152). Therefore, when applying protective agents with a brush, it is impossible to achieve complete protection against fungi that attack wood. If the wood inside is always wet with a moisture content above 30%, then, despite the chemical protection of the wood (when protecting the surface) and the coating, the risk of rotting inside remains, especially with large cross-sections of wood. Most often, wood-destroying fungi become partially active only when the moisture content is significantly higher than the saturation state of the fibers⁵. Color-changing fungi (causing blue discoloration) do not attack resistant tree species such as pine sapwood with a moisture content above 18–20%.

The most important feature of chemical fire protection is that it reduces the thermal stability of the material in the area the temperature preceding combustion, and does not lead to its increase, as with fire protection based on physical phenomena. However, this decrease and change in the direction of wood decomposition inside of the formation of non-combustible products of thermal destruction turn out to be most beneficial for suppressing the subsequent burning.

The simplest method of fire retardant wood processing is impregnation with fire retardants, which can be surface and deep. According to the data, for translation wood into a flame-resistant material must be achieved wood absorption of fire retardant in terms of dry matter in the amount of 30-45 kg / m³, and for low-combustible material – 60–85 kg / m³, which achieved by deep flame retardant impregnation.

Surface fire-retardant impregnation of wood provides two types of treatment, namely: multiple application of flame retardant products to the surface without drying between intervals and with drying. In this case, the quality of impregnation is characterized by retention of a protective agent or is regulated by the cost impregnating agent.

Fire retardant impregnation of wood, carried out according to the method heating-cold bath or soaking a hot wood in a cold fire retardant solution, provides for penetration fire retardant to a depth of at least 3 mm for heavy impregnated areas and at least 5 mm - for easily impregnated areas. On the practice, three options are used for impregnating wood by the method applying protective agents to the surface. Impregnation can carried out by immersing the tree in an impregnating solution, applying the solution to the wood surface with a brush, and spraying with a spray gun. All three options simple, do not require special equipment or equipment for carrying out fire retardant works. However, with this method of impregnation the depth of penetration of fire retardants into the wood does not exceed 3 mm for lightly impregnated areas and 1 mm for heavily impregnated areas.

Results and Discussion. In these cases, an anti-blue remedy is rational, often combined with an anti-mold agent. In this case, we are not talking about the preventive chemical protection of wood in the meaning of DIN 68800-3. Moisture (dampness) protectors will also not be effective against insects. However, smooth and crack-free surfaces can interfere with egg-laying and thus insect reproduction and structural deterioration.

REFERENCES

1. Будкевич Е.В. Древесина сосновых. Анатомическое строение и ключи для определения родов и видов / АН СССР; Ботан. ин-т им. В.Л. Комарова; отв. ред. А.А. Яценко-Хмелевский. – М. – Л.: Изд-во АН СССР, 1961. – 152 с.
2. Григорьев М.А. Справочник молодого столяра и плотника: Учебн. пособие для профтехучилищ. – 2-е изд. – М.: Лесн. пром-сть, 1984. – 239 с.
3. Григорьев, М.А. Материаловедение для столяров, плотников и паркетчиков: Учебн. пособие для ПТУ. — М.: Высш. шк, 1989. – 223 с.
4. Яценко-Хмелевский, А.А., Никонорова, Е.В. Строение древесины основных лесообразующих пород второго яруса: Учебн. пособие для студентов специальности 1512 / Ленингр. ордена Ленина лесотехническая академия им. С.М. Кирова; Отв. ред. К. И. Кобак. – Л.: ЛТА, 1982. – 67 с.
5. А.А. Чернуха, А.А. Киреев, А.Я. Шаршанов. Огнезащита древесины с помощью гелеобразующих составов на основе силикатов. – Харьков, 2015.

WOOD FIRE PROTECTION MECHANISMS

F. QASIMLI, M. NASIROV

Western Caspian University, Baku, Azerbaijan

Wood is one of the oldest building materials which is widely used today. Together with a large number of positive properties of wood as a construction material, it also has negative properties. One of these properties is flammability. According to existing regulatory documents wood intended for use in construction, must be subjected to fire retardant processing.

Even Lavoisier (late 18th century) and Gay-Lussac (early 19th century) believed that substances possess flame retardant properties, which, under the influence of heating, melt and emit non-combustible gases. Scientists before the 40s of the current century held the same views. But with the improvement of research methods, it was found out that some substances that do not have the ability to release when burning, non-combustible gases can have a fire-retardant effect. Some value in reducing the flammability of protected wood began to be given the possibility of reducing temperature of the burning material due to the release of crystallization water or increasing the amount of slowly burning coal when the fire retardant interacts with the components of wood or the initial products of their decomposition.

Naturally, the explanation of the fire-retardant effect of various substances due to any one of their properties is unacceptable. Even when using fire retardants of the same type per combustion process can be influenced by a significant number of factors. In addition, the effect of two or more factors may be more than the sum of their effects due to the phenomenon of synergy.

To prevent wood fires, it is necessary to create conditions excluding excess of the temperature of heating wood above the ignition temperature. This temperature range is in the range of 200–250° C. Funds must show fire retardant effect inhibiting the development of combustion processes to the ignition temperature of wood.

Fire protection mechanisms include:

- thermal insulation of the protected surface from impact ignition source;
- heat absorption due to the heat capacity of the fire-retardant coating and flow endothermic processes in the coating;
- inhibition of the combustion process due to the death of active centers of the flame and inhibition of the chain chemical reaction of combustion;
- acceleration of the processes of decomposition of carbohydrates with the formation of non-combustible gas products of thermal destruction of water and coke oven residue, which in turn has thermal insulation properties;
- dilution with non-combustible wood decomposition products or covering flammable substances in the combustion area.

Due to the above influence of the chemical structure substances on their flammability, it can be concluded that for organic of film-forming substances, the flammability increases in the following order:

- 1) compounds that contain halogens, acid residues of phosphoric, sulfuric and sulfurous acids (per-chloro-vinyl resins, organo-phosphorus bromine polymers, sulfite alkali, etc.);
- 2) compounds that most completely passed into three-dimensional polymer. Among them, the most resistant are urea resins, resins, etc.;
- 3) connections that have partially switched to three-dimensional polymer retaining unused functional groups (films of vegetable wood oils that dry out);
- 4) high molecular weight chain compounds that have fusibility (ethyl cellulose, benzyl cellulose, etc.);
- 5) low molecular weight compounds such as bitumen;
- 6) high molecular weight chain compounds, which have kept a large number of unused and combustion-friendly functional groups (rubber, nitrocellulose, etc.). According to the above principle, the most suitable for fire retardant coating are organic film formers of the first and second group.

Studying the behavior of pine wood, treated with inorganic salts, Eikner found that the concentration of salts at which wood is least resistant to heating is 10-20%. Calculated from data statistical thermo-gravimetric analysis of the magnitude of the apparent activation energies of the wood decomposition process (with different additives) are as follows (Table 1.)

Table 1. – Values of the apparent activation energy (E) of the decomposition process wood (with various additives)

Variety salts	Content salt in sample, %	E, kJ / mol
Untreated salt	-	149,8
NH ₄ Cl	17,7	145,7
NaCl	12,0	138,1
(NH ₄) ₂ SO ₄	15,7	142,3
NH ₄ H ₂ PO ₄	45,1	138,5
(NH ₄) ₂ HPO ₄	10,8	133,5
Na ₃ PO ₄ ·12H ₂ O	18,0	122,6
Na ₂ B ₄ O ₇ ·10H ₂ O	17,4	103,4
K ₂ CO ₃	20,0	106,3

Results and Discussion. It is known that the rate of thermal destruction of wood decreases with the addition of fire retardants and depends on their quality. It has been proven that it is possible to more than double the yield of carbonaceous residue by treating pine with phosphates and borates, and the release of volatile products will change, which means that the heat of combustion of volatile combustible products and the amount of heat delivered to the surface wood. As a result, more powerful heat flux, and the coal layer, as it accumulates, will protect the inner layers of wood.

REFERENCES

1. С.Н. Горшин Консервирование древесины, Издательство «Лесная промышленность», Москва -1977.
2. А.А. Чернуха, А.А. Киреев, А.Я. Шаршанов Огнезащита древесины с помощью геле-образующих составов на основе силикатов Харьков – 2015.

APPLICATION OF THE METHOD ELECTRO-SPARK DEPOSITION WITH ADDITIONAL ULTRASONIC IMPACT
TO EXTEND THE LIFE OF THE METALWORKING TOOL

A. KASHCHONAK, N. CHIGRINOVA

Belarusian National Technical University, Minsk, Belarus

The article substantiates the possibility of using the method electro-spark deposition with additional ultrasonic impact to extend the life of the metalworking tool. Practical testing of this technology has been carried out. As a result, it was found that the number of articles manufactured using hardened tool and die tooling before their first regrinding increased 1.5-2.1 times.

Introduction. The operational wear of metalworking tools is a serious problem that can entail significant time and financial losses. Tool wear can be reduced by applying protective coatings. One of the most popular methods for creating wear-resistant coatings is the technology of electro-spark deposition (ESD) [1]. This is due to a number of its advantages: high adhesion of substrate and coating materials, the ability to carry out spot treatment of the surface, low thermal effect on the substrate, no strict requirements for surface preparation, high equipment reliability [1]. The undoubted advantage of electro-spark deposition is its suitability both for processing new and for restoring worn surfaces, which is very important for extending the service life of metalworking tools.

The disadvantage of this method is the impossibility of obtaining coatings of equal thickness and the high tension of their structure [2, 3]. Studies carried out by a number of authors [4] have shown that during electro-spark deposition there is also a problem of high roughness of the processed surface, which reduces the efficiency and quality of the tool with such a coating.

The elimination of these disadvantages is achieved through the use of an integral technology of electro-spark deposition with additional ultrasonic impact at various stages of coating creation: ESD with USI [5, 6]. The implementation of strengthening procedures is possible in two versions: according to the scheme ESD + USI and USI + ESD + USI. The choice of the processing scheme depends on the state of the worn out blade of the tool and the operating conditions of the product being processed with the hardened tool.

Methods of research. The principle of hardening the working edges of the tools by the proposed method is as follows. When a wear-resistant coating is formed according to the USI + ESD + USI option, at the initial stage, in the process of additional exposure to the surface with an alloying anode vibrating at an ultrasonic frequency, the processed material is activated, accompanied by an increase in its internal energy [5,6]. This causes the acceleration of physicochemical interactions, mass transfer processes in the anode - cathode system. During their vibro-shock high-frequency contact, a thin near-surface layer of plastically deformed metal is formed on the part cathode. The increased diffusion rate of atoms of alloying elements in the layer intensifies the process of saturation of the surface layer with them and leads, as a result of anodic-cathodic interactions, to a change in the structural-phase state of the coating being formed. Due to the reduced resistance of a metal to plastic flow under the ultrasonic impact [6, 7] and numerous vibration shock process for surface coating formation ESD method is more stable, with a stable and an active mass transfer, whereby the resulting coating has a higher thickness and a uniformity of thickness of the coating. In addition, under the influence of ultrasound, there is a redistribution, stabilization and relaxation of residual stresses over the section of the part [8]. As a result, the possibilities of controlling both the elemental composition of the hardened surface and the level and distribution of residual stresses over its cross section are expanded [9, 10].

The assessment of the thickness of the created coatings was carried out using a multifunctional device for measuring geometric parameters "Constant K-5" (TC 74.06.400.000.00). Measurements were carried out in accordance with the instructions attached to the device. The uniformity of thickness was determined by applying a grid on their surface with a uniform step, followed by precision measurement at the grid nodes of the coating thickness. After mathematical processing of the data obtained, curves were plotted that determine the change in thickness over the coating surface.

Research results. The protective coating on the surface of the cutting tool should, first of all, ensure its high performance under intense abrasive-mechanical effects.

Therefore, the processing of steel surfaces was carried out using hard-alloy electrodes of the VK (tungsten alloys), TK (tungsten-titanium alloys) groups and, for comparison, other compositions specially made for experiments, also capable of increasing the wear resistance of the treated surface.

Figure 1 shows the nature of the change in the thickness of the coatings formed by the T5K10 electrode over the entire surface of the samples according to three schemes: standard ESD - curve 1, scheme ESD + USI - curve 3 and scheme USI + ESD + USI - curve 2.

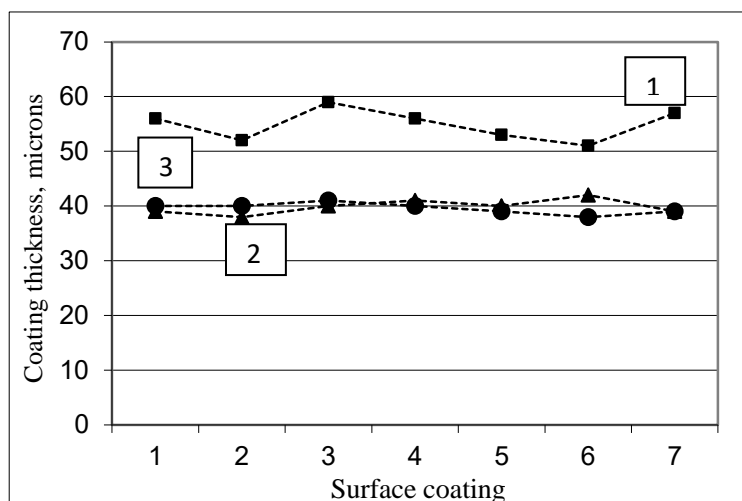


Fig. 1. – Change in the thickness uniformity of the hard-alloy coating depending on the processing scheme

The graph shows that the use of integral technology allows one to obtain a higher uniformity of thickness of the coatings created, which is very important for ensuring the required quality of the cutting edges of the tool. A similar picture of the change in the uniform thickness of the coating over the entire treatment area was also recorded when the surface was alloyed with other electrodes selected for research.

Then, according to the Knopp method, the microhardness of the obtained surfaces was measured, which is an indirect indicator of wear resistance (Figure 2).

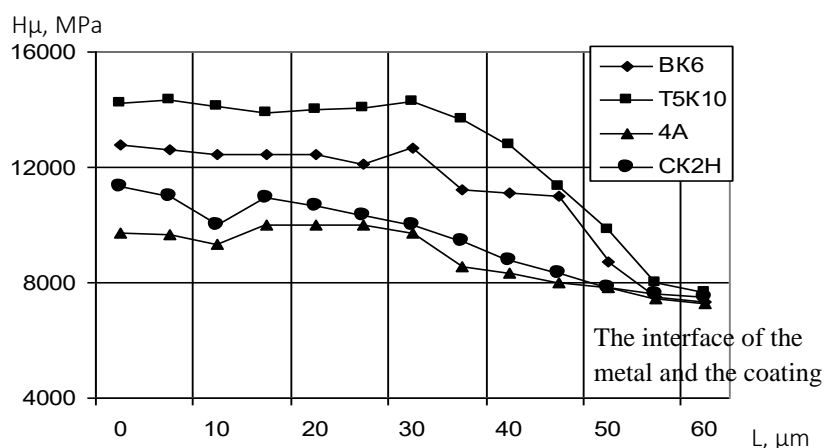


Fig. 2. – Distribution of microhardness over the cross section of the coating on R6M5 steel after its three-stage hardening with different electrode anodes

In the course of measurements, it was found that the most uniform change in microhardness along the depth of the hardened zone was recorded in the coating after three-stage hardening of the steel base with hard-alloy electrodes, in particular, with an alloying anode of T5K10 composition. It can be seen from this figure that the highest values of microhardness H_μ were observed when alloying the steel base with the T5K10 electrode. This is explained by more thermostats resistance of titanium carbide as compared to tungsten carbides and less intense carbon burn up for transfer carbides to the surface of the metal substrate.

In addition, it can be seen from Figure 2 that the composition of the electrode material also affects the depth of the hardened zone. The widest substantially commensurate with the thickness of the coating, hardened zone is formed by doping a steel cathode hard alloys by 25 - 30% less wide - in processing created by the electrode system, which, as noted above, were used for comparative tests order to optimize the formulations of reinforcing electrodes.

The roughness of the coatings was measured on a profilometer 296 in accordance with GOST 19300-86 at 5 - 8 points of the surface with control according to the criterion of the arithmetic mean deviation of the profile R_a , which is the average value of the distances of the points of the measured profile to its center line (Figure 3).

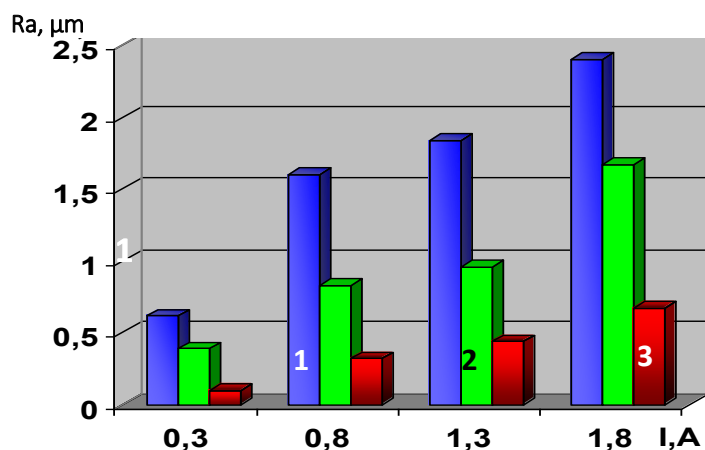


Fig. 3. – Change in surface roughness of coatings formed by methods:
ESD (1), ESD + USI (2), USI + ESD + USI (3)

Thus, the advantages of the integral method for obtaining coatings of the required quality are obvious. At the same time, it was found that the optimal variant of this technology for creating uniform-thickness coatings with a stable structure and low roughness of coatings is surface treatment according to the USI + ESD + USI scheme.

The possibility of creating high-quality wear-resistant coatings by the electro-spark deposition method with additional ultrasonic impact was tested on metal-cutting tools: cutters, cutters, drills, broaches, etc.; as well as the snap die: blanking, bending, and other dies (Figure 4).

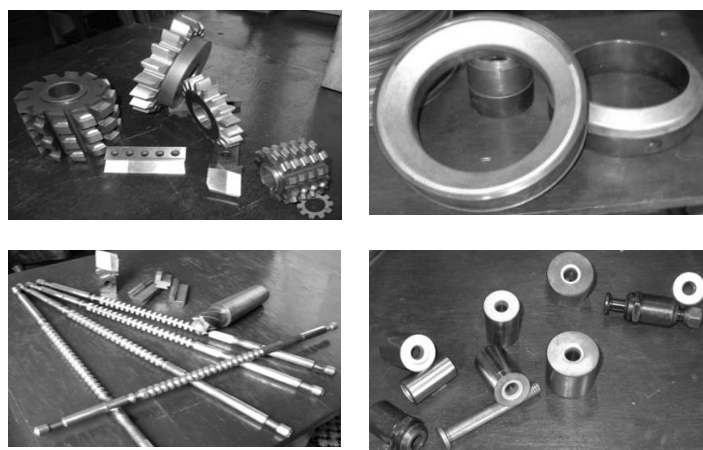


Fig. 4. – The restoration and strengthening of the integral method of electro-spark deposition with additional ultrasonic impact metal working tools and die tooling

By visual evaluation and control instrument hardened after its operation has been found the coating adhesion to the metal substrate and was maintained during the treatment and after its completion. Sticking of the product material to the coating surface was absent in all cases.

Production tests showed that the use of a hardened tool in comparison with a typical tool before the first regrinding allowed processing a larger number of parts (Table 1).

Table 1. - The number of products made with hardened and serial tools

The name of detail	Wear resistance		
	Number of parts made using standard tools, pcs.	Number of parts made using hardened tools, pcs.	Working resource increase (3 column):(2 column)
Scraper	113	200	1,77
Shell	62	116	1,87
Ring	2211	3952	1,78
Shaft	17	36	2,1
Plate	29	45	1,55

Conclusion. The hardening of the cutting surfaces of the listed tools by the ESD method with USI made it possible not only to extend the service life of the named parts, but also to return to the re-use of the product intended for disposal. As a result of the studies, it was found that the durability period of metalworking tools with a hardened coating exceeds the durability of serial ones by 1.5 times or more. It is shown that the number of articles manufactured using hardened tools and die tooling before their first regrinding increased 1.5-2.1 times. The data obtained confirm the reliability and stability of the processing of the working zones of the metalworking tool by the electro-spark deposition method with additional ultrasonic impact.

REFERENCES

1. Верхотуров, А.Д. Технология электроискрового легирования / А.Д. Верхотуров, И.М. Муха. – Киев: Техника, 2002. – 182 с.
2. Золотых, Б.Н. О некоторых закономерностях электрической эрозии металлов: автореф. дис. ...канд. техн. наук / Б.Н. Золотых. – М., 1947.
3. Лазаренко, Н.И. О механизме образования покрытий при электро-искровом легировании металлических поверхностей / Н.И. Лазаренко // Электронная обработка материалов. – 1965. – № 1. – 49–53 с.
4. Верхотуров, А.Д. Формирование поверхностного слоя металлов при электроискровом легировании / А.Д. Верхотуров. – Владивосток: Дальнаука, 1995. – 323 с.
5. Чигринова, Н.М. Технология электроискрового легирования с ультразвуковым модифицированием – эффективный способ продления ресурса рабочего времени инструмента / Н.М. Чигринова, В.Е. Чигринов // Инструмент. – С.-Петербург, 1998. – №5. – 28–32 с.
6. Способ восстановления и упрочнения штамповой оснастки и режущего инструмента: пат. ВУ 6787 / Н.М. Чигринова, В.Е. Чигринов. – Опубл. 30.03.2005.
7. Мазанко, В.Ф. Диффузионные процессы в металлах под действием магнитных полей и импульсных деформаций: в 2 т. / В.Ф. Мазанко [и др.]. – М.: Машиностроение, 2005. – 1 Т. – 339 с.
8. Белоцкий, А.В. Ультразвуковое упрочнение металлов / А.В. Белоцкий [и др.]. – Киев: Техника, 1989. – 3365 – 3371 с.
9. Чигринова, Н.М. Технология электроискрового легирования с ультразвуковым модифицированием – эффективный способ ремонта и восстановления размеров и геометрических параметров высокоточных изделий / Н.М. Чигринова, В.Е. Чигринов // Новые материалы и технологии: материалы Междунар. конгресса, Минск, май 1997 г. – Минск, 1997. – 13–17с.
10. Chigrinova, N.M. Electrospark alloying of electroconductiviting surfaces / N.M. Chigrinova, V.E. Chigrinov, E.V. Zvonarev // Materials of the International Conference of Thin Covers, San Diego, USA, April 1996. – San Diego, 1996. – 1243–1249p.

RESEARCH OF MOULD CONTAMINATION ON WOODEN SURFACES OF HISTORICAL MONUMENTS WITH MODERN DEVICES

M. NASIROV

Western Caspian University, Baku, Azerbaijan

Moisture conditions. The difference between fragments taken from contaminated surfaces can be partially caused by the differences in the material moisture conditions. As was shown in the experiments comparing fungal growth on agar and ceiling tiles, the moisture from agar can penetrate the thick layer of fungi and thus can increase the adhesion forces and reduce the release of fungal propagules. It should also be noted that the adhesion forces are higher for fungal fragments than for fungal spores due to the smaller size of the fragments.

Introduction. One of the important problems facing the architects was the problem of earthquake resistance of the structures being built. Azerbaijani masters paid serious attention to the issues of seismic resistance, the resolution of which often led to a change in the conceived architectural and planning composition.

The builders, knowing the destructive effect of the earthquake, first of all paid attention to the choice of building materials corresponding to the spatial-compositional system, the total weight of the structure, and its distribution in different parts of the building. Elastic building materials and structures are one of the most effective anti-seismic factors.

As anti-seismic measures, along with an increase in the thickness of the wall, wooden anti-seismic belts made of archan (*Juniperus L. juniper*) were inserted into every 4-5 rows of masonry.

The state of the palace, taking into account the strong seismicity of the area, testifies to the wise constructive correspondence between the mass of brickwork and the wooden frame of the building, found by the folk craftsmen-builders [1].

The quality of protective measures should be systematically controlled. Quality assessment is carried out taking into account:

- completeness and thoroughness of cleaning of structures from fungi, beetles and debris, as well as disinfection of opened parts of structures;
- the quality of chemical processing of wood (depth of antiseptic penetration into wood, lack of passes, processing of ends and cuts), the name and consumption of antiseptics;
- disposal quality of the used materials;
- moisture content of structures;
- the quality of the backfill of the floors.

Weatherproof coatings are used to protect outdoor wooden elements of buildings and structures, as well as to protect wooden structures used in conditions of high air humidity (above 61%). These coatings are good to resist the action of moisture, sunlight, sharp temperature fluctuations, weathering, etc. Various organochlorine compounds are introduced into them as binders; phosphoric acid esters and halogenated mineral oils - as plasticizers. Minerals with low thermal conductivity (asbestos, vermiculite) or salts (carbonates, borates), have the properties of fire retardants. [2].

The transition towards a digital society pushes the wood industry to apply smart and robust methods for material properties evaluation.

Ten Side-boards (the flat-sawn sapwood part of the log) of Scots pine were single stacked on stickers and naturally dried indoors at 20°C during 30 days to average moisture content (MC) of 4.6%. Another ten side-boards were dried in a small-scale laboratory air-circulation kiln. The boards were then double-stacked with the bark-side surfaces (the surface of the boards oriented to the bark-side of the tree) in each pair oriented outwards in order to get a high flow of moisture from the inner part of the boards towards the bark-side surfaces. In this way, extractives could migrate with the water transport during drying and accumulate on the wood surfaces. The total drying time was 44 hours of which 1.7 hours was a heating regime, and the cycle ended with a 5-hour cooling regime giving a final moisture content of 14%. No conditioning regime was applied in order to prevent the influence of re-distribution of extractives after drying.

A microNIR OnSite Spectrometer (VIAVI Solutions Inc., San Jose, CA, USA) with NIR wavelengths from 908 to 1676 nm with step 6 nm was used (Figure 1) was used for samples evaluation. The assessment classes were: *No mold/Mold, Drying type, Plaining depth, and NIR wavelengths* [3].



Figure 1. – MicroNIR portable spectrometer

Results and Discussion. The exploratory PCA model was initially built using the data obtained from air and kiln-dried samples containing no mould, and the same samples after mould test for discovering the grouping pattern. The drying type and planing depth were not efficient for classification of the spectroscopic data.

REFERENCES

1. М. С. Насиров, Защита деревянных конструкций при реставрации исторических памятников региона понтокаспий для развития туризма, Западно-Каспийский Университет, Кафедра Механических Устройств и Машин-2020.
2. Ю. Б. Левинский, Защита древесины и деревянных конструкций, Екатеринбург-2011.
3. Myronycheva. O, Karlsson. O, Sehlstedt-Persson. M, Öhman. M, Sandberg. D Portable microNIR sensor for the evaluation of mould contamination on wooden surfaces (2019).

PERFORMANCE OF THE TECHNOLOGICAL PROCESS OF PRINTING WITH PRINTING EQUIPMENT

M. GULIYEVA, M. NASIROV

Western Caspian University, Baku, Azerbaijan

The article discusses technological schemes of printing equipment, structure, principle of operation, design of the main units, classification of printing machines and their shortcomings that will be solved scientifically.

Introduction. The main purpose of the printing equipment is to carry out the printing process, that is, to repeatedly obtain identical prints by applying ink to the material. In addition to its main purpose, it is also used for embossing, die-cutting and perforating material. The block diagram of the printing machine is shown in Fig. 1 (its main units are represented in the rectangles, and those of them that may be absent in certain types of machines are outlined by the dashed line). The name of the device corresponds to the technological process it performs.

The classification of printing machines, reflecting only the main principles of their construction, is shown in Fig. 2. By the type of material being processed (tape unwound from a roll, or sheets fed from a stack), machines are called roll and sheet, respectively. The next feature of the classification is the shape of the actual printing surfaces. Machines in which the printing bodies are made in the form of cylinders are called rotary. Machines in which the working surface of the printing plate is located in plane, and the pressing surface is cylindrical, are called flat printing. Machines in which both working printing surfaces are flat are called crucible.

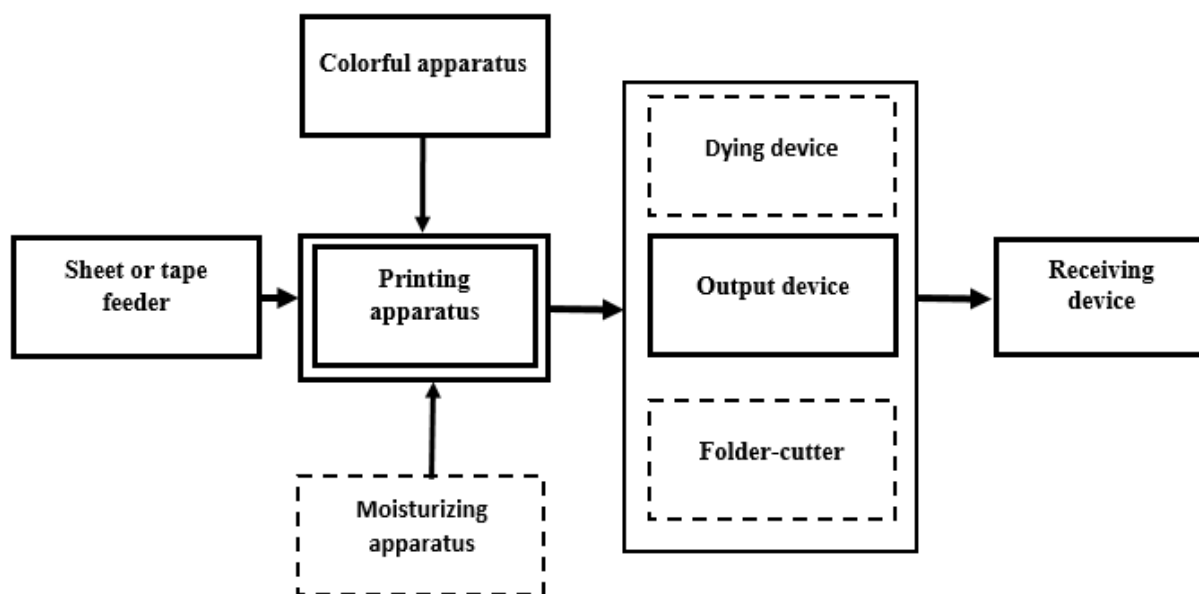


Fig.1. – Block diagram of the printing machine

Depending on the number of colors obtained on the print, the machine is called multi-color or single-color. Flat bed and crucible machines are currently produced, with rare exceptions, only in the form of single-color automatic machines or semi-automatic machines for processing sheet materials. Rotary presses are built exclusively in the form of automatic machines for printing on sheet or tape materials. At the same time, both single-color and multi-color machines are widely used. We have found double-sided rotary machines, in which the material is simultaneously or sequentially sealed from both sides. Multicolor machines which are made up of the same type of one-color printing units are called sectional, and multicolor machines containing one common impression cylinder around which other cylinders are installed (see Fig. 2) are called planetary. Flat bed and crucible presses are built for high printing method, and rotary - for high, offset and gravure printing methods [1].

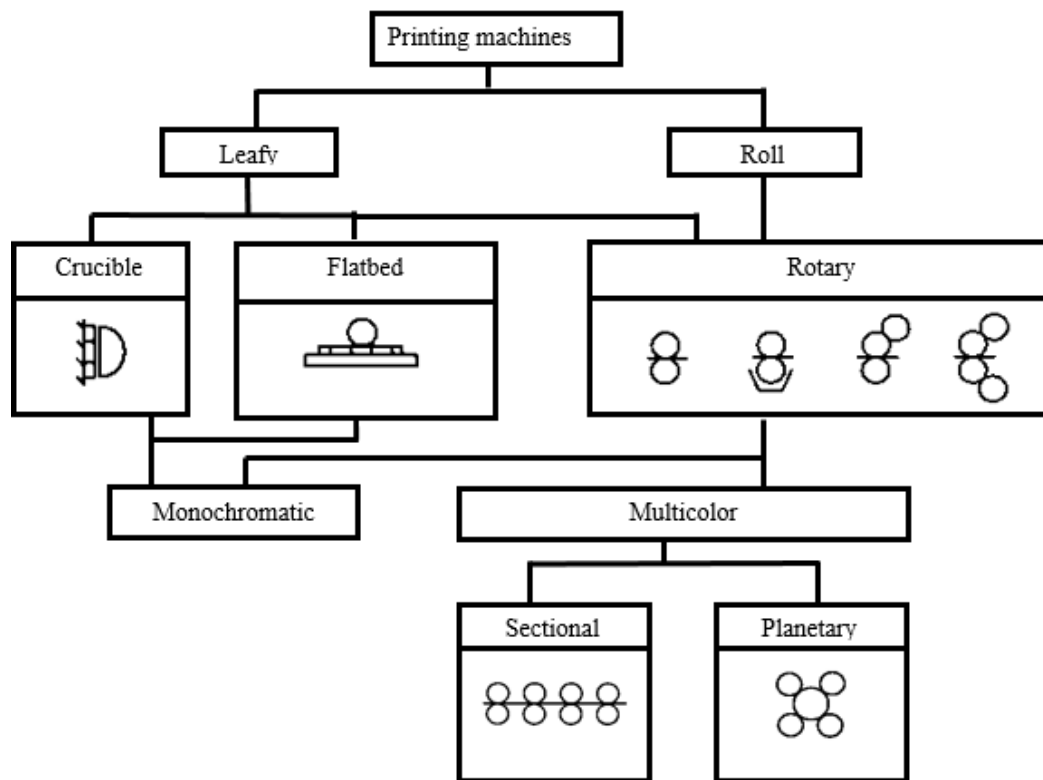


Fig.2. – Classification of printing machines

By the degree of automation, modern printing equipment is, as a rule, automatic machines, which are highly automated and high-speed high-precision mechanical systems with automatic feeding of the printed material and acceptance of finished products. Thanks to electronics, they are able to control and maintain in automatic mode the main functional units, to diagnose and adjust them. The evolution of printing equipment led not only to the increase in the operating speed of machines, but also to a sharp increase in their productivity due to a high degree of automation.

However, there are still machines with manual feed of the printed material, which belong to the class of semi-automatic devices. They are characterized by a low level of automation and low productivity.

Sheet-fed presses have lower productivity compared to web-fed presses. The speed of their operation is limited by the capabilities of the leaf feeding system, which carries out piecewise (discrete) feeding of sheet material. For medium format machines the capacity is 18,000 sheets / h at a linear sheet speed of up to 4 m / s, and for large format machines - 9000-15,000 sheets / h. Modern printing machines have wide technological capabilities to reproduce at a high quality level almost any text and illustration images with simultaneous additional finishing operations. For this, in the course of work of the PM, perforation, varnishing, numbering, die-cutting, embossing and other additional work is carried out, which expands the technological capabilities of the machine and allows you to obtain printed products of increased cost.

Sheet-fed presses are capable of printing sheet material in a wide range of formats with a sheet weight of 1 m² from 30 to 800 g and a thickness of 0,03 to 1,2mm. Sheets of paper pass through the technological sections of the machine without tension and warping, which reduces, in comparison with roll-fed machines, the likelihood of being peeled, allowing you to obtain high accuracy of color registration in one pass within $\pm 0,05$ mm.

When designing printing machines, the dimensions of the PA cylinders are selected taking into account the utilization rates of the working cycle K_u and the circumference of the printing or plate cylinders $K_n = \frac{t_n}{T}$; $K_n = \frac{l_p}{\pi D_n} \approx \frac{L_{max}}{\pi D_n}$; where t_n - sheet sealing time; T - duration of the kinematic cycle; l_p - the length of the working part of the circumference of the impression cylinder; L_{max} - the largest size of the sheet in the direction of its feeding; D_n - diameter of the impression cylinder.

The value of these coefficients is less than one ($K_u = K_n = 0,65 - 0,85$), since the cylinders of the printing CVL machines have non-working zones (recesses) for placing the actuators in them.

In roll-to-roll presses with a rotary press, the cycle time for printing and the surface of the plate cylinder are fully used, therefore $K_u = K_n = 1,0$. These machines are the fastest of all types of printing equipment, which is achieved by the continuous supply of paper tape to the rotary press. The speed of its conduction is about 18 m / s at a rotation frequency of the cylinders of the printing pair 50,000 -100,000 rev / h. Roll-fed machines have wide technological capabilities of reproducing any graphic images on the printed material together with the operations of cutting, perforating, gluing, sewing and folding. The multi-operation nature of roll-fed machines makes it possible to receive printed products at the output in the form of notebooks, sheets, rolls and even in the form of finished brochures, books and magazines when the RPM is included in the printing and finishing line. [2]

Conclusion. The disadvantages of RPM in comparison with sheet PM include:

- limited format of printed products (except for gravure printing machines), since the format can only be changed according to the width of the roll;
- limited length of tape cutting (except for gravure printing machines) due to the rigid scheme of the folder;
- lower accuracy of color registration due to the unstable behavior of the paper tape;
- limited range in thickness and weight of the sealed material when PA cylinders are force-locked to slip rings (40-210 g/m²).

REFERENCES

1. Ankuda D.A. Printing machines, automatic machines and production lines. Minsk-2018.
2. Shtolyakov V.I. Rumyantsev Printing equipment. Moscow-2011.

UDC 845.556

OVERVIEW OF THEORETICAL PROSPECTIVE METHODS TO REDUCE HYDRAULIC LOSSES IN A PIPELINE SYSTEM

V. SAVELYEVA, E. OVCHAROV, A. VARONIN

Polotsk State University, Belarus

This article is devoted to the biomimicry engineering approaches. It presents the idea of smooth antifrictional coatings, vortex flows, scaly coating, tubercle technologies and their advantages. The convenience of usage of natural mechanisms in the main pipeline transport is formulated.

Pipeline transport has a conclusive impact on the formation and development of the country's fuel and energy industry. The most important element of this industry is the main pipeline transport. This system is designed for the transportation of liquid and gaseous hydrocarbon energy resources. The main pipeline transport accounts for more than 4% of the total global energy consumption during transportation [4]. This fact is due to the high-energy demands of pumping equipment which, accounts for up to 20% of the world's electricity consumption [1]. According to energy consumption statistic, it is on the third place after urban transport and lighting. Thus, this is a significant energetic issue.

The hydraulic resistance appears from the side of the pipeline system and is estimated by the amount of specific energy losses that is irretrievably spent on the work of the friction forces where the flow undergoes deformation. The problem of reducing hydraulic losses in pipelines is very urgent. There are many methods of reducing hydraulic losses. Their practical use can significantly reduce the hydraulic fluid loss in pressure pipelines which in turn allows reducing the energy cost of transportation. One of the alternative approaches to technical problems is bioengineering.

Biomimicry is a practice that studies and imitates the strategies of adaptive mechanisms which were created by nature. Scientists have analyzed a large amount of material for the prospective application of some theories to such systems as airplanes, underwater vehicles, surface ships, trains and pipelines. During the analyzing of the bioengineering approaches, our attention was paid to the field of application in the main pipeline transport. The ideas of engineering bionics are applicable to both on-site and linear pipeline transport facilities.

A good example of biomimicry is the more streamlined Shinkansen train, which is not only quieter but also 10% faster and consuming 15% less electricity [5]. JR West's engineer and ornithologist used his knowledge of the splashless entry of kingfishers and the quiet flight of owls to reduce the noise made by trains. Kingfishers move quickly from air, a substance with low resistance, to water, a substance with higher resistance. The kingfisher's beak provides an almost perfect shape for such a strike. Similar to the streamlined beak of the kingfisher is the sand lizard, which due to its natural cover moves freely in the sand dunes. The application of this idea in the linear part of the main pipeline transport is in smooth surfaces. The main advantage of smooth coatings is the reduction of friction during transportation by reducing the roughness of the internal surface of the pipes. All that increases the throughput capacity of the pipelines.

With regard to the linear part of oil transport the ideas of the Austrian inventor Viktor Schaubberger, who was inspired by nature, are extremely important for the designers of modern gas pipelines, oil pipelines and whirlpool hydroelectric power plant [3]. The point is about using the phenomenon of swirling flow in pipelines that is still not used as a positive effect. This approach can be used to reduce the dynamic resistance of main pipelines and water pipelines of hydroelectric power plants. With a screw twist of the water flow during the feed from the reservoir to the hydroelectric turbines of hydroelectric power plants the kinetic energy of the water flow can be increased significantly. So that the height of the dam can be reduced respectively while saving the same power of electric units. Turbulent motion involves the waste of kinetic energy, turning it into heat, which is caused by randomly emerging and disappearing vortices of the liquid. The vortices randomly collide with each other, as well as with the walls limiting the flow. The natural flow of liquid and gas is a vortex motion, which makes consistent with the environment.

In traditional circular pipes the fluid tends to a natural swirling and tapering flow pattern. However, this flow shape doesn't align with the shape of the pipe. When the fluid moves in a circular pipe an intense turbulence occurs in the peripheral zones, which leads to additional hydraulic losses. Twisting the flow along the central axis using devices made of polymer coatings, such as elementary butterfly inserts or a twisted spring inside the pipe, can significantly reduce the energy cost of moving the contents up to 7 percent [2]. This is due to the more favorable energy state of the natural vortex flow of the liquid in comparison with the rectilinear one. In-

Technology, Machine-building

stalling a swirler in front of a circular pipeline allows to give the fluid flow this natural flow shape and reduce hydraulic losses. The positive effect of the device can be explained by the fact that any object or substance, being left to itself, tends to take the most energetically favorable state and moves along the most favorable trajectory, providing minimal energy loss. This installation can have the form of a vortex cutout in the polymer coating, which significantly simplifies the manufacturing process and reduces the cost.

The next effective example of biomimicry is the structure of fish scales. Researchers from the Universities of London and Stuttgart have found an opportunity to reduce the drag of airplanes and, as a result, to increase their speed [6]. Scientists have studied the topology of the scales of European sea bass and carp. The study made it possible to formulate a conclusion that overlapping areas on the surface of fish scales lead to a zigzag movement upon contact. The zigzag motion of the liquid creates a so-called "striped flow". This type of motion neutralizes unstable fluctuations that leads to turbulence. The use of this experimental approach in aviation contributed to a reduction in aerodynamic drag by more than 25%. This discovery may affect the shape of the polymer coatings on the internal surface of the pipeline, which will lead to an even greater reduction in hydraulic losses.

The additional example of the possibility of applying the natural approach in technical systems is the study of the Mako shark, which is considered to be the fastest of all existing sharks [7]. This type of shark can reach speeds of up to 100 km/h. One of the secrets of this mobility is the scales, which reduce the resistance of their body in water. The scales of Mako sharks have three "teeth". It was found that the scales create small vortices. In the course of the study the secret of the "super-speed" of this shark species was revealed. The secret consists in the ability to lift the scales, changing the angle of inclination of its plates. The use of the Mako shark scale structure has already found application in the coating of swimming suits. This idea can be applied to the adaptive internal surface of the pipeline, as a coating with small plates, which will also lead to a reduction in hydraulic resistance.

A specific feature of the scales is the absence of bacteria on it. The coating, which was copied from the scales of the Galapagos shark by Sharklet [5], is a plastic sheet product structured to prevent the growth of bacteria. This invention is used in hospitals and other places with a relatively high potential for the spread of bacteria and the occurrence of infections. While in operating oil pipelines, there is a problem of asphalt-tar-paraffin sediments on the walls of the pipeline. This technology is a potential solution to this problem.

Talking about on-site structures, the most important part is the main pumps which require a lot of electricity to convert the rotational energy into kinetic energy. In this case, observing nature can help solve the engineering problem of improving the pump's operating parameters.

It was noticed that whales have special bumps on the edge of the fin, which help them to divide the water into several streams. Studies have found that the addition of bumps to the leading edges of aerodynamic surfaces directly eliminates the fundamental limitations of conventional aerodynamic performance. Such surfaces have a number of advantages where the aerodynamic surfaces of the bumps have an increased stable lifting force.

The bumpy aerodynamic surfaces provide stable performance over an unsurpassed range of stall angles, and when they do stall, they stop gradually. That fact makes this technology even better. They literally revolutionize low-speed performance, far superior to any conventional blades. Based on this, WhalePower Corporation is ready to apply this technology to turbines, compressors, pumps and air fans [8].

At the core of wind turbines is the problem of root leakage, which deprives them of power. To solve this problem the scientists turned to the two most effective natural ways of moving in liquids: kingfisher and maple seeds [5]. As noted earlier, the kingfisher owes its reputation to the way its beak allows it to dive in the water with barely noticeable ripples and actually moving the liquid around it at a precise speed. When a maple seed falls to the ground, it moves through the air with the least resistance. The PowerCone is based on these principles of time-dependent energy efficiency. It absorbs wind gusts and smoothly directs the wind from the base to the outer spaces of the blades (smoothes incoming wind gusts and equalizes the air flow relative to the turbine blades), increasing the torque, reducing the start-up speed and increasing the power factor of the turbine. This reduces turbulence, vibration, and associated loads on the rotor, bearings, and transmission.

The engineering solutions of WhalePower and PowerCone can be used in the design of pump wheels which are a significant local resistance. Thanks to the PowerCone technology, a flow of material can be directed to the pump blades, which will rapidly reduce the local resistance of the pump. Due to the high energy consumption, increasing the efficiency by every hundredth of a percent is a win.

The aforementioned cases of the application of natural adaptive mechanisms of the environment and living organisms have shown that natural selection, which took place over 4 billion years, created optimal engineering adaptations in ecosystems with the best technical solutions. The study of existing adaptive natural structures was carried out with an emphasis on their extrapolation to the objects of the main pipeline transport.

The review has shown that such natural mechanisms can be used both on linear and on-site facilities. So, to reduce hydraulic losses in steel pipelines, smooth antifriction coatings, swirling of the flow by changing the

geometry of the internal polymer surfaces, a scaly internal polymer coating with a small size of each element and an adaptive internal coating can be used. To reduce losses in the main pumping equipment, it is possible to use the structure of special diagonal cutouts on the impeller blades and the inner surface of the pump casing, as well as a structure that directs the pumped flow from the center to the periphery of the impeller. These proposals are of a theoretical nature and require further research on physical experimental equipment or in special complexes for modeling.

REFERENCES

1. Официальный сайт информационного агентства «Деловой Петербург» / Энергетическая эффективность бизнеса: работа на будущее [Электронный ресурс] / Информационное агентство «Деловой Петербург». — Режим доступа: https://www.dp.ru/a/2020/09/28/Energojeffektivnij_biznes. — Дата доступа: 16.02.2020.
2. Иншаков Р.С., Балабуха А.В., Анисимова Е.Ю., Цырендашиев Н.Б., Панасенко Н.Л., Цыбуля И.И. / Применение завихрителя потока движущейся среды для снижения гидравлических потерь в трубопроводах // Вестник Евразийской науки, 2018 №3 [Электронный ресурс] — Режим доступа: <https://esj.today/PDF/36SAVN318.pdf>. — Дата доступа: 11.05.2020.
3. В.Шайбергер. Энергия воды. — М.: Яуза-Эксмо, 2007.
4. Official webpage of the American Information Energy Agency [Electronic resource] / American Information Energy Agency. — Mode of access: http://www.un.org/en/development/desa/policy/wesp/wesp_archive/2012chap2.pdf. — Date of access: 16.11.2020.
5. Official website of the American Institute of Biomimicry [Electronic resource] / Institute of Biomimicry. — Mode of access: <https://biomimicry.org/biomimicry-examples/>. — Date of access: 05.04.2021.
6. Muthukumar Muthuramalingam, Dominik K. Puckert, Ulrich Rist&Christoph Bruecker / Transition delay using biomimetic fish scale arrays [Electronic resource] / — Press Agency «Nature Portfolio». — Mode of access: <https://www.nature.com/articles/s41598-020-71434-8>. — Date of access: 22.01.2021.
7. Zhang, Hao Yan, Minghui Zhang, Qingshan Wu, Mingjie Liu, Lei Jiang, Cunming Yu, Mengfei Liu / Bio-inspired drag reduction: From nature organisms to artificial functional surfaces [Electronic resource] / — Press Agency «Elsevier». — Mode of access: <https://doi.org/10.1016/j.giant.2020.100017>. — Date of access: 18.02.2021.
8. Official website of the international consulting engineering company [Electronic resource] / — Consulting engineering company «WhalePower». — Mode of access: <https://whalepower.com/examples>. — Date of access: 05.02.2021.

UDC 347.842

**ABOUT THE POSSIBILITY OF PERSPECTIVE APPLICATION OF HYDROPHOBIC
AND SUPERHYDROPHOBIC MODIFIED INTERNAL COATINGS OF PIPELINES IN PIPELINE TRANSPORT****D. SARELA, A. VARONIN**
Polotsk State University, Belarus

The article considers the possibility of using hydrophobic coatings on the internal surfaces of main transport equipment to reduce the wettability zone and hydraulic roughness. This coating can be used on pipelines, pump impellers to reduce energy consumption. It was concluded that it is necessary to study further the theoretical and practical aspects of hydrophobization and the introduction of this method in large-scale production.

One of the main technological processes of the energy systems of the oil complex is the transport of hydrocarbon raw materials through pipeline systems, the functioning of which consumes a large amount of electricity. Energy saving issues are widely considered in various regulatory documents, including STB 1771-2010 Energy-consuming equipment. In the operation of pipeline systems, it is important to minimize hydraulic losses.

The main reasons that increase wear and reduce the degree of reliability of various pipeline systems are the formation of deposits on the in-pipe surfaces and corrosion processes caused by the aggressiveness of the transported fluids. Corrosion processes increase the surface roughness of pipelines and affect the increase in the coefficient of hydraulic friction, accelerating the accumulation of a layer of deposits on the inner surface. The formation of heavy oil deposits leads to a narrowing of the diameter of the passage section and, as a result, an increase in hydraulic resistance with the consumption of electricity for the transportation of liquid hydrocarbon raw materials.

In oil pipelines, to reduce hydraulic losses, depressants are mainly used, which are inhibitors of the formation of heavy oil deposits, anti-turbulent additives that change the coefficient of hydraulic efficiency, and heating of the transported fluid. In the result of applying this method, the physicochemical properties of the transported raw materials are affected.

Simultaneously for an additional effective reduction of hydraulic resistance, it is necessary to take into account the initial state of the pipeline surface. Thus, you can use a different method, affecting the inner surface of the pipeline. In the course of this method, protective smooth-walled epoxide and silicate-enamel coatings with a reduced absolute roughness coefficient are used, as well as hydrophobic coatings with a reduced surface wettability area. The use of modified internal coatings with hydrophobic properties is a promising and still insufficiently studied direction. It is possible to use internal hydrophobic coatings in the pipeline transport of oil and petroleum products, which requires additional research and refinement in the calculation of hydraulic parameters, taking into account the hydrophobicity of the surfaces and changes in the flow characteristics of the transported fluids.

The main approaches to reducing the hydraulic resistance due to the hydrophobicity of surfaces were proposed by R. N. Wenzel (1936), B. D. Cassier and S. Baxter (1944). These approaches are based on the use of such natural phenomena, in particular, on the imitation of the properties of the lotus leaf [1]. The mechanics of the lotus effect process is that due to the high surface tension, water droplets tend to shrink the surface, turning into a spherical shape. When the liquid comes into contact with the surface, the adhesion forces cause the surface to be wetted. The degree of wetting depends on the structure of the surface and on the tension of the liquid drop. The degree of wetting depends on the surface structure and the liquid tension of the drop [2].

The essence of hydrophobization for prospective use in the internal surfaces of pipelines is to achieve the lotus effect in technical systems by modifying the surface relief with its subsequent hydrophobization, in particular, by means of surfactants in the transported liquid or using hydrophobic compounds in the inner coating. The contact area of a liquid drop in a conventional pipeline is much larger than the contact area of a liquid drop in a pipeline with a hydrophobic coating. Presumably, the free area under the liquid is supposedly filled with gas. All this helps to reduce hydraulic resistance.

It is well known that the hydraulic resistance of the pipeline is determined by the Darcy-Weisbach formula:

$$\Delta P = \lambda \cdot \frac{v^2}{2g} \cdot \frac{L}{d} \quad (1)$$

where ΔP – pressure drop, Pa;

λ - dimensionless coefficient of hydraulic friction, which generally depends on the Reynolds number and the relative roughness of the inner surface of the pipeline;

L - pipeline length, m;

d – pipeline diameter, m;

ρ - density of the pumped liquid, kg/m³;

v – pumped medium speed, m/s.

From this formula it follows that the main influence on the hydraulic resistance is exerted by the density and speed of the pumped medium, the diameter of the pipeline, its length and the roughness of the in-pipe surface.

The resistance of pipelines with a modified hydrophobic surface cannot be correctly calculated using formula (1) due to changes in the surface wetting conditions and flow structure in the near-wall zone. The generally accepted characteristic of surface wettability is the contact angle θ between the droplet and the surface plane. However, for the surface of pipelines, the roll angle α and the equivalent roughness k_e , which characterize the hydraulic properties of the surface, play a more important role. Based on formula (1), it can be concluded that with constant parameters d , l , ρ , the hydraulic resistance is determined by the value of the coefficient λ , which is a function of the wetting characteristics, i.e. $\lambda = f(\theta, \alpha, k_e)$ [1]. In this regard, it is of great interest to establish the dependence of the decrease in hydraulic resistance on the state of surface wetting, in particular, on the basis of the results of experimental physical research or computer simulation.

The advantages of using hydrophobic coatings have been experimentally confirmed in a number of scientific studies. Thus, a study conducted on pumping equipment [2, 3] showed that the modified coating had a positive effect on the hydrodynamic effect of the elements of the flow part of rotary pumps and certain types of losses in centrifugal pumps. Due to the hydrophobization of the elements of the flow part of rotary pumps, there was a decrease in vibration by 25-30%, acoustic noise by 10-15%, wear of mechanisms by 2-5 times, as well as a decrease in power consumption by an average of 7-10 W per 1 m^3 of pumped liquid. It is also advisable to apply this approach to the pumping equipment of the main pipeline transport.

The possibility of using hydrophobic coatings in water supply networks was proposed in [4, 5, 6]. Modification of the inner surface of the pipeline was carried out by introducing surfactants with the formation of molecular layers. As a result of experiments on a laboratory bench, optimal values of hydraulic resistance reduction were obtained for the Dn50 pipeline with a length of $l=4$ m at a wetting angle of $\theta=141^\circ$ and a rolling angle of $\alpha=32^\circ$. With an increase in the internal diameter of the pipeline, the maximum reduction in hydraulic resistance decreases, for the DN50 it was approximately 30%, depending on the flow rate. It was noted that there are optimal characteristics of the hydrophobizing layer (the thickness of the molecular layers of surfactants, the angle of wetting and rolling), leading to the maximum reduction in resistance for each pipeline diameter.

The use of hydrophobic coatings has also found a place in the oil production industry [2]. In oil production, one of the most common causes of failure of oil-submersible equipment is salt deposition on the submersible electric motor, working bodies of electric rotary pumps, in filter systems. The share of failures of electric rotary pump installations reaches up to 30% of the total number of failures. Effective methods in combating salt deposition in electro-rotary pumps are the use of low-adhesion working bodies of electro-rotary pumps made of polymer materials with increased resistance to salt deposition. Impellers of electric rotary pumps with a hydrophobic coating based on polyphenylene sulfide successfully cope with salt deposition. The filters of the input modules of electric centrifugal pumps coated with a hydrophobic coating have a number of advantages over other filters: low hydraulic resistance, high throughput, regenerability, elastic properties of the material that ensure long-term and efficient operation of the equipment, reducing salt deposition on the filter elements of the grid, increasing the operating time. In addition, filter elements with a hybrid hydrophobic coating can theoretically be used for the separation of petroleum products from the watered reservoir fluid.

An important feature is the choice of a specific hydrophobic material for each specific task. The materials for the hydrophobic coating are fluorotelomers such as tetrafluoroethylene, sulfonate fluorotelomer, acrylate fluorotelomer, and methylacrylate. They have properties such as heat resistance, low surface tension, chemical resistance, repels water and grease. These materials have properties that correspond to those required to give hydrophobicity to the internal surfaces of pipelines, nodes and parts of pumping units, as well as for equipment used in oil production [7]. The task of choosing the material for the internal surfaces of the main pipeline may depend on the physicochemical characteristics of the pumped liquid and needs further research.

In the future, as a surface imparting hydrophobicity, it may be possible to use a special laser technology to impart superhydrophobic properties to the metal, first carried out at the University of Rochester [8]. The essence of this technology lies in the fact that micro- and nanoscale structures are applied to the metal surface using a femtosecond laser, which are capable of capturing and retaining air. Products made of such materials do not sink in water, even after damage and punctures, which may indicate their durability and resistance to mechanical stress. When a metal plate is immersed in water, an air bubble forms around it, which pushes it to the surface. The process of applying the structure is very time consuming and costly. It takes an hour to process a surface of 2.5 cm^2 . This method of hydrophobization is very promising and has a very huge potential in pipeline transport in order to reduce hydraulic resistance, but for treating a surface with a large area, very powerful and expensive lasers are required, and the refinement of the very technique of applying the structure, which does not make it possible to use this method on large-scale goals to date.

When analyzing the works concerning the application of the method of surface modification using the application of hydrophobic coatings and the creation of micro- and nanoscale structures, it can be concluded that this method is effective in the pipeline transport and oil production industry. To introduce hydrophobization into large-scale use, it is necessary to carry out additional research using computer modeling and make additional calculations to clarify the coefficient of hydraulic resistance, which affects the hydraulic resistance of the pipeline.

REFERENCES

1. Расчёт трубопроводных систем с учётом степени гидрофобности внутренних поверхностей / М.А. Морозов [и др.] // Трубопроводный транспорт нефти – 2016. – №4. – 131-134 с.
2. Гибридные гидрофобные поверхности в борьбе с солеотложениями на деталях нефтепогружного оборудования / С.В. Ладанов [и др.] // Добыча нефти и газа – 2020. – №6. – 52-55 с.
3. Повышение ресурса динамического оборудования путём модификации поверхностей фторосодержащими поверхностно-активных веществ / К.А. Путиев, А.А. Случаев // Вестник арматурщика – 2015. – №8. – 42-48 с.
4. О возможности снижения гидравлического сопротивления трубопроводов систем теплоснабжения / В.А. Рыженков, А.С. Седлов, А.В. Рыженков // Энергосбережение и водоподготовка – 2007. – №5. – 22-26 с.
5. Морозов М.А. Расчётно-экспериментальные исследования гидравлических характеристик трубопроводов систем теплоснабжения с учётом степени гидрофобности функциональных поверхностей: диссертация на соискание ученой степени кандидата технических наук: 05.14.04 / М.А. Морозов. – Москва, 2016. – 134с.
6. Г.П. Хованов Исследование влияния гидрофобности поверхностей элементов проточной части на эксплуатационные качества и отдельные виды потерь центробежных насосов: автореферат диссертации на соискание учёной степени кандидата технических наук: 05.04.13 / Г.П. Хованов – Москва, 2012 – 20 с.
7. Официальный сайт представительства компании DuPont / Фторированные ПАВ. Применение при разработке нефтяных месторождений [Электронный ресурс]. – Режим доступа: <https://tio2-titan.ru/Ftor-PAV.pdf>. – Дата доступа: 02.04.2021.
8. Highly Floatable Superhydrophobic Metallic Assembly for Aquatic Applications / Z. Zhan [et al.] // Applied materials and interfaces – 2021. – №11. – P. 12-17.

UDC 658.5

RESEARCH OF METHODS AND ALGORITHMS FOR SOLVING PRODUCTION PLANNING PROBLEMS

K. ZADOROVA, D. LUKIN, O. KOSENKO
Southern Federal University, Rostov, Russia

Improving efficiency of production systems is the main task of each manufacturing enterprise, and ensuring the coordinated work of all production links is the main goal of operational and production planning. This article discusses the need and relevance of the development and research of methods for optimizing the production process.

Today, the important task of every manufacturing enterprise is to improve efficiency of production systems management.

Generally speaking, an enterprise is a collection of diverse and interrelated processes distributed in space and time. Since the available production and time resources are limited, it is advisable to use production planning in enterprise management. There are many methods of operational planning process (OPP). However, it should be understood that it is necessary not only to predict the volume of products produced in order to meet the demand, but also to identify possible problems or difficulties that may arise. Determine ways to avoid and solve them. It is important to choose a management plan for the production system that will maximize profit with the least cost of resources.

At the same time, planning is often carried out under conditions of partial or complete uncertainty of the input parameters, which depend on various factors.

Thus, the task of analyzing and improving production planning methods under conditions of uncertainty is urgent.

Mechanical engineering, like any manufacturing enterprise, is a complex structure consisting of certain objects, processes and the relationships between them.

According to the timing of planning, long-term (strategic), medium-term (current) and short-term (operational and production) planning are distinguished (fig. 1).

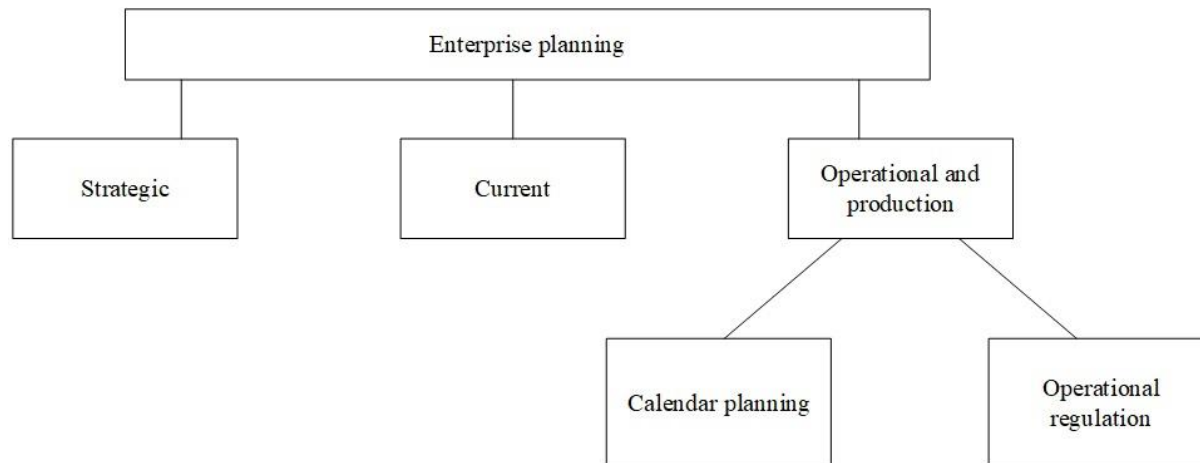


Fig. 1. – Types of planning in the enterprise

Let us take a closer look at operational production planning. Its main goal is to ensure the coordinated work of all production links to manufacture products in accordance with a given quantity, nomenclature and on time.

To achieve the main goal of the PPO it is necessary [1]:

- to develop calendar-planning standards;
- create a production plan for the enterprise for each month of the year;
- draw up operational and calendar plans for the production of products by workshops, sections by quarters, months, weeks, days, shifts;
- calculate the load of equipment;
- make shift planning.

Operational management is carried out using functional, elementary and organizational subsystems. Operational planning subsystems are shown in figure 2.

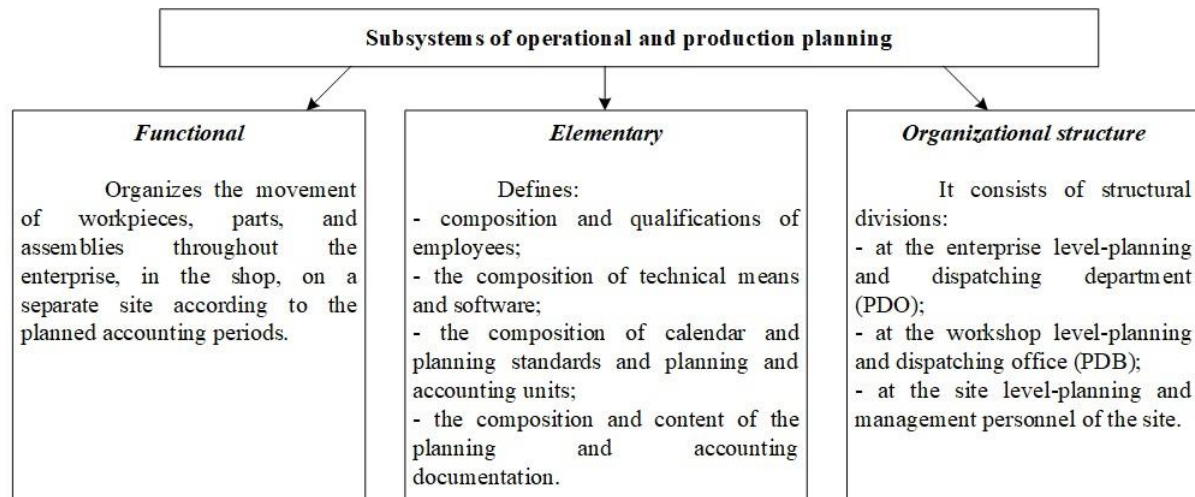


Fig. 2. – Subsystems of operational and production planning

The production dispatch department (PDO) develops operational and calendar standards, determines and establishes plans for the release of parts in workshops, and monitors the implementation of the schedule.

The production dispatch bureau (PRB) determines the places and dates of the beginning and end of processing of each detail of the operation, draws up a calendar schedule for the work of the shop sections for a quarter, month, week, day, shift, and also ensures the well-organized work of the shops to fulfill the given program.

Operational-production planning must necessarily take into account the industry specifics, serial production, design and technological features of the products, the features of the technologies used at the enterprise and other various factors.

The system of operational and production planning consists of the following interrelated and interdependent elements:

- planning and accounting periods - time intervals for which the plan is drawn up;
- planning and accounting units - a detailed planning object (order, assembly, part, etc.);
- scheduling standards - quantitative and time values of indicators (for example, batch size, duration of the production cycle, etc.);
- systems of operational production planning - a set of methods for calculating the planned parameters for the production output.

When choosing an OPP system, it is important to take into account such factors as the dynamics of demand for manufactured products, the cost of borrowed material resources, the indicator of material consumption of products, the cost of labor, the number of technological redistributions, the coefficient of coverage of general production costs, the coefficient of production specialization.

The type of production (single, batch or mass) affects both the various elements of the OPP and the features of the control and management of the production process [2].

Based on the foregoing, the expediency of developing and researching methods for optimizing the production process, taking into account the uncertainty of the initial data, as well as the formalization of a fuzzy model of the production system, is confirmed.

REFERENCES

1. И.В. Ершова, Т.А. Минеева, Е.В. Черепанова. Оперативно-производственное планирование. Екатеринбург: Изд-во Урал. ун-та, 2016.–96 с.
2. А. Кислов, С. Лебедев. Модели цифрового предприятия на базе 1С:ERP для практико-ориентированного обучения Электронный ресурс // 1С:Учебный центр № 1 («1С-Образование») - подразделение фирмы 1С [сайт]. [2020]. URL: https://kpk.1c.ru/digital_enterprise (дата обращения: 29.03.2021).

UDC 656.073.7

DIGITAL TWINS AS A TRANSPORT LOGISTICS TOOL

V. HAIKOVA, K. FILIMONOVA, P. LAPKOVSKAYA

Belarusian National Technical University, Minsk, Belarus

The article discusses digital trends for logistics transforming – digital twins. This trend contributes to the improvement of supply chains and affect transport operations in general. New technologies help companies to reduce costs, increase productivity and efficiency, and optimize maintenance.

In the modern world, there are more and more new technologies that are gradually being introduced into various areas of production, and logistics is no exception. Manual processing of information is replaced by computer, in the world there are automated systems that make it possible to simplify the process of work in enterprises. With the use of these technologies, production processes are optimized, data processing time is reduced and the efficiency of enterprises is increased. One of the such technologies is digital twin technology (see Fig.a) [1].



Fig. a. – Digital twins in logistics

A digital twin is a representation of a physical object, process or service, such as a jet engine or wind farms, or even larger items such as buildings or even whole cities and supply chains. The digital twin technology is used for copying processes in order to help company to predict how these processes will perform. These programs can integrate the Internet of things, artificial intelligence and software analytics to improve the results.

With the progress of machine learning and factors such as big data, these virtual models have become a big step in modern engineering to drive innovation and improve performance [2]. Creating digital twin can allow to avoid costly failures in physical objects, by using advanced analytical test processes and services, monitoring and predictive capabilities.

The lifecycle of a digital twin starts with experts in applied mathematics, data science researching the physics and operational data of a physical object in order to develop a mathematical model that simulates the original. The developers who create digital twins have a warranty that the virtual computer model can get feedback from sensors that gather information from the real world version. This lets the digital version simulate what is happening with the original version in real time, creating opportunities to collect insights into performance and any other potential problems.

A digital twin can be complex or simple, with differing amounts of data determining how clearly the model simulates the real world physical object [5]. The twin can be used with a prototype to offer feedback on the product as it can even act as a prototype in its own right to model what could happen with a physical object when built.

Since it can be used across a wide range of industries, from healthcare to automotive and power generation, it has already been used to solve a large number of problems. A digital twin allows users to explore solutions for product lifecycle increase, manufacturing and process improvements, and product development and prototype testing. A digital twin can virtually show a problem so that a solution can be invented and tested in the program rather than in the real world.

Aftermarket logistics services can be developed by linking digital twins of manufactured products with logistics services. With a digital twin of any physical object, such as goods or vehicles, the role of the logistics service provider can become extremely important, acting on insights from the virtual reality. For instance, if a vehicle receives damage and requires spare parts, the supply chain is able to react quicker (or even proactively) and more efficiently with notifications from the digital twin, detailing exactly the required parts and where they need to be sent.

Technology, Machine-building

Digital twins help companies to solve problems by simulating all assets in a complex supply chain. A company can make decision across multiple planning horizons:

- short-term planning and realization;
- sales and operations planning;
- longer-term planning.

Designing, monitoring, and managing packaging and containers creates a number of challenges for the industry. The growth of e-commerce such as packaging variety and driving up demand. This produces significant reduces operational efficiency through poor volume utilization. The application of material digital twins could help the development of better and more environmentally friendly packaging materials. In efforts to improve stability, companies are exploring the application of a range of new materials including compostable plastics and materials with a high percentage of post-consumer recycled content. Material digital twins can help companies understand and forecast the performance of new materials in packaging applications, can model material behavior under the temperature, vibration, and shock loads experienced in transit [4].

Digital twins could also help logistics participants manage container fleets more efficiently. Reusable containers are an industry standard in multiple logistics flows. They include standard ocean containers, reusable crates to transport car parts between factories, and containers for food and drinks delivery to retail stores and consumer homes.

Nowadays, the engineering, manufacturing, energy, and automotive industries are leading the way in impact digital twins to manage their most critical assets, followed by healthcare, logistics and even supply chain. As the necessary technologies continue to become more available, the logistics sector is only just now beginning its digital twin way and early examples of the first supply chain facilities using digital twins are beginning to appear. Perhaps more important for logistics professionals to consider in the near term is not how to use digital twins for direct management of supply chain operations, assets, and facilities but rather how to develop the supply chain [3].

For digital twins and their physical twins to work together optimally, there is an increasing need for logistics professionals to improve sensitivity, service quality, availability, and delivery accuracy to ensure the thing performs in optimal harmony with its intended design and performance.

Thanks to this trend, we can expect the technology to also be accepted for certifications such as security and environmental standards. In the future, products will be delivered with their digital twins. That will permit users, for example, to test and predict how modifications to an electric motor, a building's design, or a factory's production process will affect energy use and efficiency. Digital twins may become an integral part of our everyday lives by enabling individuals without previous technical knowledge to finally get simple answers to complex questions.

Customers today understand the value of digitalization, and are already ready to pay for both a physical product and a virtual one. Demand is growing, and tomorrow in highly competitive markets, it will be possible to sell only the product that has a digital twin.

The most successful retailers are those that are already recognizing and implementing technologies such as digital twins, artificial intelligence and machine learning – they are the ones that are staying ahead of the curve in tough times. If businesses are to survive and thrive in the new normal, they must implement the right enabling technology that will help them gain insights into their supply chains and make them more agile to respond to rapidly changing conditions [6].

Table 1. – Global digital twin market forecast

Year	Analysts' assessment
2019	\$ 1,9 bn
2023	\$ 16 bn
2025	\$ 32,3 bn

In conclusion, we can say that a new splash of interest in digital twins in the future will only grow. The first examples of the implementation of modern digital twins are already presented, and we can expect new ones from day to day. Some technology providers already have digital twins in their platforms, which allows to monitor the state of all processes in the enterprise. The Coronavirus pandemic has fueled wider adoption of digital twin technology. International research firm MarketsandMarkets estimates that the U.S. digital twin industry will grow from \$ 3.8 billion in 2020 to nearly \$ 36 billion by 2025, in part due to the COVID-19 pandemic.

REFERENCES

1. What is a digital twin? [Electronic resource]. – Mode of access: <https://www.ibm.com/topics/what-is-a-digital-twin>. – Date of access: 06.04.2021.

2. Digital Logistics: What Is It, and How Will It Impact Your Organization? [Electronic resource]. – Mode of access: <https://www.logmore.com/post/digital-logistics>. – Date of access: 06.04.2021.
3. Wang, Z. Digital Twin Technology / Z. Wang. – Taiyuan: North University of China, 2020. – 114 p.
4. Fuller, A. Digital Twin: Enabling Technologies, Challenges and Open Research / A. Fuller. – Staffordshire: Keele University, 2019. – 21 p.
5. GEODIS and Accenture Reveal eCommerce Surge and Challenges [Electronic resource]. – Mode of access: <https://www.supplychaindigital.com/logistics-1/geodis-and-accenture-reveal-ecommerce-surge-and-challenges>. – Date of access: 06.04.2021.
6. Parrott, A. Industry 4.0 and the digital twin / A. Parrott. - Deloitte Consulting LLP, 2017. – 20 p.

PRODUCTION MANUFACTURABILITY ASSESSMENT OF THE PRODUCT DESIGN

E. TIKHON, N. POPOK
Polotsk State University, Belarus

On the basis of technical and economic analysis of the relations properties between design and technological solutions, method for assessment production manufacturability by combining various manufacturability coefficients, taking into account the degree of their influence on the labor intensity production.

The influence of design characteristics on the labor intensity of technological preparation and products production. Example of the influence of production design (PD) characteristics on the types of labor intensity of PD production (table 1).

Table 1. – Influence of product design characteristics on labor intensity subspecies

№	Product design characteristics	Labor intensity specie (L _i)								
		L ₂			L ₃					
		L ₂₁	L ₂₂	L ₂₃	L ₃₁	L ₃₂	L ₃₃	L ₃₄	L ₃₅	L ₃₆
1	Amount of purchased elements	+		+	+	+	+			
2	Amount of repeatable details	+		+	+					
3	Amount of repeatable connections		+	+				+		
4	Precision methods		+						+	
5	Amount of borrowed elements	+		+						
6	Amount of typical details	+								
7	Details precision					+				
8	Surface roughness of details					+				
9	Material hardness of details					+				
10	Mass of product elements						+			+
11	Amount of connection types								+	
+ – influence of characteristics on labor intensity subspecies										

On the basis of the data in table 1, a coefficients list of manufacturability PD manufacturing was determined [1] and their calculation formulas were developed [2]:

1. Purchased coefficient (C_p):

$$C_p = a_2 a_{21} \frac{\sum E_{P_i} b_{com_i}}{E} + a_2 a_{23} \frac{\sum E_{P_i} b_{com_i}}{E} + a_3 a_{31} \frac{\sum E_{P_i} b_{com_i}}{E} + a_3 a_{32} \frac{\sum E_{P_i} b_{com_i}}{E} + a_3 a_{33} \frac{\sum E_{P_i} b_{com_i}}{E}, \quad (1)$$

where E_{P_i} - the i -th purchased element; b_{com_i} - coefficient reflecting the level of structure complexity of the i -th element; E - the total number of elements in the PD; a_2 - the influence degree L_2 on L ; a_3 - the influence degree L_3 on L ; a_{21} - the influence degree L_{21} on L_2 ; a_{23} - the influence degree L_{23} on L_2 ; a_{31} - the influence degree L_{31} on L_3 ; a_{32} - the influence degree L_{32} on L_3 ; a_{33} - the influence degree L_{33} on L_3 .

2. Repeatable details coefficient:

$$C_{RD} = a_2 a_{21} \frac{\sum (D_{RD} - D_{RD.B} - 1) b_{com_i}}{D - D_p - D_B} + a_2 a_{23} \frac{\sum (D_{RD} - D_{RD.B} - 1) b_{com_i}}{D - D_p - D_B} + a_3 a_{31} \frac{\sum (D_{RD} - D_{RD.B} - 1) b_{com_i}}{D - D_p - D_B}, \quad (2)$$

where $D_{RD.B}$ - the number of repeated borrowed details, D_{RD} - the number of repeatable details of the i -th group.

3. Repeatable connections coefficient:

$$C_{RC} = a_2 a_{22} \frac{\sum (C_{RC} - 1) b_{com.c_i}}{C} + a_2 a_{23} \frac{\sum (C_{RC} - 1) b_{com.c_i}}{C} + a_3 a_{34} \frac{\sum (C_{RC} - 1) b_{com.c_i}}{C}, \quad (3)$$

where C_{RC} – the number of repeated connections of the i -th group; C - the total number of connections;

$b_{com.ci}$ - coefficient of the connection structure complexity level of the i -th group; a_{22} - the influence degree L_{22} on L_2 ; a_{34} - the influence degree L_{34} on L_3 .

4. Coefficient of details material hardness:

$$C_H = a_2 a_{22} \frac{\sum n_{Hi} b_{Hi} b_{SHi}}{n}, \quad (4)$$

where n_{Hi} - the details number of the i -th material hardness value; n - the number of details in the product; b_{Hi} - the influence degree of the i -th value of the details material hardness on the labor intensity.

5. Borrowing coefficient (C_B):

$$C_B = a_2 a_{21} \frac{\sum E_{Bi} b_{com_i}}{E - E_p} + a_2 a_{23} \frac{\sum E_{Bi} b_{com_i}}{E - E_p}, \quad (5)$$

where E_{Bi} - the i -th borrowed element.

6. Typification coefficient:

$$C_{TYP} = a_2 a_{21} \frac{\sum D_{TYPi} b_{com_i} b_{TYPi}}{D - D_p - D_B - D_R}, \quad (6)$$

$\sum D_{TYP}$ - the details number of the i -th typical representative group;

b_{TYPi} - the influence degree of typical details to reduce the labor intensity of their manufacture; b_{com_i} - coefficient of the details design complexity level of the i -th typical representative group.

7. Details precision coefficient:

$$C_{PR} = a_3 a_{32} \left(1 - \frac{n_s}{\sum A_i b_{PRS_i} b_{PRI}}\right), \quad (7)$$

where A_i - the value of the i -th precision quality of the details size in the product; b_{PRI} - coefficient taking into account the labor intensity of achieving precision A_i when the part is processed; n_s - the number of details surface areas in the product; b_{PRS_i} - the area fraction of the i -th detail surface from the total surface area of all details in the product taken as a unit.

8. Coefficient of details surfaces roughness:

$$C_{RN} = a_3 a_{32} \left(1 - \frac{n}{\sum B_i b_{RNI} b_{SRNI}}\right), \quad (8)$$

where B_i - the value of the i -th details surface roughness parameter in the product; n - the number of details surfaces in the product; b_{SRNI} - the area proportion of the i -th details surface from the total surface area of all details in the product taken as a unit; b_{RNI} - the influence degree coefficient of B_i on labor intensity of processing the i -th surface.

9. Coefficient of precision methods efficiency:

for the closing links of dimensional chains.

$$C_{MDCH} = a_3 a_{35} \frac{CI \cdot b_{P.CI} + ICI \cdot b_{P.ICI} + GI \cdot b_{P.GI} + ADJ \cdot b_{P.ADJ} + FT \cdot b_{P.FT}}{CI + ICI + GI + ADJ + FT}, \quad (9)$$

where CI - the number of dimensional chains assembled by the complete interchangeability method; ICI - the number of dimensional chains assembled by the incomplete interchangeability method; GI - the number of dimensional chains assembled by the group interchangeability method; ADJ - the number of dimensional chains assembled by the adjustment method; FT - the number of dimensional chains assembled by the fitting method.

10. Connection coefficient:

$$C_C = a_3 a_{35} \frac{\sum n_i b_{Ci} b_{SCi}}{n}, \quad (10)$$

n_i - the number of i -th type connections; n - the number of connections in the product; b_{Ci} - the influence degree of the i -th connection type on labor intensity (for cylindrical movable ones b_{Ci} will have a minimum value and for welded joints it will be maximum); b_{SCi} - the contact areas proportion of the i -th connection type from total contact area of all joints in the product taken as a unit; a_{35} - the influence degree of L_{35} on L_3 .

11. Element mass coefficient:

$$C_M = a_3 a_{33} \frac{\sum n_i b_{M_i}}{n} + a_3 a_{36} \frac{\sum n_i b_{M_i}}{n}, \quad (11)$$

where n_{Mi} - the number of the i -th mass value elements; n - the number of elements in the product; b_M - the influence degree of the i -th element mass value on the labor intensity; a_{36} - the influence degree of L_{36} on L_3 .

Conclusion. The given calculation formulas of manufacturability coefficients make it possible to determine an integral assessment of the manufacturability level at the manufacturing PD stage by summing their values.

The manufacturability coefficients of disposal preparation and design production preparation are determined by the same method.

REFERENCES

1. Базров, Б.М. Анализ коэффициентов технологичности конструктивного исполнения изделия / Б.М. Базров, А.А. Троицкий // Научно-технические технологии в машиностроении. 2018, №7. - С.23-26.
2. Попок, Н.Н. Мобильная реорганизация машиностроительного производства / Н.Н. Попок. – Минск: Технопринт, 2001. – 396 с.

UDC 482.689

ON THE POSSIBLE APPLICATION OF MICROBUBBLE CAVITATION IN PIPELINE TRANSPORT

M. STUDENKOVA, A. VARONIN

Polotsk State University, Belarus

The article discusses the possibility of using microbubble cavitation in pipeline transport to reduce hydraulic losses due to a decrease in total resistance due to air bubbles. It was also concluded that further research of this phenomenon and its implementation in this industry is necessary.

In addition to the fact that pipelines guarantee the energy independence of our country, they allow to reduce transport loads on railway transport, thereby, contributing to an increase in the volume of transportation of other equally important cargo. The length of pipeline transport is growing more and more, technologies are being improved, technological re-equipment of existing pipeline systems is being carried out, more advanced and modern means of control and communication are being introduced, methods of delivery of high-viscosity and solidifying oils are being modernized.

The problem of reducing hydraulic losses in pipelines is very urgent. This is due to the huge energy and economic costs of transporting the product. Therefore, at present, there is an active development of reliable and effective devices for reducing hydraulic losses in pipelines using the example of various methods in other industries and in nature. So, it has been observed that emperor penguins in Antarctica represent an exceptional skill for reducing hydrodynamic drag when accelerating in water or jumping out of water onto slippery surfaces [8]. In addition to the streamlined body shape, studies have shown that the special structure and wettability of penguin feathers also play an important role in reducing fluid resistance. It turned out that small bubbles emerging from the entire plumage of the penguin could develop into a smooth layer - a bubble cloud, which can effectively reduce the resistance force that promotes its jumping out of the water or high-speed movement.

In 1973, McCormick first illustrated the drag reduction of a microbubble by electrolysis. Experiments have shown that bubbles can effectively alter both laminar and turbulent boundary layers resulting in significant drag reduction. In 1976, Bogdevich studied the effectiveness of reducing the resistance of microbubbles on the porous surface of a thin plate. The maximum reduction in the local resistance to friction of the wall was about 90%. It was found that a flat plate at a speed of 5 m/s showed a better drag reduction, while a plate with a porous surface was 15 m/s. The decrease in the resistance of microbubbles on the surface of the flat plate mainly occurred near the boundary layer, and they lose the decrease in resistance with distance from the boundary layer of the wall [8].

This phenomenon of bubble formation is called cavitation. This physical of the formation of bubbles (cavities, or voids) in liquid media is followed by their collapse and the release of a large amount of energy, which is accompanied by noise and hydraulic shocks [1]. Cavitation occurs as a result of a local decrease in pressure in a liquid, which can occur either with an increase in its speed, for example, behind a ship's propeller (hydrodynamic cavitation), or with the passage of a high-intensity acoustic wave during a half-period of rarefaction (acoustic cavitation). There are other reasons for the appearance of the effect as a result of external physical influences. Moving with the flow to a region with a higher pressure or during a half-period of compression, the cavitation bubble collapses, while emitting a shock wave. Basically, cavitation has the same mechanism of action as a shock wave in air, which occurs at the moment a solid body overcomes the sound barrier. The leading role in the formation of bubbles during cavitation is played by gases released inside the formed bubbles. These gases are always contained in the liquid, and with a local decrease in pressure, they begin to vigorously evolve into these bubbles.

The phenomenon of cavitation is also used in the military industry [2]. The Shkval complex was put into service in 1977. The cruising speed of a supercavitation torpedo of 375 kilometers per hour is achieved by moving in a cavitation cavity (vapor bubble), which reduces water resistance, and using an underwater jet engine powered by solid hydroreactive fuel. The use of cavitation significantly reduces the possibilities for maneuver, and instead of the homing head, a receiver of sea water is installed in the nose of the rocket, which is necessary for the engine to operate. Supercavitation is the movement of a solid object in an aquatic environment with the formation of a "cocoon" around it, inside which there is only water vapor. Such a bubble significantly reduces the resistance of the water. It is inflated and supported by a special cavitator containing a gas generator for pressurizing gases.

The sustainable examples of the use of the phenomenon of microbubble cavitation can be seen in marine navigation. Recently, of practical interest is the "air lubrication" of the bottom with the creation of a thin air film that reduces friction and increases the speed of the ship. The first proposals for the use of air lubrication on ships appeared more than a hundred years ago. So, back in 1865, Scott Russell wrote about this in his book "Modern Systems of Marine Architecture". Another famous shipbuilder, William Froude, also mentioned this. In practice, the

Technology, Machine-building

first attempt to implement the idea of "transforming a surface in contact with water into a surface in contact with air" - a substance much less dense and viscous, was made in 1882 by the famous Swedish engineer-inventor Laval. He received a patent in England and built an experimental boat with air supply under the bottom through pipes. However, Laval failed to achieve a positive effect.

In 1887, mechanical engineer S. Timokhovitch made an application for granting him a privilege for "a method of reducing the friction of ships on water and sticking it to their surface." His idea was to supply air or water-oil emulsion to the underwater part of the hull through specially arranged pipes, the layout of which varied depending on the shape, purpose and dimensions of the vessel. In the United States, the first privilege to use a similar method was issued in 1911. The American engineer D. Moore proposed supplying air under a specially shaped bottom. The vessel was supposed to have a triangular shape and gradually turn into a back-keeled ("sea sled") in the stern. The air was supposed to flow under the hull through pipes brought out to the deck - through holes in the bottom, equipped with special visors-deflectors. The author believed that when the vessel is planing, the vacuum created by the deflectors will cause a natural suction of air under the bottom.

In the 1920s and 1950s, many researchers turned to the idea of "air lubrication". In the USSR, L.M. Lapshin, N.N. Kabachinskiy, L.G. Loitsiansky were engaged in this issue. K.K. Fedyaevskiy and other scientists. At the suggestion of L.M. Lapshin, the air was to be pumped by a special installation, and the bars placed along the bottom were to prevent it from leaking to the sides. In 1924, on the Livenka River, L.M. Lapshin began experiments with a rough model of a shallow-draft flat-bottomed river vessel measuring 2.5x0.22x0.02 m, and later continued experiments on a 25-meter plank. The air intake under the bottom gave an overall drag reduction of about 20%. It is also worth noting the experiments of N.N. Kabachinskiy with models that had a bottom of a special shape - with a recess of the "air bell" type. These experiments, carried out at the Gorky Industrial Institute in 1936, showed a decrease in the total resistance due to the supply of air under the bottom by 17%, and the frictional resistance by 30%.

After World War II, warships began experimenting with a system called the Prairie-Masker, which pushed bubbles through the hull and tips of the propeller blades in an attempt to disguise the acoustic signature of the ship's equipment as a defense against submarines. In the process, they also found that these bubbles increase the efficiency of the hull when moving in water. The first tests of full-scale air-lubricated vessels were carried out two years later. In the course of these experiments, it was possible to reduce the total resistance of a specially equipped wooden barge with a length of 25 m by 22.6%; in addition, an important fact was established of the dependence of the blowing efficiency on the air flow rate. During experiments in 1957, air supply under the bottom of a serial-built steel dry-cargo barge provided an increase in travel speed by about 6.5%, which corresponds to a decrease in drag by 20% [3].

The accumulated research experience is now being applied at the Japanese company Nippon Yusen Kaisha, which completed two years of experiments with air lubrication systems installed on two of the group's carriers, Yamato and Yamatai [4]. The air lubrication system effectively reduces the frictional resistance between the bottom of the boat and the seawater due to the bubbles generated when air is blown to the bottom of the boat. In fact, it was the world's first stationary blower system. The system was installed on two ships during their construction, and experiments were carried out during the sea voyage. After analyzing the data obtained by two vessels over two years under various weather and sea conditions, the optimal mode of bubble behavior control in real sea conditions was confirmed. Compared to a 10% reduction measured in sea trials, CO₂ emissions have been proven to be reduced by an average of 6% under various weather and sea conditions.

For nearly a decade, Samsung Heavy Industries and Mitsubishi Heavy Industries have been experimenting with "air lubrication" to reduce fuel consumption on flat-bottomed ships. To do this, there are many small holes on the bottom of the vessel. Air is pumped through them under the water. The resulting bubbles create an "air cushion" that saves 4-5% of fuel. For example, DSME built the first LNG tanker using bubble cavitation technology. DSME is considering the use of air lubrication systems for other types of vessels: LPG carriers, medium tankers and large container ships [5, 6].

Additionally, model tests of this technology have been carried out in the Marin test pools in the Netherlands [7]. Damen's R&D and Marinvention team developed a completely new concept that utilized a corrugated body design. After successful testing, the traditional flat-bottomed ship models were completely changed to an air-lubricated design. Results ranged from 5% to 40% fuel economy, with a total calculated annual savings of 15% with normal seaworthy design. It was noted that fuel economy improved at lower speeds. In addition, Marinvention found that it was much easier to make a corrugated bulkhead for meridian sailing directions. The height of the corrugations depends on where the force is applied - there is a less humid area - since the gaps are filled with air. There is also an underwater hull system that allows a small amount of air to pass to the propeller, which reduces propeller vibration.

In the research, it can be concluded that this method is effective in the pipeline transport industry. This porous structure approach can be applied to the internal polymer coatings of main steel pipelines. To introduce microbubble cavitation into large-scale use, it is necessary to carry out additional studies using computer modeling and make additional calculations to clarify the coefficient of hydraulic resistance, which affects the hydraulic resistance of the pipeline.

REFERENCES

1. Башта Т. М. «Машиностроительная гидравлика», М.: «Машиностроение», 1971.
2. Официальный сайт информационного портала «Военный обзор». Торпеда «Шквал» [Электронный ресурс] / Информационный портал «Военный обзор». – Режим доступа: <https://militaryarms.ru/boepripasy/torpedy/reaktivnaya-torpeda-shkval>. – Дата доступа: 15.02.2021.
3. Официальный сайт электронного журнала «Катера и яхты» / «Воздушная смазка» днища катера для уменьшения трения о воду [Электронный ресурс] – Режим доступа: http://www.barque.ru/shipbuilding/1971/air_lubrication_boat_bottom. – Дата доступа: 22.02.2021.
4. Официальный сайт электронной газеты «Работник моря» [Электронный ресурс] – Режим доступа: <http://seafarers.com.ua/maersk-is-testing-air-lubrication-system/5186/>. – Дата доступа: 05.04.2021.
5. Официальный сайт информационного портала «Нефтегаз» [Электронный ресурс] – Режим доступа: <https://yandex.by/turbo/neftegaz.ru/s/news/Suda-i-sudostroenie/507103-zakazchiku-peredan-pervyy-v-mire-gazovoz-spg-s-vozdushnoy-sistemoy-smazki>. – Дата доступа: 05.03.2021.
6. Интернет-сайт информационного новостного портала «Businessman» [Электронный ресурс] – Режим доступа: <https://businessman.ru/s/post/vozdushnaya-smazka-sdelaet-bolshie-sudna-bolee-effektivnyimi-i-menee-zatratnyimi-novaya-razrabotka-pozvolit-znachitelno-snizit-rashod-topliva-za-schet-millionov-kroshechnykh-puzyrkov.html>. – Дата доступа: 02.04.2021.
7. Официальный сайт компании «Damen» / Преимущество судов с применением воздушной смазки подводной части их корпусов [Электронный ресурс] – Режим доступа: <https://www.damen.com/ru-ru/innovation/some-key-projects/inland-ships-benefit-from-air-lubricated-hulls>. – Дата доступа: 06.04.2021.
8. Zhang, Hao Yan, Minghui Zhang, Qingshan Wu, Mingjie Liu, Lei Jiang, Cunming Yu, Mengfei Liu / Bio-inspired drag reduction: From nature organisms to artificial functional surfaces [Electronic resource] / – Press Agency «Elsevier». — Mode of access: <https://doi.org/10.1016/j.giant.2020.100017>. – Date of access: 18.02.2021.

RESTORING REGULATORY DEPTH OF TRUNK PIPELINES

N. BOGDANOVICH, L. SPIRIDONOK

Polotsk State University, Belarus

Aging of pipelines is accompanied by a change in the position of the pipeline, this occurs under the influence of changes in the landscape, due to natural and human influence. These changes can lead to emergencies that entail significant material damage and have a detrimental effect on the environment. It is necessary to restore the standard depth of the main pipeline to prevent accidents.

On the territory of the Republic of Belarus, the routes of trunk oil and product pipelines are laid in 6 technical corridors with a total length of 1233 km. The total length of all main oil pipelines in single-thread terms is about 4000 km.

The country's main gas pipelines cross the country from north to east and from south to west. Gas pipelines pass through a variety of landscapes (swamps, hills and water bodies).

Oil and gas transport enterprises annually carry out a set of measures for the diagnosis, maintenance and reconstruction of gas-oil-transport system facilities, automation of production processes, which contributes to their reliable and stable functioning [1-2].

The actual life of most trunk pipelines in the Republic of Belarus is approaching a period of increasing accidents. Aging of the pipelines reduces their reliability and increases the likelihood of accidents. The aging of pipelines is accompanied by a change in the position of the pipeline, this occurs under the influence of changes in the landscape, due to natural and human impacts. These changes can lead to emergency situations, which entails significant material damage and has a detrimental effect on the environment. Therefore, it is necessary to restore the normative depth of main pipeline.

Restoring regulatory depth of trunk pipelines

Introduction

On the territory of the Republic of Belarus, the routes of trunk oil and product pipelines are laid in 6 technical corridors with a total length of 1233 km. The total length of all main oil pipelines in single-thread terms is about 4000 km.

The Republic of Belarus also has a developed system of gas pipelines. Currently, gas supply to the Republic of Belarus and its transit to third countries is carried out by Gazprom Transgaz Belarus. The country's main gas pipelines cross the country from north to east and from south to west. Gas pipelines pass through a variety of landscapes (swamp landscapes, hills and the intersection of water bodies).[3]

Repair of sections of the linear part of the main pipeline with an abnormal depth is carried out in the following ways:

1) Restore the normative depth of the main pipeline sections without deepening (the first method can be applied in two ways)

- a) Restoration of the normative depth of bedding by filling with imported soil on uncultivated lands (slide)
- b) Restoring the normative depth of bedding by filling with imported soil on cultivated lands (slide)

2) Restore the normative depth of the sections of the main pipeline, with deepening (the second method can be applied in three ways)

- a) Digging
- b) Deepening with laying in a combined trench
- c) Deepening using soil jumpers

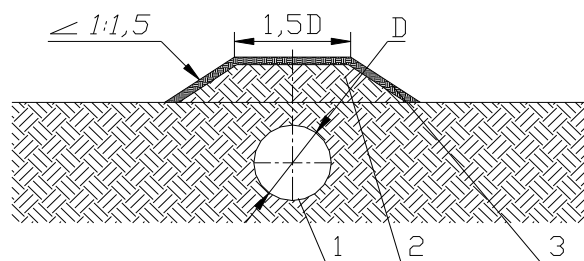
Ways to restore normative depth:

1) Restore the normative depth of sections of the main pipeline, without deepening

This method of restoring the normative depth can be used on uncultivated land or on areas of cultivated land. Such sections of the main pipeline can include: sections adjacent to the nodes of valves, intersections with field and forest roads and local property areas. Restoration of the standard depth is carried out by filling with imported soil, followed by compaction.

- a) Depth restoration on uncultivated lands.

Ground filling is carried out in the form of a roller. The soil must be leveled and compacted. Sand can be used as a soft bed for soil.



1 – main pipeline; 2 – mineral soil; 3 anti-erosion materials and structures

Fig.1. – Restoration of the normative depth of bedding by filling with imported soil on uncultivated lands

b) Depth restoration on cultivated lands.

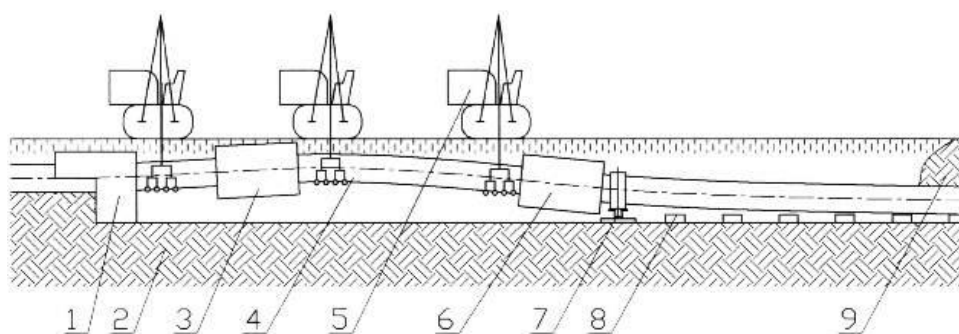
The normative depth on cultivated lands should be restored by pouring mineral soil and laying reinforced concrete slabs

2) Restoring the depth of sections of the main pipeline, with deepening.

This method of restoring the standard depth is used when it is impossible to use the recovery method with backfill

a) Deepening of the main pipeline with digging

The method of deepening a pipeline with digging without stopping the pumping can be used for pipelines of all diameters, in all soil conditions, except for rocky soils. Undercut excavation involves laying the main pipeline on supports of a given height and pouring with soil followed by compaction. Bags of non-rotting materials with a filler can be used as supports of a given height,.



1 – a digging machine or manual excavation; 2 – mineral soil; 3 – cleaning machine; 4 – MT; 5 – pipe layer; 6 – isolation machine; 7 – safety support; 8 – support of a given height; 9 – mineral soil backfill

Fig.3. – Deepening main pipeline with a tunnel

b) Deepening of the main pipeline with laying in a combined trench

The method of deepening the main pipeline with laying in a combined trench is used in the absence of the possibility of deepening extended sections of the linear part. This method consists in laying the pipeline in a parallel trench dug up to the standard depth in advance. The scheme is shown in (Figure 4)

c) Deepening of the main pipeline using ground lintels.

The method of deepening of the main pipeline using ground lintels is used in case of deformation of the pipeline being repaired. The main pipeline section is deepened by decreasing manually the height of the ground lintels (supports), with uniform removal and gradual placing of the main pipeline on the ground. For the optimal depth restoration of the main pipeline it is necessary to study the position relative to the horizon of the earth, pipes and the territory where the main pipeline is laid. [4]

Conclusion. The development of optimal methods for repairing pipelines will reduce the cost of the repair process and increase the safety of main pipelines. This approach to the choice of repair was used in the development of the enterprise standard for OAO Gomeltransneft Druzhba.

REFERENCES

1. Закон Республики Беларусь «Об охране окружающей среды» от 26 ноября 1992 года № 1982- XII.

Technology, Machine-building

2. ГОСТ 12 3 016-87 Система стандартов безопасности труда. Строительство. Работы антикоррозионные. Требования безопасности.
3. РД Технология ремонта трубопроводов в местах недостаточной глубины залегания. Методика расчёта технологических параметров заглубления трубопроводов – М: ОАО ВНИИСТ, 2008.
4. Инструкция по производству работ в охранных зонах магистральных трубопроводов. Утверждена постановлением Проматомнадзора от 29 мая 1998 г. № 6 с учётом изменений внесённых постановлением МЧС от 01 апреля 2002 г. № 7.

UDC 532.5

COMPARISON OF OPERATION OF PHYSICAL AND SIMULATION MODEL OF PROPORTIONAL DISTRIBUTOR

V. ARTEMIEV, A. NEVZOROVA

Gomel State Technical University named after Sukhoi, Belarus

The paper presents the development of a test bench for a proportional valve using Festo equipment and a simulation of the bench operation in the Fluidsim software. Analysis of the data obtained allows us to conclude that the developed simulation model adequately describes the behavior of a real object.

Introduction. Modern hydraulic drives are complex mechatronic systems, in the design of which it is necessary to take into account the operation of the hydraulic drive itself, the electronic control system, the kinematics and dynamics of the machine movement. The creation of a new technical object is a complex and time-consuming process, in which the design stage is of decisive importance in the implementation of the idea and achievement of a high technical level. Modeling is one of the most important stages in the design of any technical object, including modern hydraulic systems, allowing you to replace or significantly reduce the stages of adjustment and field tests [1].

To simulate the operation and control of hydraulic drive systems, a program developed by Festo Didactic is used in most part to design hydraulic drive and hydraulic circuits with manual, electric and electronic control [2]. Such a program makes it possible to study the work of the compiled circuits in various modes using animation [3, 4].

Simulation modeling makes it possible to solve the problems of control, regulation, statics, kinematics, dynamics and power engineering of hydraulic mechanisms from a single methodological point of view and represents the unifying core of the calculation complex.

Purpose of work - to create a physical model of a test bench for a proportional valve of wide application using Festo equipment and to simulate the operation of the bench in the FluidSim software.

Research methods. For the development of the stand, instrumentation was used, as well as hydraulic control equipment and a tested hydraulic valve from Festo.

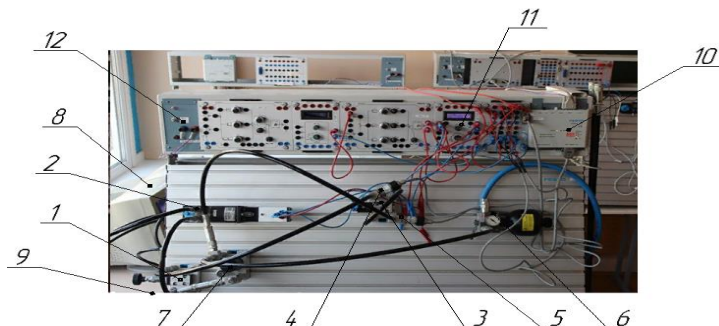
For the test bench, I-30A oil was used. The preparation of the research began with the preparation of the liquid - heating (cooling) to a given temperature.

The stand of the hydroelectric power station was located in a room with an ambient temperature of $5 \pm 2^\circ \text{C}$, providing conditions close to the working one. When the pump is turned on, the oil overflows through the safety valve (Fig. 1, item 1), due to which it gradually heats up to the required temperature. The liquid temperature is monitored by a tank thermometer and a temperature sensor (fig. 1, pos. 4). Then the oil enters the battery capacity, while the battery is being charged (Fig. 1, pos. 6). As soon as the heating of the fluid reaches the required temperature, the hydraulic unit is turned off. In this case, the valve spool is brought to the closed position, the oil value is set.

With the closed position of the valve spool (Fig. 1, item 3), the amount of fluid leakage was determined.

With the help of the control device (pos. 11 Fig. 1), the proportional magnet of the valve was used to regulate the value of the current at which the movement of the valve spool begins, which corresponds to the force of displacement of the spool in a directly proportional relationship.

To determine the time moment of the start of movement of the distributor spool, a flow meter was used (item 2, Fig. 1), since when the spool is displaced, the fluid passage into the control line of the distributor opens. The readings of the control and measuring devices were displayed in real time on a computer monitor. Measurements for each experiment were carried out 3 times with constant specified parameters.



- 1 - pressure valve; 2 - flow meter (0 - 10 V, 0-10 l / min); 3 - tested valve; 4 - temperature sensor (20-30V, 0-100 ° C);
5 - pressure sensor (15 - 30V, 10 MPa); 6 - battery (6 MPa); 7 - filter (5 μ m); 8 - personal computer (PC);
9 - pumping station; 10 - analog converter providing communication with PC;
11 - proportional magnet control device, 12 - power supply

Fig. 1. – Research stand

Then, based on the physical model of the stand, a simulation model was developed in the form of a hydraulic circuit (Fig. 2) and its operation was checked. This simulation model allows you to see how oil flows through the system and how the valve spool opens.

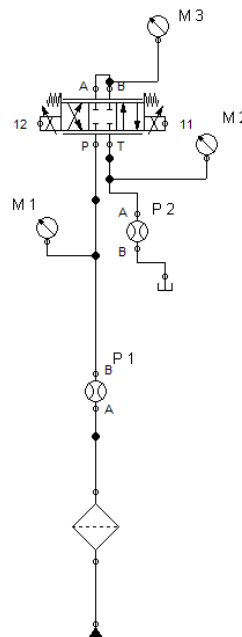


Fig. 2. – The created circuit in the FluidSim program

Results. The following was taken as the initial data: oil consumption 5 l / min and pressure 2.5 MPa. The results of the physical model (Fig. 3) and the simulation model (Fig. 4) were compared.

According to the work of the test bench of the proportional distributor, the following indicators were obtained:

- flow rate 2.5 l / min;
- pressure at the inlet, after the distributor and at the outlet from 2 to 3 bar.
- temperature 2.50C.

According to the work of the simulation model of the proportional valve test bench:

- flow rate from 0 to 5 l / min;
- inlet pressure from 0 to 2.5 MPa;
- pressure after passing through the distributor from 0 to 1.2 MPa;
- outlet pressure from 0 to 0.0035.

By establishing the adequacy, the result did not reveal design and technical errors in the real and simulation schemes. The formulated simulation model allows you to obtain a high level of adequacy in the study of the scheme using the algorithm of the FluidSim program.

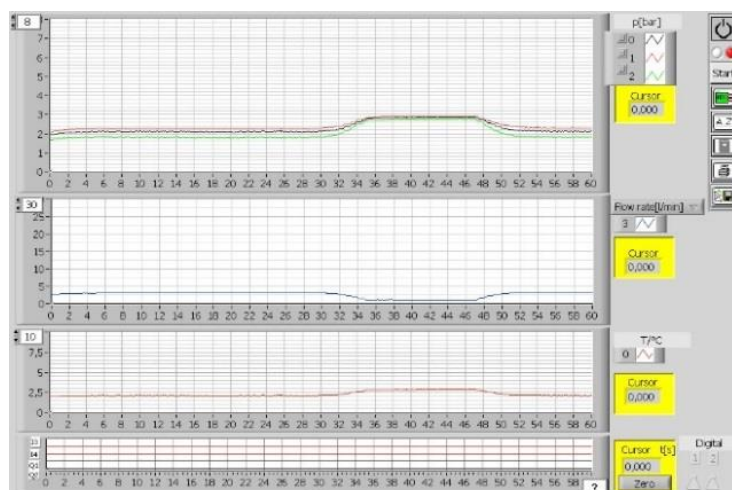


Fig. 3. – Screenshot of test bench measurements

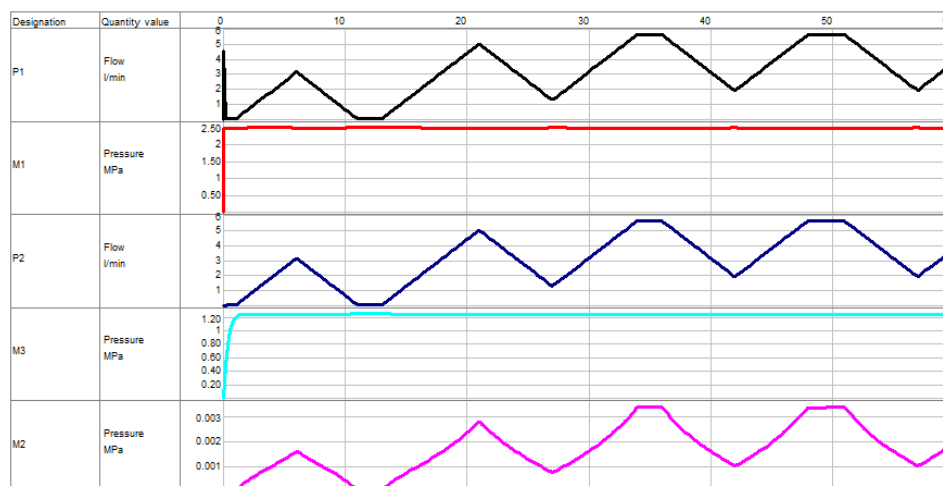


Fig. 4. – The result of the simulation model of the created program FluidSim

Conclusion. Based on the results obtained, we conclude that the developed calculation method allows us to build a simulation model that correctly reproduces the operation of the distributor regulator in a given hydraulic system (at the stand), and the results obtained allow us to understand some subtle points in the specifics of its work, which is of practical interest and can be used in mechanical engineering, machine tool building, and combine building to simulate the work of the designed hydraulic units.

REFERENCES

1. Shornikov Yu. V., Myandin S. A. Computer modeling of hydraulic systems // Young Scientist. - 2017. - No. 22. - S. 104-110.
2. Borovikov A.V. Research of hydraulic drive operation using fluidsims program // International student scientific bulletin. - 2019. - No. 5-1.
3. Sbrodov, N.B. Design and modeling of electropneumatic automation systems. Methodical instructions for practical exercises. - Kurgan, 2015.-30 p.
4. Hydro-pnevmo.ru. Calculations, design. Design documentation. In which program to create hydraulic and pneumatic circuits. [Electronic resource] - Access mode: <http://www.hydro-pnevmo.ru/topic.php?ID=7...> - Date of access: 13.04.2021.

CHARGE ELECTRIC VEHICLES

HUANG NAN, A. ADAMOVICH

Polotsk State University, Belarus

The advantages and disadvantages of charging stations for electric vehicles, including domestic and public ones, are considered. Methods of charging electric vehicles and the problems of frequent charging are considered. The existing problems arising during the operation of batteries are listed.

The development of electric vehicles includes the research and development of electric vehicles and energy supply systems. The energy supply system refers to charging infrastructure, power supply, charging and battery systems, and energy supply modes. Electric vehicle charging technology is a new field of science and technology. Countries all over the world are involved in the research of charging technology and plan to make charging technology standards, which will take the lead in the development of future enterprises.

At present, the lack of integrated technology for power supply, charging and battery system application and related standards and specifications is still the main weak link in the promotion and application of electric vehicles, which brings great difficulties to the next development of electric vehicles and the unified planning of charging facilities. There is no mature product for the charging station monitoring system that can ensure the normal operation of large-scale charging stations. There is no unified standard for the communication protocol and communication interface between the charging station monitoring system and the charger, and there is no information connection between charging stations.

Commonly used charging modes of electric vehicles. According to the technology and usage characteristics of electric vehicle power battery packs, there are certain differences in the charging modes of electric vehicles. For the selection of charging schemes, there are currently three modes of household charging piles, public charging piles and battery replacement.

The first is a household charging pile. When buying an electric car, a home charging pile is generally given with the car, and technicians will be arranged to install and debug at the door. The charging time of this charging method is not bad, and it will vary with the brand and model of the vehicle, but the premise is There must be a parking space, and the property allows you to install household charging points in the parking space.

The second way is public charging piles. The advantage of this charging method is that you can choose between DC fast charging and AC slow charging according to the actual situation, and it is also the only place that supports DC fast charging, but the disadvantages are also obvious. Public charging piles are currently under construction and difficult to find. It is not easy to take up afterwards, and the charging cost is relatively high.

The third charging method is to change the battery. This is also the last trick for electric vehicles. Specially trained technicians can replace the battery within 2-10 minutes through fully automatic or semi-automatic technology to achieve electrical energy replenishment, so as to achieve a speed comparable to that of fuel vehicles. But this The shortcomings of this method are also obvious. It can only be operated by professionals in professional locations, and the replacement of batteries is uneven, which is worrying.

Generally speaking, the charging methods of electric vehicles are more flexible and diverse. You can choose the charging method scientifically and reasonably according to your actual situation. This can not only achieve the normal use of electric vehicles, but also save charging costs, and is economical.

The main factor affecting the safety of electric vehicles is the charging process of the battery. The inconsistency of battery technology is one of the basic characteristics shared by all types of batteries, which is mainly manifested in the capacity error, internal resistance error and voltage error of the battery. The consistency error of a few batteries is not obvious, but the capacity error, internal resistance error and voltage error of the electric vehicle battery pack composed of dozens or even hundreds of battery cells will become prominent. In the process of electric vehicle charging, it is impossible to sequentially charge the battery cells, but to charge the entire battery pack. During the charging process, due to the internal resistance error, the voltage at both ends of the battery cells in the entire battery pack forms an error. The larger the internal resistance error, the more obvious the voltage error formed. Although the charging voltage at both ends of the entire battery pack will not exceed the rated voltage, the voltage at both ends of an individual single battery may exceed its rated voltage, which may easily lead to unbalanced charging of the battery pack and different charging capacities of single batteries. If the voltage error of the battery is too large, it may exceed the safe capacity of battery charging, causing the battery to overheat and cause an accident. Therefore, the charging device for electric vehicles must have technical measures to prevent the battery system cell voltage and temperature from exceeding the allowable value to improve the safety of the electric vehicle charging process.

Electric vehicles can also make full use of the surplus electricity during the night when the electricity is low for charging, so that the power generation equipment can be fully utilized day and night, and its economic benefits are greatly improved. It is these advantages that make the research and application of electric vehicles a "hot spot" in the automotive industry.

REFERENCES

1. 周建伟 · 吴方捷. 新能源电动汽车充电技术研究[J]. 决策探索, 2020(01): 96.
2. 刁力鹏 · 张亮 · 曾雁鸿. 新能源电动汽车充电技术与应用浅析[J]. 电器工业 · 019(10):70 - 73.

WASTE OF THE AGROINDUSTRIAL COMPLEX OF TURKMENISTAN AS A RAW MATERIAL BASE FOR OBTAINING OIL SORBENTS

G. ANNAYEV, S. YAKUBOUSKI, Y. BULAUKA

Polotsk State University, Belarus

The physicochemical and sorption properties of such wastes of the agro-industrial complex of Turkmenistan as seed husks, tumbleweeds and cotton bolls have been studied as a potential raw material for the production of oil sorbents.

Introduction. In recent years, agriculture has been rapidly developing in Turkmenistan along with other sectors of the economy and is one of the most significant sectors of the country's modern economy. The main types of agricultural crops are wheat, cotton, rice, sugar beet, fodder, vegetable and melon and fruit and berry crops. At present, all efforts of the state in the field of waste management are aimed at finding alternative ways of their rational use.

At the same time, there are two large oil refineries in Turkmenistan, one of which is the "Turkmenbashi complex of oil refineries" located on the shores of the Caspian Sea, which determines a significant risk of oil spills.

Oil and its components, getting into the environment, be it air, water or soil, cause a change in their physical, chemical and biological characteristics, disrupting the course of natural biochemical processes [1]. The problem of localization and elimination of emergency spills of oil and oil products lies not only in its scale, but also in the development of criteria and effective methods for combating this complex and variable in its composition pollution [1,2]. That is why the study, development of methods and technologies for the localization and elimination of emergencies associated with the spill of oil and oil products in the process of their transportation and movement is currently an urgent and important task.

Despite the developments in this direction, in recent years, a search has been actively carried out in the field of obtaining new inexpensive oil sorbents for collecting hydrocarbon spills. The issues of studying the collection of oil and oil products from various surfaces, as well as assessing the effectiveness of the use of sorbents based on wood waste and crop waste, have not been given sufficient attention, which helped to determine the purpose of this study [3-22].

Task formulation. The actual direction of research at the present time is the study of wastes of the agro-industrial complex of Turkmenistan as a raw material base for the production of oil sorbents.

Methods of research. The study determined the physicochemical properties of the wastes of the agro-industrial complex of Turkmenistan, namely: humidity according to GOST 12597-67, bulk density according to GOST 16190, hydrogen index according to GOST 32327-2013, adsorption activity for iodine according to GOST 6217-74 and adsorption activity for methylene blue in accordance with GOST 4453-74.

Results, their discussion and perspectives. The following samples of fractions with a particle size of 0.25-1 mm were used for the study: sunflower seeds (seed peel), tumbleweed (prickly), tumbleweed (soft), cotton bolls. For them, the main physical and chemical properties are determined, the generalized results are presented in Table 1.

Analysis of the results given in Table 1 made it possible to conclude that the moisture content in the wastes of the agro-industrial complex of Turkmenistan is from 2 to 7.5% by weight, which indicates a high ability to dry the samples; potentiometric titration established that the aqueous extract has a weakly acidic environment, and the bulk density of the samples is on average 100 ... 110 g / 100 cm³, which is comparable with industrial sorption materials.

Almost all samples, except for thorny tumbleweed, have a similar adsorption activity with respect to iodine with the enterosorbent of the Polypham brand (23-24%), i.e. almost the same microporosity (pore size about 1 nm). The adsorption activity (capacity) for methylene blue, the molecule of which has relatively large linear dimensions and molar mass, indirectly characterizes the sorption capacity in relation to petroleum products [1-4]. It was found that the adsorption activity for methylene blue of the test samples from the wastes of the agro-industrial complex of Turkmenistan is similar to this indicator for activated carbon (210 mg / g) and "Polyphepan" (125.8 mg / g).

Table 1. – Physicochemical properties of agro-industrial waste in Turkmenistan

Sample name	Sunflower seeds (Helianthus annuus)	Cotton bolls (Gossypium)	Tumbleweed (Rollin stone)	
			prickly	soft
1	2	3	4	5
Moisture,% mass according to GOST 12597-67	3.5	6.5	7.5	2.0

The ending of table 1

1	2	3	4	5
Bulk density, g / 100 cm ³ in accordance with GOST 16190	99.84	104.09	110.11	107.09
Hydrogen exponent, pH of water extract according to GOST 32327-2013	5.0	4.4	5.5	4.9
Adsorption activity for iodine, % according to GOST 6217-74	21.08	20.2	13.6	20.5
Adsorption activity for methylene blue, mg / g according to GOST 4453-74	127.5	88.0	98.75	347.5

Conclusion. Thus, the obtained results of the study of wastes of the agro-industrial complex of Turkmenistan make it possible to predict their high ability to sorb oil and oil products. Utilization of such large-tonnage waste as an inexpensive volumetric porous sorbent in the technological processes of purification, concentration and removal of oil products is a promising direction that will reduce the burden on the environment and obtain an economic effect.

REFERENCES

1. Emergency sorbents for oil and petroleum product spills based on vegetable raw materials / Y A Bulauka, K I Mayorava, Z Ayoub // IOP Conference Series: Materials Science and Engineering. – 2018. – Vol. 451 (1).- art. no. 012218.- DOI: 10.1088/1757-899X/451/1/012218.
2. Получение сорбента для сбора нефти и нефтепродуктов при их разливах путем утилизации отходов агропромышленного комплекса / Якубовский С.Ф., Булавка Ю. А., Майорова Е. И. // Вестник Полоцкого государственного университета. Серия В, Промышленность. Прикладные науки. - 2017. - № 11. - С. 84-89.
3. Рациональное использование отходов сельского хозяйства в целях снижения экологического ущерба от разливов нефти/Ю.А. Булавка, С.Ф. Якубовский, Е.И. Майорова// Вестник НЦБЖД- 2019. - № 1(39). - С. 71-78.
4. Использование отходов агропромышленного комплекса для получения нефтяных сорбентов /Булавка Ю.А., Якубовский С.Ф., Майорова Е.И.//XXI век. Техносферная безопасность. 2017. Т. 2. № 4 (8). С. 38-47.
5. Использование отходов сельского хозяйства в целях снижения экологического ущерба от разливов нефти/ Майорова Е.И., Якубовский С.Ф., Булавка Ю.А.// Системы обеспечения техносферной безопасности: материалы V Всероссийской научной конференции и школы для молодых ученых (с международным участием) (г. Таганрог 4-5 октября 2019 г.) – Таганрог: ЮФУ, 2019. – С. 69-70.
6. Вовлечение отходов сельского хозяйства в производство нефтяных сорбентов /Е.И. Майорова, С.Ф.Якубовский, Ю.А. Булавка//Наука. Технология. Производство – 2019: материалы Международной научно-технической конференции, посвященной 100-летию Республики Башкортостан / редкол.: Н.Г. Евдокимова и др. – Уфа: Изд-во УГНТУ, 2019. –С.330-332.
7. Рациональное использование отходов сельского хозяйства в целях снижения экологического ущерба от разливов нефти / Ю.А. Булавка, С.Ф. Якубовский, Е.И. Майорова// Инновационные подходы к решению проблем «Сендайской рамочной программы по снижению риска бедствий на 2015 – 2030 годы»: сборник материалов международной научно-практической конференции, 19 – 20 октября 2018 г. – Казань: Изд-во КНИТУ-КАИ, 2018. –С.215-219.
8. Использование отходов сельского хозяйства в производстве сорбционных материалов для сбора нефти и нефтепродуктов / Булавка Ю.А., Якубовский С.Ф., Майорова Е.И. //IX Сибирская конференция молодых ученых по наукам о Земле: материалы конференции / Ин- т геологии и минералогии им. В. С. Соболева СО РАН, Ин-т нефтегазовой геологии и геофизики им. А. А. Трофимука СО РАН, Новосиб. гос. ун-т. – Новосибирск: ИПЦ НГУ, 2018. - С.85-87.
9. Ликвидация аварийных разливов нефти и нефтепродуктов с использованием сорбента/ Майорова Е.И., Якубовский С.Ф., Булавка Ю.А.// Сборник тезисов докладов 73-й Международной молодежной научной конференции «Нефть и газ – 2019» (22-25 апреля 2019 г. Москва). – Том 5.– М.: Издательский центр РГУ нефти и газа (НИУ) имени И.М. Губкина, 2019. –С.470-471.
10. Природные сорбирующие материалы для ликвидации нефтяных загрязнений /Майорова Е.И., Булавка Ю.А. // Безопасность – 2019 : материалы докладов XXIV Всероссийской студенческой научно-практ. конф. с междунар. участием «Проблемы экологической и промышленной безопасности современного мира» (г. Иркутск, 16–19 апр. 2019 г.). – Иркутск : Изд-во ИРНИТУ, 2019. –С.277-278.

Technology, Machine-building

11. Особенности микроструктуры отходов сухой окорки сосны как сырья для получения нефтяных сорбентов / С.Ф. Якубовский, Н.В. Ощепкова, Ю.А. Булавка, С.С. Писарева, Л.А. Попкова // Вестник Полоцкого государственного университета. Сер. В, Прикладные науки. - 2011. - № 11. - С. 154-157
12. Микропористость сорбентов на основе растительной биомассы/ С.Ф. Якубовский, Ю.А. Булавка, С.С. Писарева, Л.А. Попкова// Техника и технология защиты окружающей среды: материалы докладов Международной научно-технической конференции. – Минск: БГТУ, 2011.-С. 136-139.
13. Нефтяные сорбенты на основе растительной биомассы/ С.Ф. Якубовский, П.В. Коваленко, Ю.А. Булавка// Надежность и безопасность магистрального трубопроводного транспорта: материалы VII междунар. научн-техн. конф., г. Новополоцк, 22-25 ноября 2011г. / Полоцк. Гос. Ун-т; под общ. ред. д-ра техн. наук, проф. В.К. Липского. - Новополоцк, 2011.-С.242-244.
14. Растительная биомасса – альтернативное сырье для получения нефтяных сорбентов / Якубовский С.Ф., Коваленко П.В., Булавка Ю.А. // Надежность и безопасность магистрального трубопроводного транспорта: сб. науч. тр. / Полоц. гос. ун-т; под общ. ред. д-ра техн.наук, проф. В. К. Липского. – Новополоцк, 2011. – с.262-265.
15. The microporosity of sorbents which based on the plant material /S. Pisarava, Y. Bulauka// Materials of IV junior researchers' conference «European and National dimension in research», Polotsk State University, Novopolotsk, April 25 - 26, 2012: in 3 p. - Novopolotsk: PSU, 2012. - Issue 4. Part 3: Technology. p. 82-84.
16. Нефтяные сорбенты на основе растительной биомассы/ Писарева С.С., Попкова Л.А. Якубовский С.Ф., Булавка Ю.А // Нефть и газ – 2012: сборнике тезисов 66-й Международной молодежной научной конференции (г. Москва, 17-20 апреля 2012 г.).- Москва: РГУ нефти и газа им. И.М. Губкина, 2012 . -С.409.
17. Исследование влияния концентрации гидроксида натрия на выход веществ фенольной природы из коры сосны /Писарева С.С., Попкова Л.А., Якубовский С.Ф., Булавка Ю.А. //Новые материалы и технологии их обработки: сборник научных работ XIII Республиканской студенческой научно-технической конференции: [23-27 апреля 2012 г.] / Белорусский национальный технический университет, Механико-технологический факультет. – Минск: БНТУ, 2012. –С.268-270.
18. Ликвидация аварийных разливов нефти и нефтепродуктов сорбентами на основе растительной биомассы/ Попкова Л.А., Писарева С.С., Булавка Ю. А. Якубовский С. Ф. // Обеспечение безопасности жизнедеятельности: проблемы и перспективы: сборник материалов VII международной научно-практической конференции курсантов (студентов), слушателей магистратуры и адъюнктов (аспирантов). – В 2-х ч. Ч.1. – Минск: КИИ, 2013. – С.183-184.
19. Нефтяные сорбенты на основе отходов переработки древесного целлюлозосодержащего растительного сырья/ Булавка Ю. А., Попкова Л.А., Писарева С.С., Якубовский С. Ф.// Наука – образованию, производству, экономике : материалы XVIII(65) Региональной научно-практической конференции преподавателей, научных сотрудников и аспирантов, Витебск, 13–14 марта 2013 г. / Вит. гос. ун-т ; редкол.: А.П. Солодков (гл. ред.) [и др.]. – Витебск : ВГУ имени П.М. Машерова, 2013. – Т. 1. – С.63-65.
20. Adsorption of petroleum products on sorbents which based on the plant material / L.Papkova, Yu. Bulauka // Materials of V junior researchers' conference «European and National dimension in research», Polotsk State University, Novopolotsk, April 24 - 25, 2013: in 3 p. - Novopolotsk: PSU, 2013. - Part 3: Technology. p. 87-89.
21. Сорбционные свойства природных целлюлозо- и лигнинсодержащих отходов для сбора проливов нефтепродуктов/ С.Ф. Якубовский, Ю.А. Булавка, Л.А. Попкова, С.С. Писарева // Вестник Полоцкого государственного университета. Сер. В, Промышленность. Прикладные науки.– 2013. – № 11. С.110-115.
22. Анализ адсорбционной активности по метиленовому синему отходов деревообработки и растениеводства/ Якубовский С. Ф., Попкова Л.А., Писарева С.С., Булавка Ю. А. // Химия и технология растительных веществ: Тезисы докладов VIII Всероссийской научной конференции. Сыктывкар-Калининград. 2013. - С.265.

UDC 621.9.06 + 536.75

FEATURES OF DETERMINING LABOR INTENSITY OF THE DESIGN AND TECHNOLOGICAL CUTTING TOOLS PRODUCTION PREPARATION

I. KHMIALNITSKAYA, N. POPOK

Polotsk State University, Belarus

Three levels of cutting tools indicators are considered; coefficients of acceptability, durability, accuracy and cost cutting tools are proposed, and desirability of coefficients set, which makes it possible to evaluate the effectiveness of cutting tools use at the design and technological production preparation stage.

Specific features of determining the production preparation labor intensity. In modern conditions of frequent production diversification the approach to determining the manufacturability coefficients should be refined for the design and technological production preparation. In particular, it is necessary to determine the frequency and duration of the use tools and equipment in the production process.

The details number and the frequency of structural elements meeting the same type in terms of their characteristic standard size, for example, the diameter of the hole in the parts, are determined in the product [1]. At the same time, in the process of design preparation for production, the structural elements sizes are estimated, which determine their production by cutting tools. Further, if necessary, in the process of technological production preparation, the duration of the use auxiliary tools and equipment, machines and devices is taken into account.

Statistical data analysis can be represented by histograms of the frequency and duration of the encounter and the use structural elements, cutting and measuring tools, etc.

Those constructive elements and, accordingly, tools that are rare, can be unified and replaced with frequently occurring ones.

The efficiency of using the cutting tool at the first level can be estimated by the coefficient of the conditional duration of use.

$$C_{Ui} = F_i \cdot D_i, \quad (1)$$

where F_i and D_i - the frequency and duration of the detail element meeting and the use of the cutting tool, respectively.

Tools that are common and can be replaced by new, more effective ones should be evaluated by the second level indicators. This compares the indicators of the basic (previously used) and new instruments.

The criteria can be used:

tool life coefficient:

$$C_{TL} = F_N / D_B, \quad (2)$$

where T_N and T_B - the durability periods of the new and basic instruments, respectively;

detail material machinability coefficient:

$$C_M = V_N / V_B, \quad (3)$$

where V_N and V_B - cutting speeds with new and basic tools, respectively;

precision and quality coefficient:

$$C_{PQ} = (IT, Ra)_B / (IT, Ra)_N, \quad (4)$$

where $(IT, Ra)_B$ and $(IT, Ra)_N$ - the precision and roughness of the machined surface of detail structural element with the basic and new cutting tool, respectively.

Indicators or criteria of the third level characterize the cutting tool at the manufacturing stage. In particular, the cost coefficient of the cutting tool:

$$C_{COST} = C_B / C_N, \quad (5)$$

where C_B and C_N - the cost of the basic and new cutting tools, respectively;

Technology, Machine-building

payback coefficient of the cutting tool:

$$C_{PB} = COST_N / (C_B - C_N), \quad (6)$$

where $COST_N$ - costs for a new cutting tool.

The effectiveness of one or more candidate tools can be assessed at each of the given levels or in aggregate in points:

$$C_{EF} = C_U \cdot C_{TL} \cdot C_M \cdot C_{PQ} \cdot C_{COST} \cdot C_{PB}, \quad (7)$$

or by the generalized desirability function:

$$C_{DEF} = f(C_U, C_{TL}, C_M, C_{PQ}, C_{COST}, C_{PB}). \quad (8)$$

The cutting tool with the highest C_{EF} score is considered the most effective.

Desirability refers to one or another level of a parameter or criterion for assessing the effectiveness of the cutting tool use. On a special scale, the desirability value can vary from 0 to 1 (fig. 1).

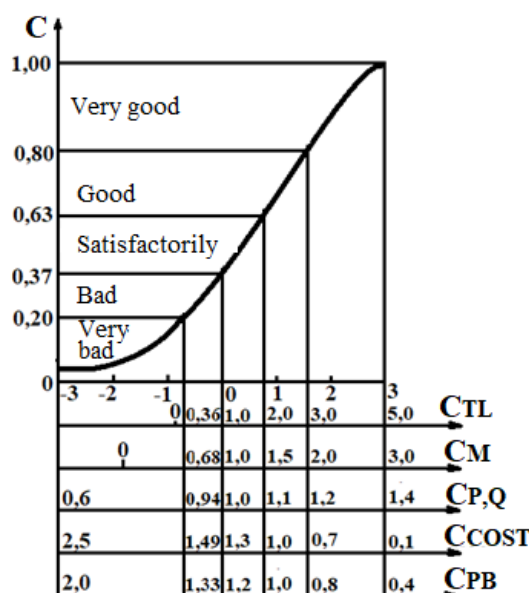


Fig.1. – Generalized desirability function of efficiency coefficient set of the tool use in production

The values of $C_{DEF} = 1$ correspond to the maximum possible criterion level, and $C_{DEF} = 0$ - the minimum.

The desirability function is described by the expression:

$$C_{DEF_i} = \exp(-\exp(C_i)), \quad (9)$$

where C_i - the dimensionless value of a parameter or criterion, given in accordance with the desirability scale. The generalized desirability function is formed as the geometric mean of the desirability parameters:

$$C_{DEF} = \sqrt[n]{C_{DEF_1} \cdot C_{DEF_2} \cdot \dots \cdot C_{DEF_n}}. \quad (10)$$

Conclusion. As a result, to determine the effectiveness of the tool use an expert system has been proposed, which includes: a database on certain parameters of products, parts, cutting and measuring tools and other objects of the technological environment; analysis methods using mathematical statistics of the frequency and duration of the detail elements, tools and other objects meeting; procedures for assessing the condition of the instrument at the stages of its manufacture, operation and disposal.

REFERENCES

1. Попок, Н.Н. Мобильная реорганизация машиностроительного производства / Н.Н. Попок. – Минск: Технопринт, 2001. – 396 с.

UDC 621.37/39(075.8)

COMMUNICATION 5 GENERATION

N. SYTOVA, V. YANUSHKEVICH

Polotsk State University, Belarus

This article discusses the construction of the fifth generation networks. Their characteristics are considered. Development prospects are analyzed.

The telecommunications market is developing dynamically. Creation of communication networks of the next generation 5G is the main condition for the development of the information society and the digital economy. The main advantages of 5G networks are high access speed with minimal delays, support for many concurrent devices, high energy efficiency. Fifth-generation networks will provide an opportunity to introduce smart home technologies, smart cities, artificial intelligence, the Internet of Things, and unmanned vehicles into everyday life.

The main requirements for the 5G standard, which are put forward by the International Telecommunication Union:

- data transfer rate in Downlink mode - up to 20 Gbps;
- data transfer rate in Uplink mode - up to 10 Gbps;
- the number of supported devices in an area of 1 square kilometer - at least 1 million;
- delay for eMBB (high-speed communication) services - no more than 4 ms;
- delay for URLLC (ultra-reliable communication) services - no more than 0,5;
- for point-to-point connections, it is also planned to use additional bands 71-76 and 81-86 GHz.

These requirements are achieved at the expense of multichannel (parallelism in frequencies and base stations), increasing the carrier radio frequencies from units to tens of GHz (radio channel bandwidth).

The alignment of standard 4G and 5G by technical characteristics is shown in table 1

Table 1. – Comparison of 4G and 5G standards

Network Generation	Maximum throughput, GBits/sec		Network latency, ms	Spectral efficiency bit/Hz		Device connection density per 1 sq. m
	Uplink	Downlink		Uplink	Downlink	
4G	1,5	3	5	15	30	—
5G	10	20	0,5 — 4	6,75	15	1 million

For networks of the fifth generation, it is proposed to use the radio frequency ranges of 700 MHz, 3.6 GHz, 26 GHz. Low frequencies range 600-850 MHz provide full coverage of the territory. This is about the same range that existing 4G networks use, with a data transfer rate of 50–250 Mbit/s. 5G-compatible devices can connect to low-frequency 5G networks and operate at speeds similar to those of 4G / LTE networks.

The medium frequency range of 2.5-3.7 GHz provides the ability to transmit data at a speed of 100-900 Mbit /s. Despite the smaller coverage radius of each cell tower, this type of 5G will become the most common practical solution for 5G networks for many years. This is a good ratio between the speed of the network and the signal propagation range-both in urban areas with an average density of buildings, and in rural areas with less dense buildings.

High frequencies in the 25-39 GHz range are required for applications that require high data rates. The disadvantage of high-frequency 5G networks is that millimeter-wave transmitters have a very limited coverage radius. The normal operation of the network requires the installation of many small transmitters, and this is only possible in urban agglomerations, where transmitters can be installed near buildings.

When implementing fifth-generation networks, the following disadvantages must be taken into account: the availability of the radio frequency spectrum, compliance with the requirements for protection from the effects of electromagnetic fields created by base stations, payment for the allocation and use of the radio frequency spectrum for the 5G standard.

In Belarus, 5G networks were tested by operators MTS, Unitary Enterprise A1, Belarusian Cloud Technologies, Beltelecom in the cities of Minsk, Kopyl (fig.1), Gomel, the Great Stone Industrial Park.

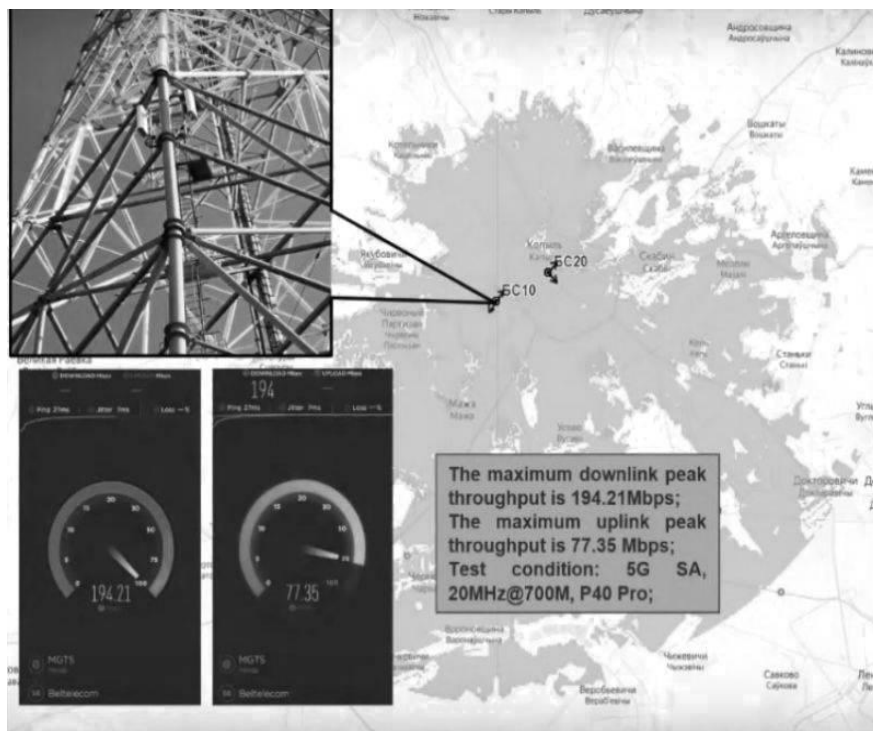


Fig.1. – 5G test in Kopyl

The conditions for the use of the radio frequency spectrum are developed after the definition of a model for the implementation of 5G networks.

The infrastructure model involves the construction of 5G infrastructure by a single operator.

The competitive model involves the construction of a passive and active 5G network infrastructure by each of the operators. In order to optimize costs, it is assumed that operators will jointly participate in the construction of transport infrastructure – fiber-optic communication lines.

The passive infrastructure sharing model involves the construction of an active 5G network infrastructure by each of the operators within the allocated radio frequency spectrum, and the construction of a passive infrastructure – a transport network, antenna-mast structures, fiber-optic communication lines-by a single infrastructure operator. The joint use of active and passive infrastructure can be carried out by all operators, provided that appropriate changes are made to the legislation governing the use of the radio frequency spectrum.

The basic principles of building 5G networks are as follows: the division of network nodes into elements, the division of network elements into network layers (Network Slicing), implementation of network elements in the form of virtual network functions (Virtual Network Functions), support for simultaneous access to centralized and local services, defining a converged architecture, combining different types of access networks, support of uniform algorithms and authentication procedures, support for stateless network functions (stateless), support for roaming with traffic routing both through the home network (Home routed) and with local landing (Local breakout) in the guest network (VPLMN).

REFERENCES

1. Тихвинский В.О. Сети мобильной связи 5G. Технологии, архитектура и услуги. Москва: Медиа Паблшер, 2019. - 375 с.
2. 5G: как работает технология и зачем нам это нужно [Электронный ресурс] – URL: <https://rb.ru/longread/what-is-5G/>.

UDC 665.75

RATIONAL REFINING OF HEAVIER CUT OF PYROLYSIS GAS OIL

Y. BULAUKA, S. YAKUBOUSKI, N. VASHKOVA
Polotsk State University, Belarus

The composition of the fractions of the heavier cut of pyrolysis gas oil production was investigated by gas chromatography. In order to increase the profitability of pyrolysis units, it is recommended to organize complex technological schemes for the processing of the heavier cut of pyrolysis gas oil.

Introduction. The general power of pyrolysis processes in the world exceeds 130 million tons per year. The process of getting light olefins is accompanied by forming about 20% coproducts. The usage of these coproducts is a serious technical and economic problem that is associated with increased profitability of production. In order to remain competitive in the ethylene business for steam crackers, more effort must be made to upgrade all of the byproducts that are formed by liquid crackers. Producers who do not upgrade these by-products will face growing tension on the plant margins owing to competition from the world's low-cost regions [1].

One of these coproducts is the heavier cut of pyrolysis gas oil (PGO). The heavy distillates of the steam-cracked naphtha contain aromatic hydrocarbons that boil above 180 Celsius degrees. Only in Russia the production of PGO exceeds 325000 tons per year. Belarussian petrochemical Plant "Polymir" which is part of JSC "Naftan" is able to produce from 12000 up to 16000 tons of PGO yearly [2,3].

The issue of rational use of PGO is relevant for Belarus due to the future plans to increase the capacity of the enterprise, which will lead to an increase in the amount of by-products and amount of problems associated with their marketing.

Nowadays, PGO is used as a source of boiler heater. It is possible to obtain from the heavy pyrolysis tar not only boiler fuel but also carbon black, inactive carbon black, coke, dark petroleum resins, concrete superplasticizing agents, plasticizers, bitumen materials and to extract individual aromatic hydrocarbons (Naphthalene, 1-methylnaphthalene, 2-methylnaphthalene, etc.).

With the increasing global market demand for naphthalene, naphthalene refining technology is extensively studied internationally. Industrial naphthalene from coal tar accounts for 85% of total naphthalene production in the world. Naphthalene is produced from a high heteroatoms content coal-tar resin. In order to remove these heteroatoms expensive cleaning operations are used [4-16].

Up to date, there is still a problem to release pure naphthalene from coal tar and from components with similar boiling point to Naphthalene (217,97°C), such as Thionaphthene (219,90°C) and 2,3-Xylenol (216,87°C). It should be noted that the PGO of a wide fraction of light hydrocarbons, in contrast to coal tar, does not contain heteroatomic compounds, including Thionaphthene and Xylenols, and therefore is the preferred raw material for producing high purity Naphthalene [1].

Task formulation. The composition of the fractions of PGO production was investigated by gas chromatography.

Methods of research. Gas chromatography identifies resin ingredients by peak area, evaluate their quantitative content with high accuracy.

Results, their discussion and perspectives.

As a result of fractional distillation of PGO according to Engler, the yield of fractions is the following: b.b.-180°C was 1.89% wt., fraction 180-210°C was 18.76% wt., fraction 210-230°C was 14.45% wt. and semi-solid non-distillable residue of polymeric nature (pitch) was 64.90% wt. We have analyzed the Belarussian heavy pyrolysis resin (tar) and identified individual substances. PGO liquid concentrate is a mixture of various groups of hydrocarbons, primarily aromatic, both monocyclic and polycyclic. Also, all fractions contain isoparaffin, unsaturated, naphthenic and paraffinic hydrocarbons.

Table 1 presents data on the group hydrocarbon composition of individual fractions of heavy pyrolysis resin, produced at the factory "Polymir".

While the content of aromatic hydrocarbons in PGO reaches to 68%wt., in particular, naphthalene is up to 18 % wt. More than 75 individual aromatic hydrocarbons were found in the PGO liquid concentrate and their content increases with the weighting of the fractional composition.

The main component of the liquid product of PGO with boiling point up to 230°C is naphthalene and its alkyl derivatives.

Technology, Machine-building

Table 1. – The group hydrocarbon composition of individual fractions of PGO

Groups of hydrocarbons	Fractions of PGO, % wt.			
	b.b.-180°C	180-210°C	210-230°C	Total fraction
Paraffins	2,04	0,94	0,43	0,79
Isoparaffins	10,96	13,29	14,04	13,47
Aromatics	62,82	66,30	70,47	67,82
Naphthenes	7,30	5,26	1,94	4,00
Olefins	13,09	5,26	3,43	6,70
Unknown	3,79	5,64	9,69	7,22

Naphthalene plays an irreplaceable role in Fine Chemical Industry. Naphthalene is used for the synthesis of sulfonic acids, phthalic anhydride, azo dyes, plasticizers, decalin, tetralin, naphthol and others. Sulfonic acids from naphthalene are good surface-active substances (surfactants). The way of the derivation of superplasticizers for concrete from naphthalene is actively developing now.

The output of naphthalene at the factory "Polymir" from the PGO fraction with boiling point up to 230°C can be about 1000 tons per year. Naphthalene recovery is economically feasible. The results of chromatographic analysis show that in the process of obtaining high-purity naphthalene from PGO, separation of homogeneous azeotropes (naphthalene & 1-methyl naphthalene; naphthalene & 2-methyl naphthalene; naphthalene & biphenyl and others) might be a problem.

Various product derivatives can further increase the profitability of naphthalene recovery (Xu, 2012). Methyl naphthalenes are used as insecticides, solvents and starting materials in the synthesis of dyes, to produce sulfonic acids of mono- and dimethylnaphthalenes, used as surface active substances. Besides:

- 2-Methylnaphthalene is a valuable raw material for the production of synthetic vitamin K3 (2-methyl-1,4-naphthoquinone, menadione), which is widely used in medicine as a drug to increase blood clotting.
- 1-Methylnaphthalene is a reference when determining the cetane number of diesel fuel (for 1-methylnaphthalin, it is assumed to be zero).
- 1,4-dimethylnaphthalene is used to suppress the germination of potatoes and vegetables.
- 2,6-dimethylnaphthalene is oxidized to 2,6-naphthalene dicarboxylic acid used in the production of polyesters and polyamides.

The theoretical output of 2-methylnaphthalene at the factory "Polymir" from a liquid product PGO can reach 250 tons per year, for 1-methylnaphthalene is about 170 tons per year, for 1,4-dimethylnaphthalene is about 18 tons per year, for 2,6-dimethylnaphthalene is about 15 tons per year.

Cymols of PGO liquid product can be widely used for the synthesis of cresols, highly effective antioxidants, phthalic acids (mainly isophthalic and terephthalic acids), flavors, etc. The use of cymols in petrochemical synthesis allows sprawling of the raw material base for the production of alkylaromatic hydrocarbons. The theoretical output of cymols at the factory "Polymir" from PGO with boiling point up to 230°C can be: for 1-methyl-2-isopropyl benzene is about 630 tons per year, for 1-methyl-3-isopropyl benzene is about 125 tons per year and for 1-methyl-4-isopropyl benzene is about 2 tons per year.

Indane (2,3-dihydroinden) is the starting material for the synthesis of 2-, 4- and 5-indanols, which are used in the preparation of medicines. The theoretical output of indane from the liquid fraction of PGO can be up to 80 tons per year.

Tert-butylbenzene is the starting compound in the preparation of valuable fragrances, and is also used as a solvent and raw material for alkyl polystyrenes. It is potentially possible to organize the production of tert-butylbenzene from PGO liquid product up to 68 tons per year.

Pseudocumene (1,2,4-trimethylbenzene) is used in the production of trimellitic acid and its anhydride, pseudokumidin, vitamin E. The theoretical output of 1,2,4-trimethylbenzene from the liquid fraction of PGO can be more than 55 tons per year.

Biphenyl is used as a precursor in the synthesis of polychlorinated biphenyls, as well as other compounds used as emulsifiers, insecticides and dyes. It is possible to extract about 50 tons of biphenyl per year from PGO liquid product.

It is expedient to use the residue of the distillation of PGO as a raw material for the production of pitches and carbon fibers.

Conclusion. In order to increase the profitability of pyrolysis units, it is recommended to organize complex technological schemes for the processing of PGO.

REFERENCES

1. Bulauka Y.A., Yakubouski S.F. PGO Processing with azeotropic rectification to extract naphthalene // Topical Issues of Rational Use of Natural Resources 2019- Litvinenko (Ed), 2020 Taylor & Francis Group, London, DOI: <https://doi.org/10.1201/9781003014638.-Volume 2 - P.495-501>.

2. Bulauka Yu.A., Liakhovich V.A., Yukhno D.S., Yakubouski S.F. Rational refining of heavier cut of pyrolysis gas oil of hydrocarbon feed // Сборник докладов 72-й Международной молодежной научной конференции «Нефть и газ – 2018» (23-26 апреля 2018 г. Москва). – Том 3.– М.: Издательский центр РГУ нефти и газа (НИУ) имени И.М. Губкина, 2018. –С.293.
3. Bulauka Yu., Yakubouski S. Rational refining of heavier cut of pyrolysis gas oil // Abstract book of 10th International Youth Scientific and Practical Congress «Oil and Gas Horizons», Moscow, November 19-22, 2018.- Gubkin Russian State University of Oil and Gas (National Research University).-Moscow, 2018.-p.61.
4. Stalmakh D.V., Bulauka, Y.A, Yakubouski S.F. Complex of Technology for Processing Heavier Cut of Pyrolysis Gas Oil // European Association of Geoscientists & Engineers. Conference Proceedings, Tyumen 2021, Mar 2021, Volume 2021, p.1 - 5 DOI: <https://doi.org/10.3997/2214-4609.202150056>.
5. Bulauka Y.A., Yakubouski S.F. Process to extract high purity naphthalene from the heavier gas oil fraction from naphtha crackers producing ethylene // Scientific Conference Abstracts of XV International Forum-Contest of Students and Young Researchers « Topical issues of rational use of natural resources», St. Petersburg, May 13-17, 2019.- Saint-Petersburg Mining University. - St. Petersburg, 2019.- P. 24.
6. Булавка Ю.А., Якубовский С.Ф., Хохотов С.С., Ляхович В.А. Инновационный подход к переработке тяжелой смолы пиролиза углеводородного сырья // Актуальные проблемы развития нефтегазового комплекса России: Сборник тезисов XII Всероссийская научно-техническая конференция (12-14 февраля 2018 г., г. Москва).- РГУ нефти и газа (НИУ) имени И.М. Губкина.- Москва, 2018.-С.209.
7. Булавка Ю.А., Ляхович В.А., Якубовский С.Ф. Рациональная переработка тяжелой смолы пиролиза углеводородного сырья // Tatarstan UpExPro 2018: материалы II Международной молодежной конференции (14–17 февраля 2018 г., Казань). – Казань: Изд-во Казан. ун-та, 2018. –С.120-121.
8. Булавка Ю.А., Якубовский С.Ф., Хохотов С.С., Ляхович В.А. Инновационный подход к переработке тяжелой смолы пиролиза углеводородного сырья // Сборник трудов XII Всероссийской научно-технической конференции «Актуальные проблемы развития нефтегазового комплекса России». – М.: Издательский центр РГУ нефти и газа (НИУ) имени И.М. Губкина, 2018. –С.23-26.
9. Булавка Ю.А., Якубовский С.Ф., Хохотов С.С. Получение нового для белорусского рынка продукта нефтехимии – нафталина // Горизонты и перспективы нефтехимии и органического синтеза: материалы Международной научной конференции-Уфа: Изд-во «Реактив», 2018.-С.138-139.
10. Булавка Ю.А., Якубовский С.Ф., Ляхович В.А. Получение товарных продуктов из тяжелой смолы пиролиза // Актуальные вопросы современного химического и биохимического материаловедения: материалы V Международной молодежной научно-практической школы-конференции (г. Уфа, 4-5 июня 2018 г.) / отв. ред. О.С. Куковинец. - Уфа: РИЦ БашГУ, 2018.-С. 54-57.
11. Булавка Ю.А., Ляхович В.А., Москаленко А.С. Современные направления переработки тяжелой смолы пиролиза углеводородного сырья // Новые технологии – нефтегазовому региону: материалы Международной научно-практической конференции/ отв. ред. П. В. Евтин. – Тюмень: ТИУ, 2018.- С.31-33.
12. Булавка Ю.А., Якубовский С.Ф., Ляхович В.А. Получение нафталина - нового для белорусского рынка продукта малотоннажной химии // Сборник материалов 4-го Белорусско-Балтийского форума «Сотрудничество – катализатор инновационного роста», Минск, 31 мая-1 июня 2018 года, г. – Минск: БНТУ, 2018. – С.62-63.
13. Шульга Е.А., Ляхович В.А., Якубовский С.Ф., Булавка Ю.А. Направления рационального использования тяжелой смолы пиролиза // Сборник научных работ студентов Республики Беларусь «НИРС 2019».- Минск : Издательский центр БГУ, 2020. - С. 208.
14. Казак Е.В., Якубовский С.Ф., Булавка Ю.А. Азеотропная ректификация нафталинсодержащей фракции тяжелой смолы пиролиза // Сборник научных работ студентов Республики Беларусь «НИРС 2016» / В. Л. Богуш (председатель) [и др.].- Минск : Издательский центр БГУ, 2017. - С. 97-98.
15. Якубовский С.Ф., Булавка Ю.А., Казак Е.В. Сравнительная оценка растворяющей способности углеводородов и спиртов по отношению к нафталину // Вестник Полоцкого государственного университета. Серия В, Промышленность. Прикладные науки. - 2016. - № 3. - С. 160-163.
16. Якубовский С.Ф., Булавка Ю. А., Шульга Е.А., Вашкова Н.С. Суперпластификаторы для бетонной смеси на основе тяжелой смолы пиролиза // НЕФТЕХИМИЯ – 2020: материалы III Междунар. науч.-техн. форума по хим. технологиям и нефтегазоперераб., Минск, 2–3 декабря 2020 г. – Минск : БГТУ, 2020. – С.14-17.

ANALYSIS OF THE POSSIBILITIES OF USING PETROLEUM COKE IN VARIOUS INDUSTRIES

A. LITVIN, I. KOVALENKO, M. PUGACHEV, E. SAFRONOVA
Polotsk State University, Belarus

The efficiency of the delayed coking process lies in the fact that along with the production of petroleum coke, a significant amount of distillate products is formed that is suitable for the production of high-quality motor fuels. It is possible to process oil sludge and other waste. The raw materials are heavy fractions of oil formed as a result of atmospheric and vacuum distillation of oil (fuel oil, semi-tar, tar), cracking-residues from thermal cracking of fuel oil and tar, heavy gas oils of catalytic cracking, residues of oil production (asphalt of propane deasphalting of tar, extracts of phenolic oil purification, etc.)

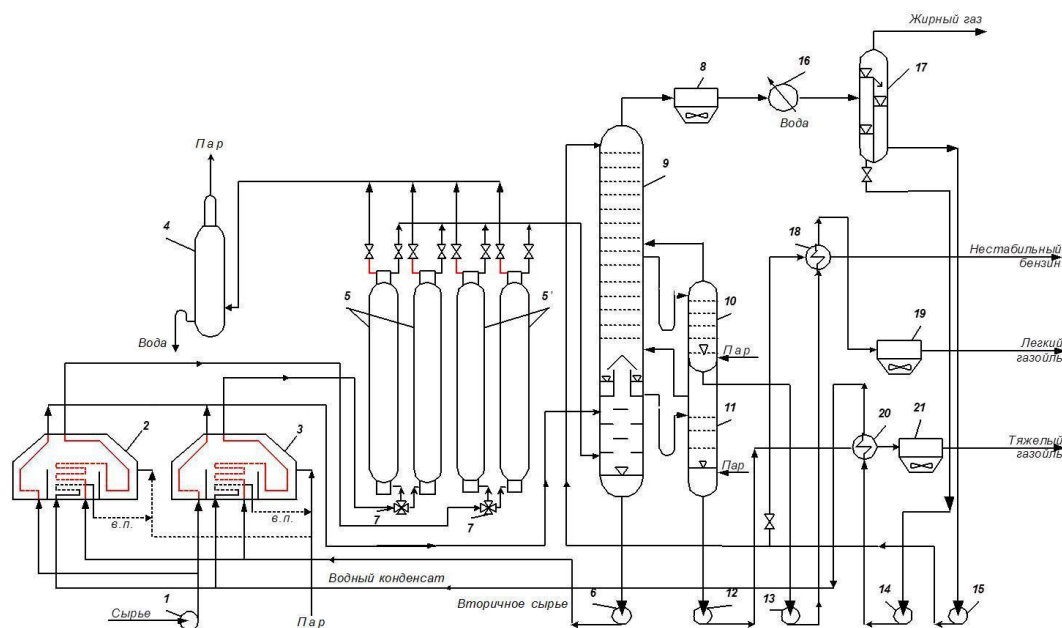


Fig. 1. – DCU (delayed coking unit) scheme

Technological devices and equipment:

1, 6, 12-15-pumps; 2, 3-tube furnaces; 4-receiver; 5, 5' - delayed coking chambers; 7-four-way cranes; 8, 19, 21-air cooling devices; 9 – rectification column; 10, 11-steam columns; 16-refrigerator; 17-water and gas separator; 18, 20-heat exchangers.

The industrial coking process is carried out on 3 types of installations: periodic coking in coke cubes, delayed coking in chambers, continuous coking in the fluidized bed of the carrier coke.

Delayed coking

Delayed (semi-continuous) coking is the most widespread in the world practice. The raw material, pre-heated in tubular furnaces to 350-380 °C, is continuously fed to the cascade plates of the distillation column (operating at atmospheric pressure), flowing down where it contacts the rising vapors supplied from the reaction apparatuses.

As a result of heat and mass transfer, some of the vapors condense, forming with the raw material the so-called secondary raw material, which is heated in tubular furnaces to 490-510 °C and enters the coke chambers-hollow vertical cylindrical apparatuses with a diameter of 3-7 m and a height of 22-30 m. The reaction mass is continuously fed into the chamber for 24-36 hours and coked due to the heat accumulated by it. After filling the chamber with 70-90% coke, it is removed, usually with a high-pressure water jet (up to 15 MPa).

The coke enters the crusher, where it is crushed into pieces of no more than 150 mm in size, after which it is fed by an elevator to the screen, where it is divided into fractions of 150-25, 25-6 and 6-0.5 mm. The chamber from which the coke is discharged is heated with hot water vapor and steam from the working coke chambers and filled again with the coked mass.

The volatile coking products, which are a vapor-liquid mixture, are continuously removed from the operating chambers and sequentially separated into gases in the distillation column, water separator, gas block and steam column.

Typical process parameters: temperature in the chambers 450-480 °C, pressure 0.2-0.6 MPa, duration up to 48 hours. The advantage of slow coking is the high yield of low-ash coke. From the same amount of raw materials, this method can produce 1.5-1.6 times more coke than with continuous coking.

As a result of delayed coking processes, lumpy petroleum coke with the following characteristics is obtained:

- 1) the amount of coke fines (particle less than 10 mm) = 30-50%
- 2) coke humidity = 5-7 %
- 3) volatile matter yield 8-15%

Lump coke is divided into fractions by size and subjected to calcination.

Quality of anodic (calcined) coke:

- 1) sulfur content up to 3%
- 2) nickel content 200 weight parts per million
- 3) vanadium content 200 parts by weight per million
- 4) ash 0,3%
- 5) grinding capacity less than 90%
- 6) the content of volatile fuels in-in 0,3%

Petroleum coke, which is a solid porous product from dark gray to black color, is obtained by coking petroleum raw materials. The main quality indicators are the content of S, ash, moisture (usually no more than 3% by weight), the yield of volatile substances, granulometric composition, mechanical strength.

Petroleum coke is divided: by the content of S into low-sulfur (up to 1%), sulfur (up to 2%), high-sulfur (more than 2%); by the content of ash into low-ash (up to 0.5%), medium-ash (0.5-0.8%), high-ash (more than 0.8%); by the granulometric composition into lumpy (fraction with a particle size of more than 25 mm), "nut" (6-25 mm), small (less than 6 mm).

Application of coke:

- aluminum industry, where coke serves as a reducing agent (anode mass) when smelting aluminum from aluminum ores (bauxite). The specific consumption of coke is 550-600 kg / t of aluminum.
- raw materials for the manufacture of electrodes used in steelmaking furnaces;
- for the production of carbides (calcium, silicon), which are used in the production of acetylene;
- production of grinding materials,
- in the manufacture of conductors, refractories, etc.

Before use, petroleum coke is usually subjected to refining (calcination) at refineries immediately after receipt or from the consumer. During calcination, volatiles and partially heteroatoms (e.g., S and V) are removed, and the electrical resistivity is reduced. In the food industry coke is used in the production of sugar to replace blast furnace coke. Low-quality sulfur coke is used as fuel.

REFERENCES

1. Method for obtaining sulfocationite: pat. 6210 Rep. Belarus, IPC7 c 08 J 5/20, From 08 G 2/30/ L. M. Lyakhnovich, S. V. Pokrovskaya, I. V. Volkova, S. M. Tkachev; applicant Palace. State Un-T.- no. b 0000011; declared. 04.01.00; publ. 30.06.04 // official byul. / National Intellectual Center. ownership. - 2004. - No. 2. - p. 174.
2. Akhmetov M. M., Karpinskaya N. N., Telyashev E. G. Petroleum coke: production, quality, calcination, areas of use. - Ufa, Publishing House of JSC "INKHP", 2018. – 584 p.
3. Yanko E. A. Requirements for calcined petroleum coke for the production of anode mass and burnt anodes. Collection of reports of the inter-industry conference "Oil refining and aluminum industry-development of cooperation, optimization of relations for the supply of petroleum coke". Krasnoyarsk, March 27-29, 2001, pp. 33-37.
4. Valyavin G. G. Technology of industrial production of petroleum coke of needle structure. Production of carbon products. Problems of providing carbon raw materials. Collection of works. Issue I. M., D. I. Mendelev Russian State Technical University, 2002, pp. 51-61
5. Valyavin G. G., Zaporin V. P., Gabbasov R. G., Kalimullin T. I. The process of delayed coking and the production of petroleum cokes specialized for use. - Territory of Neftegaz. - No. 8, 2011, pp. 44-48.
6. Rabin P. B., Vorobyov N. I., Sayfullin N. R., etc. Problems of coke for the production of graphite electrodes. Sat.trudov. "Modern problems of production and operation of graphitized carbon". Chelyabinsk, 2000, pp. 28-34.

SIMULATING THE INFLUENCE OF THERMAL EXPOSURE ON THE MAIN ELEMENTS OF A CUTTING TOOL IN SOLIDWORKS

D. MAKSIMENKO, A. PORTYANKO, N. POPOK, S. PORTYANKO

Polotsk State University, Belarus

The results of experimental studies of the effect of thermal action on the main elements of the cutting tool in the SolidWorks software environment are presented.

Introduction. In the process of cutting, the cutting tool heats up; therefore, it is required to predict its behavior at different temperature operating conditions. Experimental theoretical studies were carried out. Experimental studies consist of real heating of a 3D model of a cutting tool, and theoretical studies consist of simulating the heating of cutting tools using the SolidWorks software environment. The main structural components of the block-modular end mill were investigated: the screw, the block and the body [1]. The reliability of the developed system for fixing the cutting plate in the cutting block and the cutting block in the housing modules is considered in [2].

Basic information on the materials and tools used. During the experiment, a hot air gun "Stern HG2000ACN" was used for heating. Table 1 shows its technical characteristics.

Table 1. – Technical characteristics of a hot air gun «Stern HG2000ACN»

	
Power	2000 W
Number of temperature modes	2
Temperature range	350 – 550°C
Airflow	300 – 500 lpm
Number of air flow rates	2
Overheat protection	+

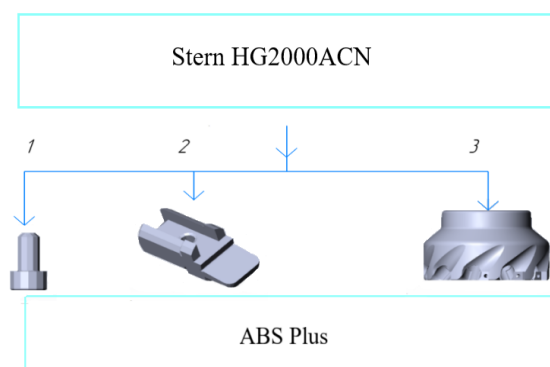
The temperature in the first position reaches 350 °C. In the second position - 550 °C.

The 3D models of the screw, the block and the cutter were 3D printed on the Mass Portal Pharaoh XD 30. They were made of ABS Plus plastic. The characteristics of the plastic are shown in table 2.

Table 2. – ABS Plus Plastic Specifications

Density	1,05 g/cm ³
Tensile strength	30 MPa (2400MPa (23°C))
Impact strength	130 (at 23°C), 100 (at 130°C) kJ/m ²
Tensile modulus	1627 MPa
Tensile modulus at 23 °C	1700 – 2930 MPa
Flexural modulus	1834 MPa
Elongation ratio	6%
Electrical strength	12-15 MV/m
Moisture absorption	0,2-0,4 %
Softening point	~ 100°C
The melting temperature	~ 220°C
Autoignition temperature	~ 395°C
Flame classification	HB

Investigation of the thermal effect on the main elements of the cutting tool. In the laboratory the screw, the block and the cutter body were heated to the melting temperature and their behavior under the influence of temperature was investigated. Figure 1 shows the order of the experiment.



1 – screw; 2 – block body; 3 – end milling cutter body

Fig. 1. – Experiment layout

The calculated formula for the temperature from a heat point source is presented below [3]:

$$\theta(x, y, z, \tau) = \frac{q_T}{\lambda \sqrt{\omega} (4\pi\tau)^{\frac{3}{2}}} \exp \frac{-(x_u - x)^2 + (y_u - y)^2 + (z_u - z)^2}{4\omega\tau} =$$

$$= \frac{20}{0,2 \times \sqrt{1,1} \times (4 \times \pi \times 20) \times \frac{3}{2}} \times \exp \frac{-(0-0)^2 + (24-0)^2 + (0-0)^2}{4 \times 1,1 \times 20} = 175,96^\circ\text{C} \quad (1)$$

where: $\theta(x, y, z, t)$ – temperature of any point of the body;

x, y, z – body point coordinates;

x_u, y_u, z_u – heat source coordinates;

τ – source time;

λ and ω – coefficients of thermal conductivity and thermal conductivity of the body material respectively;

Next, the heating of the screw, the block and the cutter body was simulated in the SolidWorks environment program.

Ambient temperature is 20 °C. The screw, the block and the cutter body were heated to a temperature of 150 °C, since further heating is not advisable and leads to spontaneous ignition (see Table 2). The simulation parameters are presented in Table 3.

Table 3. – SolidWorks Modeling Options

Model material	ABS plastic Plus
Ambient temperature	20°C
Final temperature	150°C
Heating time	3 sec (screw), 5 sec (block body and end milling cutter body)

The results of the study are presented in Table 4.

Table 4. – Research Results in SolidWorks

Screw				
0c ($T_{\max}=20^\circ\text{C}$)	2,25c ($T_{\max}=52,5^\circ\text{C}$)	2,5c ($T_{\max}=95,83^\circ\text{C}$)	2,75c ($T_{\max}=128,33^\circ\text{C}$)	3c ($T_{\max}=150^\circ\text{C}$)

The ending of table 4

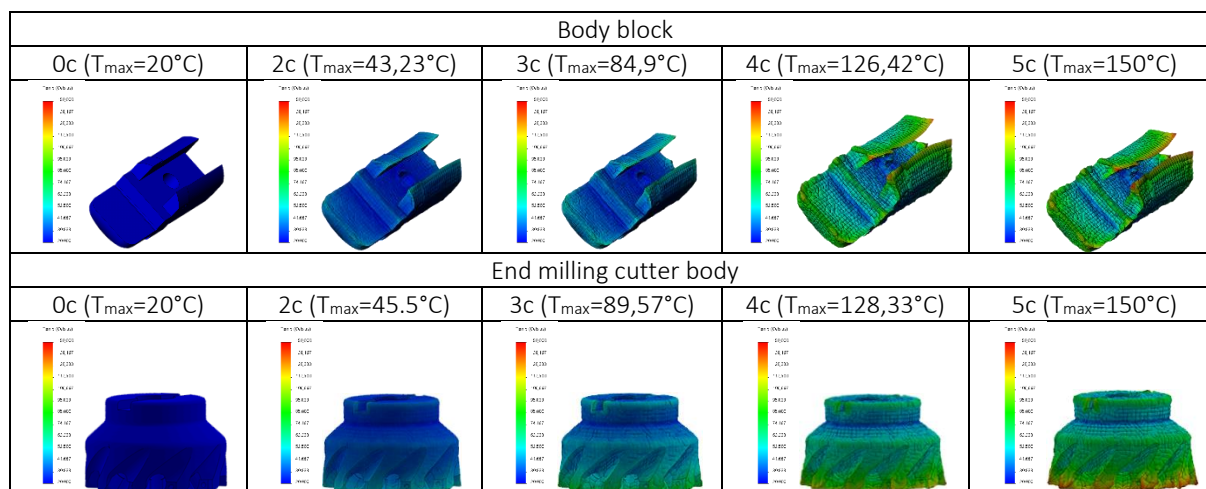


Table 1 shows that all models within 1-5 sec began to deform under the influence of temperature, changing the geometric parameters.

Conclusion. If we make a comparison of practical and theoretical studies, it can be seen that they differ in terms of the manifestation of deformations and temperatures. Practical and theoretical experience did not coincide as in real life heating after the heat source is turned off, the temperature continues to rise.

As a result of thermal deformation modeling, the following can be noted [4]:

1. When the fastening screw heats up, it lengthens, which must be taken into account when designing a threaded connection.
2. The cutting tool insert increases in diameter, which must be taken into account when determining the size of the groove for its placement;
3. The body of the tool block increases in size, the side walls of the longitudinal groove for the stuck accommodation are subjected to the greatest thermal deformation, which must be taken into account when assigning tolerances to the width of the groove and the stuck.
4. Thermal deformations of individual structural elements of the cutter block affect the overall deformation of the cutter block assembly - the cutting tool insert enters the body and the grip; the dimensions of the grip change in height, width, and length; the shape of the hole for the pin is deformed; the diameters of the pin and clamping screw increase. These thermal deformations must be taken into account in the dimensional analysis of the tool block assembly.
5. Qualitative changes in the thermal deformations of the end mill indicate their maximum values in the cutting tool insert and the cutting block, however, they cannot be neglected when designing the cutter body, especially in the part of the end key, which the mill is fixed in the shank with.

REFERENCES

1. Попок, Н. Н. 3D-моделирование конструкций блочно-модульных торцовых фрез / Н. Н. Попок, С. А. Портянко, Г. И. Гвоздь // Информационно-коммуникационные технологии: достижения, проблемы, инновации (ИКТ-2018) : электронный сборник статей I международной научно-практической конференции, посвященной 50-летию Полоцкого государственного университета, Новополоцк, 14–15 июня 2018 г. / Полоцкий государственный университет ; пред. редкол.: Д. Н. Лазовский. – Новополоцк, 2018. – С. 190.
2. Попок, Н.Н., Максимчук, А.С., Портянко, С.А. Совершенствование системы закрепления пластин режущих и блоков резцовых в блочно-модульных режущих инструментах/ Вестник ПГУ, сер. В – 2015 - №2, с. 16-22.
3. Попок, Н.Н. Теория резания : учебное пособие / Н.Н. Попок. – Минск : ИВЦ, Минфина, 2019 г. – 372 с.
4. Методология исследования работоспособности фрезерных и осевых режущих инструментов на основе 3D прототипирования / Н.Н. Попок, С.А. Портянко – Вестник ПГУ, сер. В. Промышленность. Прикладные науки. 2020 г. – с. 29-39.

UDC 621.91.01

MODELING THE OPERATION OF END MILLS IN THE CINEMA 4D PROGRAM

R. DMITRIEV, D. MATVEENKOV, N. POPOK, S. PORTYANKO

Polotsk State University, Belarus

For successful work with milling cutters, it is important to understand the interaction of their design with the aero-hydrodynamic environment. The purpose of the research work is to study the impact of aero-and hydro-dynamic environments on the design of milling cutters and their performance. Various methods for measuring surface friction stresses are proposed. Pneumometric methods for indirect determination of the vector of surface friction stresses in spatial flows are developed. The simulation of the dynamics of milling cutters in a viscoliquid medium is shown. The results of the research are also presented. New scientific results have been obtained and methodological justifications are of scientific and practical value for the further development of the design of end mills and cutting tools.

Introduction. The use of prefabricated cutting tools in the industry reaches 70% of the total number of tools, with one third of these tools being prefabricated end mills. Prefabricated end mills consisting of interchangeable modules are becoming more and more common, the use of which significantly reduces production costs.

Currently, almost the only method for determining the flowability of structures is the floating weight element method. However, its application on surfaces with a large curvature or under the action of significant alternating inertial loads is difficult.

Of the indirect pneumatic methods, the use of Preston tubes, the Stanton nozzle, is more common. These methods are also used for measuring shear stresses in spatial flows, and the direction of the shear stress vector is previously determined using the oil drop method or a thermal meter.

The use of these pneumometric methods is difficult or even impossible in highly directional currents, as well as under the action of significant inertial loads on the object under study.

Indirect methods for determining shear stresses in the wall include the method of fluorescent coatings, the method for measuring tangential stresses along the length of strokes as a result of spreading oil droplets applied to the surface, as well as methods using the Reynolds analogy between temperature and dynamic boundary layers (Figure 1) [1].

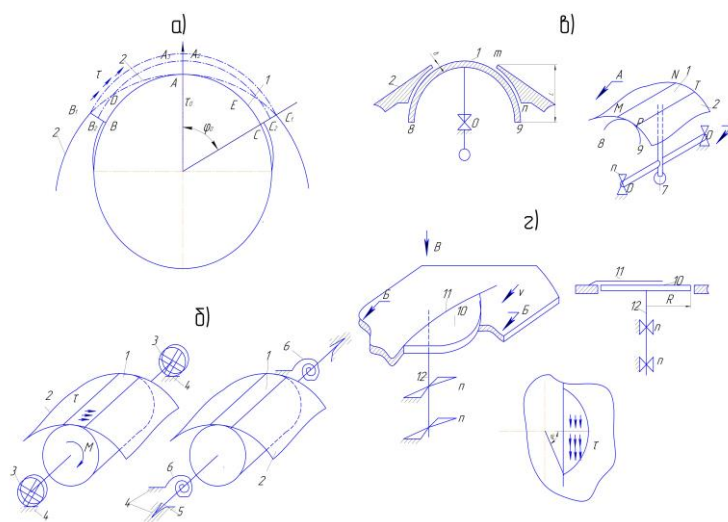


Fig. 1. – Description: a-cylindrical element touches the surface of the circle; b-modification with strain weights; c-part of the cylindrical surface; d-sensitive element in the form of a flat disk

Description of the Cinema 4D software product. For 2020, Cinema 4D is the easiest-to-use program for 3D artists, at least as stated on the developers' website. All the main advantages are also present: ease of use, everyone's favorite intuitive interface, stability, integrated help, a procedural workflow and the availability of the program in different versions, depending on the purpose of use.

Cinema 4D is a universal program for 3D modeling, editing objects and creating effects. It also renders objects using the Gouraud method (the shading method, which is based on intensity interpolation and is known as the Gouraud method (after its developer), allows you to eliminate the discreteness of intensity changes). Renderers can be either "native" or embedded directly into the program itself using plugins and connectors.

Students love to use this program, as it does not take much time and effort to learn the principles of work. It was in this editor that the operation of milling cutters in a visco-liquid medium was investigated.

Plugins and settings for Cinema 4D. To simulate the operation of milling cutters in a liquid environment, the "RealFlow" plugin was used. This plugin is designed for modeling and simulating a variety of physical bodies in dynamics and is intended for use primarily in the computer graphics, animation, and special effects industries, rather than in scientific calculations and research. Basically, it uses particle systems to calculate the dynamics of the shape of physical bodies. The "RealFlow" calculation algorithm uses the method of smoothed particle hydrodynamics (eng. Smoothed Particle Hydrodynamics (SPH), which allows the particles modeling the environment to interact with each other. The essence of SPH is that, depending on the distance between two particles, these particles can "stick together" or "push apart". Each particle can have its own mass and the so — called "smoothing length", which determines at what distance this particle will be attracted to others, and at what distance it will repel. All bodies modeled by "RealFlow", built on point particles, the mechanism of which is described above. Initially, "RealFlow" was intended for modeling only fluid and viscous bodies, primarily liquids, but later the set of supported physical bodies has significantly expanded. As a result, "RealFlow" version 5 supports solid and deformable bodies, gases, and "meshes".

"RealFlow" can work as a completely separate (standalone) application, and can be used as a component (plugin) to other programs, such as 3D Max, Maya, LightWave, Softimage, Cinema 4D and Houdini.

In the project where the study was conducted, the following elements were used (Figure 2):

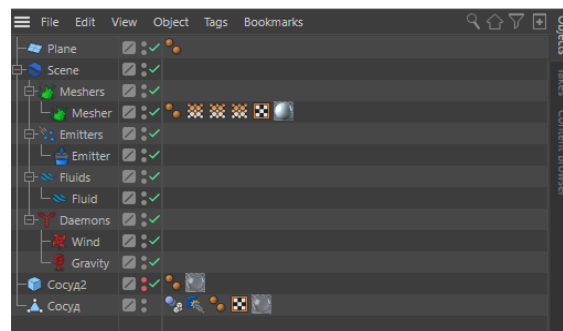


Fig. 2. – Project elements

The plugin creates a "Scene" section that contains all the elements and settings of the fluid.

"Meshers" is the texture of the water itself. The "Emitters" object stores all the configurable water properties that can be changed at any time (Figure 3). Where the "Body" indicates the "Vessel" object, so that water does not spill through it.

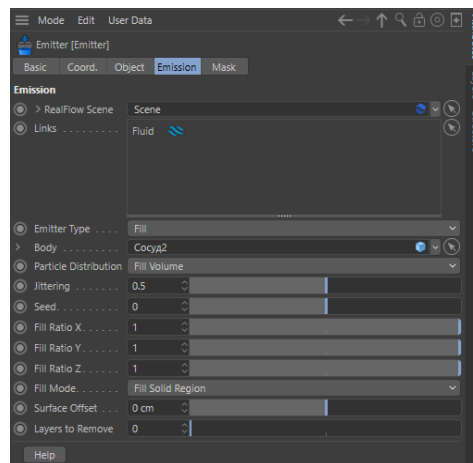


Figure 3. – Setting up "Emmitter"

"Fluids" is responsible for the quality and resolution of the granules that make up the water. In this case, the water resolution is set to 5 (Figure 4).

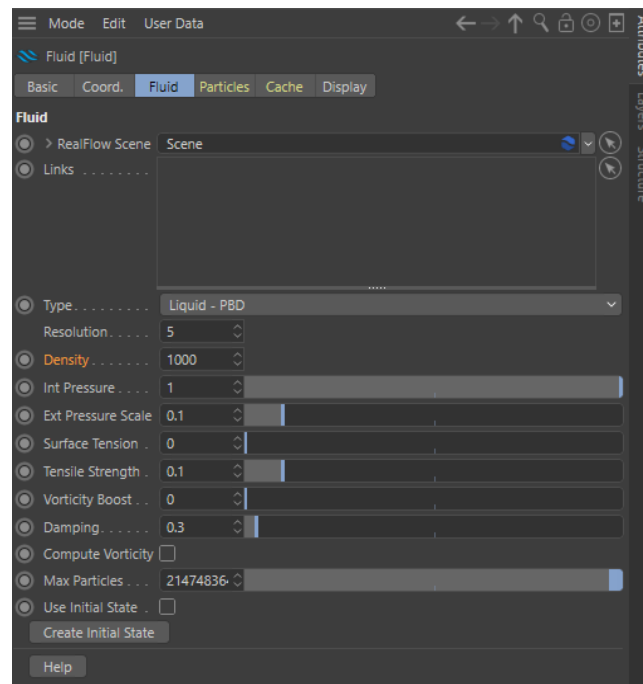


Fig. 4. – Setting up "Fluid"

The "Daemons" section stores all the physics of water ("Wind", "Gravity"). Where "Wind" is responsible for the wind created by the rotation of the cutter, and "Gravity" is responsible for the gravity of the water

Research. Table 1 and 2 show the frame-by-frame (fragmentary) changes in the liquid (waves, flows, splashes) over a certain period of time $t=1, 2, 3$ s.

Table 1. – Investigation of the dynamics of the first milling cutter in a liquid medium

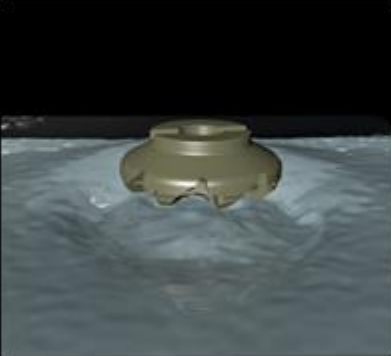
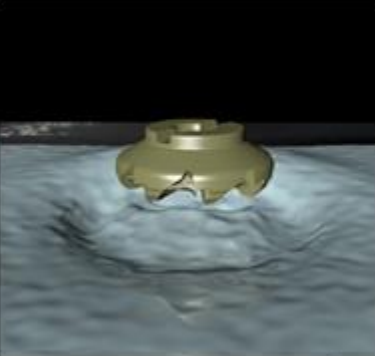
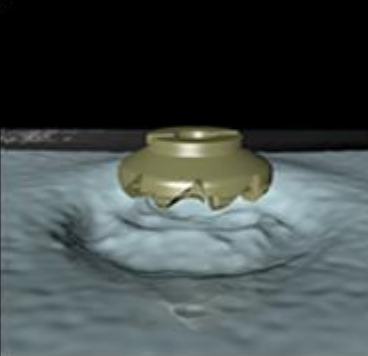
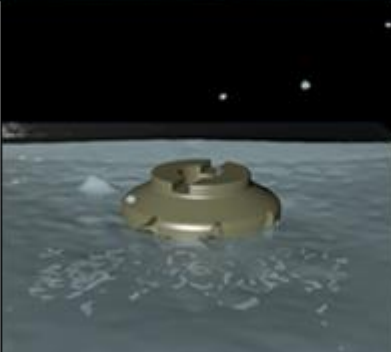
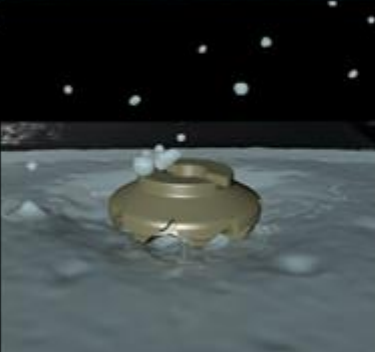
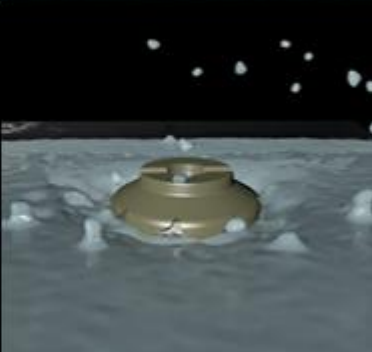
	t=1 c	t=2 c	t=3 c
ABOVE THE WATER			
IN THE WATER			

Table 2. – Investigation of the dynamics of the second milling cutter in a liquid medium

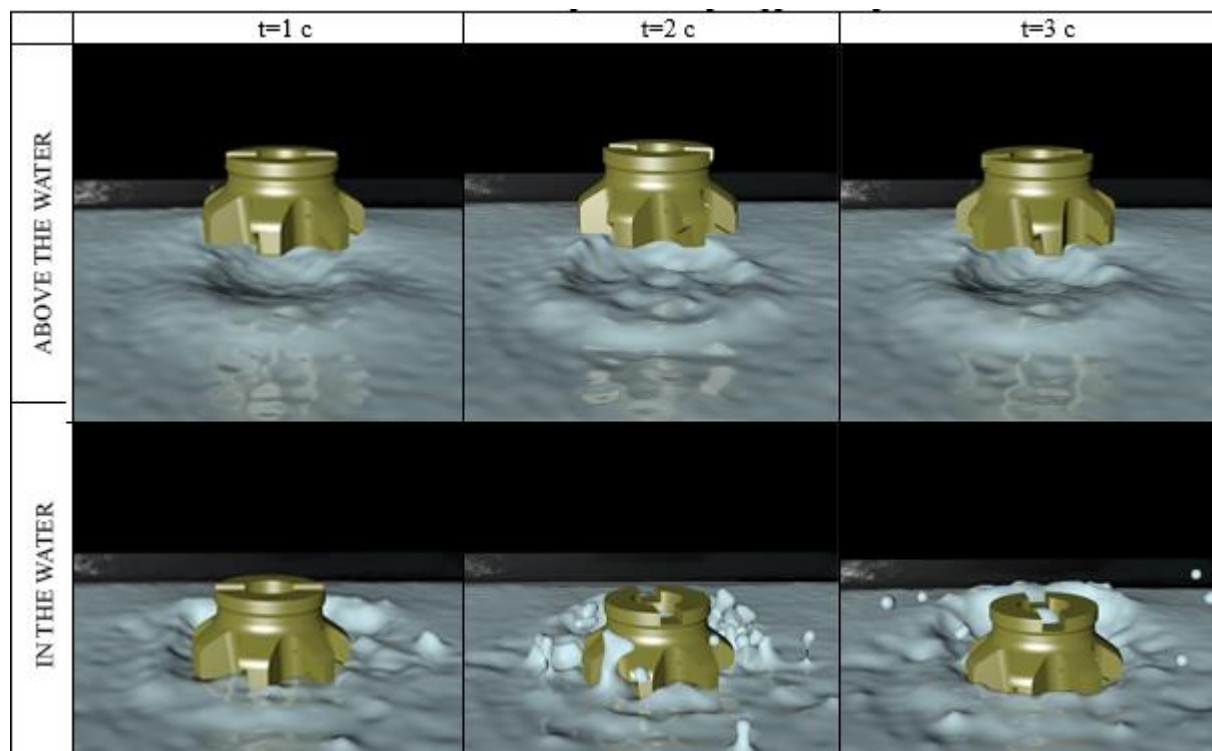
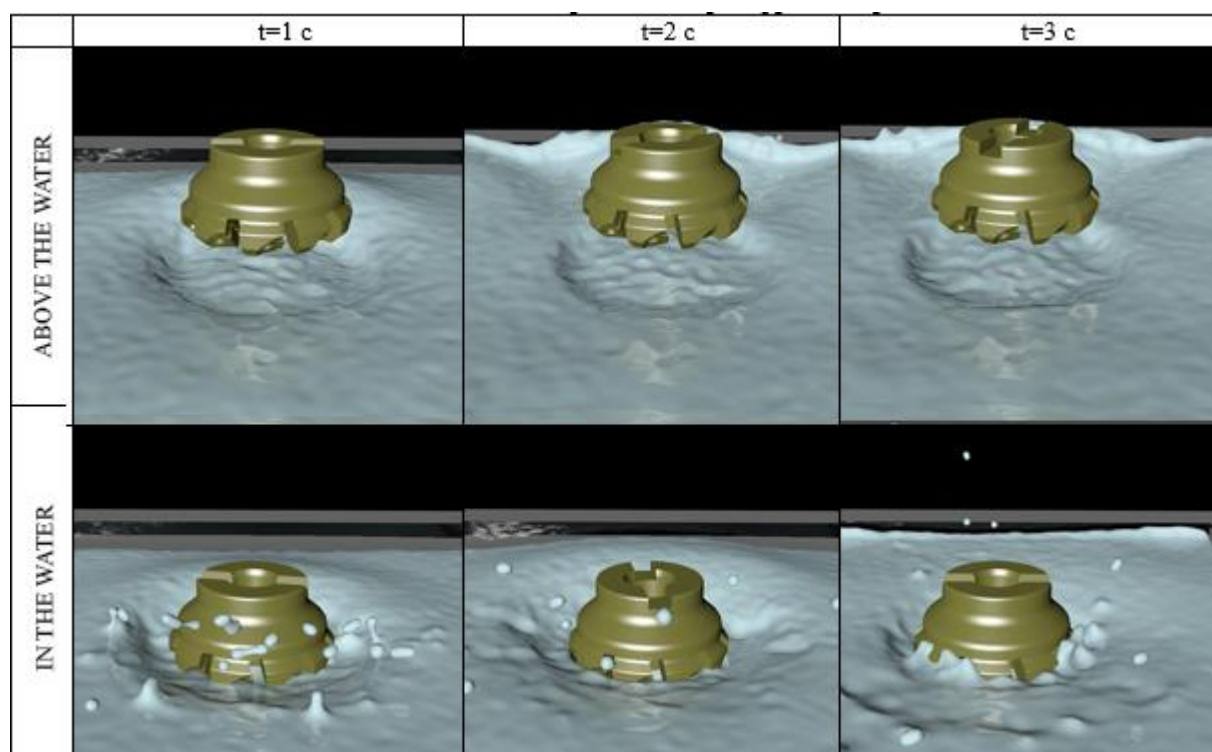


Table 3. – Investigation of the dynamics of the third milling cutter in a liquid medium



Description. Milling is one of the most common processing methods. In terms of productivity, milling is superior to planing and in large-scale production is second only to external stretching. The kinematics of the milling process are characterized by a rapid rotation of the tool around its axis and a slow feed movement. The feed movement during milling can be straight-forward, rotational, or helical. In the rectilinear movement of the feed, the milling cutters process all kinds of cylindrical surfaces: planes, all kinds of grooves and grooves, shaped cylindrical surfaces.

Experimental studies were conducted in the Cinema 4D software, using an additional plugin that allows you to simulate the behavior of the liquid and interaction with it. The results of the study are presented in the tables, which show the impact of the milling cutters on the surface of the liquid. In our case, the surface is the surface of the liquid, which is affected by the milling cutter air flow. Each milling cutter rotated on its axis above the surface, acting on the liquid. machine spindle speed n : 1000 rpm. Due to the different sizes of the grooves on the milling cutter design, they have different properties of passing air flows through them.

The milling cutter 2 affects the surface of the liquid least of all, since it has a large area. In the case of the 1 and 3 milling cutters, they affect a smaller area, but with greater force, as can be seen in the images in the tables.

If you put the rotating cutters in the liquid, we will see that during the rotation, the cutters will divert water through the grooves and form waves, bursts on the surface of the liquid. The milling cutter with a larger area during rotation, a larger number of waves are formed, when the milling cutters 1 and 3, with a smaller size of the grooves, more liquid is discharged, which causes a larger number of bursts.

Conclusion. In the course of the study, the possibilities of the methodology for studying the aero-hydrodynamic flowability, the effect of air flows on the shape of the milling cutter design were revealed. Also, using the Cinema 4D software and the "RealFlow" add-on, we modeled a simulation of the liquid environment for interaction with the 3D model of various milling cutters, respectively, we studied the effects of chip removal grooves on the liquid environment, both with the help of air passing through them, and the direct interaction of the cutter with water.

REFERENCES

1. Методы определения вектора аэрогидродинамических напряжений трения на поверхности тел, обтекаемых пространственным или плоским потоком. [Электронный ресурс]. – Режим доступа: <https://cyberleninka.ru/article/n/metody-opredeleniya-vektora-aerogidrodinamicheskikh-napryazheniy-treniya-na-poverhnosti-tel-obtekaemykh-prostranstvennym-ili-ploskim/viewer/>. – Дата доступа: 20.09.2020.
2. Методология исследования работоспособности фрезерных и осевых режущих инструментов на основе 3D прототипирования / Н.Н. Попок, С.А. Портянко – Вестник ПГУ, сер. В. Промышленность. Прикладные науки. 2020 г. – с. 29-39.

AIRFLOW SIMULATION IN SOLIDWORKS FLOWSIMUTALION

D. ABRAGIMOVICH, ISSA ABAKAR AHMAD ILYASS, N. POPOK, S. PORTYANKO

Polotsk State University, Belarus

Creation of a model of air flow propagation of end mills for subsequent analysis of aerodynamic properties for materials by cutting.

To create a model of the distribution of an air flows, we need: 3D - model of the investigated object; 3D - model of the body that fixes the object. The next step is to create an assembly of the model under study (Fig.1).

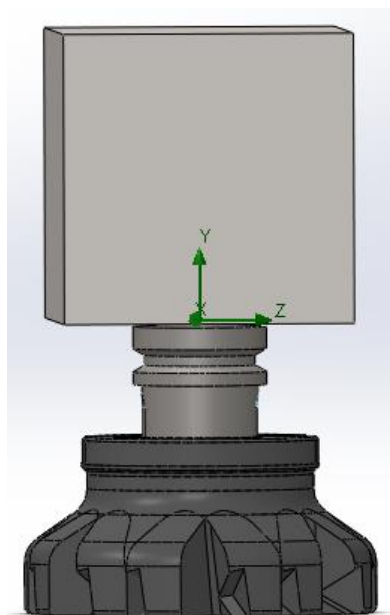


Fig. 1. – Assembling the model under study

Then we need to add a three-dimensional model, using a sketch and extrusion, select the area of rotation of the model under study (Fig. 2).

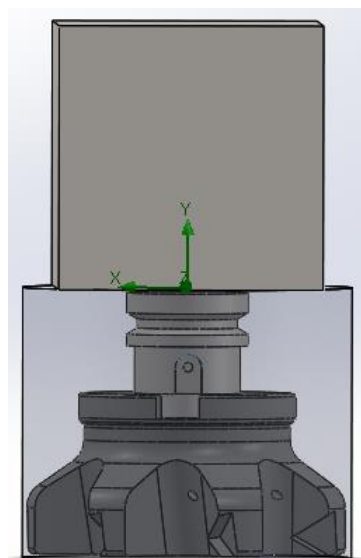


Fig. 2. – Assembly with the area of rotation

Then using FlowSimulation we launch the project master using the appropriate button. After that in the window that opens we select the metric system, the type of simulation (in our case, rotation), the type of gas or liquid. Next in a new project we set the area of rotation and the speed of rotation, using the created part, and the boundary condition that fixes our part (Fig.3).

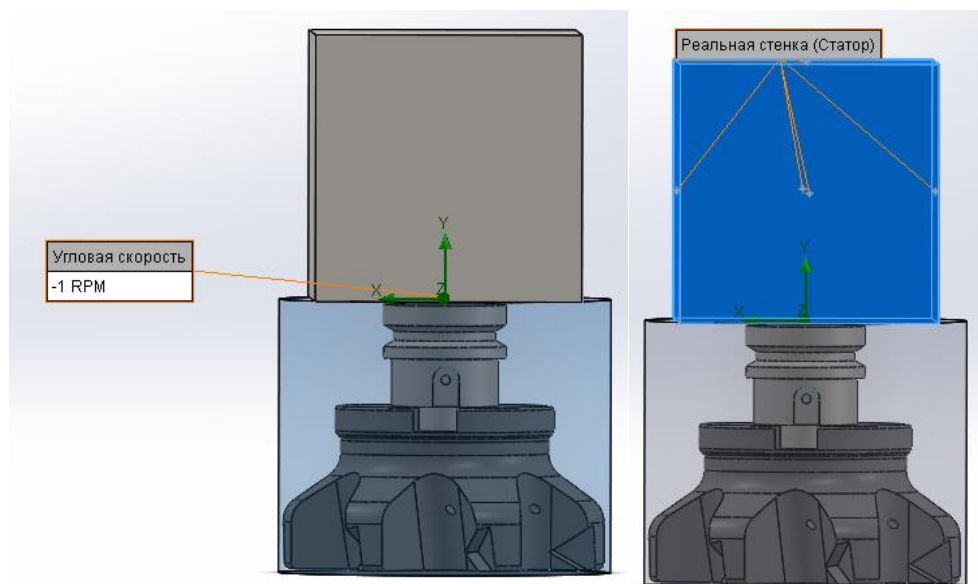


Fig. 3. – Domain of rotation and boundary conditions

After that our project is ready for modeling. We start the calculations using the appropriate button "Start". After completing the calculations, open the results section and add the flow trajectory for visualization (Fig. 4).

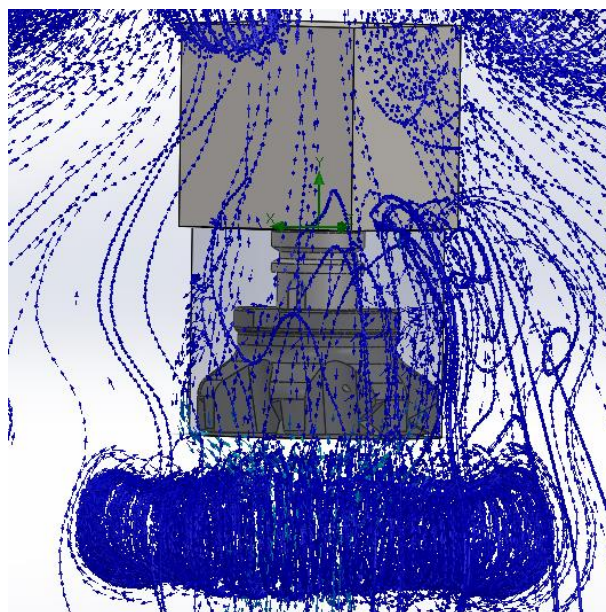


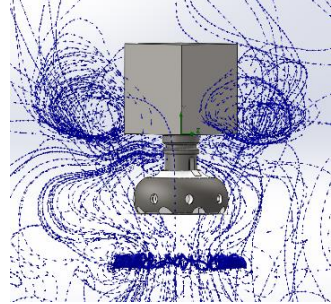
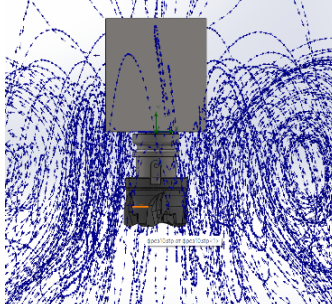
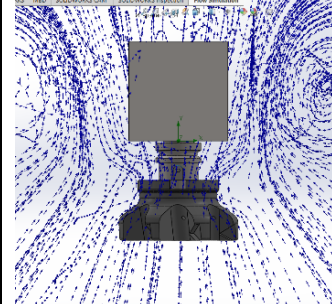
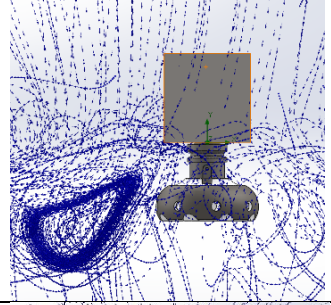
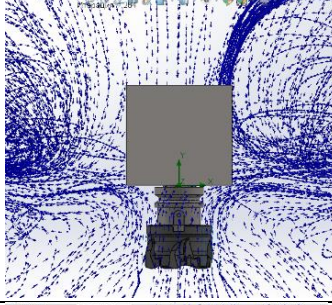
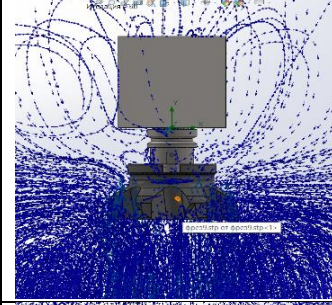
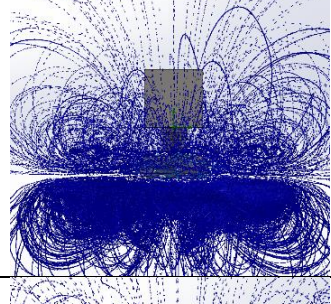
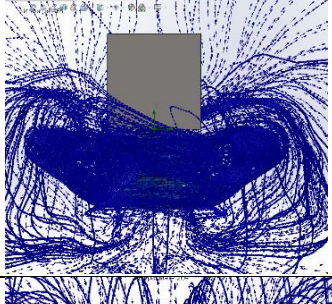
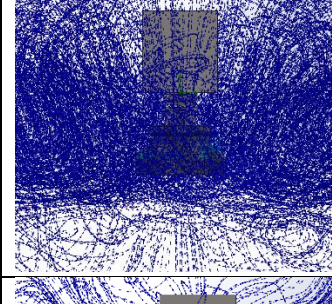
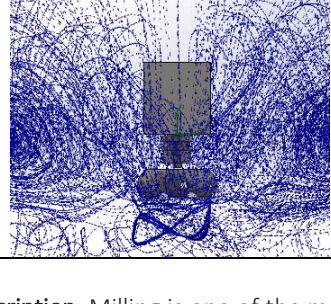
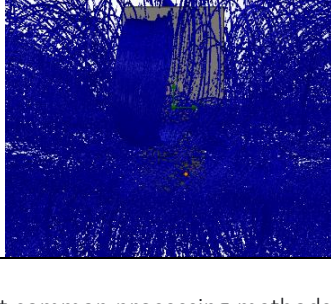
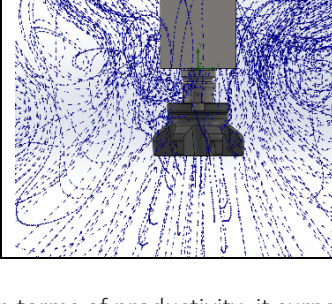
Fig. 4. – Distribution of air currents

With FlowSimulation, we can analyze and compare the air flows generated by different cutters. For experience, select milling cutters: 1-End milling cutter, 2-Milling cutter FF FWX D066-05-22-08, 3-Milling cutter HP F90AT D50-4-22-19.

For testing, select angular speeds: 1 rpm, 10 rpm, 100 rpm, 1000 rpm.

Let's compile a table with the results of all experiments. The table shows the direction of the air flow depending on the angular velocity.

Table 1. – Study of the dynamics of the work of cutters in the air

Speed of rotation	Milling cutter 1	Milling cutter FF FWX D066-05-22-08	Milling cutter HP F90AT D50-4-22-19.
1 rpm			
10 rpm			
100 rpm			
1000 rpm			

Description. Milling is one of the most common processing methods. In terms of productivity, it surpasses planing and in the conditions of serial production is second only to external pulling. The kinematics of milling processes are characterized by fast rotation around its axis and slow feed movement. The feed movement during milling can be rectilinear-translational, rotary, helical.

For milling cutter 1: at a speed of 1 rpm, a small amount of air flow is noticeable, most are projected onto the machining plane, but a significant part is chaotically scattered. With an increase of speed, we see an increase in number of air flows, they are mainly located on the projected plane, their trajectory resembles a torus. However, at 1000 rpm, we see that most of the air flows are scattered, and a distinct frieze outline is formed at the base.

For the FF FWX D066-05-22-08 cutter: at 1 rpm, air currents are sucked in, after which they create vortices on the sides of the cutter. As the speed increases to 10 rpm, the radius of the vortices increases, while the amount of air flows changes insignificantly. However, when the speed rises to 100 rpm, the amount of air flows increases significantly. The streams are highly concentrated around the frieze. This is due to the shape of the teeth. Having increased the speed to 1000 rpm, we observe a colossal amount of air flows. They form a huge torus around the cutter.

For the HP F90AT D50-4-22-19 cutter: at an angular speed of 1 rpm, a rather small number of threads are formed, relative to the rest of the cutters, however, after increasing the speed to 10 rpm, the picture changes significantly. The number of air flows increases, while the direction remains the same, the flows rise from top to bottom, spraying in a vertical plane along a parabolic trajectory. When the speed increases to 100 rpm, the air flow is redirected. There is a swirling uplift, rather concentrated, relative to the other cutters. The vortex shape is a torus. However, with an increase in the rotation speed to 1000 rpm, the speed of movement of the flows themselves increases, thereby distributing them less densely, but at a distance significantly greater than in other cases, the number of flows, in turn, decreases.

Conclusion. During the work we learn the methodology for studying the direction, quantity, speed of air flows, aerodynamic streamlining of end mills was studied. All calculations, the creation of a model of the movement of air flows were carried out in the SolidWorks software with the FlowSimulator plug-in installed.

REFERENCES

1. Методология исследования работоспособности фрезерных и осевых режущих инструментов на основе 3D прототипирования / Н.Н. Попок, С.А. Портянко – Вестник ПГУ, сер. В. Промышленность. Прикладные науки. 2020 г. – с. 29-39.

COMPARATIVE ANALYSIS OF 3D PRINTERS BASED ON FDM AND SLA TECHNOLOGIES

D. MAKSIMENKO, V. KUDRYAKOVA, N. POPOK, S. PORTYANKO

Polotsk State University, Belarus

Introduction. Modeling by the method of fused deposition (FDM) and stereolithography (SLA) are the two most popular 3D printing technologies. Both technologies are adapted and improved, which makes them more accessible, easy to use, and more functional.

The simulation of the application method of layer-by-layer material is the most widely used 3D printing technology at the consumer level. FDM works by extrusion of thermoplastics, such as ABS, PLA, through a heated extruder, material melting and applying plastic layer. These types of 3D printers are well suited for basic models, verification of the concept, as well as for quick and inexpensive prototypes creation.

Stereolithography was the world's first 3D printing technology. Invented in the 1980s, and still remains one of the most popular technologies for professionals. SLA uses a laser for curing a liquid resin into a hardened plastic in the process, called photopolymerization.

3D SLA printers have become extremely popular due to its ability to produce high-precision, isotropic and waterproof prototypes and parts from the most modern materials with excellent characteristics and a smooth surface. Resinous compositions SLA offer a wide range of optical, mechanical and thermal properties that correspond to the properties of standard, technical and industrial thermoplastics.

SLA is a great option for high-precision prototypes that require rigid tolerances and smooth surfaces, such as forms, patterns and functional parts. SLA is widely used in various industries: from mechanical engineering and design of products to production, dentistry, jewelry, creating models and education.

Comparison of 3D printing technologies FDM and SLA. Quality and print accuracy. When the processes of 3D printing create parts layer by layer, each layer also makes inaccuracy. The process of forming layers affects the quality of the surface, the level of accuracy and, therefore, the overall quality of printing.

FDM 3D printer's layers may not fully stick to each other, layers, as a rule, are clearly visible on the surface, and in the process there is no ability to reproduce complex, small details that other technologies can offer.

In SLA 3D printing, allows you to get smaller parts and is more reliable for multiple achievements of high-quality results. As a result, SLA 3D printing is known for its excellent characteristics, a smooth surface, the highest accuracy of details.

Using light instead of heat for printing is another way for SLA machines to guarantee reliability. When printing parts are at a temperatures close to room temperature, they do not suffer from thermal expansion and artifacts compression that may occur during FDM printing.

While FDM creates a mechanical connection between layers, SLA 3D printers create chemical bonds by transverse stitching of photopolymers between layers, resulting in completely dense, waterproof and airtight parts. These bonds provide a high degree of lateral strength, which leads to isotropic details. Which means that the ruggedness of the parts does not change with the orientation. It makes SLA especially ideal for mechanical engineering and production, where the properties of the material are important.

Materials. FDM 3D printers work with a number of standard thermoplastics, such as ABS, PLA and their various mixtures. The popularity of FDM in space for lovers led to abundance of color options. There are also various experimental mixtures of threads to create parts with a surface similar to a tree or metal.

Engineering materials such as nylon, PETG, PA or TPU and high-performance thermoplasty, such as PEEK or PEI, are also available, but are often limited to elected FDM professional printers that support them.

SLA resins have the advantage of a wide range of configurations of the compositions: materials can be soft or solid, strongly filled materials, such as glass and ceramics, or filled with mechanical properties, such as high heat deviation temperature or impact resistance. Various resin compositions offer a wide range of optical, mechanical and thermal properties to comply with the properties of standard, technical and industrial thermoplastics.

Description and Specifications of 3D printers**Premier3D N1 3D Printer (FDM)****Pic. 1. – 3D printer Premier3D N1**

The impressive size of the print area, components of the 200x200x200 mm. Together with a compact case and low weight, will allow the use of Premier3D N1 at home without any problems without any limiting space.

The print speed is impressive being 70 mm / s with the thickness of only 0.1 mm. Such productivity was achieved by applying special print head algorithms. The LCD panel responsible for setting up the printer has high informativeness and a large number of functions, allowing you to configure Premier3D to print any models using the necessary type of plastic [1].

Table 1. – Technical characteristics

The main	
Type	FDM printer
Minimum layer thickness	100 mkm
Technical characteristics	
Print area length, width, height	200 mm
Supported materials	PLA, ABS
Material thickness	1,75 mm
Table temperature	60 – 120° C
Extruder temperature	190 – 260° C
Maximum print speed	70 mm/s
Dimensions and weight	
Length, width, height	480x505x450 mm
Weight	19,9 kg

3D Printer Stratasys Mojo (FDM)

3D printer Mojo from Stratasys is a reliable and fast three-dimensional printing system that will easily fit on your desk.



Pic. 2. – 3D printer Stratasys Mojo

Easy to use and high-quality in the results – the MOJO printer is specially created for quick printing prototypes using a durable ABSplus plastic. The low cost, reliability and simplicity of use make Mojo an example of an available 3D printer with good characteristics. This is the best choice for those who want to get acquainted with the capabilities of three-dimensional printing. Printer's work technology – FDM is the most popular 3D printing technology in the world. The stability of printing results also provides advanced software and automatic temperature control inside the construct chamber. This will allow you to get high-quality high-definition prototypes without leaving the workplace [2].

Table 2. – Technical characteristics

Printing technology	
FDM	layered applying molten plastic thread
Working chamber size (the size of the construction area)	
Length, width, height	127 mm
Printing options	
Material thickness	0,178 mm
Print mode	adjust
Parameters of printing block	head – 1; nozzle – 2
Color printing support	9
Supported materials	
Total	1
Materials	ABSplus-P430
Model support material	SR-30 Soluble
Cartridges	2 coils (655 sm ³)

3D Printer Form3 (SLA)

Form 3 uses low power stereolithography technology (LFS) with a flexible tank and linear illumination, which provides impeccable print quality and printer reliability. The parabolic mirror ensures that the laser prints perpendicular to the plane, providing uniform print quality throughout the platform [3].



Pic. 3. – 3D Printer Form3

Form 3 constantly monitors printing performance, built-in sensors help to maintain ideal conditions and send the printer status alerts. Optical sensors constantly adjust the scale and power, and can even detect dust. The automated resin feed system allows you to print more products and leave less used materials, as well as increase the lifespan of the bath for printing. Printing chamber with air auto-heating is up to 35 ° C.

Table 3. – Technical characteristics

The main	
Type	SLA printer
Case	closed
Minimum layer thickness	25 mkm
Technical characteristics	
Print area length, width, height	145x145x185 mm
Positioning accuracy X, Y, Z	25 mkm
Supported materials	Photopolymer
Power consumption	220 W
Management	Touch display
Interfaces	USB, Wi-Fi, Internet
Supported file formats	.stl, .obj
Laser power	250 mW

3D Printer Mass Portal Pharaon

The quality of 3D printers Mass Portal is both the quality of their assembly, ensuring reliability and uninterruptedness and quality, and the accuracy of work, which gives the best printing results, allowed them to spread across multiple continents and attract well-deserved attention to themselves.

The feature of the XD series, which represents XD 20, XD 30 and XD 40 – the ability to print multiple materials at the same time [4].



Pic. 4. – 3D Printer Mass Portal Pharaon

More about them all – in the table below. There are also prices in the table, but they are approximate – the price of any 3D printer can both grow and decrease, accurate better to learn on the site.

Table 4. – Technical characteristics

The main	
Type	FDM printer
Minimum layer thickness	10 mkm
Technical characteristics	
Print area length, width, height	300x300x300 mm
Positioning accuracy X, Y	6 mkm
Positioning accuracy Z	5 mkm
Supported materials	PLA, ABS, PVA, Nylon, PET, HIPS, FLEX, PC, TPU, PP, PETG
Material thickness	1,75 mm
Table temperature	120°C
Extruder temperature	300°C
Supported file formats	.stl, .obj, gcode
Interfaces	USB, Wi-Fi, Internet
Power consumption	360 W
Complete set	
Nozzle	0,1 – 1 mm
Dimensions and weight	
Length, width, height	480x505x450 mm
Weight	19,9 kg

Conclusion. In the process of analyzing 3D printers based on FDM, SLA, we revealed their differences. The effect of the printer based on the temperature of the extruder, the heating of the table, power consumption, supported materials, the influence of various factors on the print speed. We also studied the thickness of materials, the minimum thickness of the layers. The dimensions of each printer, the size of the print area have been analyzed. The print area of the printers under consideration based on FDM is from 145 to 300 mm, and the printer based on SLA is significantly less than 127 mm. In printers operating on FDM technology, the minimum thickness of the layer is 100 mm, when based on SLA – 127 microns. There is also a difference in printing technology. 3D printers FDM form layers by applying molten plastic lines. In this process, the resolution of the part is determined by the size of the extruder. In the process of analyzing 3D printers based on FDM, SLA, we revealed their differences. In this process, the resolution of the part is determined by the size of the extruder nozzle, and voids occur between the rounded lines when the nozzle is precipitated. In SLA 3D printing, the liquid resin is cured by a high-precision laser for the formation of each layer, which allows you to get smaller parts and is more reliable for repeatedly achieving high-quality results.

REFERENCES

1. 3D - принтер Premier 3D N1. [Электронный ресурс]. – Режим доступа: <https://easycraft.by/3d---printer-premier-3d-n1/>. – Дата доступа: 20.09.2020.
2. 3D принтер Stratasys Mojo [Электронный ресурс]. – Режим доступа: <https://3d-m.ru/3d-printer-stratasys-mojo/>. – Дата доступа: 22.09.2020.
3. Form 3. [Электронный ресурс]. – Режим доступа: <https://formlabs.com/ru/3d-printers/form-3/>. – Дата доступа: 28.09.2020.
4. Mass Portal. [Электронный ресурс]. – Режим доступа: <https://massportal.com/>. – Дата доступа: 29.09.2020.

ANALYSIS OF THE DIELECTRIC CHARACTERISTICS OF COMPOSITE MATERIALS BASED ON A POLYMER MATRIX

A. TACHILO, D. TARASHKEVICH, T. MOLODECHKINA

Polotsk State University, Belarus

Currently, polymeric materials are widely used in every branch of industry and human activity. On the basis of high molecular weight compounds, rubbers, fibers, plastics, films and paint coatings are manufactured. Polymers are the basis for the production of composite materials.

Polymers belong to the class of high molecular weight compounds and are characterized by chemical structure, molecular weight, molecular weight distribution, polarity, conformational flexibility of the chain, the ability to form supramolecular structures, etc.

The widespread use of polymeric materials is due to their *unique properties*, including: low density, high plasticity, elasticity, thermal and wear resistance, chemical and radiation resistance, low electrical and thermal conductivity, crack resistance under high-intensity loads, etc.

The properties of polymers, in turn, depend on the chemical nature of the monomer, production technology, the arrangement of molecules in space and the degree of their branching, as well as external conditions (pressure, temperature).

Composite materials are compositions, i. e. in their composition, in addition to the main component, called the matrix, other components (fillers) that differ from it in properties are included in certain ratios. The peculiarities of polymers are determined primarily by the properties of the binder. The filler usually imparts these characteristics [2]. The characteristics and properties of the produced material also depend on the choice of technology for their connection with the filler. After different components are combined, the resulted material has conductive property set, which reflects not only the initial characteristics of the generators of its components, but new properties which starting components do not possess. This makes it possible to create materials with predetermined or improved properties, which is an *undoubted advantage of composites* over traditionally used materials.

Previously we had conducted research that helped establish the dependence of ϵ_{pr} composites on the type and amount of filler. The highest dielectric strength was found in materials based on a silicone matrix filled with glass fiber (fiber). This will make it possible to use composite materials as sealants for electronic components.

The relative permittivity of a dielectric material is defined as the ratio of the capacitance of a capacitor, in which the space between and around the electrodes is completely filled with the dielectric material under test, to the capacitance of the same positioned electrodes in a vacuum.

$$\epsilon = \frac{C_x}{C_0} (1)$$

When determining the relative dielectric constant of a dielectric material according to formula (1), the interelectrode capacitance can be replaced with practically sufficient accuracy in vacuum with the interelectrode capacitance in air C_0 , since the relative dielectric constant of dry air ϵ_B , under normal atmospheric conditions is close to unity ($\epsilon_B = 1.00053$).

The dielectric constant depends on the presence of polar impurities and moisture in the polymer.

Permittivity is related to polarization, i.e. with the occurrence of certain electric moment in the unit. Electric point volume is the geometric sum unit - IU dipole moments which are included in this volume.

The article presents the results of research on composite materials based on a polymer matrix. Silicone and acrylic were chosen as matrix materials.

Samples for testing the dielectric constant were made in accordance with GOST 22372-77 [1].

Sample making technology:

1. We took silicone and acrylic sealant as a matrix.
2. The required amount of silicone and acrylic sealant used as a matrix is determined by weighing.
3. The percentage of fillers was calculated.
4. We combine the calculated filler with the matrix by stirring.
5. Apply the prepared mixture on a round-shaped substrate according to GOST 22372-77. [1]
6. After 24 hours, the samples were ready for measurements.

Samples shall meet the following requirements:

1. Samples for testing solid dielectric materials should be made in the form of round, square plates or cylindrical tubes.
 2. The surface of the sample should be flat, smooth, without cracks, folds, dents, scratches, foreign inclusions and other defects. If necessary, the surface of the sample should be cleaned with a solvent that does not affect the properties of the material.
 3. The thickness of the sample should be determined as the results of its measurements at not less than five points evenly spaced along the surface of the sample.
 4. Measurement of the dielectric constant of the material should be made on the same sample.
- The method for determining the dielectric constant was carried out in accordance with GOST 22372-77 [1]. The capacitance was measured on an E 7-8 installation that meets the requirements of GOST 22372-77 [1]. Arrangement of electrodes in a sample using a two-electrode system.

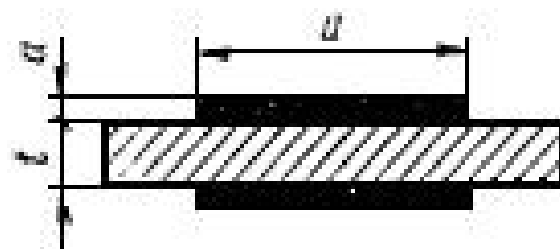


Figure 1. - Arrangement of electrodes in a sample using a two-electrode system

Formula for calculating C_0 interelectrode capacitance

$$C_0 = 0,0695 \frac{d^2}{t} \quad (2)$$

The results of these studies are presented in Tables 1-4.

Table 1. - Test results for interelectrode capacitance and dielectric constant on the E7-8 device

Silicone newsealant		
	ϵ	C_0
PC 10%	2.594	15.216
PC 20%	3.286	15.419
Fiberglass (Fiber)	5.217	15.334
Fiberglass (Canvas)	2.609	25.273
Coal 10%	5.447	14.686
Coal 20%	1.727	23.167
Soot 10%	2.969	16.838
Soot 20%	3.314	15.088

Table 2. - Test results for interelectrode capacitance and dielectric constant on the E7-8 device

Acrylic sealant		
	ϵ	C_0
PC 10%	0,48	29.030
PC 20%	0,71	20.871
Fiberglass (Fiber)	0,61	21.173
Fiberglass (Canvas)	0,42	28.138
Coal 10%	0,37	31.663
Coal 20%	0,633	25.249
Soot 10%	0,44	29.512
Soot 20%	0,46	32,477

Using the analysis of tables 1 and 2, we can conclude that silicone sealants have a higher relative permittivity of the dielectric material than acrylic.

Table 3. - Test results for interelectrode capacitance and dielectric constant on a laboratory bench

	Siliconesealant	
	ε	C_0
PC 10%	0.195	15.419
PC 20%	0.197	15.216
Fiberglass (Fiber)	0.261	15.334
Fiberglass (Canvas)	0.189	25.273
Coal 10%	0.265	14.686
Coal 20%	0.086	23.167
Soot 10%	0.178	16.838
Soot 20%	0.199	15.088

Table 4. - Test results for interelectrode capacitance and dielectric constant on a laboratory bench

	Acrylic sealant	
	ε	C_0
PC 10 %	0,24	29.030
PC 20 %	0,43	20.871
Стекловолокна (Волокна)	0,42	21.173
Стекловолокно(Полотно)	0,35	28.138
Уголь 10%	0,18	31.663
Уголь 20 %	0,35	25.249
Сажа 10%	0,37	29.512
Сажа 20%	0,307	32.477

Using the analysis of tables 3 and 4, we can conclude that silicone sealants have a higher relative permittivity of the dielectric material than acrylic ones.

Output:

Studies have been carried out on the dielectric characteristics of composites based on silicone and acrylic. The result of studies show that most are samples of silicone excipient where the carbon makes up 10% as measured on the instrument E 7-8. The least important are the samples made of silicone, the filler of which is 20% carbon, which was determined on a laboratory bench.

This information will be used for a comprehensive assessment of the properties of composites in the selection of their performance characteristics.

REFERENCES

1. GOST 22372-77 Dielectric materials. Methods for determining the dielectric constant and the tangent of the dielectric loss angle in the frequency range from 100 to $5 \cdot 10^6$ Hz. By the termination of the State Committee of Standards of the Council of Ministers of the USSR dated February 18, 1977 N 424, the validity period was established from 01.01 1978 to 01.01 1983 - URL: <https://docs.cntd.ru/document/1200016160>. –Text: electronic.

537.533; 621.3

COMPARATIVE ANALYSIS OF SOFTWARE FOR SIMULATION OF ELECTRONIC - OPTICAL SYSTEMS

D. BIRYUKOVA, D. ANTONOVICH

Vitebsk State University named after P. M. Masherov, Belarus

A number of existing packages of applied programs for computer modeling of electron-optical systems of sources of charged particles built on the basis of analytical synthesis models and numerical methods of analysis are considered. The analysis of the main advantages and disadvantages of the packages MAGIC, MAFIA, CEM, KARAT, POISSON, TAU, ERA, BEAMCAD and their functionality is carried out.

Electron beam technologies occupy an essential place among modern highly efficient methods of metal-working and obtaining materials with new properties. Expanding the field of application of this kind of technologies in industry is necessary both to improve the quality and reliability of products and to increase their competitiveness, since the use of modern technologies, including electron beam technologies, meets the requirements of European and international quality standards. A wide range of technological capabilities of electron beam heat treatment has determined the use of electron beams in many technological processes. [1], including for cutting, melting, welding and heat treatment - hardening, hardening and surface modification. In this case, for the formation of beams of charged particles, different classes of devices are used according to the principle of operation, one of the most promising are sources of charged particles, the principle of operation of which is based on the emission of charged particles from the plasma of a gas discharge [2]. The basis of any electron-beam device is an electron-optical system (EOS), which is used to form an electron beam with certain parameters. The variety of factors affecting the parameters of the generated beams, their interrelation and mutual influence, require a large amount of experimental work to obtain electron beams with the required characteristics in the development of new EOS designs, which makes it expedient to use computer simulation technologies to reduce financial and time costs at the design and construction stage. similar devices.

The purpose of this work is some analysis of the functional capabilities of a number of existing software for modeling electro-optical systems of sources of charged particles.

Material and methods. The material for the study was software for mathematical modeling of electro-optical systems. During the research, generally recognized methods of scientific knowledge were used.

Result and its discussion.

Software for modeling electron-optical systems can be divided into three groups depending on the intensity of the simulated beam of charged particles: for calculating low-current electron beams (taking into account only the effect of their own space charge), for calculating high-current electron beams, and for calculating high-current electron beams in complex gas-dynamic conditions.

Each of the programs has its own sources of errors, since they are based on analysis methods or synthesis methods. In methods of analysis, errors, as a rule, arise due to the discretization of the flow of charged particles and the computational domain, in addition, errors arise associated with numerical methods for solving differential and integral equations of problems of mathematical physics. In synthesis methods, errors proceed from the approximate nature of the solution of both the internal and external problems in the approximation of asymptotic expansions.

To simulate processes in low-temperature plasma, there are a large number of software systems. One of the examples of such complexes is COMSOL MULTIPHYSICS [3], in which there is a module that allows simulating plasma physics without taking into account kinetic effects. For modeling processes in low-temperature plasma, there is software that allows you to build mathematical models of these processes. Also, MAGIC (USA) [4], MAFIA (Germany, USA) [5], CEM (USA) [6], KARAT (Russia, USA) [7], POISSON (Novosibirsk, USA) can be used as examples of software systems. [8], TAU (St. Petersburg) [9], ERA (Novosibirsk) [10], BEAMCAD (Moscow) [11].

All the aforementioned application packages (APPs) use Newton's equations as methods for calculating the motion of charged particles. The first four programs use a large particle model to discretize the flow of charged particles, POISSON and BEAMCAD use a non-deformable stream tube model, and TAU can use both methods. The mobility of the EOS boundaries allows modeling only the ERA, in all other RFPs it is considered that the boundaries are immovable.

None of the above PPPs take into account secondary emission processes. Ionization processes can be simulated only by ERA and BEAMCAD, they take into account the ion flux by the method of non-deformable current tubes, the effect of paired electrons is neglected.

All programs from the list simulate an EOS with a solid-state cathode, POISSON, in addition, simulates bipolar fluxes, and ERA, in turn, allows simulating a plasma anode.

Conclusion. To date, a number of applied software packages have been developed to simulate the processes of formation of beams of charged particles, mainly in systems using emission from solid-state emitters. Such SPPs are not applicable for systems based on a plasma emitter, which have a number of physical features in comparison with systems based on solid-state emitters. In the presently existing SPP for modeling the EOS of plasma emitters, there are many unsolved problems. Namely, the shape of the emitter is not taken into account (the possibility of analyzing the shape and the possibility of changing it are not considered), secondary electron-electron and ion-electron emission are not taken into account, and the compensating charge for electron beams provided from the outside is not taken into account. In addition, the existing software does not take into account the magnetic field, which can affect the formation of the beams. Taking into account the promising application in mechanical engineering and instrument making of beam devices based on plasma emitters [12], the task of creating a software package for modeling the physical processes of the electron-optical properties of systems of sources of charged particles based on plasma emitters, taking into account the features of such EOS, is urgent.

REFERENCES

1. Electron beam processing of materials / V. N. Alekhovich, A. V. Alifanov, A. I. Gordienko, I. L. Pobol // Minsk, Belarusian Science, 2006, 320 p.
2. Physics and technology of plasma emission systems / ed. ed. V. T. Barchenko. SPb.: Publishing house of ETU "LETI", 2014. 286 p.
3. Dickinson, E. COMSOL Multiphysics (R) : Finite element software for electrochemical analysis. A mini-review / E. Dickinson, H. Ekström, E. Fontes // Electrochemistry Communications. – 2014. – Vol. 40. – P. 71-74.
4. Goplen B., Ludeking L., Mc Donald J., Warren G., Worl R. MAGIC user's manual // Mission Res. Corp. Nevington VA. Rep. MRC/WDC-R-184, Sept. 1988.
5. The 3-D MAFIA Group of Electromagnetic Codes / Ebeling F. [et al.] // IEEE Trans. Magn. – 1989. – V.25, №4. – P.2962–3064.
6. Shankar V., Hall W.F., Mohammadian A., Rowel C. Development of a CFD-based Algorithm for Computational Electromagnetics (CEM)// In: Computational Fluid Dynamics Review 1995. John Wiley&Sons, NY, 1995.P.821-836./ Ed. Hafez M., Oshima K.
7. User's manual for code KARAT // V.P. Tarakanov and Berkley Research Associates. – Inc. 1992-96.
8. Numerical Simulation of Diodes with Plasma Electrodes / V. Astrelin [et al.] // Proceedings of 15th International Symposium on High Current Electronics. – Tomsk: Publishing house of the IAO SB RAS, 2008. – P.11-15.
9. Tregubov V.F., Tregubov A.V. Program package TAU. Structure and applications for electron device simulation. Proceedings of the 7-th International conference on electron beam technologies. 2003. Varna. Bulgaria. P.39-41.
10. Sveshnikov, V.M. Sveshnikov V.M. Solution of the optimization problem for intense beams of charged particles in the ERA SPP / V.M. Sveshnikov // Technology of modeling problems of mathematical physics. - Novosibirsk: Computing Center of the Siberian Branch of the USSR Academy of Sciences. - 1989. - S. 134-141.
11. Dzagurov, L. Yu. Numerical modeling of electron-optical systems with gas filling / L.Yu. Dzagurov, Yu.A. Kovalenko // Radio engineering and electronics. - 1987. - T. 32, No. 4. - S. 847-854.
12. Antonovich D.A. Plasma emission systems for electron and ion-beams technologies / D.A. Antonovich, V.A. Gruzdev, V.G. Zalesski, I.L. Pobol, P.N. Soldatenko // High Temperature Material Processes: An International Quarterly of High-Technology Plasma Processes. – 2017. – vol. 21. iss. 2 p.143-159.

ICT, ELECTRONICS, PROGRAMMING, GEODESY

UDC 537.533; 621.384

METHODS OF FORMING CHARGED PARTICLE BEAMS OF LARGE CROSS SECTION

P. SOLDATENKO, Y. GOLUBEV

Polotsk State University, Belarus

D. ANTONOVICH

Vitebsk State University named after P.M. Masherov, Belarus

Improving the efficiency and quality of electron-beam surface treatment of materials is one of the important issues in the process of developing technological equipment. To solve this problem, it is proposed to use electron-beam assistance, which implies alternating or simultaneous exposure to beams of charged particles of both types on the treated surface. In this paper, we consider a method capable of providing such an impact.

The development of the theory and practice of the formation of beams with a large cross section is associated with the prospects of their use for materials surface treatment. Such processing by beams in vacuum and in the residual atmosphere of various gases is used in plasma-chemical technologies, heat treatment of various materials, coating deposition, etc. In a number of cases, a significant increase in the quality of such technologies and the productivity of technological equipment involves the simultaneous action of electron and ion beams. At the moment, this technology is usually provided by using separate electron and ion sources. In this case, the most widespread application for the formation of plasma surfaces emitting ion or electron beams has received gas-discharge electrode structures in which magnetron discharges are excited [1; 2], or discharges with electron oscillations of the "Penning" type (PIG) [3], or with a hollow cathode [4; 5]. Under technologically necessary conditions of low gas pressure, to reduce the discharge voltage and the density of the emitting plasma in gas-discharge structures, hot cathodes are used [6]. A significant drawback of such sources is their fragility in gas discharges.

In the above sources, the emitting plasma is separated from the electrodes of the gas-discharge structure by near-wall electrical layers, the parameters of which are determined by the potential difference between the plasma and each electrode, as well as by the plasma density, as is customary at present, by the condition that the electric field strength at its boundary is equal to zero [7]. The emitting plasma surface also obeys this condition [8]; therefore, the electron (ion) optical conditions in the acceleration gap of electrons (ions) and beam formation depend on the position and shape of the emitting plasma boundary; on the accelerating voltage, the geometry of the electrodes and their potential. This creates certain difficulties in the formation of beams with a large cross section [9].

At the same time, the efficiency of using plasma sources in technological applications is due to the achievement of the necessary parameters of the beam itself in these sources, first of all, the energy of ions and electrons, the surface current density in the beam, and the current density distribution over the beam cross section. The inhomogeneity of the distribution of the current density over the cross section of the ion-electron beam will lead to uneven processing of the material surface; therefore, achieving a uniform distribution of the beam current density is an important task.

The known effect of the possible formation of secondary plasma in the accelerating gap [10] can provide a significant improvement in the emission-optical properties of a source with a plasma emitter: a decrease in the beam divergence due to a decrease in the radial potential gradient in the accelerating gap; an increase in the emission current due to the reverse flow of charges from the secondary plasma into the emitting plasma [11]; increasing the perveance of the accelerating system due to partial compensation of the space charge of the beam.

Also there are known works on electron-beam processing of surfaces when exposed to dielectric materials, in which the features of the effect of the surface charge introduced by an electron beam to the surface are studied. It is shown that this charge is effectively "removed" by the secondary plasma of the electron beam. However, the features of the formation of a "plasma blanket" over a large area to be treated when exposed to ion-electron beams have not been studied. Studying the behavior and parameters of plasma near the surface, depending on the beam current, energy of charged particles and gas pressure, will make it possible to determine and optimize the parameters of a multi-discharge system created for processing large surfaces.

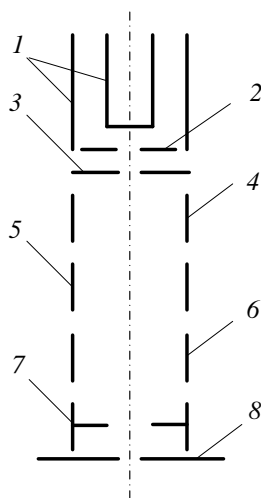
The above suggests:

1) the possibility of creating a plasma object with electrostatic layers in it, capable of providing the formation of ion and electron beams combined in a single space;

2) the multifactorial nature of such a structure and the absence of the necessary algorithms currently complicates the numerical simulation of such structures;

3) an experimental study of such structures at this stage seems to be the most effective for creating technological sources of combined ion-electron beams.

A schematic of the electrode structure of the experimental source is shown in Figure 1. In the volume bounded by electrode 1 (cathode) and electrode 2 (anode), a discharge with electron oscillation is excited [12; 13], from the plasma of which the electrons emission and acceleration is provided by the electrode 3. Electrodes 3–7 form a gas-discharge structure that forms a plasma, which is a source of sputtering ions. This structure consists of two PIG-type gas-discharge cells connected in series (along the axis). Elements 4 and 6 of this structure are the anodes of the discharge cells; elements 3, 5 and 7 - cathodes. A voltage is applied between the electrodes 7 and 8, which accelerates the ions to the energy of the sputtering ions required by the technology. At the same time, in this gap (between electrodes 7 and 8), the deceleration of the electron beam accelerated between electrodes 2 and 3 is carried out.



1, 5, 7 – cathodes; 2, 4, 6 – anodes; 3 – accelerating electrode (electrons); 8 – accelerating electrode (ions)

Figure 1. – Schematic electrode structure of a multi-discharge system

Conclusion. The proposed concept of the source shows the possibility of creating multi-discharge panels that allow solving urgent problems of forming technologically combined electron and ion beams for the implementation of electron-beam assistance to plasma-chemical processes or combined exposure to electron and ion beams. Sources of this type can become a unique universal tool for applying film coatings for various purposes. Such systems can be of interest both as separate sources and as cells of a multi-discharge source for the formation of an impact on large areas.

REFERENCES

1. Барченко, В.Т. Физика и технология плазменных эмиссионных систем / В.Т. Барченко. – Санкт-Петербург: Изд-во СПбГЭТУ «ЛЭТИ», 2014. – 286 с.
2. Кузьмичёв, А. И. Магнетронные распылительные системы. Кн. 1. Введение в физику и технику магнетронного распыления / А.И. Кузьмичёв. – Киев: Аверс, 2008. – 244 с.
3. Penning FM. Coating by Cathode Disintegration. US Patent 2,146,025; N.V. Philips, Gloeilampenfabrieken, Eindhoven, The Netherlands; 1939
4. Москалев, Б.И. Разряд с полым катодом / Б.И. Москалёв. – Москва: Энергия, 1969. – 184 с.
5. Крейндел, Ю.Е. Плазменные источники электронов / Ю.Е. Крейндел. – Москва: Атомиздат, 1977. – 145 с.
6. Алямовский, И.В. Электронные пучки и электронные пушки / И.В. Алямовский. – Москва: Советское Радио, 1966. – 454 с.
7. Груздев, В.А. О механизме возникновения электрического поля в плазме при эмиссии электронов / В.А. Груздев, В.Г. Залесский // Вестник Полоц. гос. ун-та. Сер. С, Фундаментальные науки. – 2014. – № 4. – С. 103–108.
8. Груздев, В.А. Формирование эмиссионного тока в плазменных эмиттерах электронов. / В.А. Груздев, В.Г. Залесский // Прикладная физика. – 2009. – № 5. – С. 82–90.

9. Gruzdev, V.A. Electron-optical characteristics of the beam generated by the electron plasma sources / V.A Gruzdev, V.G. Zaleski // *Electrotechnica and electronica (Bulgaria)*. – 2014 – V. 49, № 5-6. – P. 264–268.
10. Gruzdev V.A. Emission current formation in plasma electron emitters / V.A. Gruzdev, V.G. Zaleski // *Plasma Physics Reports*. – 2010. – №36. – p. 1191-1198
11. Залесский, В. Г. Эмиссионные и электронно-оптические системы плазменных источников электронов : дис. ... д-ра физ.-мат. наук : 01.04.04 / В. Г. Залесский. – Минск, 2015. – 316 с.
12. Gruzdev V.A. Universal plasma electron source / V.A. Gruzdev, V.G. Zaleski, D.A. Antonovich, Y.P. Golubev // *Vacuum*. – 2005. – №77. – p. 399-405.
13. Zaleski V.G. Peculiarities of plasma electron sources operation at high pressures / V.G. Zaleski, D.A. Antonovich // *Journal of Physics D: Applied Physics*. – 2007. – №40. – p.7771-7777.

RESEARCH OF CURRENT MARKET NEEDS USING MODERN METHODS OF DATA ANALYSIS

E. GAYCHUKOV, V. LIVINSKAYA

Belarusian-Russian University, Mogilev, Belarus

The article shows the results of a study of the market for vacancies in the field of information technology. The study was conducted to determine the most demanded specializations, programming languages, as well as salary levels, depending on the professional gradation and the programming language that is used.

The problem of training specialists who will be in demand in the labor market has become especially urgent in recent years. This is especially noticeable in the field of information technology. In the recent past, all development associated with the accurate computations, belonged mainly to military and space fields. Now there is a huge variety of domains where such specialists are needed, for example, e-commerce, bioinformatics, medical research, geology, product quality control etc. The rapid digitalization of all areas related to the life of society implies that graduates of the IT profile of universities will be able to demonstrate their knowledge and skills regardless of the subject area, which makes special requirements for the developers of educational programs. It is necessary to regularly analyze the labor market in this category and make changes that allow students to master the necessary competencies.

This study analyzes the vacancies of IT-profile specialists posted on the HeadHunter website, one of the largest job search and employee search resources in the world (according to the Similarweb rating). The site has 49 million resumes in the database, 793 thousand vacancies, 1423 thousand verified companies regularly place their ads. The website is visited by 18 million visitors monthly, leaving about 1 billion responses to vacancies.

Special program was written using Python language to collect data from the site. The HeadHunter service provides a special API (application programming interface) that makes it possible to get information about applicants and companies. The main activity of the company is the sale of information from the resume database (information about the database and the opportunity to post a vacancy for employers are carried out on a paid basis). The search in the vacancy database is provided free of charge for applicants, which made it possible to organize the collection of data using the API for this study. The company regularly publishes analytical information on the state of the labor market, publishing information on the annual or monthly dynamics of vacancies and resumes. The hh-index is a coordination statistic that is used to characterize the relationship between supply and demand. It shows how many resumes are per vacancy. The more important this index is, the higher the competition in the analyzed professional sphere is.

Python has been used to connect to the databases of the HeadHunter site. This programming language also has been used to collect and process information.

API HeadHunter can be used to access the database of vacancies of companies in Ukraine, Belarus, Azerbaijan, Uzbekistan, Kazakhstan, Georgia, Kyrgyzstan. This opportunity allows large companies to expand their business outside of Russia. It also helps citizens of the former Soviet Union to find jobs in Russia.

We have analyzed 17,620 ads in the Information Technology, Internet, Telecom category published on the website from January 11 to February 27, 2021. Vacancies were organized into a dataframe (a special table that consists of records whose fields are variables of various types) using a special algorithm. The bounds of the salary range are a quantitative attribute of a vacancy. It is present in the records if it is completed by the employer. The rest of the attributes are categorical. Table 1 shows the fields that the employer fills in.

Table. – List of fields in the analyzed dataset

Field name	Semantic content
id	ad identifier
language	programming language
grade	skill level
vacancy_name	vacancy title from the website
employer	name of employer's company
city	city of employer's company location
experience	required previous experience
schedule	type of employment
published_at	publication date
salary_from	lower bound of the salary range
salary_to	upper bound of the salary range
currency	currency of salary
specialization1	subject area
specialization2	subject area

The cities with the greatest need for IT specialists and the most common programming languages were selected for conducting reliable statistical analysis. Moscow (8938 vacancies), St. Petersburg (4104 vacancies), Novosibirsk (1588 vacancies), Minsk (1223 vacancies), Yekaterinburg (902 vacancies), Kiev (864 vacancies) are cities that can be attributed to this group. We have selected vacancies with the following programming languages: 1C (795 vacancies), C# (1078 vacancies), C++ (448 vacancies), Java (1219 vacancies), JavaScript (642 vacancies).

We have conducted an analysis of variance to determine the factors that influence the salary range. As a result, we have found out that there is a difference in the average level of salaries depending on the city, currency, subject area. Figure 1 shows average values of the bounds of the salary range depending on the subject area.

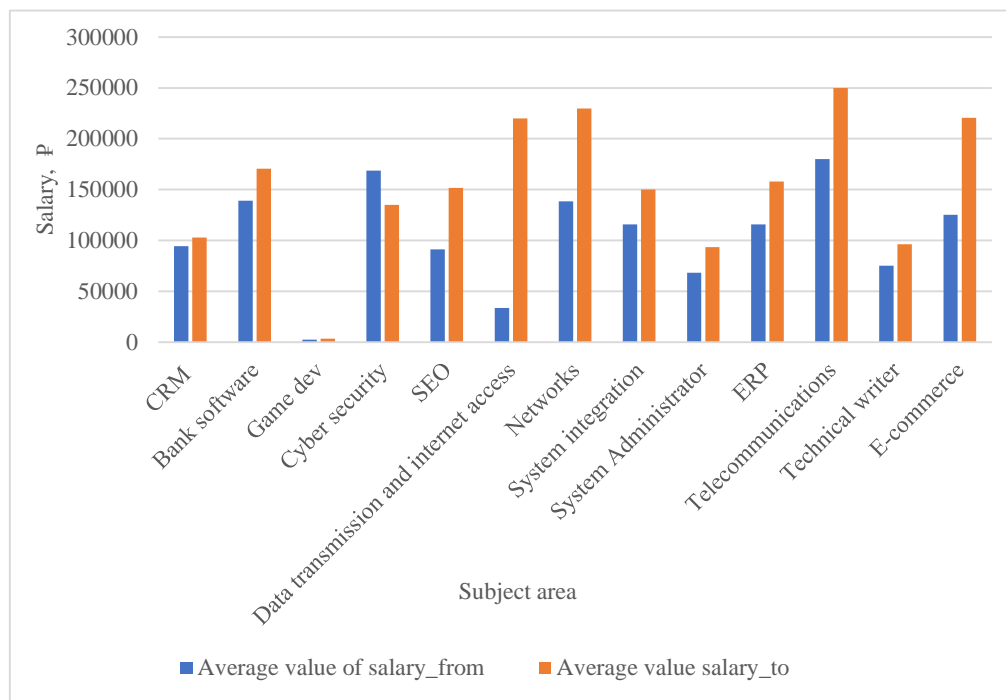


Fig. 1. – Average values of the bounds of the salary range depending on the subject area

The greatest length of the salary range is observed in the field of data transmission and Internet access. It means that professional skills are very significant in this area.

REFERNECES

1. Wikipedia.org : website. – Moscow, 2021. – Mode of access: <https://ru.wikipedia.org/wiki/HeadHunter>. – Date of access: 27.03.2021.

ANALYSIS OF THE NAND FLASH DEVICE GARBAGE COLLECTION ALGORITHMS UNDER LACK OF MEMORY CONDITIONS

I. ZAITSEV, S. ZALIVAKA

Belarusian State University of Informatics and Radioelectronics, Minsk, Belarus

The paper presents the problem of high latency requests in SSD devices with a greedy garbage collection algorithm under low memory conditions. To solve this problem, other existing algorithms (RGA, Random, FIFO) are considered. The algorithms are implemented in the MQSim simulation environment. As a result, it is shown that in lack of memory conditions, the FIFO algorithm can reduce the latency of command executions by an average of four times compared to the greedy algorithm.

Nowadays, solid-state drives (NAND Flash SSD – Solid State Drive) are widely used in many computer systems, along with traditional hard disk drives (HDD – Hard Disk Drive). Solid-state drives have become widespread in comparison to traditional hard drives due to several advantages: faster access time, lower power consumption and compact package. It is also important that due to the lack of moving parts, solid-state drives have better vibration resistance. The disadvantages of solid-state drives include: a higher cost per bit of information storage, a lower throughput and latency during service procedures (e.g. garbage collection, wear leveling, etc.), and a smaller number of erase/write cycles for each block of memory [1].

SSD devices support three basic operations: read, write, and erase. The read and write operations work within the page, while the erase operation works within the block (block is a collection of pages) [2].

Each page in the SSD has one of three possible states: valid, invalid, and free/erased. The write operation can only be applied to a page in a free state. When a write operation is applied to a page, its state is changed from free to valid. Fig. 1 shows a case when data needs to be overwritten, which leads to the latency increase during a write operation. To optimize the write request, the data is written to a free block and the address mapping table (L2P – Logical to Physical Table) is updated. All pages of the old block are marked as invalid. With this optimization, all pages will gradually change their state from free to valid and invalid. The garbage collection procedure is used to restore invalid pages [2].

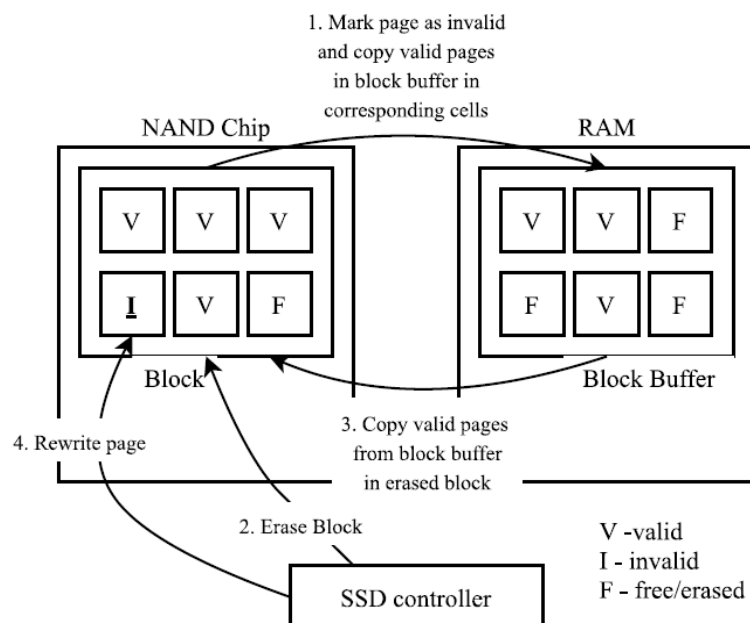


Fig. 1. – Page rewriting process

Garbage collection algorithm have such parameters as a threshold for the garbage collection procedure and a victim block selection policy. The threshold determines the number of free pages when the garbage collection procedure starts (triggered). The victim block selection policy determines which criteria are used to select a block to erase.

Garbage collection leads to significant latency overhead, so when garbage collection is performed, the delay in operational requests increases. In lack of memory conditions, the performance of an SSD device can significantly drop (at least 16 times, according to the modeling results shown in Fig. 2). Therefore, it is necessary to use an algorithm that would reduce the impact of the garbage collector on the device performance in such conditions.

This problem is typical for SSD devices with a greedy garbage collection algorithm. The purpose of the research is to find an algorithm that would reduce command execution latency in lack of memory conditions and compare it to the greedy algorithm performance.

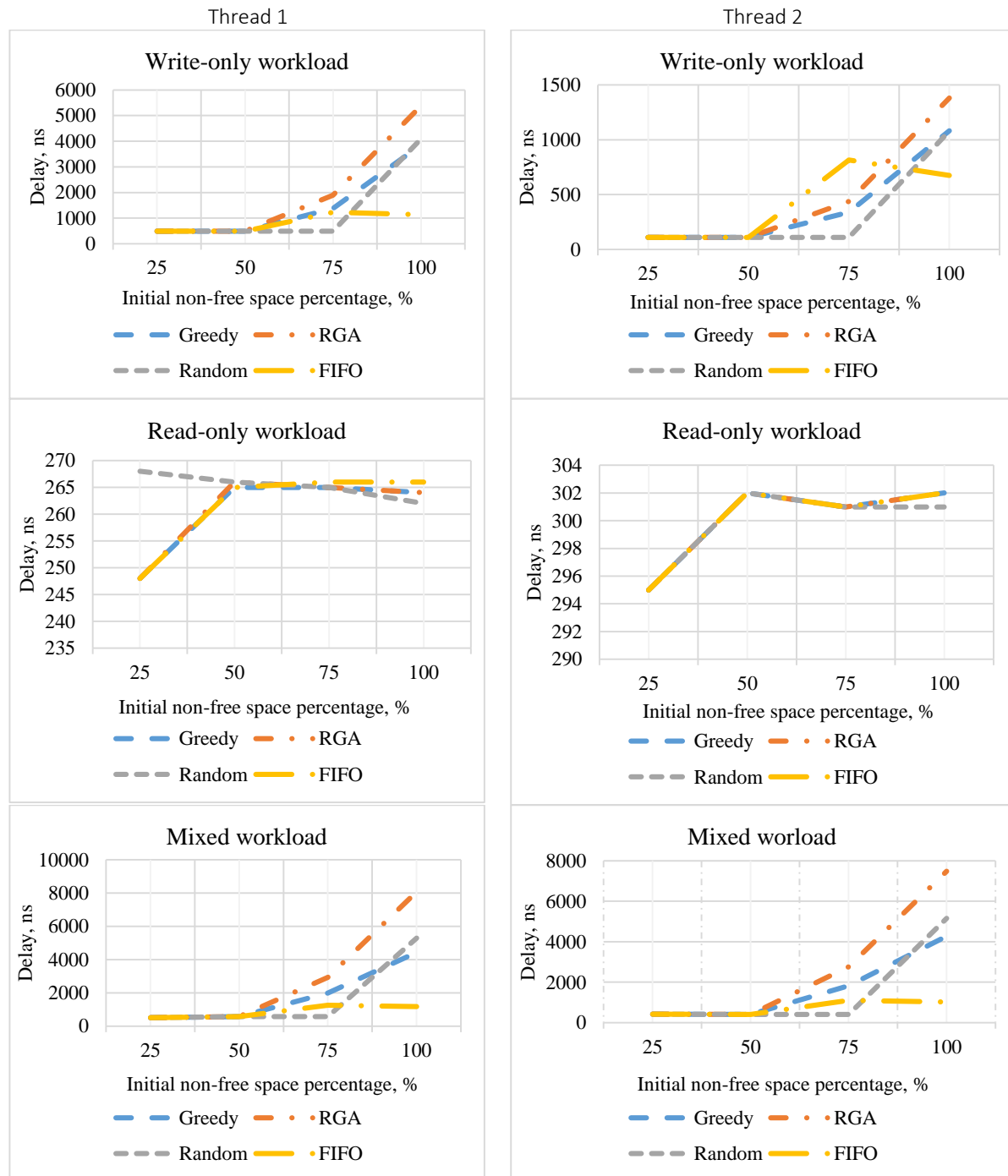


Fig. 2. – Delay values obtained during simulation of considered algorithms under different workloads

There are four garbage collection algorithms analyzed in this work:

1. **Greedy.** The block with the largest number of invalid pages is selected [3].

2. **RGA (Random Greedy Algorithm)**. The block with the largest number of invalid pages is selected from a random set of blocks [4].

3. **Random**. A random block is selected [4].

4. **FIFO (First In – First Out)**. A queue-based algorithm, i.e., each victim block is added to the queue when it is fully written. If the drive needs to perform a garbage collection procedure, the victim block is chosen as a result, i.e., the least recently written block [3].

The MQSim simulator is chosen as the environment for the experiment [2]. In this environment, the workload (the sequence of requests of the same or different types) can be reconfigured, the parameters that are responsible for the ratio of write and read requests, and the initial non-free space percentage of the disk can be set. Also, in this environment, it is possible to run simulations using multiple threads to execute requests. The simulation is performed with three types of workload: write commands only, read commands only, and mixed workload (read and write commands). In all cases, the number of requests is 1.2×10^5 and the two-threads mode is set.

Fig. 2 shows the measured delays for each algorithm. The first column shows the results for Thread 1, and the second column shows the results for Thread 2. The first row shows the results for write-only workload, the second row – for read-only workload, and the third row – for mixed workload (for Thread 1 read percentage is 80, for Thread 2 read percentage is 30).

Based on the results shown in Fig. 2, it is possible to make the following conclusions:

1. The read delay is approximately the same for different algorithms under conditions of varying degrees of free disk space.

2. Under write-only and mixed workloads the first three algorithms show almost the same behavior of the delay dependency despite of free disk space changes.

3. The FIFO algorithm can be described by a different behavior and shows the maximum delay value not when the disk is full. Then it shows almost a constant delay value, which is 5-6 times (on average) less than the value shown by other algorithms in lack of memory conditions. Based on the simulation results, FIFO algorithm shows the best performance in both cases, lack of memory conditions (disk is almost full) and free disk space around 25% or less.

Figs. 3 and 4 show the average number of page movements for GC (Garbage collection) and total number of GC executions for write-only and mixed workloads.

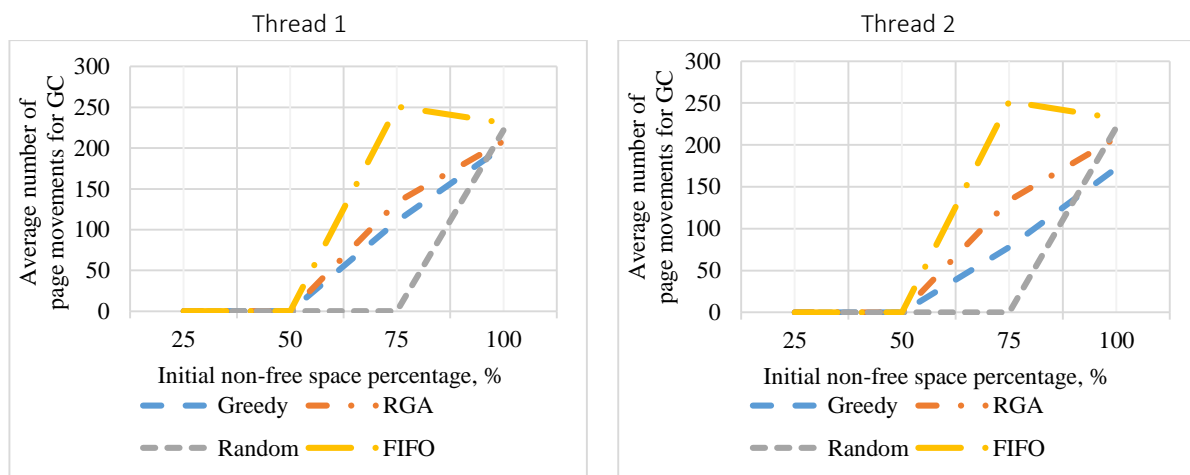


Fig. 3. – Average number of page movements for different garbage collection algorithms

Based on the obtained data, it can be concluded that:

1. The number of page movements and total number of GC executions are correlated to the delay value, i.e., with a decrease of free disk space, the write delay, number of page movements and total number of GC executions will increase. This can be explained by the fact that as the device has less free space, there are fewer free pages and the probability of getting a rewrite request increases, which leads to a search of a free block, the absence of which triggers the garbage collection procedure.

2. The conclusions described above (point 1) does not match the FIFO algorithm. Average number of page movements and total number of GC executions are almost equal after reaching the minimal value (25% of free disk space).

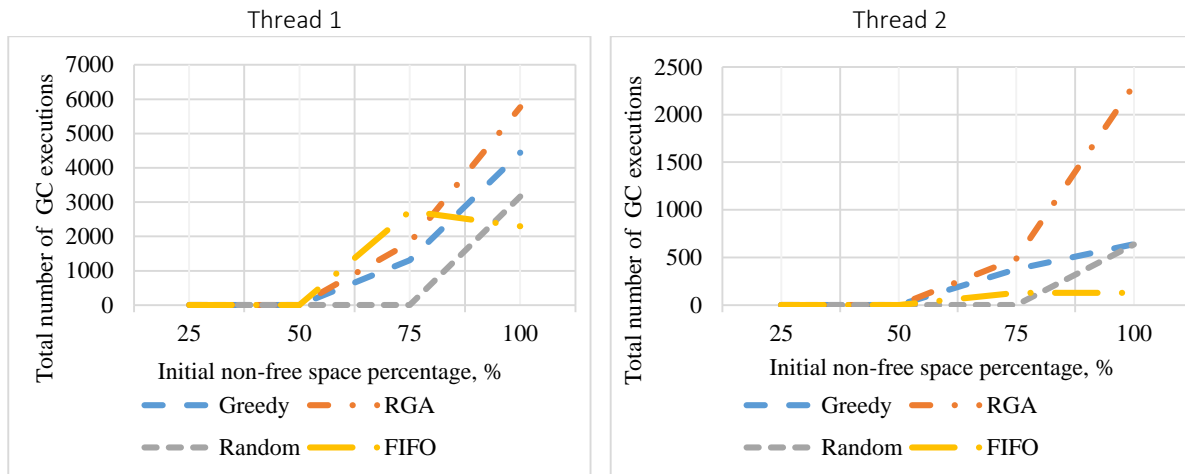


Fig. 4. – Total number of GC executions for different algorithms

Fig. 5 shows the total number of WL (Wear Leveling) executions for whole device.

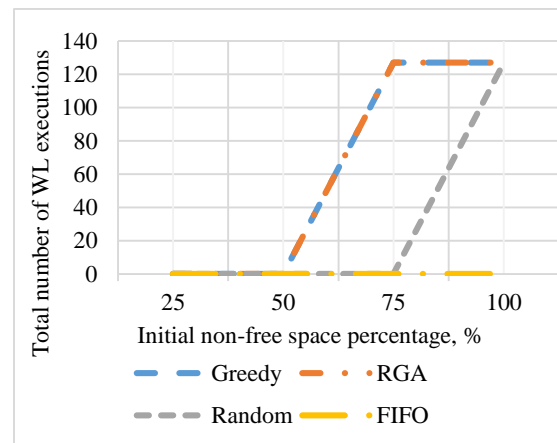


Fig. 5. – Total number of WL executions for different algorithms

Based on Fig. 5, the following conclusions can be drawn:

1. For the FIFO algorithm, wear leveling is not applied, because the victim block for garbage collection is selected from the head of the queue. In this case, the blocks will wear out equally, as least recently written blocks will be selected as victim blocks. Thus, the FIFO algorithm provides a built-in algorithmic level of uniform distribution of wear out levels for the blocks.

2. The other algorithms show approximately the same performance.

During the experiment various algorithms (Greedy, RGA, Random, FIFO) have been compared under lack of memory conditions using the MQSim simulation environment. The results of the experiment have shown that the FIFO algorithm is four times more efficient in terms of requests latency comparing to the greedy algorithm. Usage of the FIFO algorithm reduces the latency of requests by reducing the number of the garbage collection procedure calls and ensures an almost uniform page wear leveling in the device.

REFERENCES

1. Kim Y., Taurus B., Gupta A., FlashSim: A Simulator for NAND Flash-based Solid-State Drives.
2. Tavakkol A., Gómez-Luna J., Sadrosadati M., MQSim: A Framework for Enabling Realistic Studies of Modern Multi-Queue SSD Devices.
3. Houdt B. V. Performance of garbage collection algorithms for ash-based solid state drives with hot/cold data.
4. Houdt B. V. A Mean Field Model for a Class of Garbage Algorithms in Flash-based Solid State Driver.

AMPLITUDE-TYPE SENSORS IN FIBER-OPTIC DEVICES

A. MOROZ, V. YANUSHKEVICH
 Polotsk State University, Belarus

This article describes the process of intellectualization of the fiber-optic sensor (FOS) system. The block diagram of the intelligent system is shown. The modeling of the flowchart of FOS intellectualization in the LabVIEW program is shown.

The object for intellectualization is a fiber-optic sensor used to measure movements.

FOS intellectualization is achieved through the use of digital filtering, an error correction unit, a displacement parameter calculation unit, as well as an information signal generation unit, while automatic correction is possible in each digital unit depending on the requirements and operating conditions.

Figure 1 shows a block diagram of the intelligent system.

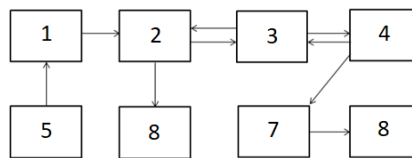


Figure 1. - Block diagram of the intelligent system

5-power supply unit; 1-radiation source; 2-beam splitter; 3-optical fiber 1, 7-optical fiber 2; 4 – the object under study; 8-output device.

The creation of the primary converter was performed according to the block diagram in Figure 2.

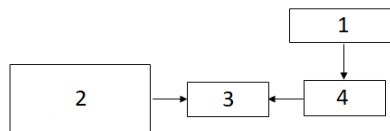


Figure 2. - Block diagram of the intelligent displacement converter system

The information signal from the sensor (1) via the NI-6009 ADC (4) is sent to the PC (3) on which the LabVIEW software package is installed (2). This program allows you to measure, filter, graphically display the signal in real time and perform various operations on the information signal.

The developed intelligent sensor system (Figure 3) consists of 11 blocks:

- a generator that simulates an information signal (1);
- the signal from the primary transmitter (7);
- an external and internal signal control unit (6);
- a filter block (2);
- an error correction unit (3);
- a calculation block X-displacement, V-speed, a-acceleration (4);
- a display (output of calculated values X, V, a) (5);
- a flash memory (11);
- graph 1 (displaying the signal before the filter block) (8);
- graph 2 (display of the signal after the filter block) (9);
- graph 3 (displaying the signal after the error correction block) (10).

The development of the appropriate software allows you to automatically determine the signal level, analyze it, and perform further operations with it: storing, transmitting, processing, and displaying data. Using the self-monitoring mode allows you to automatically detect and correct errors.

A program written in the LabVIEW environment is usually called a virtual device (VD), or a virtual instrument (VI). This follows from the fact that any program created in LabVIEW is presented in the form of a device, the main components of which are the front panel, the flowchart, the icon and the connecting panel. Figure 4 shows the developed block diagram of the intelligent fiber-optic motion sensor system.

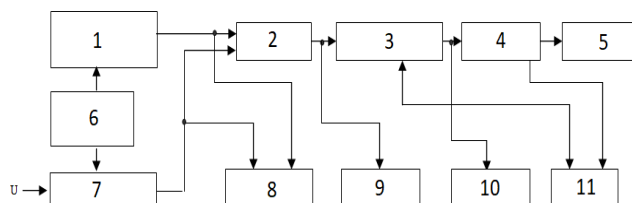


Figure 3. - Block diagram of an intelligent system integrated into a single-board computer

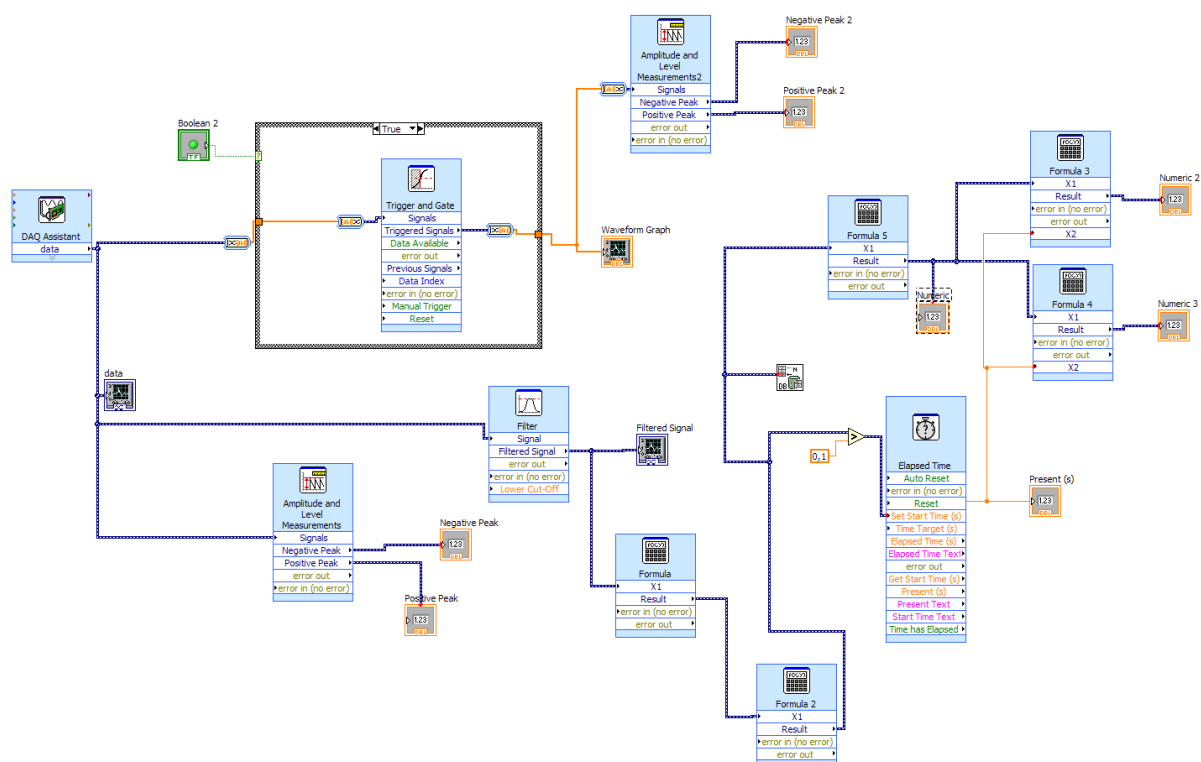


Figure 4. - Block diagram of the intelligent fiber-optic motion sensor system

REFERENCES

1. Бусурин В. И. Волоконно-оптические датчики: Физические основы, вопросы расчета и применения / В. И. Бусурин, Ю. Р. Носов. – М.: Энергоатомиздат. –1990. – 256 с.
2. Айфичер Э. «Цифровая обработка сигналов: практический подход, 2-е издание» / Пер. с англ. – М.: Издательский дом «Вильямс», 2004. – 992 с.
3. Сергиенко А. Б. Цифровая обработка сигналов: Учебник для вузов. 2-е изд. – СПб.: Питер, 2006. -751 с.

PROSPECTS FOR THE DEVELOPMENT OF OIL FIELDS IN LEBANON

M. MTAYREK, A. NEVZOROVA

Gomel State Technical University named after P.O. Sukhoi, Belarus

The search for oil fields near the coast of Lebanon is of current importance for the forecast assessment of the country's energy security. The paper attempts to analyze and understand the basics of the oil/water/surface interaction in the presence of surfactants and their effect on improving the displacement of water by oil from the surface.

Introduction. Early estimation of Lebanon's offshore reserve potential ranges into the hundred of millions of barrels of oil and 25 trillion cubic feet (Tcf) natural gas resources located in its offshore territories. These estimations are based on 2D and 3D seismic studies and are mainly performed by Petroleum Geo Services (PGS) and Spectrum. The first offshore exploration well was drilled and completed in Block 4 on 8 May 2020. The drilling activities started with the arrival of the *Tungsten Explorer* drillship on 25 February 2020. Traces of gas were observed, confirming the presence of hydrocarbon reserves. However, these traces are not enough to yield a commercial quantity (EUROMENA Energy). Furthermore, the gas-bearing Tamar sands formation, located beneath the Mediterranean Sea, was not encountered in this well, indicating that the well was not extended to this formation.

According to the report published in March 2010 by U.S. Geological survey (USGS) [7], the Levant basin, which covers Lebanese, Palestinian and part of Cyprus offshore, has mean probable undiscovered oil resources of 1.7 billion barrels and, more significantly, mean probable undiscovered resources of natural gas resources of 122 Tcf. Total had already drilled a well in Block 4 earlier that year but it did not find sandstone reservoirs such as those found in Palestine and Cyprus (Fig. 1). "The lithology Total found in block 4 exploration well had a carbonated formation which could be a reservoir rock but these types of rocks need to be further evaluated since the drilling focused only on sandstone reservoirs. The Jurassic carbonate platform in Lebanon, as well as in the neighbouring countries, includes thick pervasive dolostones (exceeding 1000m in thickness) which are believed to have resulted through hydrothermal dolomitisation of pre-existing Early Jurassic, seepage reflux dolostones and Middle-to-Late Jurassic limestones [1].

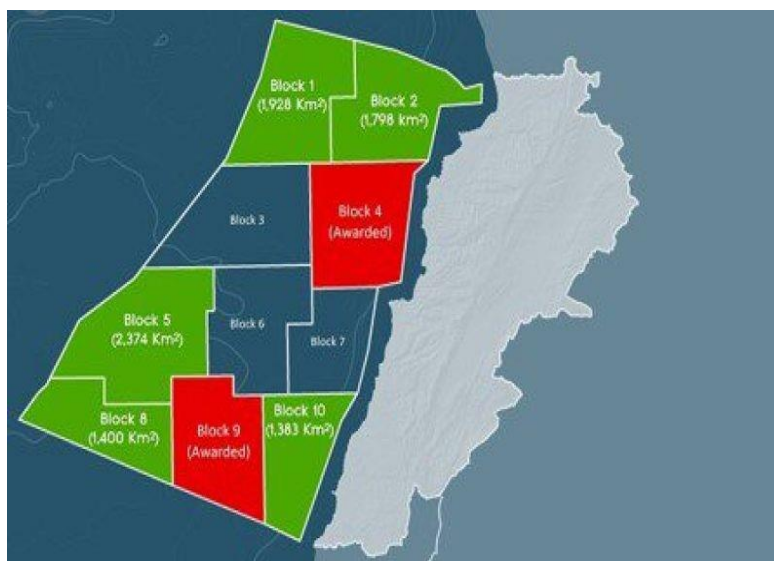


Fig. 1. – Offshore blocks in Lebanon. Source: Lebanese Petroleum Administration

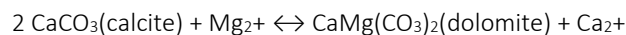
Dolomitisation took place during a time span stretching from the Late Jurassic to the Early Cretaceous (ca. 10 million years approximately), coinciding with major uplifts and subaerial conditions that occurred together with faulting and volcanic activities. Recent fieldwork led to the discovery of a 'tongue'-shaped dolostone body (350m in length) within the latest Jurassic limestone strata in central Mount Lebanon. Sampling was performed systematically along four almost parallel profiles crossing the dolomite 'tongue' lengthwise. In total, 70 core-drilled samples were collected from the dolostones, as well as from the nearby partly dolomitised limestones, sandstones and volcanic deposits.

Purpose of the work – to assess the problems of extracting oil in Lebanon and put forward some solutions.

Methodology. A project started to understand the fundamentals of "Chemical Injection based Enhanced Oil Recovery in Hydrocarbon Reservoirs". QCM-D for the purpose. This research will help understand the fundamentals of the interaction of oil/water/surface in the presence of surfactants and the impact of these surfactants on changing the wettability of the surface and, hence, improve water displacing oil from the surface. Very few people used QCM-D for such applications. Therefore, we believe that this research will lead to new and innovative results. The research will benefit from the cross-domain expertise in the Chemical and Petroleum Engineering Department. The first environmental impact assessment (EIA) study for petroleum activities was conducted in line with the Lebanese regulations by the operator block 4 for the upcoming petroleum activities and was approved by the ministry of environment in February 2020. Carbonate reservoir modeling: How can you ensure optimal drilling and production in carbonate reservoirs? It requires new tools, techniques, and interpretation methodologies that harness and utilize borehole measurements with high-resolution 3D surface seismic surveys.

Near-wellbore scale: As carbonate rock has been compressed over geological time, its character has changed from its original state due to diagenesis. This process caused the pores to change in size and geometry and may have also created stylolite flow barriers over large areas. Evaluating the complex heterogeneous rock can therefore be problematic, particularly as rock properties may vary greatly across the field. Porosity, permeability, and saturation are therefore some of the most important factors for reservoir modeling and production planning. Our proprietary interpretation methodology and workflow provide a rapid, robust, and comprehensive petrophysical description, including evaluations of lithology, porosity, pore geometry, fluid saturations, relative permeability, and primary drainage capillary pressure curves. This information can aid in detecting fractures, optimizing completion program design, and estimating recoverable reserves. With an understanding of the carbonate rock formation at the micro and macro scale, specific intervals can also be reopened using hydraulic fracturing techniques. Postulated Palaeozoic facies also offer favorable potential. The effects of limited extrusive phases in the Late Jurassic/Early Cretaceous and the Late Neogene are examined and considered as non-critical to hydrocarbon accumulation other than on a very limited local structure scale, while the structural effects of Neogene horizontal displacements along the length of the country are taken into account in the presentation of three exploration options designed to look thoroughly at pre-Jurassic prospects.

A two-stage dolomitisation model for the Jurassic carbonates in Lebanon has recently been proposed by the authors. According to this model, second-stage Late Jurassic hydrothermal dolomitisation is believed to have occurred as a result of the circulation of mixed dolomitising fluids along fault. Dolomitization is a geological process by which the carbonate mineral dolomite is formed when magnesium ions replace calcium ions in another carbonate mineral, calcite. It is common for this mineral alteration into dolomite to take place due to evaporation of water in the sabkha area [1]. Dolomitization involves substantial amount of recrystallization. This process is described by the stoichiometric equation:



Results. Dolomitization depends on specific conditions which include low Ca:Mg ratio in solution, reactant surface area, the mineralogy of the reactant, high temperatures which represent the thermodynamic stability of the system, and the presence of kinetic inhibitors such as sulfate [2]. Diagenesis may include conversion of limestone to dolomite by magnesium-rich fluids. There is considerable evidence of replacement of limestone by dolomite, including sharp replacement boundaries that cut across bedding. Ordinary seawater is capable of converting calcite to dolomite, if the seawater is regularly flushed through the rock, as by the ebb and flow of tides (tidal pumping). Once dolomitization begins, it proceeds rapidly, so that there is very little carbonate rock containing mixed calcite and dolomite. Carbonate rock tends to be either almost all calcite/aragonite or almost all dolomite [5].

In Case 1, the concentration of SO_4^{2-} in the injected water was 10 times higher than that in the Base Case (Fig. 2).

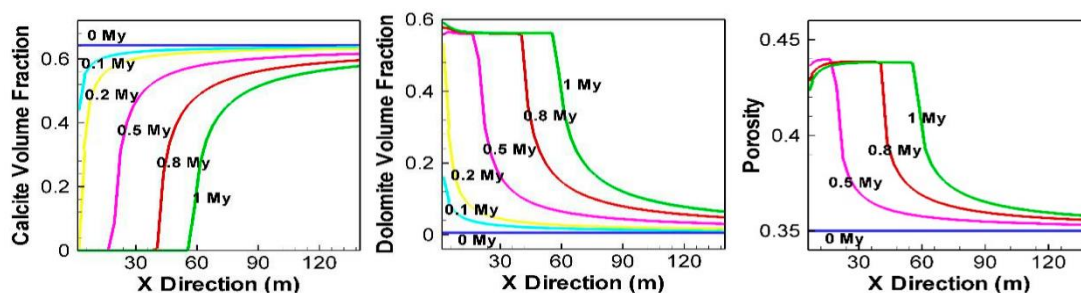


Fig. 2. – Calcite and dolomite content and porosity evolution (Base Case)

Results in Fig.2 show that the calcite nearest to the injection point dissolved first and gradually transformed to dolomite. No calcite was found within 70 m of the injection point after 1 My, when the dolomite content was up to 0.55. During the transformation of calcite to dolomite, the generated Ca^{2+} moved continuously to the right area as the water flows. When Ca^{2+} and SO_4^{2-} concentrations in the system reached the conditions for gypsum precipitation, gypsum was formed. As the curve of gypsum content shows, the content reached the highest value at a distance of 10 m from the injection point after 0.5 My. With continuous injection of external fluids, more and more gypsum precipitated. The gypsum content was close to 0.4 between 20 and 80 m from the injection point after 1 My. The porosity increased to about 0.45 within 20 m of the injection point after 0.5 My, whereas it decreased to about 0.05 between 20 and 80 m from the injection point after 1 My.

Conclusions. A series of test analysis and numerical simulation were combined to study the effects of various factors (such as temperature, flow rate, seawater concentration, Mg/Ca ratio, pH and SO_4 s concentration) on dolomitization during diagenesis in carbonate reservoirs. The degree of dolomitization varied with the flow rate and other hydrodynamic conditions of the external fluid. The better the hydrodynamic conditions were, the faster the fluid migration was, which then pushed the reaction and expanded the scope of dolomitization. Different solution properties and minerals also led to various levels of dolomitization. During successive diagenetic stages under different sedimentary environments with various temperatures, minerals, solutions and other conditions, reservoir experienced complicated fluid–rock reactions. The diagenetic process and porosity evolution curves in four different sedimentary environments were reestablished in the studied area. The main controlling factors of dolomitization were identified, which is helpful to clarify the genesis and distribution of carbonate reservoirs. As the fluid–rock interaction mechanism in carbonate reservoirs is a complex process, further experimental and numerical simulation studies are planned to elaborate and enhance our understanding.

REFERENCES

1. Ehrenberg, S.N.; Walderhaug, O.; Bjorlykke, K. Carbonate porosity creation by mesogenetic dissolution: Reality or illusion? AAPG Bull. 2012, 96, 217–233.
2. Read, J.F.; Husinec, A.; Cangialosi, M.; Loehn, C.W.; Prtoljan, B. Climate controlled, fabric destructive, reflux dolomitization and stabilization via marine- and synorogenic mixed fluids: An example from a large Mesozoic, calcite-sea platform, Croatia. *Palaeogeogr. Palaeoclimatol. Palaeoecol.* 2016, 449, 108–126.
3. <https://jpt.spe.org/twa/what-concealed-beneath-lebanese-offshore>.
4. http://www.xinhuanet.com/english/2020-06/04/c_139114407.htm.
5. <https://www.aub.edu.lb/msfea/research/Pages/oil-and-gas.aspx>.
6. Read, J.F.; Husinec, A.; Cangialosi, M.; Loehn, C.W.; Prtoljan, B. Climate controlled, fabric destructive, reflux dolomitization and stabilization via marine- and synorogenic mixed fluids: An example from a large Mesozoic, calcite-sea platform, Croatia. *Palaeogeogr. Palaeoclimatol. Palaeoecol.* 2016, 449, 108–126.
7. <https://www.lpa.gov.lb/english/about/partnerships/sustainable-oil-and-gas-development-in-lebanon>.

UDC 621.37/39(075.8)

FIBER-OPTIC COMMUNICATION LINE RECEIVERS

D. BUDKO, V. YANUSHKEVICH
 Polotsk State University, Belarus

This article discusses the application of fiber-optic receivers used in fiber-optic communication systems. The characteristics of the optical network have been studied. The reasons for the occurrence of reverse optical losses are analyzed.

The main task of the optical receiver is to convert the modulated light flux coming from the optical fiber into a copy of the original electrical signal sent to the transmitter. Usually, a PIN or avalanche photodiode mounted on an optical connector (similar to that used for light sources) is used as a detector in the receiver. Photodiodes usually have a fairly large sensor element (several micrometers in diameter), so the requirements for the positioning accuracy of the optical fiber are not as strict as for transmitters.

The actual sensitivity of the receivers is determined by many factors: the normalized value of the error coefficient, the shape of the pulse, the speed of information transmission, the bandwidth of the receiver, and the noise of optical radiation. Therefore, practically, in the specifications the sensitivity of the receiver is set only for a well-defined transmitter, the transmission rate of binary signals and their shape.

With an increase in the data transfer rate, the sensitivity deteriorates (i.e. increasing) in linear units approximately proportional to the speed B , bit/s. The sensitivity of modern digital high-speed receivers based on PT-photodiodes is determined by the thermal noise of a transimpedance amplifier [1].

Networks built on the basis of fiber-optic cable have the following advantages in comparison with networks based on coaxial cable:

- less signal attenuation;
- less exposure to interference;
- greater broadband and, therefore, capacity;
- a single optical cable can contain a large number of fibers, each of which carries a high-speed information flow and provides an independent information service (or a group of services).

All this allows you to deliver a signal over long distances with high quality and, in addition, to build integrated networks based on a single fiber network. Such an integrated network can provide a subscriber with television services (analog, digital, high-definition), high-speed data transmission, and telephony.

An important parameter of the optical network is the wavelength used. For cable television networks, the wavelength ranges of 1310 and 1550 nm are used. Transmitting equipment for a wavelength of 1310 nm is significantly cheaper, but the attenuation in the fiber is higher here. The optical cable lengths of equal attenuation for the wavelengths of 1310 and 1550 nm are approximately related as 5:8, that is, a 5 km length of optical fiber at a wavelength of 1310 nm has the same attenuation as an 8 km length at a wavelength of 1550 nm. However, in small-scale networks, it is usually preferable to work at a wavelength of 1310 nm.

The reverse optical loss represents the total power of the light reflected back to the source from the optical gap which includes the back-scattered light from the fiber, expressed in decibels, defined as:

$$ROL = 10 \log \frac{P_{ip}}{P_{rl}} \quad (1)$$

Where P_{ip} is the input power and P_{rl} is the reflected light power, Watts.

A high level of ROL will reduce the performance of some transmission systems. For example: high back-reflection can distort the quality of the analog video signal, resulting in poor video quality.

The higher the OOP is estimated and the lower the reflected power is, the smaller the effect of reflection will be. This means that the $ROL = 40$ dB is better than the $OOP = 30$ dB. The ROL is expressed as a positive decibel value, while the connector reflection is expressed as a negative value [2].

If the ROL value is too high, the light may resonate in the cavity of the laser diode, causing it to become unstable. As a result:

- Increased transmitter noise reduction of the optical signal-to-noise ratio in analog video transmission systems and an increase in the ratio of the number of mistakenly received bits to the total number of received bits in digital transmission systems;

ICT, Electronics, Programming, Geodesy

- Increase in light source interference change in the wavelength and output power of the central laser;
- Higher probability of damage to the transmitter.

And if the ROL value is too small, then we use:

- low reflection connectors;
- optical isolators near the laser to reduce back reflection.

The FOCL receiver can be used in various receiving television antennas, and will be in demand in both wireless and cellular communications, radio broadcasting, GPS, ground stations and VSAT data networks.

REFERENCES

1. Оптоволоконные линии связи [Электронный ресурс]. – Электронные данные. – Режим доступа: <https://www.avclub.pro>. – Дата доступа: 13.01.2020.
2. Убайдуллаев Р.Р. Протяженные ВОЛС на основе EDFA. Lightwave Russian Edition, № 1, 2003, с. 22–28.

UDC 621.37/39(075.8)

FIBER-OPTIC COMMUNICATION LINE AMPLIFIERS

I. MAKRIDIN, V. YANUSHKEVICH

Polotsk State University, Belarus

This article discusses the application of fiber-optic amplifiers used in fiber-optic communication lines, considers the characteristics of fiber-optic amplifiers, and analyzes the main classes of EDFA amplifiers.

Optical amplifiers are an integral part of fiber optic communication systems of various types. The most popular type of such amplifiers is based on an erbium – doped optical fiber (EDFA). Due to a number of their characteristics, EDFA amplifiers are widely used in optical information transmission systems, including systems with dense spectral densification DWDM.

The need for optical amplifiers (OP amps) for digital fiber-optic networks arose already with the introduction of SDH (synchronous digital hierarchy) technology. At high transmission speeds (from 2.5 Gbit / s and above) and fairly long sections of fiber-optic communication lines (FOCL), it was often necessary to use various types of converters – electro – optical (EOP) and optoelectronic (OEP), as well as regenerators-devices that restore the original form of the transmitted signal after passing the regeneration section. At the same time, since the 1980s, the direction of purely optical signal processing has been developing. In optical regenerators, as a rule, the optical signal is received, amplified, restored in shape, and transmitted to the input of the next regeneration section. Today, it is not possible to implement a fully optical circuit in a fiber optic communication system, but this is a matter of the near future. However, using the OP-AMP, you can significantly increase the length of the regeneration section, reduce their number. This simplifies the transmission scheme and reduces the cost of equipment. Optical amplifiers are also successfully used in CATV analog cable television networks, when a single common signal is transmitted to a significant number of consumers. For reliable reception of analog CATV signals, a higher signal-to-noise ratio on the receiver side is required than for digital systems. The overall signal in CATV networks should be very powerful, as it is distributed among hundreds and thousands of subscribers. OUS are able to solve such problems. They will also find application in FTTH technologies (Fiber to the Home – fiber to the apartment). Indeed, in this case, it is necessary to provide subscribers with inexpensive, and therefore not very sensitive receivers. Consequently, high signal strength is also required in FTTH networks.

EDFA-amplifiers-general principles

Most often, doped segments of optical fibers are used as the active medium of the OP AMP. In such a fiber, signals of certain wavelengths can be amplified by the energy of the external radiation of the pump. Rare-earth elements are used to dope the fiber. So, neodymium (Nd) and praseodymium (Pr) are used in the OP amp operating in the 1300 nm range, for the 1550 nm range – erbium (Er), in the 1470-1650 nm range, another rare earth element – thulium (Tu) is used.

The most widely used op-amps are based on erbium – doped fiber-EDFA (Erbium Doped Fiber Amplifier). This is mainly due to the development of dense optical multiplexing (DWDM) technology. It is thanks to the advent of amplifiers with such a combination of qualities as EDFA, communication lines and networks based on DWDM systems have become economically attractive. Indeed, conventional electronic regenerators, in order to restore the level of the optical signal, convert the input optical signal into an electrical one, with subsequent amplification and shape correction, and then convert it again into an optical signal. Considering that DWDM technology uses up to several dozen channels at different wavelengths within the transparency window, the regenerator becomes the most complex and expensive part of the system. In contrast, EDFA amplifiers do not recognize or convert the signal, but simply increase its power, immediately in the entire operating band – from about 1525 to 1565 nm. Therefore, unlike regenerators, they are practically independent of the protocol and the transmission speed. The operating range of the EDFA with a width of about 40 nm almost exactly corresponds to the transparency window of the quartz fiber. These 40 nm can accommodate several dozen DWDM channels.

Since EDFA amplifiers are independent of the network protocol, they can be directly connected to different equipment without fear of interfering with each other. Networks with EDFA amplifiers have a number of advantages. For example, the capacity of such networks can be increased economically and gradually, adding new channels as the demand increases. The use of EDFA optical amplifiers allows you to create fully optical networks in which signal processing by electronic devices occurs only at the start and end points of the network.

Of course, the use of EDFA is not a panacea for all problems. After all, an amplifier without a regeneration function increases the total power of the input signal, including additive noise – as a result, the signal-to-noise ratio decreases. It also does not compensate for the effects of various nonlinear effects, including dispersion of different nature (unless, of course, the amplifiers are equipped with built-in dispersion compensators). Therefore, despite the certain ease of use of the op-amp, it is necessary to carefully consider their parameters and some features of the application. First of all, a decrease in the signal-to-noise ratio at the output of the op amp leads to a decrease in the threshold sensitivity of the terminal receiver. Moreover, this ratio is less, the more OP-AMP is used when creating a specific communication line. Therefore, in SDH networks on long-distance sections, it is preferable to use conventional electro-optical regenerators with the restoration of the shape of the transmitted optical signals. The disadvantages of using an OP AMP in DWDM systems include the non-uniformity of the amplitude-wave characteristic. Its compensation leads to a decrease in the output power and, consequently, to a decrease in the length of the fiber optic cable. Let's consider the main parameters of EDFA and their impact on the use of OP-amp in fiber optic communication systems.

In addition to similar characteristics to electronic amplifiers, such as gain, noise factor, dynamic range, and amplitude-wave response, the OP AMP has its own unique parameters. The main ones are the saturation power, the medium gain, the enhanced spontaneous emission (SPI), and the sensitivity to the polarization of the input optical signal.

As in electronic amplifiers, the gain of the OP amp depends on the level of the input signal. Up to a certain (small) level of the input signal, the gain is almost constant. Further, it begins to fall exponentially with an increase in the input power level. This flat part of the characteristic is the OP AMP saturation region and is explained by a decrease in the multiplication factor k caused by a shortage of working particles capable of generating secondary photons with an increase in the input signal. This region can be characterized by the P_h saturation power at the output of the amplifier at the level of -3 dB of the output characteristic (the gain of the medium drops twice). It should also be noted here that the amount of gain can be affected by the polarization of the input signal, which is not controlled in the FOCL, but can change under the influence of random changes in the shape of the core and other reasons.

Dynamic range (SNR) is defined as the range of input power of an optical signal at which the gain remains constant. Naturally, it is associated with another parameter-the noise coefficient, which depends on the level of USI, the residual pump signal and crosstalk. The greatest influence on the noise factor is exerted by the USI. It occurs under the influence of random disturbing factors, for example, when the op-amp is heated. This noise not only reduces the dynamic range, but also reduces the maximum allowable gain.

The decrease in the dynamic range is characterized by a noise coefficient $F = SNR_{xx}/SNR_x$, where SNR_{xx} and SNR_x are the values of the dynamic range at the input and output of the op amp.

The gain in the OP amp is caused by the fact that under the influence of laser diode (LD) radiation in some active medium having two energy states, an increased population of the level with a higher potential energy is created. As a result of this pumping, the medium becomes active, i.e., capable of generating secondary photons with a multiplication factor of k . Some op-amps use a more complex, three-level interaction mechanism for pumping. The scheme for creating overpopulation is as follows: from the first level, the particles are transferred to the second, from which they move to the third level as a result of relaxation. Due to the significant difference in the time of life at the third level, a sufficient population is created for strengthening. This type of OP AMP also includes EDFA.

LDS with wavelengths of 980 and 1480 nm are suitable for pumping EDFA. LD at 980 nm uses a three – level model of interaction with the active medium, and LD at 1480 nm-a two-level model. LDS at 980 nm allow you to get a very low noise factor, 3-5 dB, which is better for multi-channel systems and preamps of DWDM systems. On the other hand, LDS at 1480 nm with a noise factor of 5 dB are more reliable and cheaper. Some models of EDFA amplifiers use pumping at two wavelengths, which to some extent allows you to combine the advantages of both methods.

In EDFA with single-stage pumping, the maximum achievable output power is about 16 dBm. At the same time, the noise coefficient in the low-power signal region is 5-6 dB. In the double-pumped EDFA (980 and 1480 nm), higher output power values are achieved – up to 26 dB. To reduce the noise level in such a design, a multi-stage scheme is used: after the first gain stage, an optical insulator is placed, which prevents the propagation in the opposite direction of the USI of the second stage.

The amplitude-wave characteristic (AVC) of EDFA with an unevenness of ± 10 dB practically covers the band of 1520-1570 nm, has a maximum gain (40 dB at $R_{vc} = -30$ dBm) at a wavelength of 1535 nm and a plateau (gain of 30 dB) in the range of 1540-1569 nm. You can align the characteristics of the amplifier for use in DWDM systems by using various filters. As a result, it is possible to achieve an uneven ABC of 0.1–0.2 dB. However, the gain is reduced to 16-18 dB in the OP AMP with one pump LD and to 19-22 dB - with two LDS. Another way to reduce the unevenness of the ABC is to use fluoride-based fibers as the active medium, since they have a more uniform spectral distribution of the gain than for quartz fibers. But such amplifiers have a higher noise level.

To equalize the time delays that occur during the propagation of signals of different wavelengths in the fiber optic system, EDFA (especially two-stage) uses dispersion compensation devices.

EDFA amplifiers can be divided into three main functional classes:

- high-power amplifiers (boosters) installed directly behind the transmitter. They work with a large input signal, provide the maximum allowable gain and a high output signal level, and are not critical to the noise level;
- line amplifiers are installed on the communication line as repeaters. They amplify the signal as much as possible, while introducing as little noise as possible;
- preamps installed directly in front of the receiver. They work with very weak signals (from -45 to -30 dBm) and are therefore extremely critical to the noise level of the amplifier.

REFERENCES

1. Оптоволоконные линии связи [Электронный ресурс]. – Электронные данные. – Режим доступа: <https://www.avclub.pro>. – Дата доступа: 13.01.2020.
2. Убайдуллаев Р.Р. Протяженные ВОЛС на основе EDFA. Lightwave Russian Edition, № 1, 2003, с. 22–28.

COMPARATIVE ANALYSIS OF MODELS AND FORECASTING METHODS

D. VASILYEVA, D. GLUKHOV
Polotsk State University, Belarus

In this article, work has been done on the study and comparison of forecasting methods, namely the methods: ARIMA, LSTM, Facebook Prophet. Examples of the work of these methods are given, and the best one for the implementation of the "Forecast of natural gas consumption in Belarus" is selected.

Study of forecasting methods. Forecasting gas consumption is the basis not only for planning purchases of natural gas from gas traders, but, no less important, for developing measures to manage energy consumption in the municipal economy, especially during the heating season.

One of the best methods to construct a forecast of the consumption of a particular resource is a neural network approach, since it is free from model constraints and is equally suitable for linear and complex nonlinear problems, as well as classification problems. Technically, training consists in finding the coefficients of connections between neurons. In the process of training, the neural network is able to identify complex dependencies between input data and output data, as well as perform generalization. This means that in case of successful training, the network will be able to return the correct result based on data that was absent in the training sample, as well as incomplete and / or "noisy", partially distorted data.

Therefore, there are many different approaches for time series forecasting such as ARIMA, LSTM, Facebook Prophet, regression models, etc.

A popular and widely used statistical method for forecasting time series is the ARIMA model. It explicitly serves a set of standard time series data structures and, as such, provides a simple yet powerful technique for making sophisticated time series predictions.

ARIMA stands for AutoRegressive Integrated Moving Average. It is a model class that captures a set of different standard time structures in time series data.

Using ARIMA it is possible to make predictions on non-stationary data due to the introduction of integration into the model. This is achieved by taking differences - subtracting the levels of the time series from each other.

Given the seasonality of the time series, short-term components are likely to make a significant contribution to the model. Thus, the model also needs to take into account seasonality - seasonal ARIMA. The most important steps are the estimation of model coefficients. If variance grows over time, variance-stabilizing transformations and taking differences should be used.

One of the obvious shortcomings of the models is the requirement for data series: to build an adequate ARIMA model, at least 40 observations are required, and for SARIMA, about 6–10 seasons, which is not always possible in practice.

The second serious drawback is the inadaptiveness of autoregressive models: when new data is received, the model must be periodically reevaluated, and sometimes re-identified.

The third disadvantage is that building a satisfactory ARIMA model is resource and time consuming. The very construction of the model is more likely an "art", i.e. requires a lot of experience on the part of the forecaster.

The whole construction of ARIMA models is based on the assumption that the time series is generated infinitely in accordance with some function, the parameters of which we need to identify and estimate, i.e. the ARIMA approach is based on the assumption of the frozen nature of the ongoing processes, evolutionary nature as such is not taken into account in the model. This is primarily due to the fact that the models were originally developed for modeling physical and technical processes, in which almost all types of processes are described either as stationary or as stationary in differences. From which we can conclude that the use of these models will not allow us to give accurate predictions.

To solve the problem of storing a small number of previous observations, LSTM networks have been developed.

Long short-term memory neural network is an artificial convolutional neural network used in the field of deep learning. Unlike conventional feedforward neural networks, LSTM networks have feedback loops. Such networks are capable of processing not only individual single data, but also entire data sequences. LSTM neural networks are well suited for classification, processing and forecasting based on time series, where interrelated phenomena can occur with an indefinite time lag. This time lag leads to difficulties in using classical neural networks in solving these problems due to the fading of the gradient, while LSTM networks are insensitive to the value of the time lag.

There are 3 types of layers in LSTM networks:

1. Forget gate layer
2. Layer "memory" (Memory gate)
3. Output layer (Output gate)

First, the "forgetting filter layer" determines what information can be forgotten or left behind. The values of the previous output and current input are passed through the sigmoidal layer. The obtained values are in the range [0; one]. Values closer to 0 will be forgotten and values closer to 1 will be left. $h_{t-1}x_t$

$$f_t = \sigma(W_f[h_{t-1}, x_t] + b_f) \quad (1)$$

Next, it is decided what new information will be stored in the cell state. First, a sigmoidal layer called the "input filter layer" determines which values to update. The tanh layer then builds a vector of new candidate values c that can be added to the cell state.

$$i_t = \sigma(W_i[h_{t-1}, x_t] + b_i) \quad (2)$$

$$C_t = \tanh(W_c[h_{t-1}, x_t] + b_c) \quad (3)$$

To replace the old state of the cell with the new state, it is necessary to multiply the old state by forgetting what you decided to forget earlier. Then we add $C_{t-1}C_t f_t i_t * \dots$. These are the new candidate values multiplied by C_t - how much to update each of the state values.

At the last stage, it is determined what information will be obtained at the output. The output will be based on our cell state, with some filters applied to it. First, the values of the previous output and the current input are passed through the sigmoidal layer, which decides what information will be output from the cell state. The cell state values are then passed through the tanh layer to output values in the -1 to 1 range and are multiplied with the output values of the sigmoidal layer, which allows only the information required to be displayed. h_{t-1}

$$o_t = \sigma(W_o[h_{t-1}, x_t] + b_o) \quad (4)$$

$$h_t = o_t * \tanh(C_t) \quad (5)$$

where x_t is the input vector; h_t - output vector, h_t - vector of states; x_t h_t C_t W and b - matrices of parameters and a vector; i_t is the vector of the forgetting gate; the weight of storing old information; i_t is the vector of the input gate; the weight of receiving new information; i_t is the vector of the output gate, the candidate for the output. f_t i_t o_t received in this way and are transmitted further along the chain. h_t C_t

Facebook Prophet is an open source forecasting tool available in Python, and R. Prophet is optimized for business forecasting tasks, which typically have any of the following characteristics:

- hourly, daily or weekly observations with a history of at least several months (preferably a year);
- strong multiple seasonality: day of the week and season;
- a reasonable number of missing observations or large outliers;
- historical changes in trends;
- trends, which are non-linear growth curves when the trend reaches a natural limit or reaches saturation.

There are anti-aliasing options for seasonality that allowing to tune how closely historical cycles are matched, and there are anti-aliasing options for trends that allowing to tune how aggressively changes are followed in historical trends. For growth curves, you can manually specify "powers" or the upper limit of the growth curve, allowing you to enter your own preliminary information about how the forecast will rise (or decline).

In fact, Prophet is an additive regression model consisting of the following components:

$$y(t) = g(t) + s(t) + h(t) + \epsilon_t \quad (6)$$

where the trend is; $g(t)$ - seasonal components; $s(t)$ - abnormal days; $h(t)$ - errors. ϵ_t

1. Seasonal components are responsible for simulating periodic changes associated with weekly and yearly seasonality. Weekly seasonality is modeled using dummy variables. 6 additional signs are added, for example, [monday, tuesday, wednesday, thursday, friday, saturday], which take on the values 0 and 1 depending on the date. The sunday attribute corresponding to the seventh day of the week is not added, because it will linearly depend on other days of the week and this will affect the model. The annual seasonality is modeled by Fourier series. $s(t)$

2. A trend is a piecewise linear or logistic function. With a linear function, everything is clear. The logistic function of the form (11) makes it possible to simulate growth with saturation, when with an increase in the indicator, its growth rate decreases. A typical example is the growth of the audience of an application or site. Among other things, the library is able to select the optimal points of trend change based on historical data. But they can also be set manually (for example, if the release dates of new functionality are known, which greatly influenced the key indicators). $g(t)$

3. The component is responsible for user-defined abnormal days, including irregular ones, such as, for example, Black Fridays. $h(t)$

4. The error contains information that is not considered by the model. ϵ_t

$$g(t) = \frac{c}{1 + \exp(-k(t - b))} \quad (7)$$

An important idea in Prophet is that by doing more flexible work in adjusting the trend component, we model seasonality more accurately, and as a result, we get a more accurate forecast. The Facebook Prophet developers prefer to use a very flexible regression model instead of the traditional time series model for this task because it gives more modeling flexibility, makes model fitting easier, and handles missing data or outliers more gracefully.

By default, Prophet provides uncertainty intervals for the trend component, simulating future trend changes for a time series. Prophet and its core are implemented in the Stan probabilistic programming language. Stan performs MAP optimization for parameters very quickly (<1 second), which makes it possible to estimate parameter uncertainty using the Hamiltonian Monte Carlo algorithm and allows reuse of the fitting procedure for several interface languages.

Results, discussion and prospects. We have studied the trends of 220 natural gas consumers in the Republic of Belarus over the past 8 years (2012-2020). Moreover, the data of 2012. appear from May and data for 2020. incomplete.

All tracks have the following features:

- The data shows the presence of telemetry errors, emissions and zeros associated with temporary failure of flow sensors, or pressure and temperature, when calculating the flow rate by calculation;
- There are data gaps for the periods of scheduled and emergency gas pipeline repairs;
- There is no exact alignment of timestamps;
- The data does not reflect the fact of gas consumption, but the operating mode of the gas transmission network for the delivery of contract gas to the consumer, and accordingly reflects non-stationary processes (gas injection into the system, gas disassembly from the system in the cylinder mode, when gas flows through the gas distribution station or compressor station does not occur, and consumption gas continues);
- Gas flow rates recorded by sensors lack information on gas density;
- A part of the flow rates was obtained by calculation using a stationary non-isothermal model under boundary conditions specified through pressure and temperature;

Figure 1 shows a graph of forecasting using the ARIMA model, the graph shows the available data and the forecast itself. Calculating the root mean square error of the model, or more simply, the RMSE gave the result 0.1364, from which we can conclude that, although the model has errors, the result is still close to the real values.

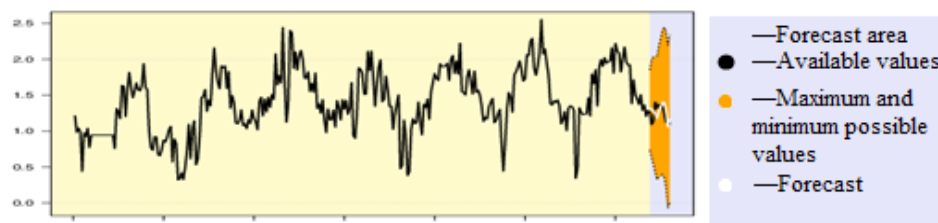


Figure 1. - Forecast for 12 weeks according to the ARIMA model (1, 0, 2) (1, 0, 1)

Figure 2 depicts the prediction of the LSTM model. Since this model is designed for forecasting small time series, it starts forecasting from the beginning of the data, gradually improving the forecast accuracy, which is very useful when some data is missing. The graph shows available data, current forecast and future. RMSE for this model = 0.3485, and it performed worse than ARIMA.

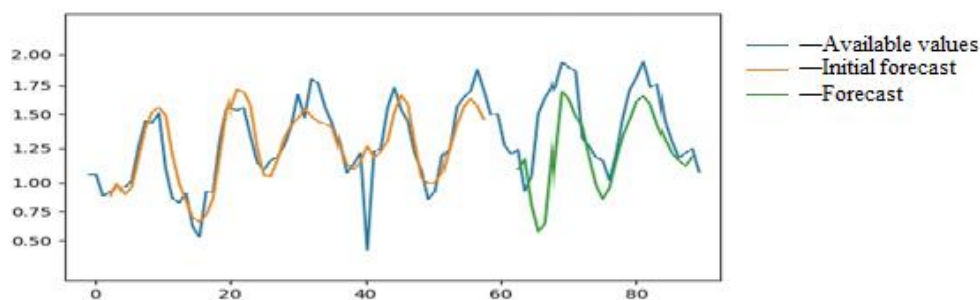


Figure 2. - Forecast for 12 weeks according to the LSTM model

Figure 3 shows Prophet at work. This model always uses only two values: date and numeric. It is designed to work with large amounts of data. It shows the available data, the maximum and minimum possible data and the forecast itself, which, like the LSTM, starts with the beginning of the data. RMSE for this model = 0.2051, but it is worth noting that with each subsequent step the forecast becomes better, based on this, we conclude that more data is needed for a more accurate forecast of this model.

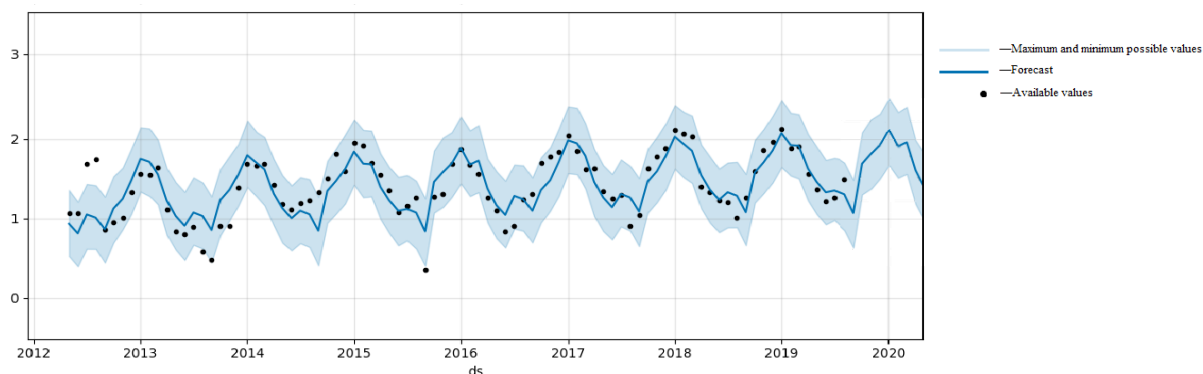


Figure 3. - Forecast for 12 weeks according to the Prophet model

Conclusion. The ARIMA model is much more expensive than the Prophet. For it, it is necessary to investigate the initial series, bring it to a stationary one, select initial approximations and spend a lot of time on the selection of hyper-parameters of the algorithm, but in this case the efforts are not in vain because the ARIMA prediction turned out to be more accurate ($RMSE_{ARIMA} < RMSE_{Prophet}$). The forecast of the LSTM model has a large error, but perhaps with its help, or with the help of Prophet, we could predict missing values in the past, in order to possibly improve the forecast of other models.

REFERENCES

1. Section "Interval forecasting of time series using recurrent neural networks with long short-term memory" on the Habr website [Electronic resource]. - Access mode: <https://habr.com/ru/post/505338/>. - Date of access: 11/16/2020.
2. Section "Facebook Prophet" on the site Facebook Research [Electronic resource]. - Access mode: <https://research.fb.com/prophet-forecasting-at-scale/>. - Date of access: 01.03.2021.
3. Section "Time Series Prediction with LSTM Recurrent Neural Networks in Python with Keras" on the Machine Learning Mastery website [Electronic resource]. - Access mode: <https://machinelearningmastery.com/time-series-prediction-lstm-recurrent-neural-networks-python-keras/>. - Date of access: 03/07/2021.
4. Section "Time series analysis using python" on the website habr.com [Electronic resource]. - Access mode: <https://habr.com/ru/post/207160/>. - Date of access: 03/14/2021.

RESEARCH AND APPLICATION OF FEEDER AUTOMATION SYSTEM IN DISTRIBUTION NETWORK

ZHOU HENGYU, D. DAUHALA

Polotsk State University, Belarus

The feeder automation system is a system that uses various devices to monitor and control the lines and equipment in the distribution network. When a fault occurs in the distribution network, the feeder automation system can automatically determine the location of the fault in a short time, and can actively isolate the fault area to restore the normal power supply of the system. With the development of Jiamusi economy, the distribution automation system built in the early stage in this area has not been able to meet the requirements of power supply reliability. In order to improve the power supply reliability of the distribution system, it is necessary to build feeder automation system in Jiamusi area that can monitor the operation of various distribution equipment and can carry out fault location and active fault isolation.

In this paper, first of all, the system mode and fault handling mode of feeder automation are described. The main station centralized control and local control combined system mode are adopted, and the current type fault handling mode is adopted for system design. Furthermore, this paper introduces the principles of various location methods under different fault conditions. According to the specific situation of a certain region, the location method based on the feeder terminal unit (FTU) and network data is finally determined to design the feeder automation system. Secondly, relying on the feeder automation transformation project of Jiamusi regional power grid company, the main station, communication system and feeder terminal of the whole automation system are designed. The overall structure of the main station and the configuration principle and specific scheme of various software and hardware are designed; the construction principle and technical route of the system communication part are designed in detail, and the required equipment is listed in the equipment list; the configuration is designed to meet the functional requirements according to the functional requirements of the system feeder terminal unit (FTU).

The line from the substation to the power user is collectively called the feeder system. The line can be a pure overhead line, a cable line, or a mixed line of the two. When the distribution network is operating normally, the system can monitor the operation of the distribution network through various devices to ensure that the line is always in reliable operation. When a fault occurs in the distribution network, the feeder automation system can automatically determine the location of the fault in a short time, and can actively isolate the faulty area and restore the normal power supply of the system's non-faulty area.

Distribution network feeder automation system mode

Feeder automation plays a very important role in providing reliable electrical energy to power users. When a fault occurs in the distribution network, the feeder automation system can automatically determine the location of the fault in a short time, and can actively isolate the faulty area and restore the normal power supply of the non-faulty area of the system, so it can reduce the impact of various faults on power users, reduce various losses caused by power outages.

The core component of the distribution network automation system is the terminal monitor. The existing terminal monitors are mainly divided into FTU, DTU and TTU according to their functions. When configuring on the actual site, it is generally configured as follows:

1. For important distribution networks and important nodes in the distribution network that require high reliability of power supply, the monitoring points generally select terminal equipment mainly based on "three

remotes". Where the optical fiber communication conditions are met, when a fault occurs, the local control and centralized control are generally used for processing; if the optical fiber communication is not satisfied, the local control is generally used.

2. For general nodes, in order to monitor the distribution network and locate faults, the "two remote" monitoring method with the help of fault indicators can be preferred. If an important branch node is encountered, a tap switch can be installed, and the branch line can be isolated on the spot when the branch circuit fails.

3. Line monitoring and fault locating devices with "one remote" or "two remote" functions are generally used on lines erected in the suburbs of cities and in the vast rural areas, so as to locate faults on the lines in the distribution network. For ordinary radial lines in the distribution network, the automatic opening and closing functions of the reclosers and sectioners installed in the line are used to remove line faults and normal power supply in non-faulty areas. The work mainly depends on local automation. The level of the equipment and the set fault removal plan use the coordination or blocking function between the recloser and the sectioner to isolate the fault.

The system generally includes communication and master station systems, power distribution switches, primary voltage transformer equipment, various power distribution line terminals and communication facilities. When the system is in normal operation, various power distribution terminal devices can be used to monitor various operating conditions in the lines and equipment in the power distribution line, and transmit this information to the master station. However, when a fault occurs in the distribution network, there is no need to use the communication network and the master station for processing. It only needs to use the distribution terminal equipment to monitor the line voltage, current and other parameters, and use the changes of these parameters and the terminal equipment itself. The protection and logic functions perform fault location, and then remove the fault area, restore the power supply in time, and allow the fault to be reported to the master station.

The system monitors the current flowing in the line and the voltage on both sides of the switch by configuring intelligent terminal equipment for the line switch, and combines the operating status of the switch, synthesizes this fault information and uses the logic judgment function of the terminal equipment itself to automatically proceed. In the judgment of the faulty section, after the faulty section is determined, the switches on both sides of the faulty section are automatically disconnected for fault isolation, and the line tie switch is closed to quickly restore the power supply of the non-faulty area.

Centralized control mode automation system

The system has the same equipment composition as the local control mode system, and also includes communication and master station systems, power distribution switches, primary voltage transformer equipment, various power distribution line terminals and communication facilities. Among them, the power distribution terminal has a "three remote" function and a fault detection function. When the system is in normal operation, various power distribution terminal devices can be used to monitor various operating conditions in the lines and equipment in the power distribution line, and transmit this information to the master station. When a fault occurs in the distribution network, the master station uses the fault information detected and uploaded by each power distribution terminal in the network, and analyzes the network structure with the help of the working status of each switch, and then determines the specific section where the fault occurs. Then the main station system automatically controls or uses manual remote control of the line switch to remove the faulty area and restore the power supply in time.

In the centralized control system mode, the fault processing is generally carried out in the system master station, mainly by using the SCADA system to collect information and data in each line in the distribution network to deal with the faults that occur. The master station analyzes the fault data uploaded by each power distribution terminal, and uses the status of each line switch and the distribution network topology to judge the

fault occurrence section, and at the same time judges the type and location of the fault according to the set fault handling procedure.

The system master station can provide one or more operation schemes that can realize fault isolation and quickly restore the power supply of the system after the power distribution network fails to help the staff perform remote control operations.

Local control and centralized control system collaboration automation system

The two modes of local control mode and centralized control mode are mutually backup. By combining these two control modes, the advantages of these two modes can be combined together. The centralized control mode of the master station can quickly remove faults. Section, and the local control mode has lower requirements on the communication system of the system. Therefore, in the design of fault removal, this article adopts a combination of "master station centralized control" and "local fault removal". The specific implementation process is: when the mains of the distribution network fail, the outgoing line at the substation after the switch is tripped, if it waits for the reclosing failure, the master station system determines that the fault is a permanent fault, and then judges the location of the fault according to the characteristics of the fault current in the line, and gives a fault handling plan.

REFERENCES

1. Ge Shuguo, Shen Jiaxin. 10kV distribution network feeder automation system control technology analysis and application [J]. / Ge Shuguo, Shen Jiaxin. // Power Grid and Clean Energy. – 2012, № 08. – P.29-34.
2. Liu Jian, Zhao Shuren, Yin Baoji, et al. Distributed intelligent feeder automation system rapid self-healing technology and reliability guarantee measures [J]. / Liu Jian, Zhao Shuren, Yin Baoji, et al. // Automation of Electric Power Systems, 2011, № 17. – P.67-71.
3. Li Jiajue. Design and research of feeder automation system [D]. Shenyang: Shenyang University of Technology, 2011.

UDC 004.620.182

METALLOGRAPHIC STUDIES

A. BESETSKAYA, R. BOHUSH
Polotsk State University, Belarus

The article discusses the directions of implementation of metallographic research. Analysis of grain counting methods and the use of these methods in metallographic analysis. The principles of implementing a web application are given.

Metallographic studies are used in many areas of industry: metallurgy; automotive industry; nuclear industry; energy; aerospace industry; research and survey work in various research and scientific centers, universities, laboratories [1]. In this case, the initial data is used as a microchip having a specially prepared surface (the structure is revealed by etching, cutting) for microanalysis, which is currently represented as a digital image. The analysis of metal images requires a large amount of time, so special algorithms for processing digital images and software tools are developed and used [2-4]. Such systems require a fairly good quality of preparation of the surface of the micro-section, since the presence of noise components leads to a decrease in the reliability of the analysis [5]. However, even the use of modern automatic machines does not allow to fully obtain the surface of the micro-section with the complete absence of interfering factors [6]. Thus, the development of algorithmic and software for the analysis of images of the metal microstructure based on modern methods of digital image processing is relevant.

The metallographic analysis uses GOST 5639-82 "Steels and alloys. Methods for detecting and determining the grain size", which contains methods: determining the grain size by comparison with reference scales; counting the number of grains; counting grain border crossings; measuring chord lengths. The method for determining the grain size by comparison with reference scales is based on a visual comparison of the target image and a set of standards, which are given in GOST 5639-82. The method of counting the grains per unit of the surface of the section consists in counting all visually distinguishable grains on the section, while the automatic processing algorithm must take into account the need to separate the grains according to the criterion of crossing the image boundaries: internal and boundary, i.e. crossing the image boundaries. The method of calculating the intersections of the boundaries of equiaxed grains by straight segments with the determination of the average conditional diameter involves measuring by constructing two perpendicular lines at the characteristic place of the image of the cut and dividing them into segments bounded by the contours of the detected grains. Next, you need to calculate the arithmetic mean of the lengths of the obtained segments, followed by comparison with the table parameter of the average conditional diameter. The method of calculating the intersections of the boundaries of non-equiaxed grains by straight line segments with the determination of the number of grains in 1 mm³ differs from the method intended for equiaxed grains by the need to use an additional image obtained across the main axis of symmetry. The analysis is performed by calculating the number of grains crossed by a line in terms of its length equal to 1 mm, which allows you to calculate their number per unit volume and compare the result with a parameter that matches the average number of grains per 1 mm³ and a certain grain score in GOST 5639-82.

In [4], a segmentation algorithm is described based on the selection of a grain contour based on the brightness difference of adjacent pixels and traversing the found border in a circle. As a preprocessing, the input image is convoluted with a kernel that allows you to select the contours of objects, in this case-the Laplace operator (Sobel or Canny operators can also be used), the resulting image is binarized. The author notes that there may be situations when the grain boundary is not closed due to the defects of the section, and the resulting gaps will be quite large. This can cause a single grain to be defined as multiple objects. In [5], an approach for preprocessing is presented using the Otsu binarization method, using the closing and opening operations to filter the binary image and further highlight the contours on it. The paper [7] presents a general scheme for processing the image of a microstructure using the "beetle" algorithm for selecting contours in the image. The methods from [5,7] will not allow for high-quality contour selection on real images, which will lead to a deterioration of the analysis.

The initial data can be used: one image of the slot along the main axis of symmetry; two images, including an additional image to the previous one, obtained across the main axis of symmetry; a set (package) of images for simultaneous processing. To improve the accuracy of determining quantitative indicators and to improve the quality of the input image, taking into account the preservation of the correct grain boundaries for further automatic processing, preliminary image preparation is required, which includes the following operations: image sharpening; brightness correction; contrast enhancement; noise filtering.

To implement the method of determining the grain size by comparison with reference scales, a universal digital standard has been developed that supports scaling, taking into account the restriction that the image resolution and the grain number are known in advance.

The task of automatic quantitative analysis requires the segmentation of the grains in the image of the section and is reduced to the selection of closed areas corresponding to the grain boundaries. One of the most common

defects is non-uniform brightness and contrast. Therefore, it is necessary to improve the original images. In existing systems for determining the grain score, the histogram alignment method is used. If the brightness distribution of the input image is not uniform, for example, one half of it is darker, this method does not work well enough, since one part of the processed image will also be darker. Therefore, it is proposed to use the adaptive histogram equalization algorithm with contrast restriction (CLAHE) to improve preprocessing [8]. With this approach, the image is processed not in its entirety, but in fragments, which, after correction, are combined using bilinear interpolation to suppress sharp transition boundaries between fragments. When using the CLAHE algorithm, there is almost no light unevenness in the output image, in contrast to the image obtained on the basis of histogram alignment. To remove Gaussian and pulse noise, two-dimensional filtering is used in the spatial domain with the corresponding types of filters and apertures of different sizes, since different types and levels of noise can be present in the images.

After pre-processing, a grain segmentation step is performed, which will allow you to apply various analysis methods in the final stages. For this purpose, it is proposed to apply adaptive binarization, remote transformation, and the watershed method to the image, as well as mathematical morphology methods for binary images.

To implement the method of counting grains, an algorithm is proposed that requires the following basic steps: segmentation of grains based on contour analysis on a binary image, each of which is described by coordinates and area; selection of grains and, calculation of the value of the total number of grains in the image; reduction to the number of grains per unit area and comparison of the result with the parameter from GOST 5639-82, which corresponds to the range of values of the average number of grains per 1mm² and a certain grain score; calculation of the numbers of grains most often found in the image.

Methods for measuring chord lengths and counting grain boundary intersections require the construction of reference lines, from which segments are distinguished in the areas where they intersect with the grains. For the method of measuring chord lengths and counting the intersections of the boundaries of equiaxed grains, the average length of segments is calculated, for non-equiaxed grains, the number of segments is calculated. The obtained values are compared with the table parameters.

Based on the considered algorithmic support, the application is presented in the form of a website. The application has several roles: administrator, registered user, and guest. Depending on the role, different application functions are provided. The guest has limited functionality, which is controlled by the administrator. A registered user can use the full list of functions. The administrator moderates users and controls access to functions for the "Guest" and "Registered User" roles» The site has registration and authorization forms. These forms use an E-mail and password or OAuth 2.0 to log in. The OAuth 2.0 authorization protocol allows users to exchange certain data with the application, while keeping their usernames, passwords, and other information secure.

After the user is logged in, the main page of the site will be displayed. This page is divided into the following sections: image, menu, toolset, dimension. On this page, you can upload an image that will be displayed in the output window with the processing of the uploaded image applied. Tools for processing the input image, tools for binarizing the data under study and working with the resulting image, and counting methods will also be available. In turn, the counting methods include the following analysis methods: the method of determining the grain size by comparison with reference scales (GOST 5639-82, p.3.3); The method of counting grains (GOST 5639-82, p.3.4); The method of counting the intersections of the boundaries of equiaxed grains (GOST 5639-82, p.3.5.3); The method of counting the intersections of the boundaries of non-equiaxed grains (GOST 5639-82, p.3.5.4); The method of measuring chords (GOST 5639-82, p. 3.6).

The method for determining the grain size by comparison with reference scales includes the following sections: image, working with a file, the list "Grain number, G", the list "Color scheme", the list "Window width and height". When you change the list "Grain number, G", the scale of the image under study automatically changes to the corresponding grain number. When you change the "Color Scheme" list, the color scheme of the reference image changes accordingly. When you change the "Window Width and height" list, the scale of the display window of the reference and the image under study automatically changes to the appropriate resolution.

The method of counting grains includes the following sections: source and final image, working with the file, "Counting grains", "Tabular data". The section "Counting grains" shows the number of detected grains in the current area and in terms of an area of 1 mm², also displays the first three numbers of grains that occupy the largest area in the image. The Tabular Data section shows the G number corresponding to the number of detected grains, the tabular value of the average diameter of the calculated grain number, and the value of the average area of the calculated grain number. Figure 1 shows the form of the grain counting method

The method for calculating the intersections of the boundaries of equiaxed grains includes the following sections: source and final image, working with the file, "Range of values". The "Range of values" section shows the number of measurements taken, the minimum and maximum grain size present in the image, calculated from the length of the segments, as well as their average value, and outputs the first three grain numbers, which are represented by the maximum number of segments. Figure 1 shows the form of the method for calculating the intersections of the boundaries of equiaxed grains.

Fig. 1. – Form of the method for calculating the intersections of equiaxed grain boundaries

The method for calculating the intersections of the boundaries of non-equiaxed grains includes the following sections: source and result images, working with the file, "Counting grains". The "Counting grains" section shows the number of measurements taken, the number of crossed grains in terms of 1 mm on each axis, and the resulting number of grains per 1 mm³, and shows the number G corresponding to the number of detected grains.

The method for calculating the chord measurement includes the following sections: the source and final image, working with the file, and the "Range of values". The "Range of values" section shows the minimum and maximum grain size present in the image, calculated from the length of the segments, as well as their average value, and outputs the first three grain numbers, which are represented by the maximum number of segments.

As a result, an application for image processing with different counting methods is presented.

REFERENCES

1. Современная металлография – основа литейного материаловедения / Анисович А.Г. – Минск, 2019. – 99-108 с.
2. Алгоритм и программное обеспечение для обработки изображений микроструктур перлитных сталей. / Чичко А.Н., Сачек О.А., Лихоузов С.Г., Соболев, В.Ф., Веденеев, А.В. – Минск, 2010. – 14 с.
3. Определение балла зерна стали компьютерными методами / Анисович А.Г., Румянцева И.Н., Бислюк Л.В. – Москва, 2019. – 100-104 с.
4. Разработка интеллектуальной системы распознавания сложных микроструктур на шлифах металлов и сплавов / Шарыбин С.И. Столбов В.Ю., Гитман М.Б., Барышников М.П. – Москва, 2014. – 50-56 с.
5. Алгоритмы предварительной обработки изображений микроструктур / Стародубов Д.Н. – Екатеринбург, 2010. – 179-185 с.
6. Автоматизированный анализ микроструктуры материалов. Анализ изображений с наличием дефектов пробоподготовки / Сивкова Т., Губарев С., Каменин И. – Москва, 2020. – 15-26 с.
7. Алгоритмы для автоматизации обработки изображений макро- и микроструктуры сплавов / Чичко А.Н., Сачек О.А., Ганжа В.А., Гашникова О.П. – Минск, 2008. – 79-84 с.
8. Adaptive Histogram Equalization and Its Variations / Pizer S. M., Amburn E.P., Austin J.D., Cromartie R., Gese-lowitz A., Greer T., Romeny B.H., Zimmerma J.B., Zuiderveld K. – New York, 1987. – 355-368 p.

THE SERVER PART OF THE ONLINE PARKING BOOKING SYSTEM

A. KHODOSEVICH, R. BOGUSCH

Polotsk State University, Belarus

The article deals with the implementation of the server part of the parking space system using a neural network. The principles and possible application of recognition of parking spaces and cars in the image are given.

Road transport is an integral part of modern society. With the growing number of cars in each city, the problem of parking is becoming more and more urgent every day. This issue is even more acute in shopping and entertainment complexes, restaurants, hotels, airports, supermarkets and nightclubs, where the competent organization of parking lots is directly related to their life support and profitability.

As long as the number of cars did not exceed a certain threshold, they could be parked at the roadsides and in other places near the desired object. But, first of all, it was not always possible to do this by observing the traffic rules. And secondly, leaving the car unattended is always associated with the risk of its theft, burglary or damage to property. This task in the city is solved by the organization of paid parking near infrastructure facilities [1].

In cities, there are a huge number of parking spaces, some of them are paid and to book a place, you need to contact the manager using a phone call. In addition, information technologies are actively developing, more and more devices are accessing the Internet, and more and more applications are moving online. Information technology has become an integral part of every person's life. Thus, it is relevant to use software to track available parking spaces based on neural networks and then book these parking spaces.

One of the most promising areas of artificial intelligence is neural networks. Now they are actively used in business, used in the field of security, entertainment and other areas. Artificial neural networks are built on the principle of biological ones, of course, with a number of assumptions, they operate a huge number of simple processes with many connections. Like the human brain, these networks are capable of learning [2].

The main task of the parking space management system is to accurately determine the available parking spaces. The first step is to recognize all possible parking spaces in the frame. Before you search for unoccupied spaces, you need to determine how the parking space will be recognized. The second step is to recognize all the cars in the frame. The third step is to determine which places are occupied by cars and which are not. To do this, you need to combine the results of the first two steps. Next, the program should display when the parking space is free or occupied. Each of these stages can be completed in different ways using different technologies. There is no single right or wrong solution to these problems, different approaches will have their advantages and disadvantages. Let's look at each step in more detail.

The source data will be an image from a video surveillance camera. This image should be scanned and get a list of places where you can park. To do this, consider several solutions.

The first option is to get an image from the video camera and select all parking spaces manually, instead of automatic recognition. But in this case, if there is a movement/displacement of the camera or use the system in another parking lot, you will have to do the whole procedure again.

The second option is to find an indicator in the image (e.g. a parking meter) and assume that there is a parking space next to each indicator. However, there are some difficulties here, since not every parking space has the ability to install an indicator and this is more expensive. Also, the location of the indicator does not explicitly indicate where the parking space is located and how it is located, but only allows you to make a guess.

The next option is to create an object recognition model that looks for the markings of a parking space located on the road. But this approach has disadvantages, such as the need to apply the marking itself on the road, which may eventually become unusable, and other lines or markers may be present in the parking lot, which may lead to erroneous recognition of the parking space.

The last option is to determine the parking space where cars have been parked for a long time. It is possible to guess where the parking spaces are if you recognize and identify cars that do not move between frames. But even in this option there are disadvantages, since in order to determine the parking space, you need to fill the parking lot with cars. This method is more suitable for determining parking spaces along roads or streets.

As a result, the first option was chosen, because it is more similar to the requirements of the system implementation.

To determine whether a parking space is occupied or not, you need to implement car recognition. On the frame, machine recognition will be a classic object recognition task. There are many machine learning-based approaches that could be used for speech recognition:

- Train the detector based on the Histogram of Oriented Gradients (HOG) and analyze the entire image to identify all the machines. This approach, which does not use deep learning, works relatively quickly, but the quality of finding machines that are located differently does not meet the requirements of the system [3].
- Train the detector based on Convolutional Neural Network (CNN) and analyze the entire image to identify all the machines. This approach works accurately, but not as efficiently, since it requires multiple image scans using CNN to find all the machines. With this method, it will be possible to find machines that are located differently, but this will require much more training data than for a HOG detector [4].
- Use a deep learning approach-Mask R-CNN, Faster-CNN, or YOLO, which combines the accuracy of CNN and a set of technical properties that significantly increase the speed of recognition. Such models will run relatively fast (on the GPU) if we have a lot of data to train the model [5].

In general, it is necessary to choose the simplest solution that will work according to the expected result and will require the least amount of training data. It doesn't have to be the newest and fastest algorithm. Having correlated all the requirements and costs, it follows that the system must use the Mask R-CNN.

The R-CNN Mask architecture is designed in such a way that it recognizes objects in the entire image, effectively wasting resources, and does not use the sliding window approach. In other words, it works quite fast [6]. With a modern GPU, it is possible to recognize objects in high-resolution video. For this system, this will be enough.

In addition, Mask R-CNN provides a lot of information about each recognized object. Most recognition algorithms only return a bounding box for each object. However, Mask R-CNN will not only give us the location of each object, but also its contour (mask).

To train the Mask R-CNN, you need many images of objects that should be recognized. One way is to go outside, take a picture of the cars and label them in the photos, which would take some time. At the moment, there are already several publicly available datasets with images of cars, since cars are one of the most common objects. One of them is the popular Common Objects In Context (COCO) dataset, which has images annotated with object masks. This dataset contains more than 12,000 images with already marked-up machines [7]. Next, you need to train the model using the COCO dataset. At the moment, there is already a trained model, as the mentioned dataset is popular. Therefore, instead of training your own model, you can take a ready-made one that can already recognize cars. For this system, you can use the model from Matterport. In the future, if the model does not match the quality of object recognition, it is possible to train your model. For artificial neural networks, learning refers to the process of configuring the network architecture (the structure of connections between neurons) and the weights of synaptic connections (the coefficients that affect the signals) to effectively solve the task. Training of a neural network is carried out on a certain sample. In the course of training, the network begins to perform tasks better and respond to the assigned commands.

As a result, the Mask R-CNN model returns 4 values for each recognized object:

1. Type of detected object (integer). The pre-trained COCO model can recognize 80 different frequently encountered objects like cars and trucks.
2. The degree of confidence in the recognition results. The higher the number, the more confident the model is that the object is recognized correctly.
3. Bounding box for the object in the form of X Y-coordinates of pixels in the image
4. "Mask", which shows which pixels inside the bounding box are part of the object. You can use the mask. data to find the outline of an object.

As a result, there are pixel coordinates of each machine. Figure 1 shows object recognition from a video camera.



Fig. 1. – Object recognition from an image

After getting the pixel coordinates, it is possible to determine whether the parking space is occupied by a car or not. To do this, each parking space is analyzed in turn and it is determined whether an object of the "car" type is located in this area or not. If the object of the "car" type is located inside the area of the parking space, then it is occupied. If the object of the "car" type is not located inside the parking space area, then the space is free and it can be reserved.

The user makes a choice of parking on the server part of the parking space system receives an image from a video camera that is located in the parking lot. The image is processed by a neural network and determines the location of parking spaces. Also, the system analyzes all parking spaces to determine which of these spaces are occupied and which are free. This data is written to the database.

At this time, the client part is updated and displays the current data. Figure 2 shows the form for selecting a parking space and booking this parking space.

Fig. 2. – Parking space selection form

REFERENCES

1. Проектирование магазинов и торговых центров / Канаян К. А., Канаян Р. В. – Москва, 2015 – 68 с.
2. Нейронные сети: применение сегодня и перспективы развития / Фаустова К.И. – Москва, 2017 – 83 с.
3. Selection of Histograms of Oriented Gradients Features for Pedestrian Detection / Takuya KobayashiAkinori HidakaTakio Kurita – Tsukuba, 2004 – 308 p.
4. Grokking Deep Learning / Andrew Trask – New York, 2019 – 50 p.
5. Mask R-CNN / Kaiming H., Gkioxari G. H., Piotr Dollar, Girshick R. M. - The Hague, 2017 – 41 p.
6. Visualizing and understanding convolutional neural networks / M. D. Zeiler and R. Fergus – Berlin, 2014 – 62 p.
7. Microsoft Common Objects in Context / Michael Maire, Serge Belongie // Microsoft COCO [Electronic resource]. – Washington, 2014. – Mode of access: <https://paperswithcode.com/dataset/coco>. – Date of access: 10.04.2021.

UDK 658.52.011.5:536.5

CONTROL AND MEASURING DEVICES FOR CONTROLLING THE TEMPERATURE REGIME OF THE COOKING CABINET

D. KASIMOV, Y. ZARGARYAN

Southern Federal University, Taganrog, Russia

Many enterprises in Russia are currently engaged in the development of temperature and humidity regulators. It happens due to the fact that in every small town and even village there are manufacturers using technological processes associated with the regulation of these parameters. The article analyzes the control and measuring devices for controlling the temperature regime of the cooking cabinet. The devices of the "Thermodat" series produced by LLC "UralTeploPribor" and "MPR 51" of the company "Aries" are considered. The advantages and disadvantages of the devices are revealed. The analysis of the application of the control device for the temperature and humidity regime of the cooking cabinet is carried out.

Many enterprises in Russia are currently engaged in the development of temperature and humidity regulators. It happens due to the fact that in every small town and even village there are manufacturers using technological processes associated with the regulation of these parameters. Thus, the demand for such devices is large [1-6].

As a result of the research, it was revealed that in Russia Orel T419 devices are often used to automate such technological processes. But devices of this type can be considered obsolete, since they were developed about ten years ago. T419 has some disadvantages, one of which is the constant presence of the operator, since after each stage of the technological process it is necessary to change the set parameters.

Among the modern developments, it is possible to note the devices of the "Thermodat" series produced by LLC "UralTeploPribor" and "MPR 51" of the company "Aries".

The device "Thermodat-38N1" is designed to measure and regulate temperature and humidity. The device has two universal inputs. Each input can work with any thermocouple XA, XK, LCD, MK, NN or thermal resistance Pt, Cu. The temperature measurement range is from minus 50°C to 200°C for any sensor. Humidity is determined psychrometrically by the temperature difference measured on the first and the second channels. In this case, the first channel of the device is designed to measure the temperature of the "dry thermometer", and the second — to measure the temperature of the "wet thermometer".

In the psychrometric method, the device measures the temperature of the "dry" and "wet" temperature sensors. The device calculates the relative humidity value based on the psychrometric table based on the "dry" temperature and the temperature difference between the "dry" and "wet" temperature sensors. In the memory of the device, two tables are "sewn" - for the aspiration speed (blowing) of 0.8 m/s, corresponding to the speed of air movement in closed rooms, and 3m/s - for blowing a "wet" temperature sensor with a fan in a standard aspiration psychrometer.

As thermal sensors, two thermocouples or two thermal resistances can be connected to the device. But since the temperature difference indicated above is usually small, the use of independent sensors can give a large error in determining humidity, since the measurement errors of the sensors add up. To obtain the relative humidity value with higher accuracy, the Thermodat-38PN1 devices provide for the measurement of the psychrometric temperature difference by differential thermocouples.

Upon request, the device can be supplied complete with a combined psychrometric humidity sensor and a temperature sensor. The sensor has a glass water feeder. As a "dry" thermometer, it is equipped with a resistance thermometer Pt100. To measure the temperature difference between the "dry" and "wet" thermometers, a battery of five differential thermocouples is used. The battery of thermocouples allows you to register small temperature differences with high accuracy, which leads to an increase in the accuracy of determining humidity.

Psychrometric humidity sensors can operate in a polluted and dusty atmosphere. The time to establish the readings is about 20 minutes.

The device has two four-digit LED digital indicators for indicating temperature and humidity.

The device can be equipped with an interface for communication with a computer. The computer program allows you to accumulate measurement results, observe and print out graphs of humidity and temperature.

In devices with an archive, the measured temperature is recorded in non-volatile memory with reference to real time and the calendar. The recording period is from 1 min to 1 hour. The archive cannot be deleted by the operator, the transfer of the archive to the computer via the interface.

Technical specifications:

Power supply ~ 220V AC 50 Hz.

ICT, Electronics, Programming, Geodesy

Power consumption-no more than 10W.

The safety requirements comply with GOST 12.2.007.0-75 and GOST 12997.

Overall dimensions of the electronic counting device-96x96x110 mm, mounting cutout in the shield-92x92 mm.

Weight - no more than 0.8 kg.

Performance in terms of construction, strength and resistance to external influences.

The device is designed for panel placement according to GOST 5944-91. The electronic device for resistance and strength to temperature and moisture correspond to the performance group B1 according to GOST 12997-84 for operation in closed heated or cooled and ventilated industrial premises, the operating temperature range is +5oC... +45oC, humidity up to 75% at 30oC. The device does not contain precious metals [1].

The device "MPR 51". The device is designed to measure and regulate temperature and humidity. It performs regulation simultaneously on two channels, according to a given program. Programs are compiled by the user and can have from two to 20 steps. The device can be used in the food industry. For example, in bakeries to maintain the regime in proofing cabinets, in ovens for baking bread; in meat and fish processing plants to ensure the technological process in cooking and smoking chambers, in maturation chambers, in universal climate chambers. The device can also be used in the production of reinforced concrete products for the heat-curing process. MPR51 can help in maintaining the desired modes in the wood drying chambers.

You can use the device for controlling the temperature and humidity mode of the cooking cabinet:

- in bakeries to maintain the mode in the proofing cabinets;
- in bread baking ovens;
- at meat and fish processing plants, to ensure the technological process in the cooking and smoking chambers;
- in the maturation chambers;
- in universal climate chambers;
- in the production of reinforced concrete products for the heat-curing process;
- when maintaining the desired modes in the wood drying chambers;
- in the cooking cabinets;
- in incubator plants.

REFERENCES

1. Фролова И.Г., Фролов С.В. Нарушение температурно-влажностного режима -фактор снижение безопасности // С.В. Вестник СГАСУ. Градостроительство и архитектура. 2013. № 3 (11).
2. Кашкаров, А. П. Датчики в электронных схемах. От простого к сложному / А.П. Кашкаров. - М.: ДМК Пресс, 2015. - 200 с.
3. Рой Ю.В, Заргарян Е.В. Технологический процесс системы управления блока сепарации установки комплексной подготовки нефти. / Электронный научный журнал «Вестник молодёжной науки России», Выпуск №1, 2020, ISSN 2658 – 7505.
4. Пушнина И.В, Понаськова К.А. Анализ и принцип управления климатом инкубатора. / Электронный научный журнал «Вестник молодёжной науки России», Выпуск №5, 2020, ISSN 2658 – 7505.
5. Ганчиевский А.В, Заргарян Ю.А. Применение нечеткого контроллера в системе управления частотой вращения ротора двигателя. / Электронный научный журнал «Вестник молодёжной науки России», Выпуск №5, 2020, ISSN 2658 – 7505.
6. Запорожцева Л.С, Заргарян Ю.А. Система управления стабилизацией пневмоколёсной платформы. / Электронный научный журнал «Вестник молодёжной науки России», Выпуск №5, 2020, ISSN 2658 – 7505.

UDK 622.276.8.004

ANALYSIS OF THE PRINCIPLES OF BELT CONVEYORS

K. PONASKOVA, E. ZARGARYAN

Southern Federal University, Taganrog, Russia

In almost all industries, belt conveyors are used, which ensure the continuity of the processes of transporting various types of goods and materials. Their use allows to deliver piece loads and materials that have a bulk / lump structure to the desired object.

There are two main types of resources that a person uses: renewable and non-renewable. Renewable resources include all those resources that are restored by photosynthesis in the foreseeable future. We are talking primarily about all types of vegetation and the resources that can be obtained from it. Non-renewable resources include minerals that will not recover in the foreseeable geological time [1,2].

Today, for example, the society has a diverse structure of various household and industrial waste, using existing technological processes. The waste accumulates in the course of time and becomes a serious problem.

The relevance of this work is determined by the fact that the need to recycle waste plays a huge role in people's lives – it is a necessary condition for their health and the health of their generations.

Since the 1980s, the production of conveyors in industrially developed countries gradually became a separate field of mechanical engineering. In modern types, the main structural elements have been preserved, which have been improved in accordance with the achievements of science and technology (replacing the belt drive with an electric one, using vibration technology, using compressed air energy, etc.).

The main classification feature of conveyors is the type of traction and load-bearing body. There are conveyors with belt, chain, rope traction bodies and conveyors without a traction body (gravity, inertia, screw). Conveyors with a traction body can be belt-type, plate-type, cradle-type, scraper-type, bucket-type, etc. These are characterized by the general movement of the load on the working areas with the working body. The traction force is transmitted either by a load-bearing element, or by an element pushing or pulling the load along a fixed chute, pipe, flooring, etc.

Depending on the conditions, floor and suspended conveyors are used. Floor coverings can be stationary, mobile or portable. On the conveyor, you can move the load in a horizontal or close to it inclined plane (belt, plate, trolley, scraper, roller, screw, vibrating, swinging); in a vertical or close to it inclined plane (scraper, bucket, screw, vibrating); in any plane [1].

Special groups are elevators, vertical conveyors with suspended buckets, cradles or shelves, escalators, special plate and belt conveyors for moving people, walking conveyors, trimmers, stackers for stacking logs, as well as combined (for example, roller-belt conveyors of the "Rapistan" type, which ensure the retention of piece loads on descents at specified intervals), etc. [2].

Main types of conveyors:

1. Belt conveyors are used to move bulk, lump and piece goods over distances that sometimes reach 10-12 km or more. These are usually made up of separate sections. The conveyor route is straight in the horizontal plane, and in the vertical plane it can be inclined or have a more complex configuration.

2. Plate conveyors are designed to move in a horizontal plane or with a slight inclination (up to 35°) heavy (500 kg or more) piece loads, large-sized, including sharp-edged materials, as well as loads heated to a high temperature. Lamellar, stationary or mobile, have the same basic nodes as the tape ones.

3. Scraper conveyors move the load by moving the scrapers along the chute or pipe. These are used for processing bulk or lumpy cargo entering the chute through the loading funnel. Scraper conveyors are usually used to move cargo over distances of up to 100 m. A variety of scraper conveyors are conveyors with submerged scrapers, in which the scrapers cover only part of the section of the chute, and the load fills the entire working branch of the chute or most of it. Such trucks can have a complex track and are used to move loads (usually small-bulk) in horizontal, vertical and inclined directions at a speed of 0.1-0.25 m / s.

4. Suspended conveyors with a chain traction body are used for continuous (less often periodic) movement of piece loads. The route of such conveyors is usually spatial closed and has a complex contour. Suspended conveyors are divided into 3 groups: load-carrying (carriages for cargo are permanently connected to the traction body); pulling (carriages are also permanently connected to the traction body and have hooks for attaching trolleys moving on the floor of the workshop or warehouse); pushing (carriages are not permanently connected to the traction body and move along suspended tracks). The use of suspended conveyors makes it possible to solve the problems of complex mechanization and automation of loading and unloading and storage operations at the junction of intra-shop, intra-factory and mainline transport.

5. Screw conveyors are used to move pulverized and small-sized loads in horizontal or inclined (up to 20°) planes, less often in the vertical plane (conveyors with rapidly rotating screws). Screw conveyors are simple in design, easy to operate, especially when transporting dusty goods.

6. Roller conveyors are used for moving piece loads with a flat, ribbed or cylindrical surface. They come in 2 types: gravity and drive. In gravity conveyors installed with a slope of 2-5°, the rollers rotate freely under the influence of the gravity of the load being moved. In drive conveyors, the rollers have a group drive from the motor. These are used when it is necessary to ensure a constant speed of movement of goods, to move them in a strictly horizontal plane or to lift them at a certain angle.

7. Inertial conveyors are used for transporting bulk, less often small piece goods over relatively short distances in horizontal or inclined (up to 20°) directions. In these conveyors, cargo particles slide along the load-bearing body or fly in space under the influence of inertia. They are divided into 2 groups: swinging, characterized by significant amplitudes and low frequency of vibrations, and vibrating — with a small amplitude and high frequency of vibrations [2,3].

Knowing what the conveyor belt consists of and what the functional purpose of its elements is, it is possible to change certain nodes to achieve the appropriate technological characteristics of the entire device.

The efficiency of using conveyors in the technological process of any production depends on how much the type and parameters of the selected conveyor correspond to the properties of the cargo and the conditions in which the technological process takes place. These conditions include: productivity, length of transportation, shape of the route and direction of movement (horizontal, inclined, vertical, combined); conditions for loading and unloading the conveyor; the size of the load, its shape, specific density, abrasiveness, lumpiness, humidity, temperature, etc.; the rhythm and intensity of the feed, as well as various local factors [4-8].

REFERENCES

1. Зенков Р. Л., Петров М. М., Конвейеры большой мощности, М., 1964;
2. Спиваковский А. О., Потапов М. Г., Котов М. А., Карьерный конвейерный транспорт, М., 1965;
3. Транспортирующие и перегрузочные машины для комплексной механизации пищевых производств, под ред. А. Я. Соколова, М., 1964;
4. Спиваковский А. О., Дьячков В. Н., Транспортирующие машины, 2 изд., М., 1968.
5. Соловьев В.В., Заргарян Е.В., Заргарян Ю.А., Белоглазов Д.А., Косенко Е.Ю. Проектирование и моделирование объемного гидропривода. Ростов-на-Дону: Изд-во ЮФУ, 2015. – 97 с.
6. Рой Ю.В, Заргарян Е.В. Технологический процесс системы управления блока сепарации установки комплексной подготовки нефти. / Электронный научный журнал «Вестник молодёжной науки России», Выпуск №1, 2020, ISSN 2658 – 7505
7. Финаев В.И., Скубилин М.Д., Заргарян Ю.А Волоконнооптические преобразователи в электроэнергетике. Известия ЮФУ. Технические науки. 2018. С. 213.
8. Пушнина И.В. Алгоритмическое обеспечение автоматической работы светофора. В сборнике: Технологии разработки информационных систем ТРИС-2019. Материалы IX Международной научно-технической конференции. 2019. С. 120-124.

UDC 517.925.44

ROBUST STABILITY IN THE PROBLEM OF MOTION OF AN INVERTED PENDULUM WITH A VIBRATING SUSPENSION POINT

A. DULEPOVA, G. DEMIDENKO
Novosibirsk State University, Russia

The work is devoted to the study of the robust stability of the motion of an inverted pendulum with a suspension point oscillating according to a sinusoidal law. The case of perturbations of the amplitude of oscillations is considered, an estimate is given for the magnitude of the perturbation at which the stability of motion is preserved.

Introduction. The motion of an inverted pendulum, the suspension point of which oscillates according to a sinusoidal law along a straight line making a small angle α with the vertical, is described by the following equation:

$$\varphi'' + \varepsilon\varphi' + \frac{g - a\omega^2 \sin(\omega t) \cos \alpha}{l} \sin \varphi - \frac{a\omega^2 \sin(\omega t) \sin \alpha}{l} \cos \varphi = 0, \quad (1)$$

where $\varphi = \varphi(t)$ is the angle of deviation of the pendulum from the lower vertical position of equilibrium, ε is the friction coefficient, l is the length of the pendulum, g is the acceleration of gravity, ω is the oscillation frequency of the suspension point, and a is the amplitude of the suspension point oscillations.

It is well known that, in case of zero angle $\alpha = 0$, at a sufficiently large oscillation frequency $\omega \gg 1$ and sufficiently small amplitude of oscillations of the suspension point $\frac{a}{l} \ll 1$, the upper equilibrium position of the pendulum becomes stable. This result was predicted back in 1908 by the English mathematician Stephenson (see [1]) and was first rigorously proved by Bogolyubov in 1942 (see [2]). Namely, he demonstrated that, if the above conditions on the amplitude and frequency are satisfied and $a\omega > \sqrt{2gl}$, the upper vertical position $\varphi(t) = \pi$ is asymptotically stable. The last condition means that the maximum oscillation velocity of the suspension point must exceed the velocity of a free fall of a body from the height equal to the pendulum length. A clear demonstration of this phenomenon is provided by the Kapitza's installation [3].

At present, there are various approaches to the proof of the theorem on the stability of the upper equilibrium position of the pendulum at zero angle $\alpha = 0$ (see [4]), the classical proof is carried out using the averaging method [5, 6]. In papers [7, 8, 9] the stability problem for an inverted pendulum in the case $\alpha \geq 0$ is solved using a special boundary value problem for the Lyapunov differential equation and the principle of contracting mappings (see, for example, [10]). This approach is remarkable in that it allows not only to establish the very fact of motion stability, but also to obtain the region of attraction of the solution and an estimate of the stabilization rate at $t \rightarrow \infty$. Developing the [7, 9] approach and using the technique described in [11], it is also possible to obtain some results on robust stability (that is, stability with respect to perturbations of the coefficients of the equation) in the problem of motion of an inverted pendulum with a vibrating suspension point, which is the subject of this work.

Task formulation. Consider the movement of the pendulum in the case of a zero angle $\alpha = 0$. Then the equation (1) takes the following form

$$\varphi'' + \varepsilon\varphi' + \frac{g - a\omega^2 \sin(\omega t)}{l} \sin \varphi = 0.$$

Shifting the angle by π ($\varphi := \varphi + \pi$) and writing the result equation in the form of a system, we get

$$\frac{d}{dt} \begin{pmatrix} \varphi_1 \\ \varphi_2 \end{pmatrix} = \begin{pmatrix} 0 & 1 \\ 0 & -\varepsilon \end{pmatrix} \begin{pmatrix} \varphi_1 \\ \varphi_2 \end{pmatrix} + \begin{pmatrix} 0 \\ g - a\omega^2 \sin(\omega t) \end{pmatrix} \sin \varphi_1. \quad (2)$$

Here $\varphi_1 = \varphi$ and $\varphi_2 = \dot{\varphi}$. Due to the angle shift, the study of the upper vertical equilibrium position of the pendulum is reduced to the study of the zero solution of system (2).

Our goal is to study the robust stability of the system (2) with respect to the perturbation Δa of the amplitude of the suspension point oscillations, i.e. we consider the following perturbed system

$$\frac{d}{dt} \begin{pmatrix} \varphi_1 \\ \varphi_2 \end{pmatrix} = \begin{pmatrix} 0 & 1 \\ 0 & -\varepsilon \end{pmatrix} \begin{pmatrix} \varphi_1 \\ \varphi_2 \end{pmatrix} + \begin{pmatrix} 0 \\ g - (a + \Delta a)\omega^2 \sin(\omega t) \end{pmatrix} \sin \varphi_1. \quad (3)$$

Preliminary information. Consider a linear homogeneous system of differential equations with periodic coefficients

$$\frac{dy}{dt} = A(t)y, \quad t \geq 0, \quad (4)$$

where $A(t)$ is a continuous T -periodic matrix of size $N \times N$.

In this paper, we rely on the criterion of the asymptotic stability of the zero solution for the system (4), formulated in terms of the solvability of the following special boundary value problem for the Lyapunov differential equation

$$\frac{dH}{dt} + HA(t) + A(t)^*H = -C(t), \quad 0 \leq t \leq T, \quad (5)$$

$$H(0) = H(T). \quad (6)$$

According to this criterion (see [12]), if the zero solution of the system (4) is asymptotically stable, then for any matrix $C(t)$ continuous on $[0, T]$ and such that

$$C(t) = C(t)^* > 0, \quad t \in [0, T],$$

there exists a unique Hermitian positive definite solution $H(t)$ of the boundary problem (5)-(6).

We will further assume that the zero solution of the system (4) is asymptotically stable. Let us denote

$$\Delta = \left(1 - \exp \left(- \int_0^T \frac{1}{2} \|H(\eta)\|^{-1} d\eta \right) \right)^{-1}, \quad (7)$$

$$\mu(H) = \max_{\tau \in [0, T]} \|H(\tau)\| \max_{\xi \in [0, T]} \|H^{-1}(\xi)\|. \quad (8)$$

In our work, in the study of robust stability in the problem of motion of an inverted pendulum, we will use the following result from [11] reformulated in terms of the asymptotic stability of the zero solution:

Theorem 1. Let the zero solution of the system (4) with T -periodic coefficients be asymptotically stable. If a T -periodic matrix $A_1(t)$ satisfies the following condition

$$q = 2T\Delta\sqrt{\mu(H)} \max_{t \in [0, T]} \|A_1(t)\| < 1, \quad (9)$$

then the zero solution of the system with perturbed coefficients

$$\frac{dy}{dt} = (A(t) + A_1(t))y, \quad t \geq 0$$

is also asymptotically stable.

Results. We begin the study of the robust stability of the system (2) with the study of the robust stability of its linear approximation, i.e. we consider $\sin \varphi_1 \approx \varphi_1$ and the corresponding system is the following

$$\frac{d}{dt} \begin{pmatrix} \varphi_1 \\ \varphi_2 \end{pmatrix} = \begin{pmatrix} 0 & 1 \\ g - a\omega^2 \sin(\omega t) & -\varepsilon \end{pmatrix} \begin{pmatrix} \varphi_1 \\ \varphi_2 \end{pmatrix} = A(t)\vec{\varphi}. \quad (10)$$

The corresponding perturbed system has the form

$$\begin{aligned} \frac{d}{dt} \begin{pmatrix} \varphi_1 \\ \varphi_2 \end{pmatrix} &= \begin{pmatrix} 0 & 1 \\ g - (a + \Delta a)\omega^2 \sin(\omega t) & -\varepsilon \end{pmatrix} \begin{pmatrix} \varphi_1 \\ \varphi_2 \end{pmatrix} \\ &= \begin{pmatrix} 0 & 1 \\ g - a\omega^2 \sin(\omega t) & -\varepsilon \end{pmatrix} \begin{pmatrix} \varphi_1 \\ \varphi_2 \end{pmatrix} + \begin{pmatrix} 0 & 0 \\ -\Delta a\omega^2 \sin(\omega t) & 0 \end{pmatrix} \begin{pmatrix} \varphi_1 \\ \varphi_2 \end{pmatrix} = (A(t) + A_1(t))\vec{\varphi}. \end{aligned} \quad (11)$$

The following result holds.

Theorem 2. Let $\frac{a}{l} \ll 1$, $\omega \gg 1$ and $a\omega > \sqrt{2gl}$, i.e. the zero solution of the system (10) is asymptotically stable. If

$$|\Delta a| < \frac{l}{4\pi\omega\Delta\sqrt{\mu(H)}}, \quad (12)$$

where $H(t)$ is Hermitian positive definite solution of the problem (5)-(6) with the matrix $A(t)$ corresponding to the system (10) and the values Δ and $\mu(H)$ are defined by (7) and (8), respectively, then the zero solution of the system (11) with the perturbed amplitude is also asymptotically stable.

This theorem follows directly from the theorem 1 applied to the systems (10), (11) and namely the inequality (9). For initial nonlinear system (2) similar result is true.

Theorem 3. Let $\frac{a}{l} \ll 1$, $\omega \gg 1$ and $a\omega > \sqrt{2gl}$, i.e. the zero solution of the system (10) is asymptotically stable. If

$$|\Delta a| < \frac{l}{4\pi\omega\Delta\sqrt{\mu(H)}},$$

where $H(t)$ is Hermitian positive definite solution of the problem (5)-(6) with the matrix $A(t)$ corresponding to the system (10) and the values Δ and $\mu(H)$ are defined by (7) and (8), respectively, then the zero solution of the nonlinear system (3) with the perturbed amplitude is also asymptotically stable.

In the proof of this theorem we first show with the use of the results from [7] about asymptotic stability of zero solutions for quasilinear systems with periodic coefficients, that from asymptotic stability of the zero solution of the linear system (10) it follows that the zero solution of the nonlinear system (2) is also asymptotically stable. Thus, the statement of the theorem 3 is indeed a result of robust stability (from the asymptotic stability of the zero solution of the nonlinear system (2) follows the asymptotic stability of the zero solution of the perturbed nonlinear system (3) when the estimate (12) on the value of Δa holds). And then, using again the results from [7], we prove the statement of the theorem 3.

Conclusion. The paper studies the question of the robust stability of the motion of an inverted pendulum, the suspension point of which oscillates according to a sinusoidal law along a vertical line. Namely, the case of a perturbed vibration amplitude is considered. An estimate is given for the magnitude of the perturbation of the amplitude at which the stability of motion is preserved. The research uses the approaches from [7] and [11].

In the future, the question of robust stability with respect to other parameters of the pendulum motion (the oscillation frequency of the suspension point ω and the length of the pendulum l) is raised, and the case of oscillations of the suspension point along an inclined straight line ($\alpha > 0$) should be studied. In addition, there stays the problem of finding a solution to a special boundary value problem arising in the study of the Lyapunov differential equation (at least approximately).

REFERENCES

1. Stephenson A. On a new type of dynamical stability // *Memoirs and Proceedings of the Manchester Literary and Philosophical Society*. – 1908. – V. 52, № 8. – P. 1–10.
2. Боголюбов Н. Н. Теория возмущений в нелинейной механике // *Сб. тр. Ин-та строительной механики АН УССР*. – 1950. – Т. 14. – С. 9–34.
3. Капица П. Л. Динамическая устойчивость маятника при колеблющейся точке подвеса // *ЖЭТФ*. 1951. – Т. 21, № 5. – С. 588–597.
4. Арнольд В. И. Математическое понимание природы: Очерки удивительных физических явлений и их понимания математиками. – М.: МЦНМО, 2011.
5. Боголюбов Н. Н., Митропольский Ю. А. Асимптотические методы теории нелинейных колебаний. — М.: ФИЗМАТЛИТ, 1963.
6. Митропольский Ю. А. Метод усреднения в нелинейной механике. – Киев: Наукова Думка, 1971.
7. Демиденко Г. В., Матвеева И. И. Об устойчивости решений квазилинейных периодических систем дифференциальных уравнений // *Сиб. мат. журн.* – 2004. – Т. 45, № 6. – С. 1271–1284.
8. Демиденко Г. В., Дулина К. М., Матвеева И. И. Асимптотическая устойчивость решений одного класса нелинейных дифференциальных уравнений второго порядка с параметрами // *Вестн. ЮУрГУ. Сер. Матем. моделирование и программирование*. – 2012. – № 14, – С. 39–52.
9. Демиденко Г. В., Дулепова А. В. Об устойчивости движения перевернутого маятника с вибрирующей точкой подвеса // *Сиб. журн. индустр. матем.* – 2018. – № 4. – С. 39–50.
10. Треногин В. А. Функциональный анализ. – 4-е изд., испр. – М.: ФИЗМАТЛИТ, 2007.
11. Демиденко Г. В. Системы дифференциальных уравнений с периодическими коэффициентами // *Сиб. журн. индустр. матем.* – 2013. – № 4. – С. 38–46.
12. Демиденко Г. В., Матвеева И. И. Об устойчивости решений линейных систем с периодическими коэффициентами // *Сиб. мат. журн.* – 2001. – Т. 42, № 2. – С. 332–348.

AUTOISOMETRIES OF THE FOUR-DIMENSIONAL LIE ALGEBRA OF IV BIANCI TYPE

E. IVANOVA, M. PODOKSENOV

Vitebsk State University named after P.M. Masherov, Belarus

1. Formulation of the problem. Let a Euclidean or Lorentz scalar product be introduced in the Lie algebra \mathcal{G} . Linear transformation $f: \mathcal{G} \rightarrow \mathcal{G}$ is called an autoisometry if it is both an isometry with respect to the scalar product and an automorphism of the Lie algebra. A transformation f is called an auto-similarity if it is both a similarity and an automorphism. As shown in [1], solving the problem of finding one-parameter self-similarity groups of a given Lie algebra allows us to construct self-similar homogeneous manifolds of the corresponding Lie group equipped with a left-invariant matrix. In the same paper, all the self-similarities of the three-dimensional Lie algebra \mathcal{H}_s of the Heisenberg group were found for various ways of defining the Lorentzian scalar product on it, and the corresponding one-parameter similarity groups of the homogeneous Lorentzian manifold of the three-dimensional Heisenberg Lie group H_s were found.

The non-commutative two-dimensional Lie algebra $\mathcal{A}(1)$ is the Lie algebra of the group $A(1)$ of affine transformations of the line. The connected component of this Lie group containing the identity is the group $A^+(1)$ consisting of affine transformations preserving the orientation of the line. In [2] and [3], all ways of defining the Lorentz scalar product on two-dimensional and three-dimensional Lie algebras $\mathcal{A}(1)$ and $\mathcal{A}(1) \oplus \mathcal{R}$ were found, for which they admit one-parameter groups of auto-similarities and autoisometries, and formulas were written, on which these one-parameter groups act. This made it possible to construct self-similar connected manifolds of Lie groups $A^+(1)$ and $A^+(1) \times \mathbf{R}$. All possible one-parameter auto-similarity and auto-isometry groups for the four-dimensional Lie algebra $\mathcal{A}(1) \oplus \mathcal{R}^2$ were found in [4], and in [5] a similar problem was solved in the case of specifying a Euclidean scalar product in the Lie algebra.

The purpose of this work is to find all ways of defining the Lorentzian scalar product in the Lie algebra $\mathcal{G}_4 = \mathcal{A}(1) \oplus \mathcal{A}(1)$ for which it admits a one-parameter autoisometry group, write out the matrix defining the action of this group, and prove that it does not admit self-similarities for any way of specifying the Lorentz scalar product on it. This four-dimensional Lie algebra \mathcal{G}_4 is the only one belonging to the IV type according to the Bianchi classification.

2. Lie algebra structure. In an appropriate basis (E_1, E_2, E_3, E_4) the commutation relations of the Lie algebra \mathcal{G}_4 are given by two equalities: $[E_3, E_1] = E_1$, $[E_4, E_2] = E_2$, and the remaining brackets are equal to the zero vector. We will call such a basis canonical. The two-dimensional subspace \mathcal{H} , which is the linear span of the vectors E_1 and E_2 is the derived Lie algebra $[\mathcal{G}_4, \mathcal{G}_4]$. This is a commutative ideal. The linear spans of the vectors E_1, E_3 and E_2, E_4 will be denoted by \mathcal{L}_1 and \mathcal{L}_2 . These subspaces are two-dimensional non-commutative ideals.

The Lie algebra \mathcal{G}_4 admits a four-dimensional group of automorphisms, which it consists of transformations, which are given by matrices of the form

$$\begin{pmatrix} \alpha & 0 & \gamma & 0 \\ 0 & \beta & 0 & \delta \\ 0 & 0 & 1 & 0 \\ 0 & 0 & 0 & 1 \end{pmatrix}, \quad (1)$$

where $\alpha \neq 0$, $\beta \neq 0$, and γ, δ can take any value. Such automorphisms will be called automorphisms of the first type. The simultaneous permutation of the basis vectors E_1 and E_2 , E_3 and E_4 also preserves the bracket operation. It is given by a matrix of the form

$$\begin{pmatrix} 0 & 1 & 0 & 0 \\ 1 & 0 & 0 & 0 \\ 0 & 0 & 0 & 1 \\ 0 & 0 & 1 & 0 \end{pmatrix}. \quad (2)$$

Therefore, the composition of automorphisms defined by matrices (1) and (2) is also an automorphism. It is given by the matrix

$$\begin{pmatrix} 0 & \alpha & 0 & \gamma \\ \beta & 0 & \delta & 0 \\ 0 & 0 & 0 & 1 \\ 0 & 0 & 1 & 0 \end{pmatrix}, \alpha \neq 0, \beta \neq 0. \quad (3)$$

We will call them automorphisms of the second type. It is important to note that the determinant of matrices (1) and (3) is equal to $\alpha\beta$, i.e. is equal to the determinant of the matrix defining the restriction of the transformation to \mathcal{H} . Therefore, the transformation obtained by multiplying the identity transformation by a number is not an automorphism (we will call such transformations homotheties). A one-parameter group of automorphisms can contain only automorphisms of the first type for $\alpha > 0, \beta > 0$.

The linear span of vectors x, y will be denoted by $\langle x, y \rangle$.

3. Main results. Let the Lorentz scalar product be introduced on the Lie algebra \mathcal{G}_4 .

Theorem. 1. *There is only one way to define the Lorentz scalar product in the Lie algebra $\mathcal{G}_4 = \mathcal{A}(1) \oplus \mathcal{A}(1)$, in which it admits a nontrivial one-parameter autoisometry group. The action of this group in the canonical basis is given by the matrix (4) and the Gram matrix of the basis has the form (5).*

$$\begin{pmatrix} e^{\nu t} & 0 & 0 & 0 \\ 0 & e^{-\nu t} & 0 & 0 \\ 0 & 0 & 1 & 0 \\ 0 & 0 & 0 & 1 \end{pmatrix}, \nu > 0, t \in \mathbf{R}, \quad (4) \quad \Gamma_1 = \begin{pmatrix} 0 & 1 & 0 & 0 \\ 1 & 0 & 0 & 0 \\ 0 & 0 & 1 & 0 \\ 0 & 0 & 0 & 1 \end{pmatrix} \quad (5)$$

2. Lie algebra \mathcal{G}_4 does not admit autosimilarity for any way of specifying the Lorentz scalar product in it.

Proof. Case 1. Lorentzian scalar product is induced on the ideal \mathcal{H} . Then a Euclidean scalar product is induced on the subspace \mathcal{H}^\perp . Let $h(t): \mathcal{G}_4 \rightarrow \mathcal{G}_4$ be a one-parameter group of autoisometries or autosimilarities. Under its action, the ideal \mathcal{H} , two isotropic directions in it, and one-dimensional ideals $\mathbf{R}E_1, \mathbf{R}E_2$ should remain invariant. In what follows, we denote $E'_i = h(t)(E_i), i = 1, 2, 3, 4$.

According to [6], in an appropriate basis (e_1, e_2, e_3, e_4) , any one-parameter similarity group of a four-four-meter Minkowski space that has more than one invariant isotropic eigenvector is given by the matrix $e^{\mu t} F_1(t), \mu \geq 0$, where

$$F_1(t) = \begin{pmatrix} e^{\nu t} & 0 & 0 & 0 \\ 0 & e^{-\nu t} & 0 & 0 \\ 0 & 0 & & \\ 0 & 0 & \mathbf{Q}(t) & \end{pmatrix}, \nu \geq 0, t \in \mathbf{R}, \quad (6)$$

and $\mathbf{Q}(t)$ is an orthogonal matrix. In this case, the Gram matrix has the form (5).

In [7], all invariant two-dimensional subspaces of the transformation group were found, which is given by matrices of the form (6).

According to the theorem proved in [7] and the corollary from it holds $\mathcal{H} = \langle e_1, e_2 \rangle$, and we can conclude that $\mathbf{Q}(t) \equiv \mathbf{E}$. But it is important for us to clarify whether $h(t)$ is specified by the matrix $e^{\mu t} F_1(t)$ in the canonical basis, and also we need to find the Gram matrix of this basis. The determinant of the transformation matrix does not depend on the choice of the basis in the vector space. The determinant of the matrix $e^{\mu t} F_1(t)$ is equal to $e^{4\mu t}$, while the matrix of restriction of the transformation $h(t)$ to \mathcal{H} has determinant equal to $e^{2\mu t}$. Therefore, $\mu = 0$, and only one-parameter autoisometry group can exist.

If $\nu = 0$, then the one-parameter group consists only of identical transformations. Let $\nu \neq 0$. Then the restriction of $h(t)$ to \mathcal{H} cannot have more than two invariant directions. Therefore, E_1 and E_2 coincide with e_1 or e_2 , i.e. they are isotropic (Figure 1).

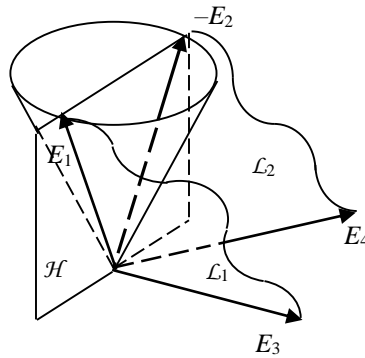


fig. 1

According to matrices (1) and (6), respectively

$$E_3'(t) = \gamma E_1 + E_3, E_2'(t) = e^{-\nu t} E_2.$$

Then

$$E_3'(t) \cdot E_2'(t) = \gamma e^{-\nu t} E_1 \cdot E_2 + e^{-\nu t} E_3 \cdot E_2 = \gamma e^{-\nu t} + e^{-\nu t} E_3 \cdot E_2.$$

The last expression must be identically equal to $E_3 \cdot E_2$. From this we obtain the identity

$$\gamma e^{-\nu t} + (e^{-\nu t} - 1) E_3 \cdot E_2 \equiv 0.$$

This is true only if $\gamma = 0$ and $E_3 \cdot E_2$ at the same time. Similarly, we get $\delta = 0$ and $E_4 \cdot E_1 = 0$. Since the scalar squares of the vectors E_1 and E_2 are equal to zero, then

$$E_3'(t) \cdot E_1'(t) = (\gamma E_1 + E_3) \cdot (e^{\nu t} E_1) = e^{\nu t} E_3 \cdot E_1.$$

This expression must be equal to $E_3 \cdot E_1$. Therefore, $E_3 \cdot E_1 = 0$, and similarly we obtain $E_4 \cdot E_2 = 0$. It means that $\mathcal{H}^\perp = \langle E_3, E_4 \rangle$. Thus, the Gram matrix of the canonical basis has the form

$$\Gamma = \begin{pmatrix} 0 & 1 & 0 & 0 \\ 1 & 0 & 0 & 0 \\ 0 & 0 & g_{33} & g_{34} \\ 0 & 0 & g_{34} & g_{44} \end{pmatrix}, \quad \begin{vmatrix} g_{33} & g_{34} \\ g_{34} & g_{44} \end{vmatrix} > 0, \quad g_{33} > 0.$$

Since $\gamma = \delta = 0$, we come to the conclusion that in the case under consideration there can only exist a one-parameter autoisometry group whose action in the canonical basis is given by the matrix (4).

Case 2. The Euclidean scalar product is induced on the ideal \mathcal{H} . Then Lorentzian scalar product is induced on the subspace \mathcal{H}^\perp , and a priori scalar squares of the vectors E_1 and E_2 are not equal to zero. Replace the basis vector E_3 by $\gamma E_1 + E_3$. Then

$$(\gamma E_1 + E_3) \cdot E_1 = \gamma E_1 \cdot E_1 + E_3 \cdot E_1$$

We will choose γ so that this expression becomes zero. In the same way, we choose δ so that the vector $\delta E_2 + E_4$ is orthogonal to E_2 , and we replace the basis vectors E_3 and E_4 with $\gamma E_1 + E_3$ и $\delta E_2 + E_4$ respectively. Let us keep the previous notation for the new basis, which will also be canonical. Also, without changing the parenthesis operation, we can make the vectors E_1 and E_2 unit.

Let $h(t): \mathcal{G}_4 \rightarrow \mathcal{G}_4$ be a one-parameter group of autoisometries or autosimilarities. The isotropic directions of the subspace \mathcal{H}^\perp must be invariant with respect to $h(t)$. Therefore, in respect to some basis (e_1, e_2, e_3, e_4) is given by the matrix $e^{\mu t} F_1(t)$. According to [7], we have $\mathcal{H} = \langle e_3, e_4 \rangle$, and thus, $\mathcal{H}^\perp = \langle e_1, e_2 \rangle$ (figure 2). From the condition on the determinant of the matrix of an automorphism, we again get $\mu = 0$ and only a one-parameter autoisometry group can exist.

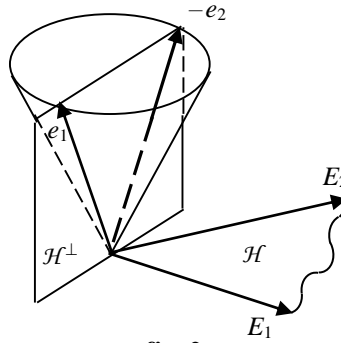


fig. 2

Moreover, the restriction of $h(t)$ to \mathcal{H} has two invariant directions. This is possible only if the matrix $\mathbf{Q}(t)$ in (6) is identically equal to \mathbf{E} . We also need to prove that $\nu = 0$.

Suppose that $E_1 \cdot E_2 \neq 0$. We have

$$E_2'(t) = E_2, E_3'(t) = \gamma E_1 + E_3,$$

$$E_3'(t) \cdot E_2'(t) = \gamma E_1 \cdot E_2 + E_3 \cdot E_2.$$

This expression must be identically equal to $E_3 \cdot E_2$. We get

$$\gamma E_1 \times E_2 = 0.$$

Hence $\gamma = 0$, and in a similar way we obtain $\delta = 0$, if $E_1 \cdot E_2 \neq 0$. It means that a one-parameter subgroup consists only of identical transformations. Therefore, we consider further only the case $E_1 \cdot E_2 = 0$. We have already proved that it is possible to choose a basis such that $E_3 \cdot E_1 = 0$. Therefore

$$E_3 \dot{\zeta}(t) \times E_1 \dot{\zeta}(t) = \gamma E_1 \times E_1 + E_3 \times E_1 = \gamma E_1 \times E_1.$$

This expression must be identically equal to zero. Hence $\gamma = 0$, and in a similar way we obtain $\delta = 0$. So, in the case under consideration, there is no nontrivial one-parameter group of autoisometries and autosimilarities.

Case 3. A degenerate scalar product is induced on the subspace \mathcal{H} . Let $h(t): \mathcal{G}_4 \rightarrow \mathcal{G}_4$ be the one-parameter autoisometry or auto-similarity group. Then the only isotropic direction in \mathcal{H} must be invariant under the action of the group. Let us first assume that it is the only invariant isotropic direction. Then, according to [6], with respect to some basis (e_1, e_2, e_3, e_4) , the group $h(t)$ is given by the matrix $e^{\mu t} F_2(t)$, $\mu \geq 0$, where

$$F_2(t) = \begin{pmatrix} 1 & t & t^2/2 & 0 \\ 0 & 1 & t & 0 \\ 0 & 0 & 1 & 0 \\ 0 & 0 & 0 & 1 \end{pmatrix}, \quad \text{and} \quad \Gamma_1 = \begin{pmatrix} 0 & 0 & -1 & 0 \\ 0 & 1 & 0 & 0 \\ -1 & 0 & 0 & 0 \\ 0 & 0 & 0 & 1 \end{pmatrix}.$$

is the Gram matrix of the basis.

It was proved in [8] that in this case all invariant two-dimensional subspaces contain the vector e_1 . Taking into account the structure of the Lie algebra, we come to the conclusion that $h(t)$ cannot be given by the matrix $e^{\mu t} F_2(t)$. Therefore, there is one more invariant isotropic direction, and in an appropriate basis (e_1, e_2, e_3, e_4) the group is given by the matrix $e^{\mu t} F_1(t)$. The subspace \mathcal{H} can be invariant only if $\mathbf{Q}(t) \equiv \mathbf{E}$.

Suppose that $\nu \neq 0$. In this case, according to [7], the two-dimensional ideals \mathcal{H} , \mathcal{L}_1 , and \mathcal{L}_2 are contained in the three-dimensional subspaces V_1 and V_2 , which are given by the equations $x_1 = 0$ and $x_2 = 0$, respectively. These subspaces are orthogonal complements to e_1 and e_2 , respectively, and have a common intersection $\langle e_3, e_4 \rangle$, so the ideal \mathcal{H} can only be contained in one of them. Let it be V_1 (figure 3). Then \mathcal{L}_1 and \mathcal{L}_2 are also contained in V_1 , since they have a nonzero intersection with \mathcal{H} . This means that the linear span of \mathcal{L}_1 and \mathcal{L}_2 is three-dimensional. We got a contradiction, since the linear hull of \mathcal{L}_1 and \mathcal{L}_2 must be four-dimensional. Consequently, the one-parameter group $h(t)$ consists only of identical transformations.

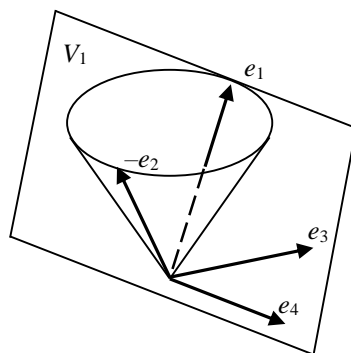


fig. 3

4. Conclusion. In this paper, we proved that four-dimensional Lie algebra $\mathcal{G}_4 = \mathcal{A}(1) \oplus \mathcal{A}(1)$ does not admit a one-parameter self-similarity group for any way of defining the Lorentz scalar product in it. Hence the corresponding connected Lie group $G_4 = A^+(1) \times A^+(1)$ equipped with a left-invariant Lorentzian metric cannot be a homogeneous self-similar Lorentzian manifold. The existing one-parameter autoisometry group for the algebra \mathcal{G}_4 allows us to construct in the future a one-parameter group of motions of the Lie group G_4 , leaving the identity of the group fixed.

REFERENCES

1. Подоксёнов, М.Н. Подобия и изометрии однородного многообразия группы Гейзенберга, снабжённой левоинвариантной лоренцевой метрикой / М.Н.Подоксёнов // Вестник Витебского государственного университета им. П.М. Машерова. – 2011. – № 5. – С.10-15.
2. Подоксёнов, М.Н. Самоподобные однородные двумерное и трёхмерное лоренцевы многообразия / М.Н.Подоксёнов // Вестник Витебского государственного университета им. П.М. Машерова, 2018. - №2(99). - С.14-19.
3. Подоксёнов, М.Н. Самоподобное однородное лоренцево многообразие трехмерной группы Ли / М.Н. Подоксёнов, А.Н. Кабанов // Наука – образованию, производству, экономике: Материалы XXIV(71) Региональной научно-практической конференции преподавателей, научных сотрудников и аспирантов, Витебск, 14 февраля 2019 г. / Витеб. гос. ун-т. – Витебск: ВГУ имени П.М. Машерова, 2019. – Т. 1. – 308 с. С. 18-20.
4. Подоксёнов, М.Н. Автоизометрии и автоподобия алгебры Ли $A(1) \hat{\mathbb{A}}^2$ / М.Н.Подоксёнов, В.В.Черных // Математические структуры и моделирование, 2020. - № 1(53). - С. 25-30.
5. Подоксёнов М.Н. Автоизометрии алгебры Ли $A(1) \hat{\mathbb{A}}^2$ / М.Н. Подоксёнов, А.К. Гуц // Наука – образованию, производству, экономике: материалы 72-й Региональной научно-практической конференции преподавателей, научных сотрудников и аспирантов, Витебск, 20 февраля 2020 г. Витебск : ВГУ им. П.М. Машерова, 2020. С. 27-29.
6. Alekseevski D. Self-similar Lorentzian manifolds / D.Alekseevski //Ann.of Global Anal.Geom.– 1985 – V.3, No.1, pp.59–84.
7. Подоксёнов М.Н. Инвариантные подпространства однопараметрической группы подобий пространства Минковского / М.Н. Подоксёнов, Е.А. Иванова // Математические структуры и моделирование. 2021. № 1(57). С. 41-45.
8. Черных В.В. Инвариантные подпространства одного специального класса преобразований / В.В. Черных // «Молодость. Интеллект. Инициатива». Материалы VIII Международной научно-практической конференции студентов и магистрантов. –Витебск, ВГУ имени П.М. Машерова. – 2020. – С. 36-38.

UDC 004.42

DEVELOPING A SYSTEM FOR AUTOMATING THE PROJECT-BASED DIDACTIC METHOD OF ACTIVE LEARNING IN THE EDUCATIONAL PROCESS

A. SHAFARENKO, D. GLUKHOV

Polotsk State University, Belarus

Nowadays, the application of the project method is becoming more and more relevant in the context of the Bologna Process, when the education system is oriented towards training specialists capable of self-learning and self-education throughout their life cycle. Automated systems that enable the organisation of project activities help to implement this method more widely and flexibly in the educational process. And this is one of the didactic methods that the MaCICT project (Modernisation of Master Curriculum in ICT for Enhancing Student Employability) is considering to improve the quality of education.

The aim of the study is to automate the process of project-based didactic method of active learning in the educational process and allow projects to be carried out remotely through the development of an appropriate information system.

Material and methods. The client-server model of the application was chosen to create the information system. For development of the server part, platform-independent programming language Java and Spring Boot framework, one of the most popular distributed application development technologies, are used. The MySQL relational database and Hibernate technology are used to store information.

The client side is a web page implemented using HTML markup language.

The FreeMarker templating engine is used to communicate between client and server. FreeMarker reads template files and combines them with Java objects to generate output HTML pages that are stored in FTLH files. By generating the user interface in FTLH files, we decouple the web pages' appearance from the program code. It becomes possible to modify the UI in a markup template file without having to change the program code.

The development environment used is IntelliJ IDEA.

Results and discussion. Project-based learning method is one of the effective methods of practice-oriented technology, which allows to rationally combine theoretical knowledge and its practical application to solve specific problems of the surrounding reality. It is fundamentally different from the classical method, as students independently set a goal and determine the ways to achieve it, search, select, summarise and analyse the information they need. The teacher acts as a consultant in this teaching method. Students' activities are organised as teamwork. The organisation of the project method of education is provided by a sequence of stages, which are limited by a specific time period (figure 1). The project method in education is used by teachers, but there are possible problems in the organisation of project-based learning methods in educational institutions: in case the teacher does not have the necessary knowledge and experience, also such projects are not scalable. Thus, there is a need for an automated system that would allow organising and supporting the project method in the educational process.

The information system under development allows to automate the organisation and remote execution of project method tasks. The application supports the division of users into three roles: administrator, teacher and student.

Common functions are implemented for each role:

- registration and authorisation in the system;
- activation in the system;
- viewing and editing your profile;
- subscribing and unsubscribing to other users' profiles for tracking purposes.

The following functions are available to the administrator:

- view the admin dashboard;
- view and manage users.

The following functions are available to the student:

- view all projects;
- view all your projects;
- viewing the project, the project teams, the stages of the teams on the project;
- changing the status of the project team stage (if the student is team captain);
- change of project team captains (if a student is team captain);
- sending the results of the project to the team at each stage;
- view your project statistics and history;
- viewing and chatting about their projects;
- viewing and communicating in team chats about their projects.

ProjectsMy projectsProjects panel

Projects / Project "INCUBATOR OF IDEAS"

Incubator of ideas

Pending

CHANGE STATUS ▾

CHAT ROOM

Delivery 18/05/2021, 22:00

Start 15/04/2021, 19:38

Objectives of the project

Develop a platform for the implementation of the most interesting and necessary ideas.

Project objectives

To study the specifics of the idea incubator sites, to make a comparative characteristic of software products of similar functional purpose, to choose design methods and tools, to design the product, to develop user interface layouts, to implement the MVP version of the product, to perform functional testing of the developed product, to develop accompanying documentation.

Description of the project

An idea incubator is a platform where users can implement their ideas together with like-minded people.

Project files

Project plan.docx

Project creator

Johns Elena

Project participants

Nash

CHAT ROOM

Smith Alex

Lopa misha

Koll

CHAT ROOM

Yapl evgen

Polk maria

Project stages

Analysis

Pending

CHANGE STATUS ▾

Delivery 16/04/2021, 12:00

Design

Pending

CHANGE STATUS ▾

Delivery 17/04/2021, 12:00

Development

Pending

CHANGE STATUS ▾

Delivery 20/04/2021, 12:00

Figure 1. – Project Method web page

The following actions are available to the teacher:

- view all projects;
- view all your projects;
- viewing the project, the project teams, the stages of the teams on the project;
- creating projects;
- creating the stages of the project;
- the creation of teams of project participants;
- changing project statuses, project phase, project team phase;
- the appointment and change of project team captains;
- assess the results of the project for the teams at each stage;
- view your project statistics and history;
- viewing and chatting about their projects;
- viewing and communicating in team chats about their projects.

The information system automates the project-based didactic method of active learning in the educational process.

Conclusion. The application of this automated system in the educational process will make it possible to organise and support the project method for training specialists ready for independent practice. The development of this information system is currently underway:

- establishment of a database of project methods in various disciplines;
- refactoring and optimising the application code;
- functionality testing;
- increasing the security of the application through protection against internet bots, hashing and creating strong passwords.

It is also planned to conduct user testing of the application and investigate the possibility of using other technologies to develop the client side of the application.

The application can be used both within the MaCICT project and in other training courses

REFERENCES

1. Polat, E.S. Method of projects / E.S. Polat // Method of projects: scientific-methodical collection / BSU, Centre for Educational Development Problems. - Minsk: RIBSH of Belarusian State University, 2003. - – C. 39-47.
2. Reshetka, V.V. Project-based learning method as a means of implementing practice-oriented technology / V.V. Reshetka // Vocational Education in Russia and abroad. - – 2013. - №2 (10). - – C. 83-36.
3. Aslyalieva, S.G. Application of the project method of learning - one of the ways to improve learning efficiency / S.G. Aslyalieva // Actual scientific research in the modern world. - – 2017. - – №1-1 (21). - – C. 32-34.
4. Yafizova, R.A. Application of project method of learning as a means to improve the quality of teaching / R.A. Yafizova // Science and modernity. - – 2011. - – №10-1. - – C. 265-268.
5. The Best Portal to Learn Technologies [Electronic resource]. - Access mode: <https://www.javatpoint.com/> - Access date: 12.04.2021.

THE DEVICE FOR DETERMINING THE DIRECTION OF THE INFRARED RADIO WAVES ARRIVAL FROM A BRIGHTLY CONTRASTING OBJECT

A. CHERNYAVSKII, V. YANUSHKEVICH

Polotsk State University, Belarus

An analysis of radar methods. Various ways of viewing are mentioned by moving the directional beam of a radar antenna. A review of the main physical phenomena directly affecting the radar. An assessment of the most promising parts of the device to accomplish the goal of the study. The characteristic of the main parameters of the key elements of the device is shown. The proposed parameters for the technical performance of this device. The results of the study can be used to develop a device for determining the direction of arrival of infrared radio waves from a brightly contrasting object.

Determining the direction of physical quantities arrival is one of the most important aspects in radar systems. Radiolocation is a field of science and technology that combines methods and means of locating (detecting and measuring coordinates) and determining the properties of various objects using radio waves. Radionavigation is a close and somewhat overlapping term, but in radio navigation an object plays a more active role, the coordinates of which are measured, most often this is the definition of its own coordinates. The main technical device radar - radar station (radar). Distinguish active, semi-active, active with a passive response and passive radar. Radars differ in the range of radio waves used, the type of the probing signal, the number of channels used, the number and type of measured coordinates, the installation location of the radar.

There are two types of radar:

1. Passive radar is based on receiving the object's own radiation;
2. With active radar, the radar emits its own probing signal and receives it reflected from the target. Depending on the parameters of the received signal, the characteristics of the target are determined.

Active radar is of two types:

With an active response - the facility assumes the presence of a radio transmitter (transponder), which emits radio waves in response to a received signal. The active response is used to identify objects, remote control, as well as to obtain additional information from them (for example, amount of fuel, type of object, etc.);

With a passive response - the request signal is reflected from the object and is perceived at the receiving point as a response one.

To view the surrounding space, the radar uses various ways of viewing by moving the directional beam of the radar antenna:

- circular;
- sector;
- overview of the helix;
- conical;
- in a spiral;
- "V" review;
- linear.

In accordance with the type of radiation radar are divided into:

- radar continuous radiation;
- pulsed radar.

Radar is based on the following physical phenomena:

- radio waves are scattered by electric inhomogeneities (objects with other electrical properties that differ from the properties of the propagation medium) encountered on the path of their propagation. In this case, the reflected wave, as well as the radiation of the target itself, makes it possible to detect the target;
- at large distances from the radiation source, we can assume that the radio waves propagate in a straight line and at a constant speed, due to which it is possible to measure the distance and angular coordinates;
- the frequency of the received signal differs from the frequency of the emitted oscillations due to the mutual displacement of the receiving and emission points (the Doppler effect), which makes it possible to measure the radial velocities of the target moving relative to the radar;
- Apassive radiolocation uses the radiation of electromagnetic waves by the observed objects, it can be thermal radiation characteristic of all objects, active radiation created by the technical means of the object, or spurious radiation created by any objects with working electrical devices.

The purpose of this work is to develop a device for determining the direction of arrival of the infrared radio waves from a brightly contrasting object [1-4].

Principle of operation of the device. The diagram contains 4 infrared receivers, they work in pairs. Those. each pair is responsible for turning the motor on its axis. With the passage of IR radiation through the lens, it will be focused at a certain point. If the spot does not uniformly illuminate all the plates, then a potential difference will occur and a pulse is generated at the receiver output, which is fed to the motors. If it is positive, then the motor moves in one direction, and if it is negative, then in the other. By the same principle, the second pair of the receiver and the motor works, the only difference is that each pair drives the motor moving along its axis, one along the X axis, and the second along Y.

Simultaneously with the work of the motors, the circuit responsible for the derivation of coordinates works. The MPU6050 chip is the main element of the GY-531 module. It has an accelerometer, a gyroscope and a temperature sensor. During the movement of the gyroscope and accelerometer, the information received is stored in the registers of the chip. The transfer of the value to the microcontroller is carried out via the I2C interface.

The microcontroller is used to control and transmit signals to other parts of the circuit. After receiving information from the sensors, the microcontroller displays data on a liquid crystal display, which has 4 lines of 20 characters each. The screen displays information received and converted from the MPU6050 chip. The first line contains the values along the three axes of the accelerometer, the second values along the three axes of the gyroscope, the third temperature, the fourth line on the left, the deflection angles according to the accelerometer and the right rotation of the Z axis according to the gyroscope. The values of the fourth row are calculated by the microcontroller itself. Also on the diagram there are 6 LEDs that light up depending on the position of the GY-531 module on the Y axis.

REFERENCES

1. Erickson, John; «Radiolocation and the air defense problem: The design and development of Soviet Radar 1934-40», Social Studies of Science, vol. 2, pp. 241—263, 1972.
2. Ширман Я. Д., Голиков В. Н., Бусыгин И. Н., Костин Г. А. Теоретические основы радиолокации / Ширман Я. Д. — М.: Советское радио, 1970. — 559 с.
3. Бакут П. А., Большаков И. А., Герасимов Б. М., Курикша А. А., Репин В. Г., Тартаковский Г. П., Широков В. В. Вопросы статистической теории радиолокации. — М.: Советское радио, 1963. — 423 с.
4. Янушкевич В.Ф. Метрология и радиоизмерения 2010 2 изд / В.Ф. Янушкевич // Полоцкого государственного университета. — Минск — 8 с. — Деп. в БелИСА 12.06.10 г. 2 изд. — С. 11.

ROC ANALYSIS AS A BINARY CLASSIFICATION TOOL

V. DASHKO, P. IVANOVA, V. LIVINSKAYA
Belarusian-Russian University, Mogilev, Belarus

The article presents a study that demonstrates the possibility of applying the method of space in the analysis of the results of clinical research.

The main purpose of this work was to identify statistically significant differences in the indicators of the assessment of the hemodynamics of the liver using reohepatography (RGG) of patients who have various pathologies and undergo treatment in the regional hospital of Mogilev [1]. This technique is based on fixing changes in the resistance of live tissue in an alternating electric field of high frequency. With the use of the Rheo-Spectrum (Neurosoft) software, certain physical characteristics of the rheographic curve (Figure 1) describing the dynamics of resistance of live tissue for a specific time interval (Table 1) were obtained.

Table 1. – Parameters of the rheographic curve

The RRG parameter	Designation
amplitude of the arterial part of the wave	A_{art}
time of pulse wave propagation from the heart	Q_x
Systolic maximum. Rheograms	A_{syst}
Time of the rising part of the wave	α
rapid blood filling time	α_1
slow blood filling time	α_2
total systole time	T_{total}
duration of catacrota	T_{cat}

As factors, we considered various parameters recorded by the device, as well as, calculated by the authors, the area under the rheographic curve (RC) as a single integral indicator. Using the R language, a dataset of 9 columns was formed from separate files in text format containing information about each patient, eight of which were physical parameters of the curve, and the ninth was responsible for the patient's belonging to one of 2 groups: patients with one of 3 pathological conditions: multiple organ dysfunction syndrome (SPOD), patients with liver cirrhosis, patients with chronic diseases of the stomach and pancreas (gastro), and the control group - practically healthy. The assignment of a patient to one of the two groups is described by a binary variable that takes two values: 1-the patient is sick, 0-the patient is healthy.

Table 2 shows the AUC values obtained by analyzing the results of measurements of the resistance of living tissue in a high-frequency alternating electric field.

Table 2. –ROC analysis results

Test Variable	Area	Std. error	Type 1 Error	Asymptotic 95% Confidence Interval	
				Lower Bound	Upper Bound
Area of RC	0,763	0,053	0,000	0,660	0,867
α_1	0,598	0,061	0,138	0,478	0,719
α_2	0,632	0,059	0,047	0,517	0,746
T_{cat}	0,663	0,058	0,014	0,550	0,776
RI	0,690	0,061	0,004	0,570	0,810
DIA	0,584	0,061	0,204	0,465	0,703
V_{max}	0,801	0,046	0,000	0,710	0,892

Analyzing the results obtained, it is concluded that the area under the rheographic curve can serve as the best predictor of pathology.

According to the available parameters, using the VBA macro, the areas under the curve were calculated for each patient using the area method:

Significant differences in the groups were identified using the nonparametric Mann-Whitney statistical test. This test is intended to compare two independent groups of a small amount of quantitative data.

The method is based on determining whether the zone of overlap of values between two variation series (a ranked series of parameter values in the first sample and the same in the second sample) is small enough. The U-test is suitable for comparing small samples: each of the samples must have at least 3 attribute values. The condition for applying the Mann-Whitney U-test is the absence of matching attribute values in the compared groups (all numbers are different) or a very small number of such matches.

The lower the value of the criterion, the more likely it is that the differences between the parameter values in the samples are reliable [2].

The result of testing the hypothesis that there are no differences in the selected groups for all parameters of the rheographic curve is presented in table 3.

Table 3. – No-Difference Hypothesis Tests

Rheographic curve parameters	U	Z	p-level
Q_x , sec	785,5000	-0,499723	0,617271
α_1 , sec	644,0000	1,773791	0,076099
α_2 , sec	613,0000	2,052916	0,040082
T_{total} , sec	585,5000	2,300526	0,021419
T_{cat} , sec	579,5000	2,354550	0,018546
RI, c.u.	391,0000	4,051808	0,000051
DIA, %	693,5000	1,328092	0,184149
V_{max} , Ohms/s	339,5000	4,448602	0,000009
V_{avr} , Ohms/s	323,0000	4,599324	0,000004
Area under curve	314,0000	4,745117	0,000002

Comparing the values of the error of the first kind of p-level with the value of 0.05, we conclude that the best factor separating the groups can be the integral indicator of the area under the curve.

To further test the possibility of using the area under the rheogram as a predictor of the patient's condition, the ROC analysis was performed. During the ROC-analysis for the factor that acts as a classifier (in our case, the area under the rheographic curve) special metrics are calculated, which are the characteristics of the quality of the partition - sensitivity (the relative index of correctly classified positive cases) and specificity (the proportion of incorrectly classified negative cases), according to which the ROC-curve is constructed.

The ROC-analysis method assumes that for each of the ordered values of the factor that determines the division into two groups (for example, whether the patient is ill or not), the proportion of truly positive cases (Se or sensitivity) and the proportion of truly negative cases that were correctly identified by the model (specificity or Sp) are calculated. Next, for all the calculated values, a ROC-curve is constructed in the coordinate system, in which the values of $1-Sp$ are plotted along the abscissa axis, and the values of Se are plotted along the ordinate axis. To quantify the classification results, the area (AUC) under this curve and the 95% confidence interval are calculated for each factor. The split is considered qualitative if the value 0.5 does not fall into the confidence interval, and the AUC itself is >0.5 . Figure 1 shows the ROC-curve for the predictor of area under the rheographic curve.

The ideal diagnostic test should have an r-shaped characteristic curve passing through the upper-left corner, in which the proportion of true positive cases is 1, and the proportion of false positive cases is 0. The closer the characteristic curve passes to the value (0; 1), the higher the effectiveness of the test. A test in which the characteristic curve passes closer to the diagonal of the graph and does not resemble an r-shape is useless. In our case, the diagnostic test is effective, because it resembles the letter "r", and is also located above the diagonal of the graph.

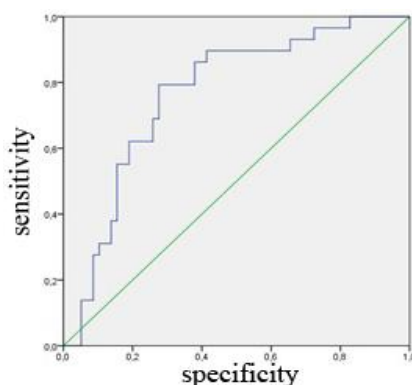


Fig. 1. – Roc-curve for the indicator of area under the rheographic curve as a predictor of disease

Quantification of the Roc-curve (AUC and 95 % interval calculated for the area by formula (1) is presented in Table 4.

$$SE(AUC) = \sqrt{\frac{AUC(1-AUC) + (n-1)(Q_1 - AUC^2) + (m-1)(Q_2 - AUC^2)}{n \cdot m}}, \quad (1)$$

For multiplicity it is indicated:

$$Q_1 = \frac{AUC}{2-AUC};$$

$$Q_2 = \frac{2 \cdot AUC^2}{1+AUC}.$$

Table 4. – Quantification of the Roc-curve

Area	Std. error	Asymptotic 95% Confidence Interval	
		Lower Bound	Upper Bound
0,765	0,053	0,662	0,869

REFERENCES

1. Точи́ло С.А. Интегративный показатель состояния артериального печеночного кровотока у пациентов при критических состояниях / С.А.Точи́ло, А.Л. Липницкий, А.В. Марочков, А.А. Антипенко, О.Л.Борисов, В.А. Ливинская //Вестник Витебского государственного медицинского университета. 2019. Т. 18. № 3. С. 52-60.
2. Библиотека постов MEDSTATISTIC об анализе медицинских данных [Электронный ресурс]. - Режим доступа: <https://medstatistic.ru/methods/methods2.html>. - Дата доступа: 28.03.2021.

UDC 621.3

PRESENT SITUATION AND DEVELOPMENT OF PHOTOVOLTAIC POWER GENERATION

LIU ZHENGMING

Polotsk State University, Belarus

Due to the global energy and environmental problems, photovoltaic power generation and other new energy generation types have been vigorously developed. This paper analyzes the current situation and development trends of photovoltaic power generation, and prospects for the future development.

a. Significance of photovoltaic power generation

In order to cope with the global energy crisis and increasingly serious environmental problems, countries all over the world are trying to explore the path of green and sustainable development of energy. The formal signing of the Paris Agreement in April 2016 demonstrates the urgency of action on environmental issues and the determination of countries to address them. Solar energy, as the representative of renewable energy has been vigorously developed. Solar energy, as an important renewable energy source, mainly includes photovoltaic and photothermal applications.

b. Current situation of photovoltaic power generation

Since 2011, with China, Japan and the United States as the lead, countries all over the world have strengthened their layout in the field of photovoltaics, and the photovoltaic market has developed rapidly. According to the International Renewable Energy Agency (IRENA), global installed capacity grew steadily between 2011 and 2020, reaching 702,909 MW in 2020, an increase of 20.32% year-on-year.

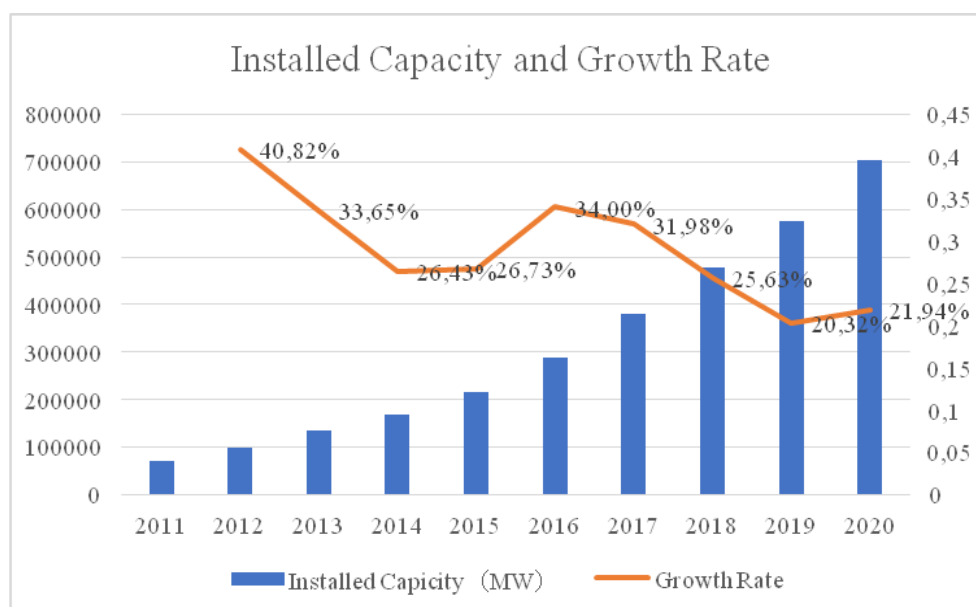


Fig. 1. – installed capacity and year-over-year growth rates in 2011-2020

Judging from the distribution of global photovoltaic installed capacity, Asia is the main market for photovoltaic industry. In 2020, Asia accounted for 45.95 percent of global installed capacity, followed by Europe with 21.77 percent.

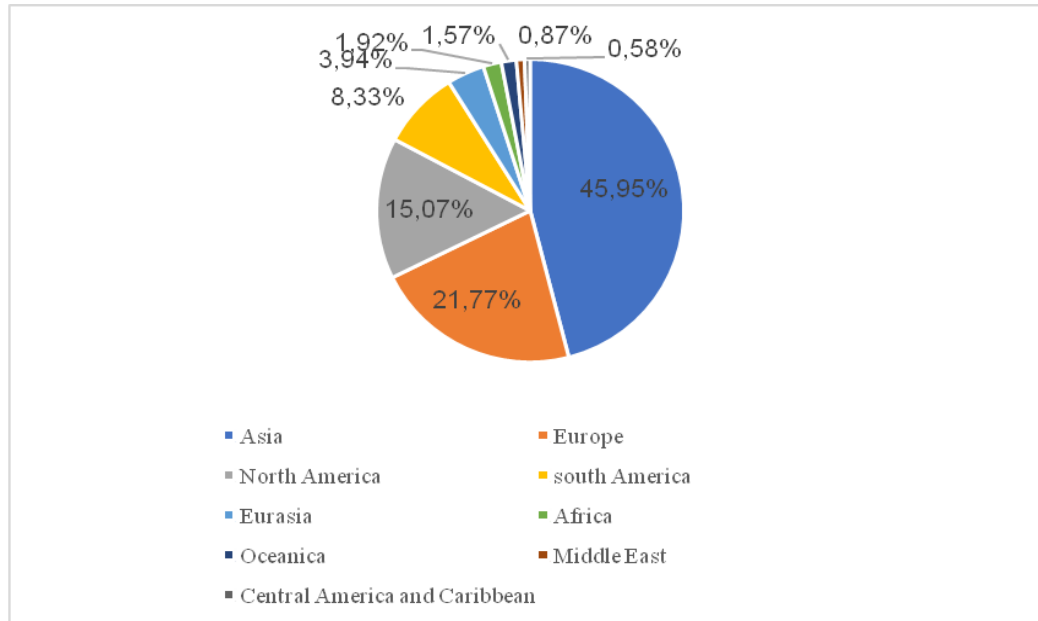


Fig. 2. – Percentage of installations in each region in 2020

In terms of countries, the top three major PV installed capacity in the world in 2020 are China, the United States and Japan.

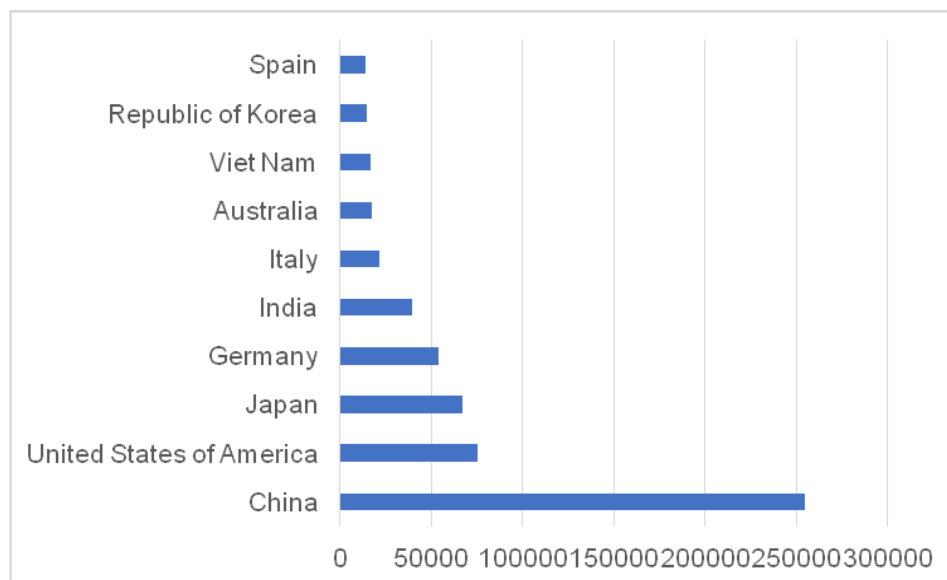


Fig. 3. – Photovoltaic installed capacity in major countries around the world by 2020

c. Development trend of photovoltaic power generation

From distributed generation to centralized power plant

The centralized large and medium-sized grid connected solar power station is the centralized infrastructure large and medium-sized solar power station. The power generation is immediately allocated to the public power grid, and the high-voltage transmission system software is connected to provide long-distance load, which can control the cost and reduce the transportation loss. The more large-scale photovoltaic power stations operate, the lower the cost of photovoltaic power generation system software is.

Light storage integrated power plant

For the photovoltaic power plants with energy storage technology stage, the integrated management and control should be carried out. Considering the maximum profit of active power output, "peak shaving and valley filling" should respond to the requirements of power grid production and dispatching, so as to ensure the power grid production and dispatching regulations immediately. The application of energy storage system can reduce the impact of battery charging on power grid and improve the quality of power grid as much as possible.

Technical application of cloud storage, cloud computing technology, digital twin, Internet big data, etc.

The application of new information technology can help photovoltaic power plants to realize intelligent system, assist photovoltaic power plants to realize intelligent operation and maintenance supervision, show the analytic function of power generation prediction and analysis, reduce the difficulty coefficient of grid connection, and improve the efficiency of power generation.

d. Summary

The fourth scientific and technological revolution will be carried out in an all-round way, and the technologies of green energy and Internet of things led by photovoltaic power generation are developing in an all-round way. According to the modern Internet of things, artificial intelligence technology and data analysis technology, we can realize the centralized operation and maintenance service of a variety of power energy including photovoltaic power generation, and create a smart power energy ecological chain. In the future, social development will build a new and upgraded energy Internet of things management system, into a low-carbon environmental protection and even carbon free period.

REFERENCES

1. Li Yankun, Zhou Rongbin. Current situation and development prospect of photovoltaic power generation [J]. Modern industrial economy and informatization, 2021,11 (01): 53-54.
2. Zhao Jianhua, Zhao Leiqing. Development status and Prospect of grid connected photovoltaic power generation and related technologies [J]. Science and technology wind, 2019 (01): 202.
3. Zhou Jingyu, Yang Pinghua, Zhao Zhipeng. Development status and trend analysis of photovoltaic power generation equipment in China [J]. Engineering construction and design, 2018 (22): 84-85.
4. Geng Na. Analysis of current situation and development prospect of solar photovoltaic power generation [J]. Modern economic information, 2018 (17): 368.

OPTICAL PROCESSORS

N. SHNIPOVA, V. YANUSHKEVICH

Polotsk State University, Belarus

It is well known that in many fields of science the main task is the processing of video information. One of these areas is exploration of natural resources of the Earth from space. To illustrate the volume of this information and the speed of its receipt, it is enough to show that only one image obtained with the multi-zone camera and covering an area of $100 * 100$ km with a resolution of 10m, contains approximately 1000 Mbit of information. Daily hundreds of such pictures are sent to Earth. To transmit this information, they serve digital radio lines operating at a speed of 10-100 Mbit / s and more.

This necessitated the development and creation of optoelectronic systems. registration, storage and processing of space video information. Optical methods make it possible to produce both analog and digital information processing. A characteristic feature of optical analog computing machines is that all elements of information on inputs are converted to the resulting output signal at the same time.

Thanks to this, huge productivity is achieved - more than $1.0e13$ op / s. However, such computers, as well as electronic analog machines have limited computational accuracy - of the order of 1%.

Interest in digital optical information processing at the initial stage was caused by the need to overcome the problems faced by analog optical computing: low accuracy of calculations and lack of flexibility inherent in electronic technology.

The need to create such computing systems is dictated by the possibility of overcoming a number of fundamental shortcomings inherent in von Neumann computers, which limit the further increase in their efficiency and productivity. Therefore, the development of such systems should be considered as one of the alternative ways of creating super-efficient computing systems along with the multiprocessor supercomputers of parallel operation being developed at present.

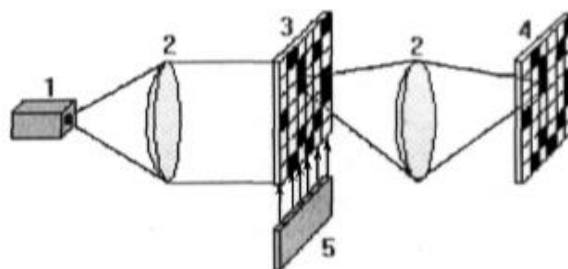
Systems for entering information into an optical processor

There are two main ways of forming images and entering them into the optical processing channel, which provide a sufficiently high input speed.

The first method is designed to input information coming in the form of a sequence of electrical or optical signals through several input channels at once. It is carried out by means of a controlled matrix transparency (SPMS - space-time light modulator), which forms an image line by line and stores information until it is read. A distinction is made between electrically and optically controlled transparencies.

The second method is designed to enter algorithms for solving problems, instructions, constants. This data is stored in permanent optical memory. Information in optical memory is stored in separate cells of a flat matrix in the form of holograms. For reading, a laser radiation addressing device is used, directing the beam to a cell with a given number. The addressing device is a multi-position laser beam deflector with arbitrary addressing. A two-dimensional image read from a hologram is fed to a transparency with an optical input and modulates its transmission or reflection function. The entrance to the banner is carried out simultaneously through all optical channels.

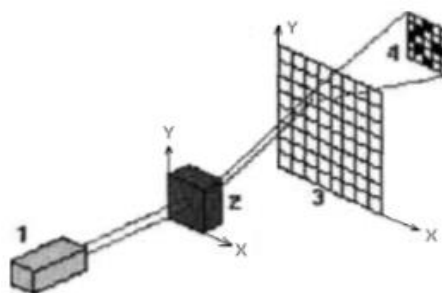
Entering information into an optical information processing device with using an electrically controlled transparency



1-laser; 2-lenses; 3-electrically controlled transparency; 4-input of the next element; 5-banner control device

Fig. 1. – Entering information into an optical information processing device using an electrically controlled transparency

Entering information into an optical information processing device using topographic storage



1-laser; 2-position baffle; 3-mattress holograms; 4-input of the information processing device

Fig. 2. – Entering information into the optical processing device information

Controlled transparencies serve for spatial modulation light beam in amplitude, phase or polarization and are used in data input-output systems.

According to the method of controlling the modulation of the light beam, electrically and optically controlled transparencies are distinguished. Both types can perform discrete or analog modulation of the light beam. In the first case, the transparency must have a nonlinear characteristic, in the second, on the contrary, it must have a linear dependence of the optical properties of the element on the control signal.

The operation of controlled transparencies can be based on various physical phenomena: electro-optical, acousto-optical, magneto-optical. Managed banners can be roughly divided into the following types:

1) Electrically operated transparencies:

- a) with electron beam addressing;
- b) with voltage addressing:
 - liquid crystal;
 - based on electro-optical ceramics;
 - on ferromagnetic materials;
 - on monocrystalline ferroelectrics;
 - acousto-optic devices.

2) Optically controlled transparencies.

The most widely used among various types of optical processors are optical correlators. There are many different options for constructing correlators, among which there are two most commonly used:

- correlator with the frequency plane;
- correlator with simultaneous transformation.

A simulcast correlator has several advantages over a frequency plane correlator:

- less tight tolerances for the accuracy of the installation of elements, since the filter obtained as a result of recording is illuminated by a flat wave;
- contrasting interference pattern and, as a consequence, good modulation of all components in the spectrum of spatial frequencies.

The correlator with simultaneous transformation is preferably used in cases where the input functions are received in real time. It should be noted that an increase in the recognition reliability can be achieved due to preliminary processing of the original image, for example, contouring, since the contour lines for most images have the greatest information content. [1]

REFERENCES

1. Янушкевич В. Ф. Устройства оптической обработки сигналов: Учебно-методический комплекс / В.Ф. Янушкевич; ПГУ.- Новополюцк, 2008.- 253 с.

THE CONCEPT OF DEVELOPING A COMMUNICATION SERVICE FOR STUDENTS, ADMINISTRATION AND POTENTIAL EMPLOYERS

U. BAKLAN, I. BURACHONAK
Polotsk State University, Belarus

This article discusses the development of a communication service for students, administration, and potential employers. A conceptual solution based on data processing and transmission technologies is proposed using the following technologies: Apache Spark, Apache Kafka, Apache Hadoop, PostgreSQL. It describes architectural approaches and solutions that increase the performance, scalability and flexibility of software for the implementation of the presented project.

The modern model of obtaining higher education in our country is collective learning. This is based on the fact that there are more students than teachers. Such a system has its advantages, but the main disadvantage is that it does not provide an opportunity for the student to focus on a specific direction, and as a result, the university graduates a specialist with a profile, covering as wide range of vacancies as possible. However, having received such a specialist, the employer has to spend additional time and money to develop their skills depending on the position. The existing education model can be improved by incorporating an element of personalized learning and automating it. The purpose of automation is to simplify teacher's interaction with a multitude of students while maintaining the element of receiving individual education, which is undoubtedly relevant.

Thus, there is a need for an automated communication system for students, administration, and potential employers, represented by the main functional subsystems (see fig. 1). The system being developed should take upon itself the solution of some of the tasks of the student and the teacher, and subsequently of the potential employer. Moreover, from student's perspective, the system should allow the student to prioritize areas; monitor progress; record achievements in one or another area as a result of which a learning map will be formed and the graduate will be able to find a position that is suitable for the acquired knowledge and skills. When it comes to teachers, the system should provide an opportunity to analyze each student's progress; create individual tasks and plans based on notes; monitor the progress of one student or the whole group, which will allow partial individual training with an acceptable amount of effort and time. The employer, on the other hand, should be able to monitor the students of interest by reviewing the learning maps of a particular person, as well as the ability to adjust the training plan at the later stages of the educational process, so that after graduation the specialist is immediately ready to work in a particular position.

The developed application has no physical load restrictions. The application can generate data and metadata in any amount. It allows you to track user behavior, service, prioritize the selection of subsequent sub-projects and analyze trends that are developed within the service.

There are three main principles of big data processing [1]:

- horizontal scalability (increase in speed and volume due to increased hardware);
- fault tolerance (failure of a certain percentage of servers does not affect the result);
- data locality (the distribution of data to each machine allows you not to lose data in case of server failure).

An example of processing large amounts of data can be ClickStream. Clickstream is a user clicks stream grouped by the user's session ID. Since the amount of data in the first stages is not huge, processing will be carried out on a cluster with a single node (this is any computer connected to the blockchain network) and all clickstream events [2] will be transmitted to the analytical system using a message broker - Apache Kafka.

Apache Kafka is a message manager that is implemented in the Java platform. Kafka has topics in which publishers enter the text of their messages and there are subscribers in threads who read these messages. All messages, without exception, are written to disk during the dispatching process.

The immediate broker message handler is an application written in Python using the Spark framework.

Spark is an Apache project that is positioned as a tool for "lightning-fast cluster computing" [3]. The project is being developed by a thriving free community and is currently the most active of the Apache projects. Spark provides a fast and versatile data processing platform. Compared to Hadoop, Spark accelerates programs more than 100 times in memory, and more than 10 times on-disk [4]. Spark was chosen based on the fact that there is a growing community of developers preferring it, it is provided with support for multiple systems and programming languages and most of the built-in elements. It allows rapid risk assessment, benchmarking, routine checks and analyzes financial and economic indicators.

In our case, the main task of the analytical service is to generate a behavioral "map" of the user, which will subsequently allow analysts and project managers to think through a product development strategy based on the user's behavioral data in a human-readable format.

To reduce the load on the system, it is planned to use Spark Streaming with Batch-mode, which will process streaming data in small batches (batches), which allows to reduce the one-time load and be able to dose the load on the cluster.

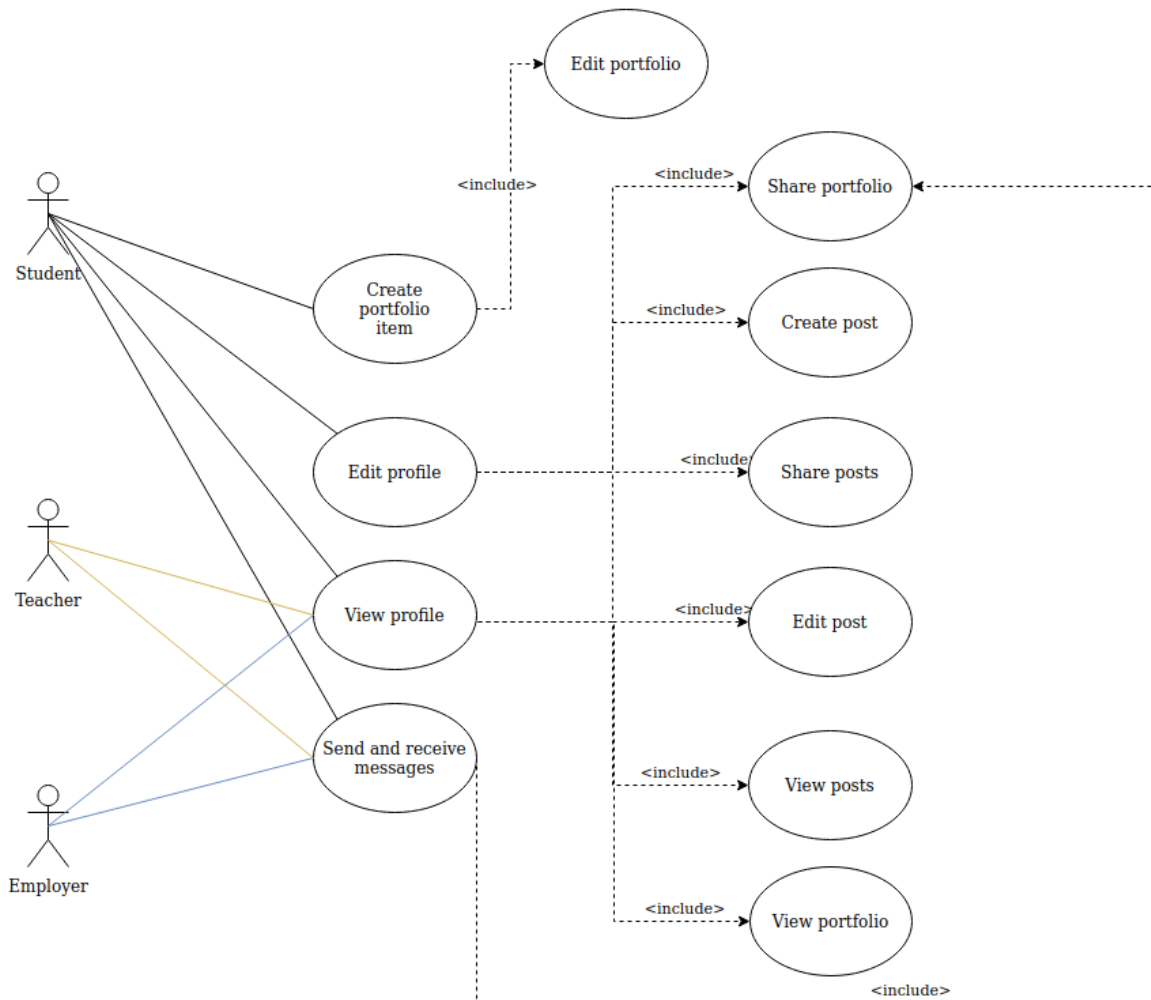


Fig. 1. – Application subsystems

As the application is initially planned to be used by a limited number of users, a minimal configuration with one master node (the node that manages the entire cluster) is sufficient for an analytics cluster. It monitors the other nodes and distributes the load between them) and one worker node (node on which containers are deployed and run), as well as the minimum level of data replication in Kafka. After processing the Spark data, the aggregated data is sent to PostgreSQL for further accessibility from a web application or for subsequent business analysis. The general architecture of data processing in the application is shown in fig. 2.

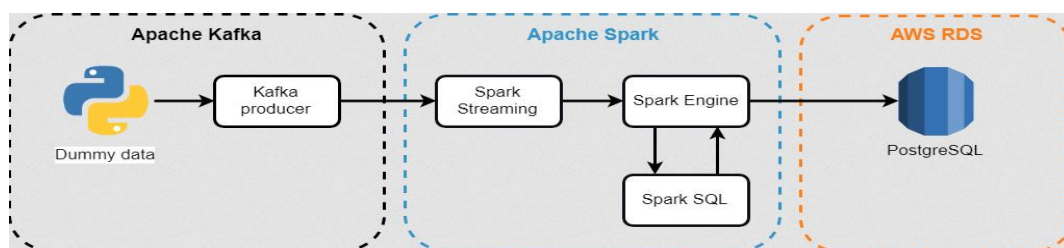


Fig. 2. – Data processing architecture

In this example of analytical processing, data loss is allowed, since a single click or a small amount of it is not critical.

Thus, the use of the presented technology stack will allow the creation of a system that is capable of processing any amounts of data, depending on the requirements and financial constraints. To further increase the amount of data or processing speed, it is enough to expand the cluster, rather than rewrite the existing code. Using the Python language allows writing a code without thinking about the intricacies of the language, which allows to speed up the development process and subsequent refinement.

The developed automated system for communication between students, administration and potential employers will allow:

- to intensify the students' activities in maintaining profiles and of all types of activities performed in the learning process (keeping their progress log allows the student to become flexible in the context of constantly evolving technologies);
- to monitor by the administration of the university the career development for each student during the educational process and the formation of their professional skills and competencies;
- to simplify the process of finding and hiring employees from university graduates for employers;
- and most importantly, based on the collected data (in our case, with the use of the presented technologies, their volume is not limited), to make forecasts of orders for personnel training for certain sectors of the country's national economy and take into account changes in the labor market, avoiding disproportions between supply and demand.

REFERENCES

1. Habr. Habr.com [Electronic Resource] / Big Data, 2021. – Access mode: <https://habr.com/ru/post/267361>. – Access date 02.03.2021.
2. Clickstream. Clickstream.cc [Electronic Resource] / Clickstream, 2021. Access mode: <https://clickstream.cc>. – Access date: 02.03.2021.
3. Wikipedia. Apache Spark. [Electronic Resource] / Wikipedia. – Access mode: https://ru.wikipedia.org/wiki/Apache_Spark. – Access date: 03.03.2021.
4. Wikipedia. Apache Hadoop. [Electronic Resource] / Wikipedia. – Access mode: <https://ru.wikipedia.org/wiki/Hadoop>. – Access date: 06.03.2021.

UDC 620.92

REDUNDANT CONTROL METHOD FOR YAW OVERLOAD PROTECTION OF WIND TURBINE

ZHENG JIEBIN, V. CHERTKOV

Polotsk State University, Belarus

This article first describes the yaw control method of the wind turbine, then analyzes the yaw control strategy of the wind turbine, and finally discusses the reasons for the yaw overload and the redundant control method of overload protection.

Introduction. By the redundant control of the yaw overload protection, extreme wind conditions can be effectively avoided. After the yaw system returns to normal, the yaw can ensure the continuous power generation of the wind turbine. At the same time, the fault shutdown will be performed when the wind direction deviation is large. To ensure the safety of wind turbines verified by the wind farm, the yaw overload redundancy control method can effectively protect the yaw equipment, reduce the number of downtimes, increase power generation revenue, and reduce operation and maintenance costs [1].

Yaw control method of wind turbine. *Rudder steering and yaw control device (Passive wind yaw control).* This yaw control method belongs to passive yaw to the wind, and its steering device is a tail rudder that makes the wind-facing surface of the wind turbine always face the direction of the incoming flow through the tail rudder swinging with the wind. Most of these wind turbines are small wind turbines, similar to the wind measurement towers used in weather stations, and the area of the tail rudder and the swept area of the wind turbine must reach a certain degree to meet the accuracy of wind. The characteristic of this yaw method is that it does not require electric or manual control.

Side wind wheel direction adjustment device (Passive wind yaw control). This kind of steering device is to install 1 to 2 small wind wheels on the side of the nacelle. The steering axis of the fan is perpendicular to the main shaft of the wind wheel. When the wind direction deviates from the main wind wheel, the side wind wheel will be blown by the wind, and the nacelle is rotated through the worm gear mechanism until the wind direction is perpendicular to the side wind wheel axis. This yaw device requires that the inclined position of the side wind turbine blades must enable the nacelle to rotate in the correct direction. The side wind wheel direction adjustment device can be used for wind turbines in the upwind direction and in the wind turbines in the downwind direction. The advantage of the wind wheel against the wind is the torque connection between the nacelle and the tower, and the yaw moment of the nacelle does not produce torque vibration excitation. The disadvantage is that when the speed of the wind wheel is high, the load is increased due to the gyro moment.

Active wind yaw control. Active wind yaw control, also known as automatic wind yaw control, mainly uses external wind speed and direction sensors to collect wind speed and wind direction signals, after it calculates the deviation angle, then it uses an electric or hydraulic drive device to make the nacelle according to the required yaw angle and the direction is deflected. This control method is more suitable for large-scale megawatt wind turbines.

The active (electric) yaw system generally includes a wind vane that senses the wind direction, a yaw motor, a yaw star gear reducer, a yaw counter, and a twisted cable alarm device. Its working principle is as follows: the wind speed and direction sensor send the collected signal to the main control system of the wind turbine, and after processing by the controller, it sends a clockwise or counterclockwise rotation command to the yaw motor. Generally, in order to reduce the gyro torque during yaw, the motor after the speed is decelerated by the gearbox, the yaw moment is applied to the large ring gear of the slewing body to drive the wind wheel

to yaw against the wind. After the wind is completed, the controller sends a stop command and the yaw process ends. In addition, this type of wind turbine must have the ability to protect the yaw torsion cable, have a yaw counter to record the total deflection angle, and automatically untwist the cable when the limit of the twisted cable is reached.

Wind turbine yaw control strategy. *Weather vane control method.* The current mainstream yaw control technology is mostly a control method based on wind direction sensor (wind vane), also known as VC control, which detects the direction of the incoming wind and wind through a mechanical or ultrasonic wind direction sensor installed at the tail, and sends the signal to the main control. The system calculates the deviation between the current cabin position and the wind direction through the main control system, and then outputs a yaw angle signal to the yaw actuator to achieve yaw control. The traditional VC yaw control method is characterized by simple control technology, strong practicability, low maintenance cost, and can basically meet the yaw control needs of large and medium-sized wind turbines in terms of wind accuracy.

Power control HC algorithm. Although the traditional wind vane control and yaw control method is simple, but due to the influence of wake and wind turbulence, the accuracy of the wind needs to be improved. When the wind direction difference is $\pm 15^\circ$, the wind vane will fail to distinguish the wind, and the wind direction sensor is used as the method of distinguishing wind is not efficient.

Compared with the traditional algorithm of power control, the HC algorithm improves the utilization rate of wind energy from the perspective of power maximization. At the same time, due to its reasonable absorption of wind load, it also increases the mechanical life of the wind turbine.

Improved V-HC algorithm program design. Although the HC algorithm can track the best power value, when distinguishing the direction of rotation: first, turn it counterclockwise or clockwise. Then see whether the direction is correct according to the power change. This step requires a long distinguish time and running time for large MW-class wind turbines.

When the wind speed is lower than the rated wind speed, the wind speed change is more complicated, and the HC algorithm is applied within $\pm 5^\circ$:

1) When the wind direction difference is greater than 15° , start the yaw, calculate the yaw direction according to the wind direction signal given by the wind vane and the current cabin position, and control the wind turbine to move in the windward direction;

2) During the yaw process, compare the feedback value of the cabin position with the wind direction signal. When the difference is less than 5° , record the power change and monitor the wind speed change. Set the calculation step to 1s.

When the wind speed is greater than the rated wind speed, the wind is higher, the airflow is relatively stable during the movement, and because the power has reached the rated power, the maximum power point can no longer be tracked. At this time, the HC algorithm is no longer needed, and the VC can be used to control the yaw. Meet the wind requirements of the unit [3].

Reasons for yaw overload. Yaw overload protection is an active power-down protection for the yaw motor protection which can effectively prevent the temperature of the yaw motor winding caused by overload, overcurrent, etc., which reduces the winding insulation life and reduces the service life of the yaw motor. Common causes of yaw overload failure include poor lubrication of the yaw bearing, high yaw pressure, and dust accumulation on the brake disc. These are all external causes, and the yaw overload is allowed; when designing the yaw system is often ignored.

Theoretically, the maximum drive torque of the yaw motor should envelop the maximum external load required by the yaw process during the design of the whole machine. Define the maximum load required for this requirement as the cut-off load. When each complete machine manufacturer designs a wind turbine, the calculation method of the cut-off value of the external load may not be consistent, but it is generally not defined

as the ultimate load in the full life cycle of the wind turbine. This is because the ultimate load is the maximum load experienced during the entire life cycle of the wind turbine. The ultimate load lasts for a short time and is a load that occurs once in several years. If the maximum driving torque of the yaw motor is required to envelop the limit load, it will cause conservative selection of the yaw motor which reduces the economy of the equipment.

Take the evaluation of the driving capability of the yaw system when a certain type of wind turbine is yaw as an example. The driving capability of the yaw system is considered to be able to successfully execute the yaw by overcoming 99% of the external load, and less than 99% of the external load It may cause an unstable state. Therefore, when the wind turbine generator yaws, there is a certain probability that the yaw drive capacity is insufficient which leads to the overload protection of the yaw motor.

In summary, when selecting the yaw motor, considering the economy of the overall system, the yaw system in the simulation design is not 100% successful in performing the yaw action, so it is necessary to study how to control the yaw overload protection redundantly [2].

Yaw overload protection redundant control method. In order to reduce the occurrence of yaw overload protection, it is proposed that when extreme working conditions cause the yaw motor protection switch to trip, the yaw stop action should be executed immediately. At this time, although the yaw motor protection switch trips, it does not affect the safety of the unit, and the wind turbine can be shut down without failure. By using hardware self-reset and software logic control to yaw again, extreme working conditions can be avoided.

There are two main types of protection for yaw motor: motor protection switch and thermal relay. After the motor protection switch is tripped, it must be closed manually. It is not suitable for use and can be changed to a thermal relay with self-reset function. The working principle of the thermal relay is that the current flowing into the thermal element generates heat, which causes the bimetallic strips with different expansion coefficients to deform. When the deformation reaches a certain distance, it pushes the connecting rod to break the control circuit, thereby making the contactor. When power is lost, the main circuit is disconnected to realize the overload protection of the motor. With disconnection of the current, the temperature of the metal sheet gradually decreases. When it is completely cooled, the metal sheet returns to its original shape and the thermal relay is automatically closed. At this time, although the thermal relay has been automatically closed, the wind turbine generator has executed the yaw stop command when the thermal relay is tripped, and the yaw motor circuit will not be turned on again due to the closure of the thermal relay. The parameters "Yaw failure times (C1)" and "Yaw failure waiting time (T1)" are added to the control. By setting the two parameters differently, diverse decisions of yaw failure can be made. The parameter "Thermal Relay Recovery Waiting Time (T2)" is added to the control to reduce the failure rate of restarting the yaw by fully considering the heat dissipation of the thermal element of the thermal relay.

Conclusion. Research on the redundant control of the yaw overload protection using the control loop of the yaw soft start is of great significance for improving the availability and power generation time of wind turbines. This article comprehensively elaborates the yaw loop hardware scheme and software scheme, and verifies it according to the usage of the wind farm.

REFERENCES

1. 风力发电机组偏航电机选型优化方法探究[J].信晶,郭宇辰,董礼.可再生能源.2019(01).
2. 论风力发电机组偏航系统的设计要点[J].信晶,袁凌,潘磊,李英昌,员一泽,郭宇辰.机械制造.2020(05).
3. 浅谈风力发电机组偏航系统现场运行技术应用[J].叶宁.红水河.2019(04).

LINEAMENT ANALYSIS OF FREE SPACE IMAGES IN LEFA SOFTWARE

P. DOLHI

Polotsk State University, Belarus

LEFA software product and its capabilities to identify lineament structures in free Landsat-8 space images are described in the article. The results obtained by the LEFA software are compared with the results of other authors.

Nowadays, remote sensing is the most important tool for research in various Earth sciences, including geodynamics. Only remote sensing can provide continuous spatial data of an areal nature. Resources with free access to data (USGS, remotepixel.ca, scihub.copernicus.eu et al. [5,7,9]) allow us to obtain information about the earth's surface in any territory in different epochs. Methods of processing remote sensing materials used in geodynamics can be divided into two groups:

- estimation of vertical displacements of the Earth's surface by interferometric processing of a pair of radar images (the most known project that provides freely distributed radar images is Sentinel-1, which consists of two satellites: Sentinel-1 A and Sentinel-1 B);
- identification of active structural elements in images in the visible and infrared bands.

Active structures identified in space images can have a linear stretch (lineaments), or be expressed in the form of ring structures. These structures can be distinguished in space images both by visual decoding and by using various automated algorithms. LEFA (Lineament Extractor and Fracture Analysis) developed by Sergey Shevyrev at the Far Eastern Federal University (Vladivostok, Russia) is one of the software products that makes an automated lineament analysis. The interface is shown in the figure 1. The product is developed on the MATLAB platform. It allows a user to perform such things as image binarization (edge detection), line detection by the Hough transform, combining lines into linear structures (faults), calculating the fractal dimension of fault systems, creating rose diagrams of the line distribution in length and direction; export the lines into a shapefile.

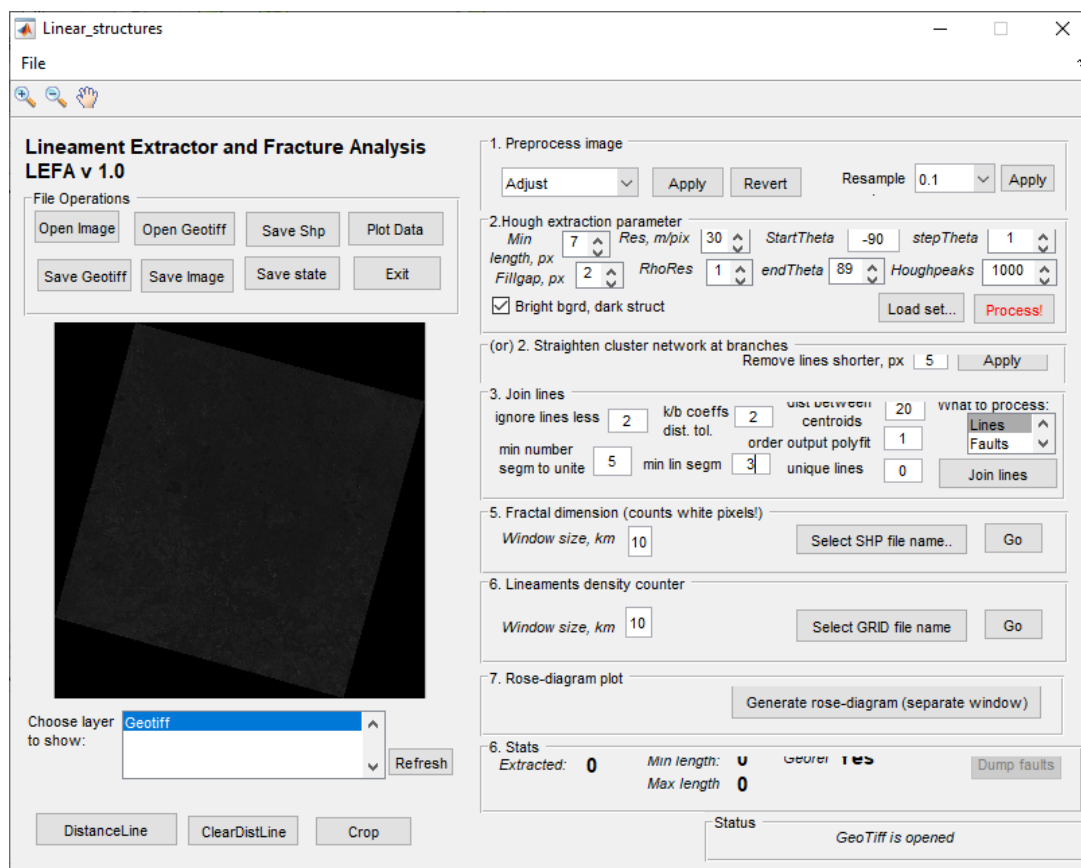


Figure 1. – Main window of the LEFA software

As the input data, the program can use grayscale images in the form of a digital elevation model (DEM), and in the form of a single-band space image. It was experimentally proven that the program was effective when processing the SRTM DEM and Landsat-8 satellite images (obtained from remotepixel.ca).

Landsat-8 data has a resolution of 15 meters in the panchromatic mode, 30 meters in the visible mode, near and short-wave infrared range, and 100 meters in the thermal infrared range. The sensing period is 16 days.

Among the possible alternatives, we can consider the images of the Sentinel-2 satellite, which have a spatial resolution in the visible range of 10 meters, 20 meters in the short-wave infrared range, as well as meteorological satellite data (TERRA (MODIS), SUOMI-NPP) with low resolution and large spatial coverage.

As the author of the program recommends, we used the 7th band of the Landsat-8 image (short-wave infrared range, with a wavelength of 2.1-2.3 microns) on the territory of the northern part of the Vitebsk region, including the Polotsk district, on various dates (table 1). Preference was given to spring and autumn images with poorly developed or withering vegetation.

Table 1. – Landsat-8 images, selected for study

Date	Cloud cover	Brief description of the conditions
11.04.2015	0,21	There is no snow cover, poorly developed vegetation
28.03.2016	1,32	There is no snow cover, poorly developed vegetation, water basins are covered with ice, light clouds are in the northeastern part.
23.09.2017	0,02	There is no snow cover, well-developed vegetation
12.10.2018	0,00	There is no snow cover, withering vegetation
06.04.2019	0,04	There is no snow cover, poorly developed vegetation

Each of the images is preprocessed according to the Canny algorithm [3,4]. A number of authors consider this algorithm to be optimal [2,8]. Then, we perform the Hough transformation, leaving default parameters (figure 2).

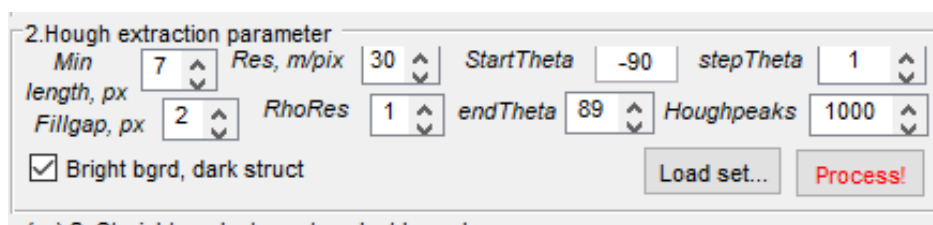


Figure 2. – Hough algorithm parameters

After finding the lines, the program joins the collinear lines into faults. We join lines (figure 3). The final fault will include at least 5 lines, with the minimum length of the fault being 2 km.

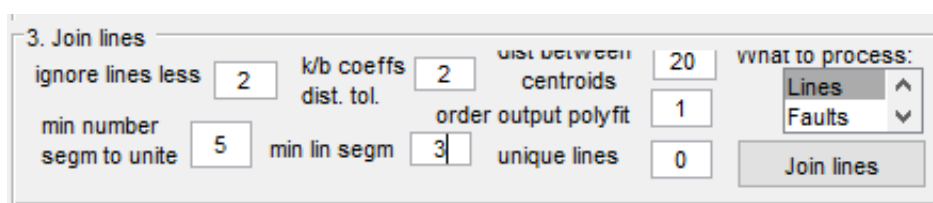


Figure 3. – Lines join parameters

We displayed the resulting faults for each epoch in the GIS-project in QGIS (figure 4, 5). As expected, the pattern of the fault network differs for different images due to different vegetation conditions, cloud cover conditions, and light conditions. However, comparing the images for different epochs, we can see that our study confirms the existence of a large latitudinal strike fault to the north of Polotsk, as well as a number of north-west – south-east strike faults. It should be noted that a number of identified structures correspond to linear objects of clearly anthropogenic origin – roads, forest clearings, etc. Such lines will not be taken into account when interpreting the result.



Figure 4. – Fault network obtained from the image on date 12.10.2018

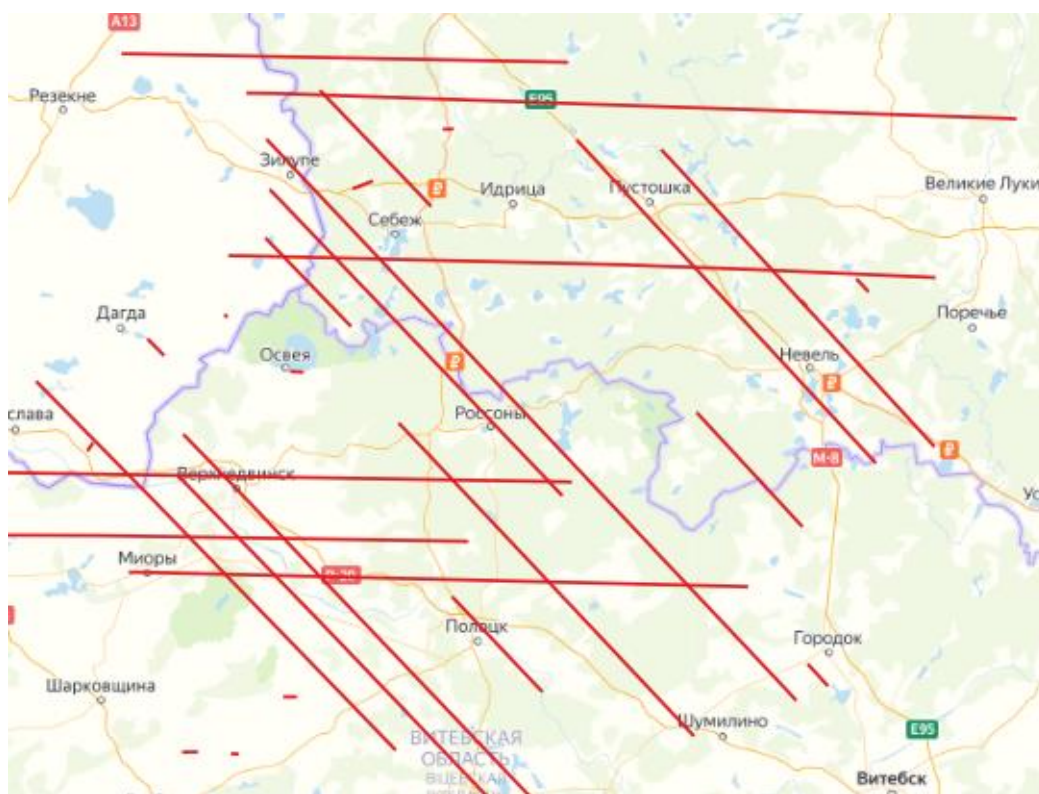


Figure 5. – Fault network obtained from the image on date 06.04.2019

We compared the resulting pattern of the fault network with the one presented on the cosmotectonic map by Garetsky, Karataev, etc. (figure 6). We can note that the directions of the main linear structures obtained by us in this region coincide to the data according to the cosmotectonic map. It can be concluded that the LEFA software product is informative for the study of the fault network based on images from the Landsat-8 satellite. Further study requires to identify algorithm parameters, as well as to develop the possibility of processing survey data from thermal, magnetic, gravimetric and other sensors.



Figure 6. – A fragment of the cosmotectonic map [1]

REFERENCES

1. Гарецкий Р.Г., Космотектоническая карта Беларуси масштаба 1 : 500 000: создание и результаты / Р.Г.Гарецкий, Г.И. Каратаев, Р.Е.Айзберг, А.К.Карабанов, А.А.Святогоров // Літасфера. – 2013. – № 1. – С. 3–30.
2. Хоан Фам Суан. Разработка технологии автоматизированного обнаружения и анализа линейных и кольцевых структур на космических изображениях: дис. канд. техн. наук: 25.00.34 / Хоан Фам Суан. / – М., 2012. – 173 с.
3. Canny J. A. // Computational Approach to Edge Detection // Pattern Anal. Mach. Intell. – 6, Vol. 8. - IEEE Trans. - 1986. - pp. 679–698.
4. Canny J.F. // Finding Edges and Lines in Images.: AITR-720 – 1983.
5. EarthExplorer // USGS.gov | Science for a changing world [Electronic resource] – 2010 – Mode of access: <https://search.remotepixel.ca/#5.42/54.946/30.862> - Date of Access: 01.04.2021.
6. LEFA for Matlab – LEFA GIS Tools // LEFA GIS Tools – Remote sensing analysis software for Earth sciences [Electronic resource]. – 2019 - Mode of access: http://lefa.geologov.net/wp-content/uploads/2018/05/LEFA_1_0_guide.pdf. - Date of access: 01.04.2021.
7. Remote Pixel | Satellite Search // RemotePixel [Electronic resource] – 2015 – Mode of access: <https://search.remotepixel.ca/#5.42/54.946/30.862>. - Date of Access: 01.04.2021.
8. R.O. Duda, P.E. Hart // Use of the Hough transformation to detect lines and curves in pictures // Comm. ACM. – Vol. 15. -1972. -pp. 11-15.
9. scihub.copernicus.eu [Electronic resource] – 2015 – Mode of access: <https://scihub.copernicus.eu/dhus/#/home>. – Date of Access: 01.04.2021.

ROBOTIC SORTING FOR THE MAIN TYPES OF SOLID HOUSEHOLD WASTE

A. LAZERKO, V. CHERTKOV
Polotsk State University, Belarus

The analysis of existing and effective methods of robotic sorting of solid household waste is carried out. The main stages of sorting solid household waste according to these methods are described.

Introduction. Municipal solid waste (MSW) has become a global problem today. Since the 19th century, the amount of garbage has increased exponentially. That was supplemented by an ever-growing demand for new products. As a result, the humanity has huge landfills filled with thousands of tons with waste. This leads to the destruction of the ozone layer and to poisoning people and animals with toxic smoke due to burning of those landfills. Landfills also serve as a halo habitat for insects, birds, and rodents who become carriers of different infections.

One of the solutions to this environmental problem that exists now is the incineration of garbage in order to stop its accumulation in landfills and to prevent soil intoxication. However, this action is not environmentally friendly. A huge amount of carbon dioxide and toxins are released into the air. Also, the burning of garbage is not profitable in terms of economy. Therefore, people began to sort the garbage. Garbage sorting is mostly done manually using a moving conveyor. Therefore, the introduction and use of automated sorting with the help of robots is an urgent task to improve the environment [1].

The main advantages of robotic MSW sorting are: the reduction of costs for manual processing (wages for workers); people are not exposed to the danger of toxins while sorting MSW; the increase in efficiency of MSW sorting [2].

Let us look closer at the promising methods of automated sorting with the help of robots.

A method of robotic sorting using machine vision. It is the main method of sorting solid waste in the modern world. It uses machine vision and advanced intelligent control system. The information from cameras and sensors is transmitted to an intelligent control system which uses a spectrometer to improve the scanning accuracy and controls the gripper manipulators.

This method involves the sequential performance of stages for sorting solid waste.

The first stage: Separation of dust, sand, and fine slag. The conveyor uses the process of separating main garbage from small parts with a radius of less than 5 cm. by using an industrial sieve and air molasses. The size of the screen grid cell is regulated by an intelligent control system.

The second stage: Separation of very large pieces of garbage for crushing. The scanner detects the size of the objects and transmits the information to the control system. The camera recognizes the objects that are larger than 1 meter and sends a command to the manipulator. The manipulators put these objects to a crushing compartment. After the crushing process, formed fragments are carried to the conveyor.

The third stage: Separation of metal objects. Metal detectors plus electromagnetic separation are used. Metal parts are extracted by using an alternating magnetic field.

The fourth stage: Sorting of the main types of MSW using machine vision. Following the previous stages, the solid waste is analyzed while on a conveyor. The sensors recognize each piece of garbage and inform the intelligent control system about its geometric location on the conveyor belt as well as about its size and the type of material (plastic, wood, glass, etc.).

The intelligent system has multiple digital cameras to use machine vision functions to recognize objects in a specific area on the conveyor belt. The software of the intelligent system implements image recognition based on a convolutional neural network and generates a list of fragments with calculated parameters (size, type of material, orientation on the tape) for further processing. The result of the software is shown on the Fig. 1 as a computer representation of the location of the debris fragments on the conveyor belt.

When the fragment reaches the area of operation of the manipulator, the latter, having received the calculated values of the size, position and the type of the material, captures and removes it from the conveyor. After, it places the fragment in a container with the appropriate type of material. The work of the manipulator is presented on the Fig. 2.

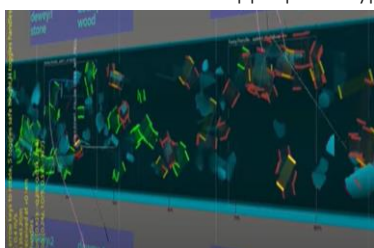


Fig. 1. – The computer vision how objects are represented on the belt



Fig. 2. – The manipulators for sorting the garbage

It is possible that some fragments of garbage will not be recognized with a high degree of probability. In this case, the manipulators will not sort them. Unrecognized fragments will be delivered by a conveyor for a specialized process, where they will be taken back to the beginning of the line for re-recognition. Due to the location on the conveyor belt and the relevance to each other, these fragments will be correctly re-recognized. The process will continue until the entire batch of garbage is decomposed according to the type of the material.

The accuracy of determining the materials depends on the degree of artificial intelligence (AI) training. The system remembers objects, color, and reflected spectrum. The speed of recognition and the number of recognized materials depends on the performance of the neural network. Machine vision can process data on various indicators simultaneously thanks to the use of high-performance neural networks. More than 90% of all existing companies use this method for sorting solid waste [5].

A list of existing companies which use machine vision in a robotic system for sorting solid household waste are the following:

a) SamurAI Robot from Canada's Machinex Technologies: recognizes plastic, cardboard, boxes, and packaging with the help of machine vision. The robot's accuracy is already equal to that of a human.

b) Russian robot for sorting waste from the GC "Environmental and Energy Technologies": recognizes 20 types of plastic among other garbage that moves along the conveyor, using not only cameras, but the spectrometer which scans chemical composition and color.

c) Finnish company ZenRobotics has developed an industrial robot and software for recycling garbage. The sensors of the system constantly monitor the flow of solid waste, and the program analyzes the data in real time. As a result, the garbage is sorted quickly and accurately.

The method of using pressure sensors. With the help of this method, the robotic system is able to determine the type of material by using tactile sensors. Such a system is able to determine whether an object is wood, metal, or plastic. The system includes a soft teflon hand that uses tactile sensors at the fingertips to determine the size and the stiffness of objects. The appearance of the manipulator equipped with a tactile system is shown on the Fig. 3.

This method was found to be 85 percent accurate when detecting materials in statics and 63 percent accurate on a real simulated conveyor belt. The most common mistake was the recognition of metal cans covered with paper. They were identified as paper.

A further development of such systems is the use of a touch-sensitive skin for the robot's grip, which provides tactile feedback that allows to distinguish between a wide range of objects, from hard to soft. On the Fig.4 a robot manipulator with teflon fingers is shown.



Fig 3. – Solid waste sorting process with the help of the robotic system that uses pressure sensors



Fig. 4. – Tactile system

When the system captures an object, it evaluates the size of the object and uses its two pressure sensors to measure the force which is required to capture the object. These indicators along with the calibration data about the size and the stiffness of the objects (which are made of various types of materials) are what gives the idea of what material the object is made of. Since the tactile sensors are also conductive, they can detect metal by the measured change in the electrical signal. The robot evaluates the size and measures the pressure difference between the current closed hand and the pressure while the hand is opened. The control system uses this pressure difference and the size to classify objects based on the available information about the objects that the machine has already measured.

The next step in the development of such systems is to compare tactile data with actual video data from the robot's digital cameras. This will improve the accuracy and will provide more subtle differentiation between different types of materials [3].

Chemical analysis method. This method, like the previous ones, uses a moving conveyor. The sorted garbage arrives at the beginning of the conveyor belt and moves to the robot manipulator. As it moves, it crosses a light beam which analyzes the chemical composition: a spectrometer is used to analyze the chemical composition. The spectrometer is assisted by machine vision cameras. Plastic is selected according to several criteria – the geometry of the container (all plastic cans, bottles, plates, packaging, etc. have a similar geometry, glass containers have a constant chemical composition).

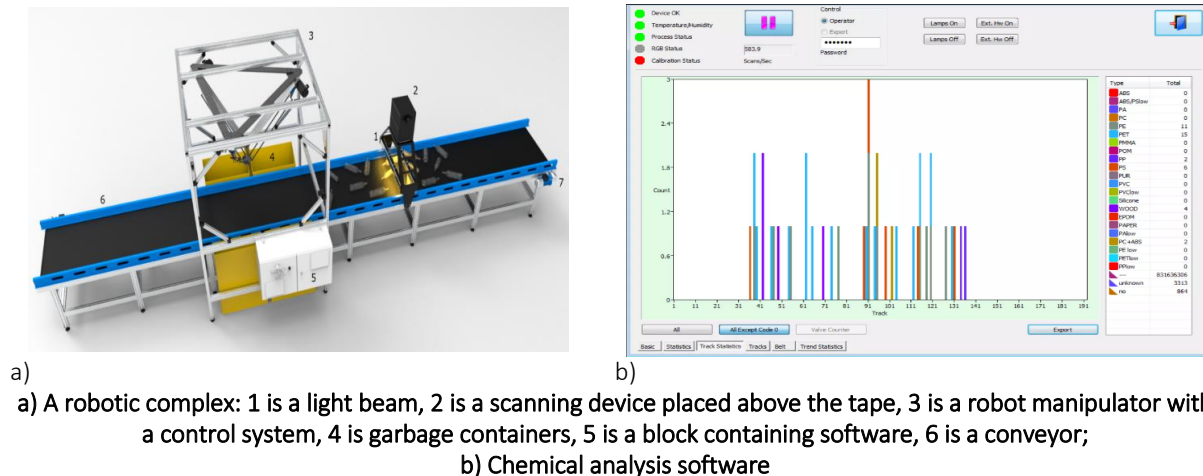


Fig. 5. – Robotic complex for sorting solid waste with chemical analysis

Therefore, it is possible to “teach” the industrial vision system to select products with the geometry needed, by using the information which is stored in its database. Solid waste color (plastic packaging is varied in color, but most often has several main colors: white, transparent, blue, red, yellow, green, and brown).

Next, the system which consists of a robot, a control system, and an industrial computer with its own software analyzes and signals to the robot where the fragment is located on the conveyor belt. It also signals about its size and the type of material. This is necessary for the correct positioning of the vacuum gripper. At present, the complex determines and sorts the types of materials according to their chemical composition: glass, plastic, and paper [4].

The development of a sorting robot based on the LEGO educational platform. At the moment, Polotsk State University has grounds for creating prototypes of robotic sorting machines based on LEGO Mindstorms EV3 educational set. To design a robot that is able to sort garbage, the experiment was carried out which includes the following steps:

The first stage. The study of the requirements for sortable objects. Here, we selected three types of objects: metal, glass, and plastic. The main task of the robot was to distinguish those three objects.

The second stage. The selection of the system as well as the model for building the robot. The LEGO Mindstorms EV3 educational system was chosen for the robot development [6]. This system allows to create complex robotic structures. It also allows to create a program which helps a robot work independently without human intervention. A mobile robot with a gripping claw was chosen as the model.

The third stage. The model was assembled. Some changes were made to the design of the robot: an additional magnetic sensor was installed which made it possible to distinguish metal objects. The principle of selecting metal objects is as follows: the robot uses its claw to grab the object; if a magnetic sensor is triggered, the object is considered metallic. The robot with a magnetic sensor is shown on the Fig 6.

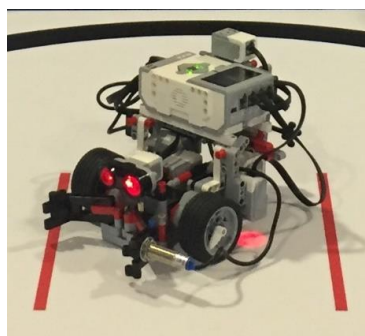


Fig. 6. – Solid Waste Sorting Robot

The fourth stage. The program is compiled in the LEGO Mindstorms environment. The program was as follows: the robot begins to rotate around its axis. When an object appears in the area of the ultrasonic sensor, the robot captures this object. The robot begins to analyze the material of the captured object. If a magnetic sensor is triggered, the robot decides that it has captured a metal object. If the magnetic sensor does not trigger, the robot tries to squeeze the object. If the robot manages to squeeze the object, it decides that it is a plastic object. It can also decide and detect when a glass object is captured.

The fifth stage. To organize the experiment for distinguishing objects made of glass, metal and plastic, the following items were selected: a metal can, an empty plastic bottle, and a glass bottle.

The experiment was conducted on a flat plastic surface. The robot was placed in the center of a circle with a diameter of 1 meter. The robot began to rotate around its axis clockwise. One item was put for the detection by the robot. Once the item was detected, the robot drove up to it, captured it, and reported the type of the captured object with sound signals. Next, the robot took the object out of the circle and returned to its original position. See, the Table 1 below.

Table 1. – The results of the object recognition experiment

Item name	Number of times displayed	Number of correct recognitions	Number of incorrect recognitions
Metal jar	30	30	0
Plastic bottle	30	23	7
Glass bottle	30	27	3

The results indicate that the developed robot has managed the tasks. To reduce the number of incorrect recognitions, it is necessary to improve the design of the robot and to add new sensors.

Conclusion. People cannot put everything on the landfill for burial. Solid household waste must be pre-sorted. This will allow sorted municipal solid waste to be used as a renewable resource for some new materials. Replacing manual labor for sorting solid waste at waste sorting enterprises will reduce personnel costs and the number of people who are endangered due to toxins of solid waste. It will increase the efficiency of sorting solid waste, thereby improving the environmental condition of the Planet.

The experiment has showed that the developed design of the sorter robot has a high percentage of object recognition. Therefore, the use of robots for sorting solid household waste is effective for saving the environment. Further research is the expansion of the line of sorted waste objects that can be used for recycling and for the production of new items.

REFERENCES

1. Ernst Weizsacker. Factor five. The formula for sustainable growth. / Ernst Weizsacker, Michael H. Smith, Carlson Hargrope // AST-PRESS KNIGA. – Moscow, 2013.
2. Catherine de Silgy. The history of garbage: From the Middle Ages to the present day.
3. Adam, C.-S. Robots that can sort recycling [Электронный ресурс]. – Режим доступа: <https://news.mit.edu/2019/mit-robots-can-sort-recycli...> – Дата доступа: 01.04.2021.
4. Роботизированный комплекс «Вектор» для сортировки пластиковых отходов [Электронный ресурс]. – Режим доступа: <https://vc.ru/tribuna/65282-robotizirovannyy-kompleks...> – Дата доступа: 01.04.2021.
5. Роботы сделают мир чистым [Электронный ресурс]. – Режим доступа: <https://habr.com/ru/post/402311/>. – Дата доступа: 01.04.2021.
6. Овсяницкая, Л. Ю. Курс программирования робота EV3 в среде Lego Mindstorms EV3 / Л. Ю. Овсяницкая, Д. Н. Овсяницкий, А. Д. Овсяницкий. – Издательство «Перо».

MODERN METHODS OF REMOTE SENSING OF THE EARTH

V. KULIK, M. VALOSHYNIA

Polotsk State University, Belarus

This article discusses the methods of remote sensing of the Earth for topographic and geodetic, cadastral purposes, presents the current trends in the industry.

Introduction. Topographic and geodetic, cartographic, as well as other sectors of the national economy, are trying to introduce and adopt modern discoveries, advanced research tools of physics, mathematics, information technologies, and methods and technologies of related industries to solve problems. On the other hand, new technologies should be analysed and investigated in order to estimate and think through the advantages and disadvantages compared with conventional methods.

Remote sensing of the Earth is the acquisition of information about the Earth's surface and objects on it, the atmosphere, the ocean, the upper layer of the earth's crust by non-contact methods, in which the recording device is removed from the object of research at a considerable distance [1]. In the narrow sense of the word, remote sensing refers to airborne and satellite surveys.

Remote sensing is an extremely valuable tool that is vital to many industries, from mining to fishing and farming to mapping and surveying operations, and the ways to use remote sensing just keep expanding [2].

The aim of the work is to study and analyze modern methods of remote sensing and processing of their results for use in topographic, geodetic, cartographic and cadastral activities.

Methods. Depending on the task, the sensors can be placed on different platforms and, accordingly, the following types of remote sensing can be distinguished: ground, airborne (aerial photography), space. Each of these types has its own capabilities, purpose and, accordingly, own characteristics and application.

Depending on the source of the registered radiation, the surveys are subdivided into active (using their own source of electromagnetic radiation to irradiate the objects being shot, e.g. radar survey), passive (recording solar radiation reflected by objects or own radiation of the Earth).

By the technology and the spectral range remote sensing methods are distinguished:

- in the optical range: in the visible and near infrared range (photographic and scanning), thermal infrared;
- in the radio range: microwave radiometric, radar.

In modern sensing systems, the multispectral principle is widely used. There are the following surveys using this principle:

- multisensor, in which imaging is simultaneously performed in several (3-7) spectral zones
- hyperspectral, in which imaging is carried out simultaneously in dozens or hundreds of narrow spectral regions,
- ultraspectral, in which imaging is carried out simultaneously in many hundreds of narrow areas of the spectrum [3].

In a radar survey, the multispectral principle is implemented using several microwave wavelengths and different polarization.

The world is changing very fast. The rapid development of information technologies, machine vision technologies, and an increase in the positioning accuracy of satellite navigation systems make it possible to introduce such methods as digital aerial photography from unmanned aerial vehicles (UAVs) and laser scanning.

The influence of the development of methods and technologies for performing topographic surveys is manifested and consolidated in technical regulations. With the entry into force building norms 1.02.01-2019 [4] in 21.09.2020, the relevance of using the aerial topographic method for surveying of large areas and long linear objects is preserved, if the required accuracy and economic feasibility are ensured. In addition to traditional aerial topographic methods such as combined and stereotopographic surveys, described in the previously valid 1.02.01-96, it is allowed to perform such surveys for engineering and geodetic surveys as aerial laser scanning in combination with digital aerial photography and digital aerial photography using UAVs.

It should be noted that such changes have long been expected by the professional community, since the possibilities of the above methods can hardly be overestimated. The advent of low-cost UAVs has been a boon to surveyors. Now they can expand their business or add value to their company by collecting high-resolution imagery. Airborne remote sensing using UAVs will remain a key science and technology for data collection. While UAVs are not yet used for national-scale mapping, they have proven to be satisfactory for smaller urban areas, industrial zones or protected areas with higher densities, resolutions and frequencies [5, 6].

Another more up-to-date trend is the use of hybrid sensor systems already for aerial photography, combining a single-camera or multi-camera system in order to integrate multiple types of data. It leads to much richer datasets and better decision making for the final users. There may be the following combining of different sources of information, such as LiDAR and optical imagery, hyperspectral scanner or other [5, 6] as well as data of different spatial resolution. The use of multisensor data leads to more comprehensive information about the object under the study.

The modern development of data processing software has led to appearing of a lot of software products. Specialists expect the appearance of a new generation of easy-to-use software, the development of automatic methods for detecting and recognizing objects, which, in turn, leads to automatic mapping. Sophisticated image processing and analysis software including deep learning technologies are in great demand [6]. For processing remote sensing data, today it is important to solve the problem of big data to extract useful information.

As for satellite remote sensing an increase in the commercial availability of high-quality satellite remote sensing data, new sensor launches for surveys and re-surveys, growth of space constellation of satellites as well as radar satellites are expected [6]. New sensors and a higher re-survey rate provide the opportunity for advanced time series analysis, e.g. geodynamic analysis.

Analyzing the world experience in obtaining spatial information, and specifically performing topographic surveys, we see that in the last 10 years, laser scanning has experienced a boom in use for obtaining accurate and detailed information about objects. Although aerial laser scanning from UAVs is not widely used due to the weight-to-price ratio, serious progress in this direction is noticeable [7].

Results and conclusion. Thus, remote sensing is intensively developing, adapting to the stages of development of society. Various global processes have a significant effect on the development of society and remote sensing as well. However, there is an increasing need for detailed, accurate spatial information, processing large amounts of information, accessibility of information processing tools, simplifying the use of software products, simplifying the integration of various types of data. The development of new modern approaches to data acquisition, analysis and the presentation should not overcome the advantages of conventional methods.

REFERENCES

1. Дистанционное зондирование земли [Electronic resource]. Mode of access: <https://aboutspacejournal.net/космические-аппараты/искусственный-спутник-земли/дистанционное-зондирование-земли/>. – Date of access: 14.04.2021.
2. Pelton J.N. (2019) Key Trends in Remote-Sensing Satellite Systems and Services. In: Space 2.0. Springer Praxis Books. Springer, Cham. [Electronic resource]. – Mode of access: https://doi.org/10.1007/978-3-030-15281-9_3. – Date of access: 14.04.2021.
3. Jensen J.R (2007) Introductory digital image processing: a remote sensing perspective. – 3rd ed. 526 p.
4. СН 1.02.01-2019 Инженерные изыскания для строительства. Утверждены и введены в действие постановлением Министерства архитектуры и строительства от 26 декабря 2019 г. № 74.
5. Smith S. (2020) GISCaFe Industry Predictions for 2020 – Part 1 [Electronic resource]. Mode of access: <https://www10.giscafe.com/blogs/gissusan/2020/01/02/giscafe-industry-predictions-for-2020-part-1/>. – Date of access: 14.04.2021.
6. Susan, S. (2020) Перевод: Дворкин Б.А GISCaFe: основные тренды развития ГИС-индустрии в 2020 году [Electronic resource]. Mode of access: <https://sovzond.ru/press-center/articles/gis-mapping/6771/>. – Date of access: 14.04.2021.
7. Воздушное лазерное сканирование [Electronic resource]. Mode of access: <http://fly-photo.ru/vodushnoe-lazernoe-skanirovanie.html> - Date of access: 14.04.2021.

UDC 621.316

IMPROVING THE EFFICIENCY OF USING REMOTE MONITORING SYSTEM OF SMART GRID

JICHANG SHANG, V. CHERTKOV

Polotsk State University, Belarus

The article describes the possibilities of using remote monitoring of an intelligent network. The architecture for intelligent monitoring systems in the power industry is considered. The equipment for remote monitoring is described.

Introduction. With the continuous development of science and technology, the benefits of remote monitoring of smart grids have undergone an essential transformation, beginning to shift from transient monitoring to real-time monitoring, forming highly efficient and intelligent monitoring content. Relevant information shows: Most smart grids in my country have built a relatively complete smart grid remote monitoring system based on communication technology, automation technology, remote measurement, etc., and built a systematic and hierarchical remote monitoring network. The development of electrical work has laid a solid foundation [1].

The development history of smart grid remote monitoring. In the process of constructing the smart grid remote monitoring system, the system equipment needs to be reasonably selected, and the corresponding equipment system must be formed in accordance with the requirements of the smart grid. In the traditional smart grid remote monitoring system, image monitoring equipment is mainly selected as the main body of remote monitoring, and digital remote image monitoring equipment is used to transmit remote information to the front-end digital host.

The TCP/IP protocol accesses the host, calls image files, and realizes remote control.

With the continuous deepening of power grid construction, the above-mentioned video monitoring system has gradually been eliminated, and the remote monitoring system with self-healing and self-protection capabilities has begun to become the core of the development of the power grid. Especially after the mature application of smart grid checking and receiving, power grid backup and self-investment to the construction of smart grid, my country's smart grid remote monitoring system has undergone an essential transformation. The current smart grid remote monitoring system mainly integrates computers, communications, sensors and other devices on the basis of traditional power grids, forming a digital, intelligent, automated, and interactive online monitoring system, which has abnormal monitoring and self-healing capabilities, and reduces The necessary manual supervision greatly improves the efficiency of remote monitoring of smart grids [2].

Construction of remote monitoring system for smart grid. In the process of this research, the application benefits of the smart grid remote monitoring system are studied mainly by taking a certain regional power supply and distribution system as an example. The current research results are as follows.

A regional power supply and distribution system is mainly responsible for regional domestic and industrial power consumption. The power supply and distribution environment is relatively complex, the area is relatively large, and the daily management work is very heavy. Since 2012, in order to further improve the efficiency of power transmission and distribution monitoring and reduce line failures and line losses, relevant departments have begun to set up an intelligent monitoring system on the basis of traditional monitoring work, and adjust the traditional video monitoring system to form a smart meter, smart The new remote monitoring architecture with switch and indoor control as the core has comprehensively improved the stability and reliability of smart grid operation. Relevant data shows: There has been no large-scale power outage in this area within 5 months

of applying the smart grid remote monitoring system, and the quality of power supply and distribution has been significantly improved, which has very high use value and reference significance [3].

Remote monitoring system settings. The remote monitoring system of a smart grid in a certain area is mainly realized through user-side control. The smart devices are set on smart meters, smart switches, and standby automatic input devices to complete online monitoring, abnormal alarms, fault location, etc., and realize power supply and distribution of the power grid. The real-time monitoring and control of power grids have effectively improved the safety and reliability of grid operation.

Smart meter settings. Choose a smart meter with energy measurement and power supervision for installation, and determine the power, rated voltage, rated current and other values according to the smart grid line conditions to ensure that the smart meter can fully collect user power information and lay a good foundation for the development of remote monitoring work. For general meter communication, RS485 bus or carrier bus can be selected, which can be appropriately selected in combination with the actual regional communication network.

The above-mentioned devices mainly collect various data in the smart grid through smart meters, transmit voltage data, current data, etc. on the corresponding circuit to the electric energy measurement device, complete the data processing in the microprocessor, and guarantee on the basis of the electric energy supervision protocol Distributed generation management works with smart meters to achieve a smooth transition of islands and upload abnormal data. With the help of smart meters, efficient calculation and analysis of voltage, current, frequency, power factor, etc. in the faulty area are used to ensure that the system can quickly complete abnormal grid operation data Processing and alarm according to fault information, minimizing the risk of smart grid operation.

Smart switch settings. During the switch setting process, ensure that it can realize line over-current and over-voltage protection, reduce line faults through switch power-off, and realize remote online protection. There are many types of smart switches in my country's smart grid. When choosing, make sure that: smart switches can realize power consumption measurement; smart switches can transmit user power consumption data and complete system data interaction; smart switches can receive user control instructions and complete the corresponding control operations, including power-off, power-on, line switching, etc. For this reason, KSC series switches and 7000 series switches are mainly used in remote monitoring of smart grids in this area. The KSC switch is small and exquisite, which can be used for smallest signal control needs, is simple to operate, and has a relatively stable communication transmission effect. "Switch" is configured to provide single-pole, double-pole and three-pole configurations with on, off and instantaneous action, which can adapt to the harsher climatic environment, and the practical application benefits are very significant.

Prepare the setting of self-investment device. In the process of transforming the smart grid in a certain area, the standby automatic input device is very important, and the paper system suitable for regional transmission and distribution has been formed by drawing on the experience of setting up the standby automatic input device of the power grid in the province. The core of the automatic input device is the UFV-200 control system, which has passed the industrial 32-level.

The ARM core realizes data processing and configures backup protection to complete the corresponding two-way backup investment according to different conditions. For example, when abnormal information is checked or the standby input is manually commanded, the standby automatic input device can perform standby automatic input operation according to specific data and instructions, realize very complicated standby power automatic input logic and two-way standby input, and minimize line failures The resulting interruption of power transmission and distribution has comprehensively improved the safety and stability of the smart grid.

Visual display system. The intelligent control module integrates the data collected by the front-end, comprehensively analyzes the position data and status data, determines the actual operating status of the lines in each area of the smart grid, and obtains that the online monitoring and processing data results are stored in the system.

This kind of data is relatively complex and often needs to be visualized and displayed. The actual operating status of smart grid lines can be displayed through images, text, videos, etc., to ensure that managers, maintenance personnel, etc. can quickly determine the actual operating status of the smart grid. Based on the data of smart meters and smart switches, the accurate location of the fault area is completed. Once a problem occurs, the remote monitoring system sends out alarm messages and control instructions to eliminate the fault in time and quickly restore regional power transmission and distribution.

Data storage. During the construction of the smart grid remote monitoring system, the data storage unit needs to be emphasized. The historical data storage unit and the report generation unit are formed according to the actual data storage requirements, and the power value, clock information, geographic information, etc. are sorted according to a certain time interval to form Complete smart grid operation status report; save the generated report through online storage of historical data, directly borrow the historical data function in the visual display to call up the visual data graph, realize quick comparison, and provide powerful data for smart grid monitoring and fault analysis support.

Application effect. During the operation of the above-mentioned monitoring system, real-time monitoring of the power consumption status of the smart grid is realized, and the line loss status in the area is comprehensively controlled and coordinated. The line loss area in the area is fundamentally reduced, and the monitoring and management of power resources are strengthened. Realize the real-time analysis of power data and form the "record" of power application, which provides a good technical guarantee for anti-theft. It can realize real-time meter reading and reduce unnecessary manual meter reading input in conventional smart grid monitoring. Greatly reduced the company's power monitoring costs; realized real-time and intelligent smart grid monitoring, provided reliable data and technical foundation for power supply marketing automation, and realized the overall improvement of the company's smart grid modern management benefits.

Optimization of Remote Monitoring of Smart Grid. *Build a remote monitoring database.* The amount of smart grid information data is relatively large, and simple remote monitoring of the smart grid cannot meet the data processing task. Therefore, database technology can be introduced in the process of daily operation, the corresponding monitoring data information can be stored through the database, and it can be digitally processed, stored and output, which lays a good digital information foundation for the development of remote monitoring of the smart grid. In the process of database construction, the binary processing method can be appropriately selected to adjust the image information, thereby increasing the storage capacity.

Adjust the communication mode of the system. With the continuous development and improvement of communication technology, the communication technology can be adjusted when the smart grid remote monitoring work is carried out, and the communication system can be reasonably optimized according to the conditions of each region, and real-time data services and status data pushes can be provided to managers to ensure that they can be comprehensive Grasp the operating status of the smart grid. If the anti-interference ability of carrier communication is poor, you can choose areas with simpler regional lines and shorter communication lines when setting up; RS485 has stronger anti-interference ability but higher cost, and it can be used in remote areas during the setting process. Areas with severe transmission and interference, etc., under the premise of ensuring the effectiveness of communication, realize the control of cost investment and maximize the operating benefits of the smart grid remote monitoring system.

Realize the professional construction of the team. In the process of improving the smart grid remote monitoring system, personnel must grasp the overall structure of smart grid remote monitoring, appropriately introduce intermediate interface equipment, and combine the four-remote system with the multimedia monitoring system to form a good monitoring structure. You can appropriately choose the form of layer-by-layer scanning to analyze the operation status of smart grid remote monitoring equipment and implement targeted

data processing. Once the displacement information is accompanied by time, immediately request the terminal to implement information control [4].

Conclusion. In the process of constructing the smart grid remote monitoring system, it is necessary to emphasize the various parts of the remote monitoring device. On this basis, set up electricity collection, intelligent control, backup protection and centralized monitoring to form a systematic functional system and view system, Management system and information processing system, so as to build a complete remote monitoring structure, realize the comprehensive control and coordination of remote information of the smart grid, and fundamentally improve the monitoring benefits of the smart grid.

REFERENCES

1. Kuang Honghai, Zhang Shuyun, Zeng Liqiong, et al. Design of remote monitoring system for rural smart distribution network based on GPRS and GPS [J] . New Technology of Electrical Engineering and Energy, 2017, 36(4): 83-88.
2. Li Bingshang, Wang Hui, Fan Zuo'e. Design of remote monitoring system for smart grid [J] . software, 2017, 38(10): 182-184.
3. Liu Shuqiang, Cheng Lianglun. Research on remote monitoring technology for power grid[J]. TV technology, 2014, 38(03): 186-189.
4. Du Chunmei, Dai Changming, Qu Jianping, et al. Research on Smart Grid Monitoring System Based on Internet of Things [J] . Power Technology, 2014, 38(5): 914-915.

SOLAR COLLECTOR CONTROL SYSTEM

V. KOVALEVSKY, V. YANUSHKEVICH

Polotsk State University, Belarus

Solar energy is one of the areas of alternative energy. Developments from this area are being implemented in many countries, as they are the most progressive and environmental friendly. The essence of this type of renewable energy source is that the energy of the Sun is drawn, and as a result, electricity is generated.

The advantages of solar energy are its availability, inexhaustibility, and the absence of by-products that pollute the environment. The disadvantages include low density and intermittent supply to the Earth's surface, associated with the alternation of day and night, winter and summer, and weather changes.

The most widespread application of solar energy is found in heat supply systems. They serve for hot water supply, heating and other needs, which can significantly reduce the use of traditional fuel resources.

Currently, solar energy is used on a limited scale in residential and other buildings. The most widely used solar collectors installed on the roofs provide cheap hot water for domestic needs. More than 1 million of these heating devices have been installed in Russia, Japan, Australia and other countries.

Depending on the type of collector, the process of converting solar energy into thermal energy has its own characteristics. However, in any case, solar radiation heats the coolant (water, antifreeze) flowing in the tubes. Further, the already heated coolant enters the remaining elements of the system and continues to circulate. In flat collectors, to convert solar energy into thermal energy, an absorber is used - metal plates (copper and aluminum), through which heat is transferred to the coolant. Vacuum collectors are two tubes nested into each other, the space between them is filled with vacuum, which makes it possible to reduce heat loss. Inside there is a copper tube through which the evaporating liquid moves. Heat is transferred from the walls of the tube to the copper tube by means of an aluminum shield. Then the heat from the vacuum tubes is transferred to the heat collector. Air is used as a heat carrier in air collectors, but this type is quite rare and is not used in our countries.

The advantages of the solar collector are:

Fuel economy. In summer, solar collectors are able to completely cover the building's hot water demand. In the off-season - in spring and autumn, collectors reduce the load on the gas boiler, which ultimately reduces gas consumption.

In winter, the collectors operate with very low efficiency.

Energy independence. By using a solar collector for heating, you reduce your own dependence on gas. The collector is an additional source of heat. At least in summer, you can get hot water for free without using gas. You can get the same result with heat pump heating.

Availability. No permission is required to install the solar collector. All you need is a straight-handed plumber and a competent salesperson who knows all the features and subtleties of installation.

Long service life. The service life of the collector is over 15 years. This means that you will be able to use free solar heat for a very long time.

Their main disadvantages are:

Cost. Prices for solar collectors for heating water range from 500 dollars to 1000 euros apiece. A complete ready-to-use system consisting of two collectors will cost from \$ 2,500. Considerable initial investment, with a payback period of 7 to 10 years.

Impermanence. The sun cannot be turned on and off at will. Therefore, the collector cannot be considered as the only source of heat.

We need a storage tank. For the operation of solar collectors, a storage tank is required. If it is not provided in your heating system, then this will entail additional costs for the purchase of collectors. As a result, based on all the information described, one can draw a conclusion: solar energy is one of the most progressive developments in the energy sector of the future, but with all its advantages, it has a number of disadvantages that cast doubt on its use. Such disadvantages are:

- long payback of equipment;
- low efficiency when using a solar collector (panel) in a temperate climatic zone.

In order to neutralize these shortcomings, it is necessary to use control systems. The main task of any control system is to increase the productivity of the controlled device. Consequently, by increasing productivity, we reduce the payback period of equipment for a solar collector. The block diagram of the developed solar collector control system is shown in Figure 1.

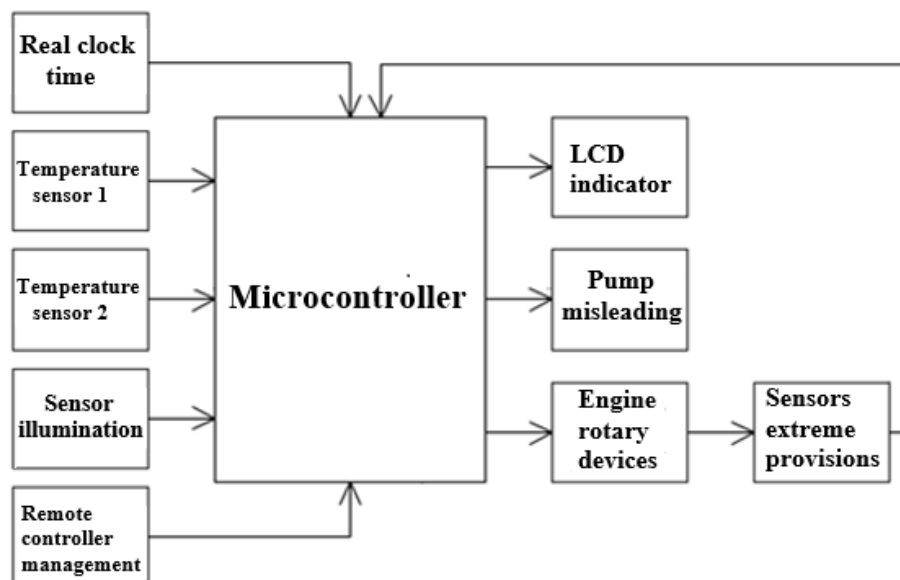


Figure 1. - Block diagram of the developed solar collector control system

Development and description of the hydraulic circuit of the device. A hydraulic diagram is a technical document containing information about the structure of a product, its constituent parts and the relationship between them in the form of conventional graphic images or symbols, the action of which is based on the use of the energy of a compressed fluid. The hydraulic diagram for connecting a solar water heater is shown in Figure 2.

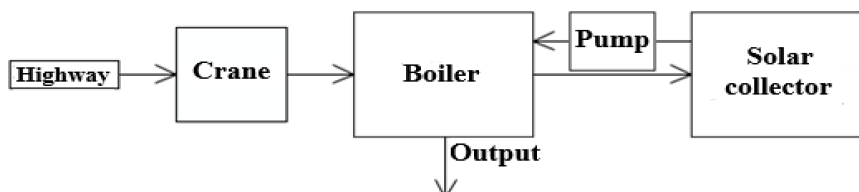


Figure 2. - Hydraulic diagram of a solar water heating installation

The solar water heating system consists of a solar collector, a boiler (water tank) and a pump. When the tap is open, water from the water main enters the boiler. Further, through the solar collector, water circulates, which is heated by the energy of the sun and is then forcibly pumped into the boiler with the help of a pump. Hot water is stored in the boiler until it is used, so it must have good thermal insulation.

REFERENCES

1. Erickson, John; «Radiolocation and the air defense problem: The design and development of Soviet Radar 1934-40», Social Studies of Science, vol. 2, pp. 241—263, 1972.
2. Ширман Я. Д., Голиков В. Н., Бусыгин И. Н., Костин Г. А. Теоретические основы радиолокации / Ширман Я. Д. — М.: Советское радио, 1970. — 559 с.
3. Бакут П. А., Большаков И. А., Герасимов Б. М., Курикша А. А., Репин В. Г., Тартаковский Г. П., Широков В. В. Вопросы статистической теории радиолокации. — М.: Советское радио, 1963. — 423 с.
4. Янушкевич В.Ф. Зондирование анизотропных сред двухчастотными и модулированными сигналами / В.Ф. Янушкевич // Полоцкого государственного университета. — Минск — 8 с. — Деп. в БЕЛИСА 12.06.97 г. - № Д 199713 / Рефер. сб. неопубликуемых работ. — 1997. — Вып. 5. — С. 11.
5. Теория электрических цепей: учеб.-метод. комплекс для студентов специальности 1-39 01 01 «Радиотехника» / С.П. Алиева. — Новополоцк: ПГУ, 2010. — 364 с.
6. Метрология и радиоизмерения: Учеб.-метод. комплекс для студ. спец. 1-39 01 01 «Радиотехника» / Сост. и общ. ред. В.Ф. Янушкевича. — Новополоцк: ПГУ, 2005. — 304 с.
7. Микроконтроллеры AVR [Электронный ресурс]. — Режим доступа: <http://www.electromonter.info/handbook/13/ElectromagneticRelay>.

GOALDIARY TIME MANAGEMENT PLATFORM

N. SMIRNOVA, I. BURACHONAK

Polotsk State University, Belarus

This article discusses the development of the time management information system. The target platform audience is students of Polotsk State University. A conceptual solution based on data processing and transmission technologies is proposed using the following technologies: TypeScript, Angular, Java, Spring, PostgreSQL. It describes the architectural approaches and solutions to solve the problem.

Today, in the era of information technology, everyone has the opportunity to use the Internet to get almost any knowledge, at the same time the volume of incoming information increases significantly and the amount of free time is limited. Only a highly organized person can do everything planned. Of course, making a to-do list and proper planning increases the awareness of their implementation. However, it is not always possible to complete tasks. In such cases, it is necessary, for example, to change tactics in order not to sink into stress or look at the tasks as a whole. Therefore, organizing planning in everyone's life is always a relevant task.

The **aim of the work** is to create a GoalDiary time management platform for the convenient scheduling of tasks in different areas of human activity and monitoring the quality of their completion.

Each individual is different and the values differ as well, dividing life into conditional areas of activity. Based on this, one of the tasks to achieve this goal is to plan the goals and objectives (keeping a diary) of a single individual and build, let's call it, its "balance wheel", as well as to obtain a report on the productivity of its activities in the form of a diagram (by category, for a time period and the ratio of planned/done).

To solve this problem, the GoalDiary time management platform has been developed using the following technologies:

- TypeScript;
- Angular;
- Java11;
- Spring Boot, Spring Security, Spring Webflux;
- R2DBC;
- PostgreSQL;
- Flyway.

A special feature of this system is the ability to divide all tasks into three types: daily tasks, weekly tasks, and monthly tasks. Each created task must be linked to a particular category that reflects the scope of the user's life. Categories are created by the user and are represented by the following types: public and private. The choice of the category type affects the formation of the productivity report. A color indication is provided, which is defined by the user.

It is important to note that the user is offered a comprehensive rating for all categories, while other users of the system can only see statistics based on public categories. Also, each participant is provided with a number of different options for specifying contact information: email addresses, mobile phone numbers, instant messaging services used, links to profiles in social networks, etc.

As for the productivity analysis, it is presented in three blocks.

The first one is a line chart, the abscissa axis indicating the days of the specified month, and the ordinate axis indicating the number of tasks. Each user category has its line, the points of which vary according to the number of completed tasks of the specified category on the dates of the given month. Such analytics reflect productivity in a complex: not only by day, but also by the life areas of the last user. A sample of these statistics is shown in figure 1.

The second type of analysis is represented by two sectors diagrams. In both diagrams, these sectors represent categories (areas of the user's life) and reflect the number of tasks associated to them according to the filtering conditions. On the first diagram, the filtering conditions are the date the task was set – it is in the specified month. On the second diagram, this filter condition is the completion date of the task in the specified month. Visually, these charts are similar, but there are still differences since it is not always possible to complete all tasks at 100%. This type of analysis allows you to evaluate productivity by category as a whole.

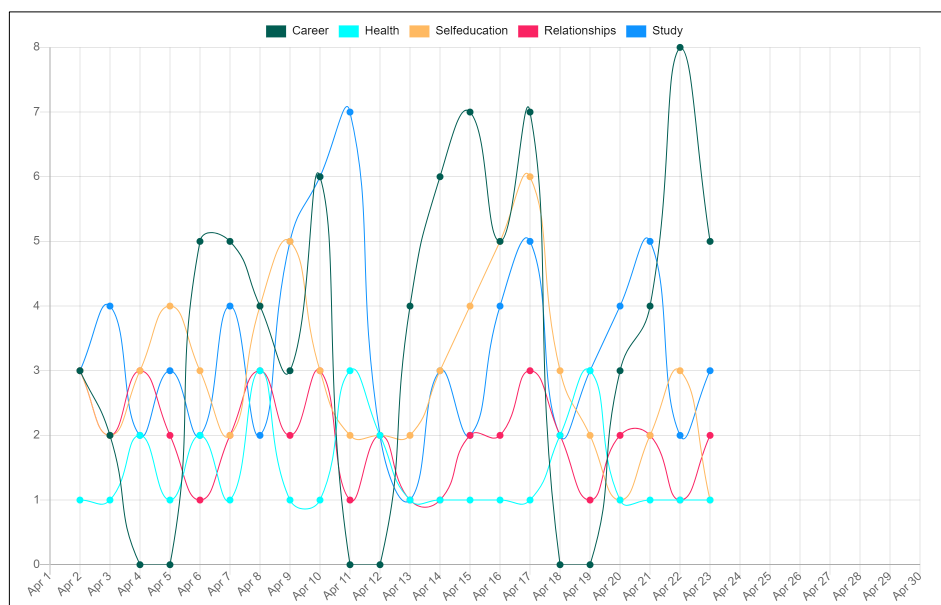


Fig 1. – Final statistics of the month

The third type of analysis is represented by a table showing the current month in the form of a familiar calendar. A special feature is the calculation of efficiency by day: the ratio of the number of tasks done to the number of tasks set. The higher the value of the resulting coefficient, the brighter the shade of green the day is highlighted, and vice versa – the lower the value, the day is marked with a brighter shade of red only. This type of analysis allows you to evaluate the productivity of each day of the month separately. A sample of these statistics is shown in figure 2.



Fig 2. – Statistics of total productivity by days

The proposed time management system developed by GoalDairy is not only about productivity. It provides its functionality to anyone, just go through the registration procedure. The developed system also includes elements of social interaction, implemented through the possibility of searching for other participants and viewing their profile. A profile can reflect public productivity statistics – what a person is willing to share with the world, thereby demonstrating their skills and willingness to develop.

The application of this system is especially useful for students who are just starting their professional growth – readiness for self-development is an important factor in obtaining a position in the profession with today's employers. The developed application can help students in time management, personal productivity, and employers in finding promising employees.

At the moment, this software is being finalized and tested.

REFERENCES

1. 10 планировщиков задач. [Electronic Resource]. – ИТС.ua, ООО «ХОТЛАЙН», 1993–2021. – Access mode: <https://itc.ua/articles/10-sovremennyh-planirovshikov-zadach/>. – Access date: 10.04.2021.
2. Chart.js – Open source HTML 5 Charts [Electronic Resource]. – Access mode: <https://www.chartjs.org/>. – Access date: 10.04.2021.
3. Angular Documentation [Electronic Resource]. – Access mode: <https://angular.io/>. – Access date: 14.04.2021.

UDC 517.983

THE SOLUTION OF THE ONE MULTIDIMENSIONAL INTEGRAL ABEL TYPE EQUATION
WITH THE HYPERBOLIC SINE FUNCTION IN THE KERNEL OVER PYRAMIDAL DOMAIN

M. PAPKOVICH, O. SKOROMNIK

Polotsk State University, Belarus

Multidimensional integral equation of the first kind with the hyperbolic sine function in the kernel over pyramidal domain is studied. Solution of this equation in closed form is established, and necessary and sufficient conditions for its solvability in the space of summable functions are given.

Let us consider the following integral equation:

$$\frac{1}{\Gamma(\alpha)} \int_{A_{c,r}(x)} \left(2 \operatorname{sh} \frac{A \cdot (x - t)}{2} \right)^{\alpha-1} f(t) dt = g(x), \quad x \in A_{c,r}(b) \quad (1)$$

Given equation generalize the corresponding one-dimensional integral equation [1, §37.1].

Let $A = \|a_{jk}\|$ ($a_{jk} \in \mathbb{R}^1$) – be an $n \times n$ ($n \in \mathbb{N}$) matrix with the determinant $|A| \neq 0$, we denote its vector-rows by $a_j = (a_{j1}, \dots, a_{jn})$ ($j=1, 2, \dots, n$), and the elements of the inverse matrix A^{-1} by a_{jk} . For vectors $x = (x_1, x_2, \dots, x_n) \in \mathbb{R}^n$ and $t = (t_1, t_2, \dots, t_n) \in \mathbb{R}^n$, $x \cdot t = \sum_{k=1}^n x_k t_k$ denotes their scalar product. For $x \in \mathbb{R}^n$ and $\alpha = (\alpha_1, \dots, \alpha_n) \in \mathbb{R}^n$, $0 < \alpha_i < 1$ ($i=1, \dots, n$) we set $x^\alpha = x_1^{\alpha_1} \cdots x_n^{\alpha_n}$, $\Gamma(\alpha) = \Gamma(\alpha_1) \cdots \Gamma(\alpha_n)$. Let $A \cdot x = (a_1 \cdot x, \dots, a_n \cdot x)$ and $(A \cdot x)^\alpha = (a_1 \cdot x)^{\alpha_1} \cdots (a_n \cdot x)^{\alpha_n}$. For $c = (c_1, c_2, \dots, c_n) \in \mathbb{R}^n$ and $r \in \mathbb{R}^1$ by $A_{c,r}(x) = \{t \in \mathbb{R}^n : A \cdot (x - t) \geq 0, c \cdot t + r \geq 0\}$ – we denote the bounded n – pyramid in \mathbb{R}^n . The expression $x \geq t$ means that $x_1 \geq t_1, \dots, x_n \geq t_n$; $dt = dt_1 \cdots dt_n$; $f(t) = f(t_1, \dots, t_n)$. A function $\operatorname{sh}(x)$ such as: $\operatorname{sh}(x) = \prod_{j=1}^n \operatorname{sh}(x_j)$, where $\operatorname{sh}(x_j)$ ($j=1, 2, \dots, n$) – hyperbolic functions [1, §28.4; 2 – 4].

The solution of the equation (1) has the form:

$$f(x) = \prod_{k=1}^n \left(\sum_{j=1}^n a_{jk} \frac{\partial}{\partial x_j} \right) \left\{ \frac{\Gamma\left(\frac{\alpha+1}{2}\right)}{\Gamma\left(\frac{-\alpha+1}{2}\right)} \int_{A_{c,r}(x)} g(t) dt \right\}. \quad (2)$$

Consider the space [2-4]:

$$L_1(A_{c,r}(b)) = \left\{ f(x) : \int_{A_{c,r}(x)} |f(t)| dt < \infty \right\};$$

$$I_{A_{c,r}}(L_1) = \left\{ \varphi : \varphi(x) = \int_{A_{c,r}(x), A \cdot (b-t) \geq A \cdot (x-t)} h(t) dt, h(t) \in L_1(A_{c,r}(b)) \right\}.$$

The space $I_{A_{c,r}}(L_1)$ plays the same role for the equation (1) as the space $AC([a, b])$ of absolutely continuous functions plays for the classical Abel integral equation [1, §2.2].

Theorem. The multidimensional Abel-type integral equation (1) $\alpha \in \mathbb{R}^n$ ($0 < \alpha < 1$) is solvable in the space $L_1(A_{\mathbf{c},r}(\mathbf{b}))$ if and only if:

$$f_{A_{\mathbf{c},r}}^\alpha(\mathbf{x}) = f(\mathbf{x}) = \frac{\Gamma\left(\frac{\alpha+1}{2}\right)}{\Gamma\left(\frac{-\alpha+1}{2}\right)} \int_{A_{\mathbf{c},r}(\mathbf{x})} g(t) dt \in I_{A_{\mathbf{c},r}}(L_1)$$

$$\text{и } \left[f_{A_{\mathbf{c},r}}^\alpha(\mathbf{x}) \right]_{\mathbf{c} \cdot \mathbf{x} + r = 0} = \left[\sum_{j=1}^n \tilde{a}_{jk} \frac{\partial}{\partial x_j} f_{A_{\mathbf{c},r}}^\alpha(\mathbf{x}) \right]_{\mathbf{c} \cdot \mathbf{x} + r = 0} = \dots$$

$$\dots = \left[\prod_{k=2}^n \sum_{j=1}^n \left(\tilde{a}_{jk} \frac{\partial}{\partial x_j} \right) f_{A_{\mathbf{c},r}}^\alpha(\mathbf{x}) \right]_{\mathbf{c} \cdot \mathbf{x} + r = 0} = 0.$$

Under these conditions, the equation (1) is uniquely solvable in $L_1(A_{\mathbf{c},r}(\mathbf{b}))$ and its solution is given by (2).

REFERENCES

1. Самко, С.Г. Интегралы и производные дробного порядка и некоторые их приложения / С.Г. Самко, А.А. Килбас, О.И. Маричев. – Минск: Наука и техника, 1987. – 688с.
2. Kilbas, A.A. On integrable solution of a multidimensional Abel-type integral equation / A.A. Kilbas, M. Saigo, H. Takushima // Fukuoka Univ. Sci. Rep. – 1995. – Vol. 25. № 1. – P. 1 – 9.
3. Килбас, А.А. Решение многомерных гипергеометрических уравнений типа Абеля / А.А. Килбас, Р.К. Райна, М. Сайго, Г.М. Сривастава // Доклады НАН Беларуси. – 1995. – Т. 43. № 2. – С. 23 – 26.
4. Скоромник, О.В. Решение многомерного интегрального уравнения первого рода с функцией Куммера в ядре по пирамидальной области / О.В. Скоромник, С.А. Шлапаков // Веснік Віцебскага дзяржаўнага ўніверсітэта. – 2014. – № 1. – С. 12–17.

UDC 004.932.

USING COMPUTER VISION TO FIND OUTLINES OF OBJECTS

S. RAHOUSKI, V. TANANA, S. VABISHCHEVICH
Polotsk State University, Belarus

The issues of using digital processing of surface images during microhardness tests to determine the geometric dimensions of prints and deformation zones are considered. An image processing algorithm has been built and a processing program has been implemented. The simulation results can be used when testing polymer films for microhardness to determine the strength characteristics: microhardness, crack resistance, specific energy of adhesion.

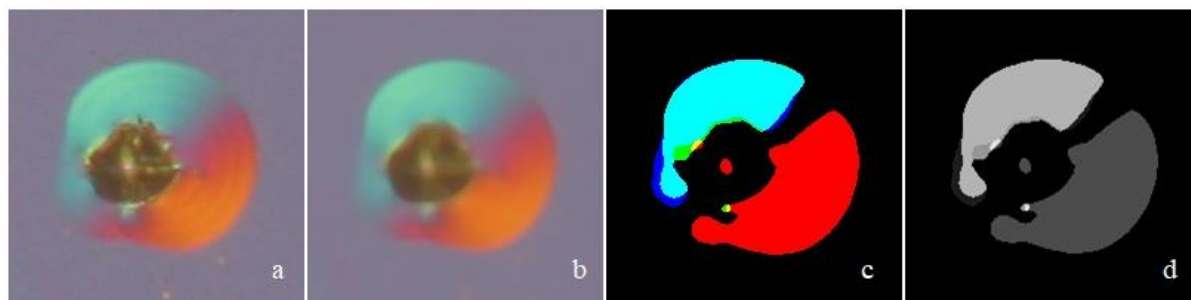
Introduction. Information technologies are widespread in all spheres of human activity. They enable us to quickly and most accurately carry out calculations, process information with the greatest accuracy and exclude subjectivity in the analysis of results.

The purpose of this work was to develop a program that allows one to obtain information on the strength characteristics of materials based on the analysis of indentations formed during microindentation of samples.

Physical aspects of the project. The modern production process of semiconductor devices involves a number of technological treatments, as a result of which, among others, the mechanical properties of materials change, which, in turn, can lead to the appearance of microcracks, scratches, chips and other surface defects. To determine the strength characteristics of silicon, various techniques are used, however, the closest to the real technological process is microindentation, since this method allows the most accurate modeling of the contact interaction of abrasive particles with the processed material [1]. There is a need to obtain a software product for recognizing digital images, which makes it possible to carry out a complete calculation of the strength characteristics of the material based on the analysis of photographs. The programming language Python was chosen as the development environment for the software product. The scheme for processing and analyzing digital image data was reduced to the following stages:

- Analysis of input image data;
- Processing of input data;
- Using the median filter;
- Image segmentation;
- Search for image contours;
- Display of contours in the image;
- Calculation of the geometric parameters of the photographing object.

Image input data. The input data are photographic images of prints during polymer indentation (fig. 1, a). In the center there is an imprint of an indenter pyramid in a polymer film surrounded by polymer heaps. The heap zone is spherical. The image was obtained by the method of differential interference contrast [2], which makes it possible to reveal the irregularities of the polymer surface. An image is made up of a collection of pixels. If you represent the image as a grid, then each square in the grid contains one pixel, where the square with coordinates [0,0] is the top-left pixel. The image size is 200x200 pixels for a total of 40,000 pixels. All pixels in the image are represented in RGB color space (red, green, blue), where one value for the red component, one for green and one for blue. Each of the three components is expressed as an integer in the range from 0 to 255, inclusive, which indicates how much color is contained.



a – input image; b – image after using the median filter; c – image after segmentation; d – binary image

Fig. 1. – Stages of processing the input image

Processing input data. To process the image data, the OpenCV library and the Python programming language were selected [3]. OpenCV (Open Source Computer Vision Library) is one of the most popular libraries for computer vision applications. OpenCV-Python is the Python version of the interface for OpenCV. The presence of the C / C ++ code of this version of the library in the backend guarantees the speed of the library, and the Python wrapper in the frontend ensures ease of customization and deployment. Thanks to this, OpenCV-Python is an excellent solution for high-load computing programs for computer vision. The library also contains a huge number of algorithms, there are interfaces for many programming languages - Java, Ruby, Matlab, Lua, C / C ++.

Input filtering. The input image contains noise that interferes with image analysis. There are many different types of noise such as Gaussian noise, salt and pepper noise, and so on. We can remove this noise from the image by applying a filter that removes it, or at least minimizes its impact. There are many different filters, such as box filter, median filter, mode filter, Gaussian filter and many others. To remove noise in our processing algorithm, we use a median filter. Median filter is a type of digital filter widely used in digital signal and image processing to reduce noise. Median anti-aliasing is widely used in edge detection algorithms because, under certain conditions, it preserves edges while removing noise.

Image segmentation. The background is characterized by a constant color value, and the trace is characterized by a sharp change in color value. To select the contour, you need to separate the trace (object) from the background. Segmentation is used to separate the trace from the background. As discussed above, an image consists of RGB components and each component has a value from 0 to 255. If you set the segmentation value to 140 in the program, then all component values above 140 will be 255, and components with values below 140 will be 0. After segmentation by In the image, the trace has a more distinct outline (fig. 1, d). Those. the background turned black and took on the values of 0, and the area inside the trace became brighter and took on the corresponding value.

Search for contours. The outline of an object is its visible edge, which separates the trail from the background. In fact, most image analysis methods work with contours, not pixels per se. The OpenCV library implements convenient methods for detecting and manipulating image contours. To find contours, use the `cv2.FindContours ()` function. This function takes three values: image, grouping mode and packing method. According to its format, this edge finder function accepts a binary image. To convert an image to binary, use the `cv2.cvtColor (image, cv2.COLOR_BGR2GRAY)` function. After applying the edge search function, the image (fig. 1, d) is ready for processing. The resulting contours of the trace must be displayed on the original image using the `cv2.drawContours ()` function. The function takes an image, outline, outline color (specified in the RGB palette), outline thickness in pixels.

The result of mapping the contour in the image is shown in figure 2, a. There are several small unnecessary outlines in the image that need to be removed. When displaying contours on the image, you need to sort them by area. Using the `cv2.contourArea ()` function, you can get the area value. The function takes all paths and outputs the area value in pixels. After that, you need to remove all unnecessary contours by sorting them by area. The area function is given by the expression: $S = cv2.contourArea (contours [i])$.



a – the image with the applied contour; b – the image with the applied contour after sorting the contours by size;
c – trace of the resulting contour on a black background; d – trail of the object on a black background
after joining the contours; e – the original image with the started contour

Fig. 2. – Stages of search and display of contours in the original image

Due to uneven lighting, we got several contours (fig. 2, c), which need to be combined into one. The contour consists of points, and when connecting the points of the contour, an object was obtained that coincided with the trace (fig. 2, c). The resulting trace coincides with the original processed image (fig. 1, a), the contour to which is the purpose of processing. To obtain a complete contour, it remains to apply the contour search function and display the resulting contour on the original image. The result is shown in figure 2, e.

The implementation of this algorithm for searching for a contour can be used to determine the geometric parameters of indentations during indentation of polymers, which makes it possible to calculate such strength characteristics as microhardness, fracture toughness K_{Ic} (stress intensity factor) and specific peel-off energy of the film, which is a characteristic of the adhesion of the polymer film to the base [4-6].

Conclusion. Thus, an algorithm for processing color images obtained by photographing the polymer surface after microhardness tests has been implemented, which aims to determine the geometric dimensions of prints, contours of heap areas, lengths of cracks and other objects. This is essential for the objective determination of the strength characteristics of materials and the automation of the measurement process in materials science.

REFERENCES

1. Litvinov, Yu.M. Methodology for determining the mechanical properties of semiconductor materials using the continuous indentation method / Yu.M. Litvinov, M.Yu. Litvinov // *Izvestiya vuzov. Electronic engineering materials*. - 2004. - No. 4. - P.11-16.
2. Anisovich, A.G. Optical effects in microscopy of nonmetallic materials / A.G. Anisovich // *Casting and metallurgy*. - 2017. - No. 1. - P.110-114.
3. Bradski, G. Learning OpenCV. Computer vision with the OpenCV library / G.Bradski, A.Kaehler // O'Reilly Media, Inc., – 2008. – 580 p.
4. Vabishchevich, S.A. Physical and mechanical properties of irradiated films of diazoquinone-novolac photoresist on silicon / SA Vabishchevich [et al.] // *Herald of Polotsk State University. Series C. Fundamental Sciences. Physics* – 2020. – No. 12. – P.60-64.
5. Strength properties of photoresist-silicon structures, γ -irradiated and implanted with B + and P + ions / S.A. Vabishchevich [and others] // *Herald of Polotsk State University. Series C. Fundamental Sciences. Physics* - 2016. - No. 12. - P.30-36.
6. Vabishchevich S.A., Brinkevich S.D., Brinkevich D.I., Prosolovich V.S. Adhesion of diazoquinon-novolac photoresist films with implanted boron and phosphorus ions to single-crystal silicon// *High energy chemistry*. – 2020. – V.54, № 1. – P.46-50.

ANALYSIS AND REDUCTION OF ENERGY LOSS IN POWER GRID OF INDUSTRIAL ENTERPRISE*LAN SHIYU, D. DAUHALA*

Polotsk State University, Belarus

With the rapid development of global economy and the continuous progress of science and technology, people's demand for electricity and the requirements of power supply quality are also increasing, and the problem of power energy is becoming increasingly prominent. Under the concept of energy conservation and emission reduction, scientists continue to optimize the use of energy, and try to create the maximum value with the lowest consumption of energy.

There is a lot of energy waste in the traditional power system [1]. The loss of power grid lines, including the loss of electrical equipment and power supply system, has become a problem that can not be ignored. It not only causes the waste of resources, but also affects the economic benefits of individuals, families, enterprises and even the country, so it is particularly important to find scientific methods to reduce the power and energy loss in the power grid.

In this paper, through the analysis of the traditional 10 kV power grid diagram of industrial enterprises, the physical quantities such as cable length, conductor section and cable rated current are measured, and the total operation time (hours) of the power network every year is counted to calculate the total cable cost. After analyzing the causes of power and energy loss in the power grid, the ways and methods to reduce the power and voltage loss of the power system are found, and then the improved cable cost was calculated according to the required physical quantities. So as to judge whether the method can really reduce the loss of power and energy in the power grid, achieve the purpose of saving resources and improving economic benefits.

Power economy is a huge and complex hierarchical system, including power supply, power and automation, electrical lighting, operation and maintenance of electrical equipment. In all aspects of the industrial power supply system, with complex electrical equipment, the related power loss also occurs [2].

Causes and solutions of power and energy loss in power grid.

1. Unreasonable wiring structure of power grid. In the power grid, the distribution lines are messy and lengthy, which often leads to the phenomenon of near power supply, far power supply and circuitous power supply. With the increase of wire length, the resistance value of wire also increases, resulting in the loss of active power of unnecessary lines. By improving the power supply mode of the circuit, the load center power supply or trunk power supply mode can be reasonably adopted to shorten the power supply radius and reduce the loss of reactive power in the line. In addition, the aging of the line, the humidity of the environment, reduce the insulation level of the wire, resulting in the loss of active power leakage. Therefore, we should regularly check and update the wire, and do a good job in 6S management, to avoid external subjective factors leading to power loss.

2. Improper conductor section. In the traditional power supply lines, due to the relatively small number of high-power equipment, for the consideration of production level and economic cost, the conductor with small cross-section and safe current carrying capacity is generally selected. The most direct impact of improper cross-section of wire is to increase the wire resistance, increase the Joule loss of wire, and there are fire safety hazards. Increasing the wire cross section can reduce the wire resistance, Joule loss and voltage loss. But increasing the cross section of conductor will increase the economic cost. When increasing the cross section of conductor, the optimal scheme between investment cost and line loss reduction should be determined by calculation, and the economic payback period should be determined by using the method of repayment period.

3. High loss of substation equipment. Loss of transformer, loss of current metering transformer and voltage transformer (including ammeter), and power consumption of substation itself. In the lower transformer, the actual total loss can reach 5-8% of the network energy consumption. Transformer loss is divided into iron loss and copper loss. Iron loss, also known as no-load loss, is its fixed loss. In fact, it is the loss caused by iron core. The loss of transformer winding is copper loss, which is also called load loss. It is mainly the loss of resistance when load current passes through winding. The copper loss is generally 0.5% of the variable loss, and the iron loss is generally 5 ~ 7% of the variable loss. The load loss is also affected by the temperature of the transformer. At the same time, the leakage flux caused by the load current will produce eddy current loss in the winding and stray loss in the metal part outside the winding. For the loss of transformer, the main solution is to choose the capacity of transformer reasonably and realize the economic operation of transformer. For a single operating transformer, the efficiency is the highest and the loss is the smallest when the iron loss is basically equal to the copper loss. Generally, two or more transformers with parallel operation and load in the distribution transformer capacity should be put into operation more when the load is large and less when the load is small, so that the transformer can always operate in the high efficiency area. Generally, the load should be operated between 40% - 65% of the distribution transformer capacity. For two or more transformers in parallel operation, more input when the load is large, less input when the load is small, so that the transformer always operates in the high efficiency area.

4. Receiver power consumption. Receiver power consumption refers to the consumption of electrical equipment. The main methods are as follows: selecting the motor according to the power and model correctly; replacing the under load asynchronous motor with the low power engine; the winding voltage of the asynchronous motor is low, and the asynchronous motor works under the low load systematically; limiting the idling movement of the asynchronous engine;

Improve the quality of motor maintenance and other factors to reduce the loss of power and energy in the grid.

5. Asymmetry of voltage and current. The asymmetry of voltage and current will lead to extra power and energy loss in power grid, shorten the life of electrical equipment, conductor and transformer, and lead to overload of each phase. It is mainly reflected in the increase of neutral line current, which leads to the increase of line loss. It can balance three-phase load and adjust three-phase voltage to reduce line loss.

Calculation of power and energy loss in power grid before and after improvement

1. After changing the wiring structure of power grid, the saved line loss is calculated by shortening the total length of wires. Further, calculation of the reduced economic cost was made.

2. The next step is selecting the appropriate wire section, calculating the reduced Joule loss, and counting the economic benefit recovery period.

3. The following steps include selecting the appropriate substation equipment and appropriate electrical equipment, calculating the economic cost rate consumed and calculating the economic benefit of recovery period.

4. Finally, the three-phase load is balanced, the three-phase voltage is adjusted, and the saved line loss is calculated. The economic cost and economic benefit recovery period after the improvement are calculated.

REFERENCES

1. Dangzhi Qiang. Power grid to reduce line loss and planning and design[J]. / Dangzhi Qiang. // China Hi tech Enterprise Technology Forum. – 2008. – DOI:10.13535/j.cnki.11-4406/n.2008.21.013.
2. Han Qinghai. Several measures to reduce the line loss of low voltage power grid[J]. / Han Qinghai. // Journal of Zhengzhou Textile Engineering College. – 1993, Vol.4, No.3. – P. 45–48.

ARTIFICIAL NEURAL NETWORKS AS A TOOL FOR SIMULATING PHYSICAL PROCESSES

D. DOVGULEVICH

Vitebsk State University named after P.M. Masherov, Belarus

In the paper various possibilities of using artificial neural networks as a tool for modeling physical processes are considered. The main advantages and disadvantages of computer modeling using ANNs in comparison with classical approaches to constructing mathematical models are revealed. The main tasks for solving the successful construction of the model are highlighted.

The machine learning techniques using artificial neural networks has been increasingly implemented in theoretical and experimental physics in recent years.

Thanks to the ability of processing large amounts of data, drawing conclusions based on characteristics without direct correlation, and high speed, the machine learning techniques can be possibly used in conjunction with classical methods of modeling physical processes, and can completely replace the latter, as well.

The purpose of this research is to determine the scope of application of artificial neural networks for modeling physical processes and to identify their advantages and disadvantages in comparison with classical methods of building models.

Methods. The research is based on mathematical models of physical processes using artificial neural networks. Generally recognized methods of scientific knowledge were used.

Discussion. A neural network in the context of mathematical modeling is a model that reflects the dependencies between input and output parameters. However, unlike models built using other approaches, in a "trained" artificial neural network, the correlation of input and output data cannot be written explicitly (for example, "the value of A is positively related to B for cases when the value of C is negative, and D tends to zero").

A neural network can produce high quality results if it was properly trained, but in essence ANNs represent a kind of "black box". Therefore, with a neural network approach in modeling, the focus is on the correctness of the model, the accuracy of predictions and application, but not on the underlying physical processes.

However, neural networks can also be used to analyze the essence of the modeled process, helping to find the most significant input variables, which facilitates further construction of the model using traditional approaches [1].

According to the Cibeko theorem (Universal approximation theorem), an artificial neural network of feed-forward with one hidden layer can theoretically approximate any continuous function of many variables with any accuracy [2]. Due to this, the models built with the use of ANN make it possible to reproduce complex dependencies occurring in physical processes and dependencies with a large number of variables, the modeling of which is extremely difficult in other ways.

Due to these properties, artificial neural networks make it possible to solve the different information processing tasks when carrying out computer modeling. For example, it is possible to approximate the original mathematical model, which not only allows to expand the range of problems that are possible to solve, but also significantly increases the speed of calculations [3].

Another task covered by using the ANN is the calibration of the model - the selection of missing parameters based on incomplete and potentially inaccurate information. Most frequently, a computer model uses a number of input parameters, and depending on the context of the application, the parameters will change, and some of them may even be unknown at all. To select the parameters using artificial neural networks, Bayesian calibration of computer models can be used [4].

When solving the problem of automation and control of processes, it is often required to model physical processes in real time. In particular, this is relevant for predicting future states of the system. An example is a system for preventing disruptions and extinguishing a plasma charge. For the correct operation of the system, it is necessary to form a breakdown precursor, i.e. to simulate the process with prediction and form the trigger of the discharge extinguishing system.

To achieve the required performance when calculating the model, the numerical solution of differential equations is replaced with a model built using artificial neural networks. Thanks to the preliminary long-term learning process of the neural network, computations are accelerated to an acceptable value [2].

The simulation using artificial neural networks also has a number of disadvantages, such as:

- Most frequently, the process of creating a model based on ANN is empirical and does not allow describing the obtained patterns in a formal language;

- A sufficient number of correctly selected datasets is required for training and testing ANN;
- ANN training can take a long time and in the case of unsuccessfully selected parameters it can come to a dead end;
- ANN behavior may not always be unambiguously predictable, which causes corresponding risks.

While modeling physical processes, the main tasks will be optimal selection of the type and parameters of an artificial neural network and gathering of training and test data samples in order to achieve the optimal ratio of the sufficient accuracy of the model and the time spent on training the ANN. But in the case of obtaining the correct construction of the model, it can significantly surpass the classical methods of modeling not only in speed, but also in the accuracy of describing physical process [5], which makes this approach popular and effective.

Conclusions. The implementation of artificial neural networks for modeling physical processes is a promising trend. ANN can be used both independently and in conjunction with other approaches. The main advantages of using ANN are higher speed (in comparison with other methods) for a large number of tasks, and an increase in the accuracy of approximating the model.

The main disadvantages when using artificial neural networks and deep learning are the need for a sufficient amount of labeled data for training, a long training time and the inability to formulate the obtained patterns in a formal language, which makes it difficult to understand the operation of the model and in some cases makes the modeling process unpredictable.

REFERENCES

1. Employing machine learning for theory validation and identification of experimental conditions in laser-plasma physics / Gonoskov, A., Wallin, E., Polovinkin, A. et al. // *Sci Rep* 9, 7043 (2019).
2. Cybenko, G. V. Approximation by Superpositions of a Sigmoidal function // *Mathematics of Control Signals and Systems*. — 1989. — T. 2, № 4. — С. 303—314.
3. Study of disruption prediction in tokamak plasma using neural networks / Kapralov V.G., Bogdanov A.M., Novokhadskaia O.E., Svintsov M.V., Totrov D.R. // 47th International Conference on Plasma Physics and CF, March 16 – 20, 2020, Zvenigorod.
4. Bayesian calibration of computer models. / Kennedy, M. C. & O'Hagan, A. // *Journal of the Royal Statistical Society: Series B (Statistical Methodology)* 63, 06 January 2002, p. 425–464.
5. Выбор метода аппроксимации экспериментальных данных / Испулов Аманбай Аватович, Сунцов Евгений Вадимович, Иванов Станислав Леонидович, Трущинский Алексей Юрьевич // *Известия ТулГУ. Технические науки*. 2019. №3.

APPLICATION OF VIRTUAL REALITY TECHNOLOGIES FOR PRACTICING HUMAN BEHAVIOR SKILLS IN EMERGENCY SITUATIONS

E. GARIST, P. SINYAK, O. GOLUBEVA

Polotsk State University, Belarus

This article describes the principle of operation of the software and hardware simulator created using virtual reality technologies and represents virtual reality as a technology for the effective development of specialized human skills. It also shows the importance of projects created for similar purposes.

Introduction. The goal of the project is to teach its users to independently prevent household hazards at the initial stages on their own and to behave appropriately, without panic.

Task Statement. The designed simulator satisfies the following necessary conditions:

- all movable objects and all sounds should either help to get out of a dangerous situation or serve to immerse the user in virtual reality. They are specially selected to keep the player's attention and stimulate him;
- all immovable objects should not create obstacles to the user or distract him;
- the user's interaction with objects should be close to reality;
- the feedback from objects and situations to the user's actions should be close to reality;
- the user should be able to interrupt, continue or replay the game;
- the user should be able to find out the reason for the loss and his mistake;
- the user should intuitively understand where an emergency will occur and how to get out of it.

The advantages of VR technologies in the project are:

- easy implementation of any complex situations;
- practical training of repetitive algorithms of actions remains in the muscle memory of the trainee;
- in the game format a person trains himself or herself and acquires skills faster;
- the player can handle specific situations after training, because he or she has successfully overcome it.

Project implementation. The software is created in a game engine called Unreal Engine 4 and based on UX – user experience. The environment was made with the use of models made in a professional program for creating three-dimensional computer graphics - Autodesk 3ds Max. The training equipment is a VR headset of the HTC Vive system.

In VR development there are no environment building templates yet, because each environment serves a unique purpose. This simulator looks like an average apartment with two locations: a kitchen and a living room. There are dangerous household situations in each location which are designed to be solved by a player.



Fig. 1. – Apartment view from above

Mostly, electrical appliance fires are presented as emergencies, because today every household has a minimum set of devices and gadgets which can catch fire due to a short circuit, network congestion or disregard for operating rules. Also, the situation of oil ignition in a frying pan is included, because if the stove is turned on and left unattended it may be dangerous. Attention is also paid to gas leak and water pipe breakout, which can occur due to poor quality of the equipment and overdue service life.

As a result, 6 dangerous situations were implemented. Each of them is possible in a residential area and each has a clear solution algorithm.

Simulator training is structured the following way: various objects are placed around the source of the danger within eyeshot. These objects are located about half a meter away from the user so that they can be easily noticed. They can be used to eliminate the hazard. There are right and wrong ways out of situations. The correct solutions can be variable, for example, they can differ in the methods of firefighting or have a certain order that is made up of several actions. The incorrect solutions are implemented in order to give the user the opportunity to make a mistake and correct it in virtual reality without damaging his health.

All situations are constructed in the same way: the use of a combination of correct actions leads to new situations and, as a result, to a successful completion. If the actions are not correct or there are no actions at all the player sees an error message with the opportunity to replay the game.

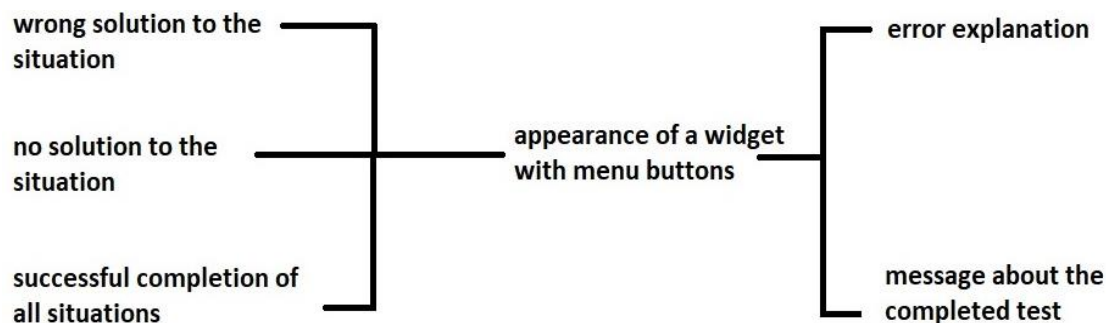


Fig. 2. – Project operation scheme

Results, discussion and perspectives. The significance of the work: the software and hardware complex based on VR technologies for developing skills of behavior in emergency situations was put into work at the Educational Center of the Ministry of Emergency Situations and is being actively used there. This center was opened in Novopolotsk on August 7, 2020. The Center aims at educating all segments of population of any age the basics of health and life safety using innovative technologies and modern equipment by immersion in a virtual environment that simulates emergency situations. This allows users to practice actions not only theoretically, but also practically. The software and hardware complex was developed under contract No. 2082 dated July 08, 2020, by order of the Representative Office of the United Nations International Children's Emergency Fund (UNICEF).

Forward-looking suggestion for development of VR: the capabilities of the simulator allow to increase training modes in order to practice actions in accordance with the rules of conduct in an emergency that may occur at the facilities of various industries. Currently it is possible to develop a simulator for practicing behavior skills in emergencies at the industrial facilities using the created software and the hardware platform. The new simulators can be used at JSC "NAFTAN" in Novopolotsk. There is also a prospect of expanding the set of emergencies in residential areas or outside them. For example, in a city, on a roadway, in a forest, near water reservoirs, and so forth.

Conclusion. The VR complex automates and gamifies the process of training in life safety and fully satisfies the requirements of the task. The user intuitively understands where to look for emergency and how to get out of it safely. If for some reason this does not happen, the player can find out about his or her mistake and try again.

The user's interaction with game objects is based on the physics simulation already existing in Unreal Engine 4 and it is close to real so a person understands how the system behaves.

The basic principles of user testing were applied to improve the product and to make it more understandable and convenient for the target audience.

REFERENCES

1. Garist, E.U. Creating three-dimensional models and audio sequences for a software and hardware VR simulator for practicing behavior skills in emergency situations / E.U. Garist, P.V. Sinyak // Electronic collection of works of young specialists of Polotsk State University. – 2020. – Release 35 (105). – Industry. – P. 30–33.
2. Garist, E.U. Creating interaction logic in software and hardware VR simulator for practicing behavior skills in emergency situations in the Unreal Engine 4 environment / E.U. Garist, P.V. Sinyak // Electronic collection of works of young specialists of Polotsk State University. – 2020. – Release 35 (105). – Industry. – P. 34–36.
3. Sinyak, P. On question about the interpolation polynomial of the function $f(\lambda)$ / P. Sinyak, N. Gur'yeva // European and National Dimension in Research: XII Junior Researchers' Conference, Novopolotsk, May 13-14, 2020 // Polotsk State University. –Novopolotsk, PSU, 2020. – P. 2 «Technology». – P. 156-157.

ANALYSIS PERSON RE-IDENTIFICATION METHODS

S. IHNATSYEVA, R. BOHUSH
Polotsk State University, Belarus

Currently, deep neural networks are used to solve a large number of applied problems, among which the re-identification problem can be distinguished. Person re-identification is a search for interest person in frames obtained from several non-overlapping video cameras. The growing computing power of computers and the growing demand for intelligent video surveillance make this task urgent.

Introductio. The widespread use of video surveillance systems leads to the need to automate the process of detection and re-identification. Re-identification implies that when processing input data, each person is assigned a unique identifier, and when this person meets on frames received from another camera, or from the same one, but after a period of time, the system must recognize him. On such shots, it is not always possible to recognize a person by face, due to different viewing angles, which leads to the need to take into account other distinctive features, for example, such as height, physique, clothing, hairstyle, etc.

For research purposes, re-identification systems of a closed-world are used. This means that homogeneous, sufficiently annotated data is used, and the image-query of the searched person exists in the gallery of the dataset. In real situations, open-world systems are used, when the input data can be heterogeneous, the bounding boxes with the person image must be generated in real time, the data often does not contain annotations, and the dataset is open and can change for time.

Re-identification task is accompanied by such difficulties as: low quality images, different viewing angles, overlaps, background heaps, illumination, etc. Systems that assume use in real conditions are additionally complicated by the fact that the dataset in which it is necessary to search has significant sizes and may constantly change, data does not have annotations, weather conditions may change, the way people move, change in appearance (hats, outerwear, glasses, bags, and other items).

Recent developments in person re-identification systems are aimed at finding solutions to existing problems, and this article conducts modern approaches research and analysis.

1. The main re-identification systems problems

In the first case, there are several people number, and you need to establish a correspondence between these people and the images in the gallery. In the second case, there is a request, and you need to establish whether this person is found in the database gallery, and, if so, find him. In general, the re-identification task can be described as establishing a correspondence between a query (or queries) and people's images in gallery from database. Features are extracted from the query-image, these features are processed using various methods and algorithms, and the system produces a person retrieval result by comparing the extracted features with objects features located in gallery. The general re-identification algorithm scheme is shown in Figure 1.

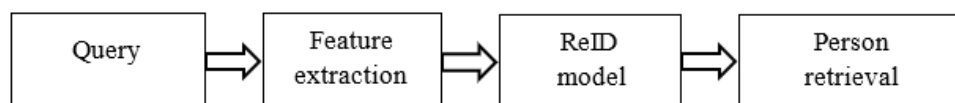


Fig. 1. – The re-identification algorithm general scheme

To extract features on the image in modern re-identification systems, a pre-trained neural network is used, which is re-trained on the dataset with which the re-identification system is to work. This approach allows you to efficiently extract a large features number. To improve training and extracted features subsequent interpretation, various re-identification models are used, with different approaches and algorithms aimed at solving re-identification problems. The main problems are the following:

1. Camera angle of view. Depending on the position in relation to the camera, the object will look completely different. Images taken from the side, from above, from behind, in front, at an angle will have completely different features for the same person, it is very difficult to distinguish something in common. In different frames, the face may be absent, the visible attributes of clothing and objects in the hands may change. For example, a backpack on the back: from the back it looks like a rectangle that obscures person part, from the side and top - a rectangle next to the person, in front - two stripes separating the arms from the body. A person easily uses a backpack as an additional feature, while this can complicate the task for an automated system.

2. **Pose's variability.** A person can take on a very large number of different positions in space. He can sit, stand, lie, raise his arms up, spread his legs, bend forward, to the side, and many other positions. And it can be extremely difficult for the system to find a common feature between a person who sits on a bench and, for example, stands on his hands.

3. **Lighting.** The color perception is highly dependent on the lighting degree at different day times, under different weather conditions, in the artificial lighting presence. A person intuitively feels the difference, while the computer vision system requires additional algorithms to solve this problem.

4. **Resolution.** Different CCTV cameras may differ in the received frames quality. Old video surveillance systems may be with resulting images low quality, which doesn't allow taking into consider small details and objects on a person's clothing, may give blur, which does not allow to clearly define the boundaries between a person and the background.

5. **Background clutters.** Re-identification task is often accompanied by a complex background presence, and the bounding boxes containing people images may contain separate other people bodies parts caught in the frame, a colorful background, objects that merge in color with clothes, hair. It also complicates the task of feature extraction.

6. **Occlusion.** The people in the video are moving and can often be obscured by other people or landscape elements. Different person parts can be hidden at different times. For example, if cameras are installed on the street, then the lower part can be hidden by benches, cars, curbs, the middle part can be blocked by a fence, the upper part - by road signs or signpost. It is impossible to predict at what point in time and how exactly a person will be partially hidden behind other objects, which makes it impossible to consider the signs of only a certain part.

7. **Appearance.** People can be dressed the same, or very similar, for different reasons. This can be a specialized uniform, such as a school uniform, or the same uniform for consultants in a shop. This greatly complicates the re-identification task, and does not allow considering only clothes as features. An extremely difficult problem is the problem of changing a person's appearance. When movement, a person can take off or put on a jacket, hat, hood. Even if the process is on camera, it is difficult for the system to determine that this is the same person, since the extracted features will have great a distance.

8. **Spatial-temporal distribution.** Person's movement trajectory, like speed, is extremely unpredictable. A person can walk slowly, then quickly, stop, turn around and go in the opposite direction, get on a bicycle or scooter and ride, run, and then sit on a bench and sit. This also affects the accuracy of re-identification.

9. **Heterogeneous data.** Sometimes, re-identification task comes down to finding a person, when the query is not an image, but a video sequence, a verbal description, a drawing, a face photograph or a frame obtained from a night vision camera, an infrared camera, while the database contains full-length images. Such a system should be use special means to solve such a problem.

2. Feature extraction

To person re-identification from an query-image in gallery, it is necessary to highlight the person characteristic features in the image, and deep convolutional neural networks are used to extract features. Networks such as ResNet-50, DenseNet-121, PCB, etc. are often used as the backbone network.

ResNet (Residual network) is a deep convolutional neural network used for feature extraction. A characteristic particularity is the use of residual blocks, that is, data from the convolutional layer output is transferred to the next layer input, and at the same time is transmitted through several layers, after which the data is combined using a shortcut connection. ResNet has modifications that differ in the convolutional layers number and can have a depth of 18, 34, 50, 101 or 152 layers. Increasing the network depth usually improves the accuracy of the algorithm, but leads to a decrease in the speed of feature extraction. Most often, researchers choose an average depth of 50 layers, thereby providing a balance between speed and accuracy.

DenseNet (Densely Connected Convolutional Network) - A neural network consisting of dense blocks, in which each convolutional layer is connected to each next layer in block, that is, each convolutional block layer receives features from all previous layers as input, and in turn, transfers them to all subsequent layers. Feature maps after each layer are concatenated. DenseNet can be 121, 169, 201 or 264 layers deep. Most commonly used DenseNet-121.

PCB (Part-based Convolution baseline) is an add-on that can be applied to any basic convolutional network without fully connected layers for classification. The idea is that an image is fed to the neural network input. At the convolutional level, this image is divided into parts, and for each part, the features are extracted and analyzed separately, which allows you to extract more complete information about the human body parts. [1]

Some researchers, when developing a re-identification method, test different convolutional networks as a backbone network. For example, in article [2], the authors conduct tests of their algorithm using ResNet-50, DenseNet-121 and PCB as the backbone network, and note that the mean average precision metric (mAP) is 72.2%, 76.9% and 82.8%, respectively, with the same other parameters for Duke-MTMC-ReID dataset. In [3], a research was also carried out on the backbone network choice influence on the algorithm accuracy, and experiments showed for ResNet-50 mAP = 32.58%, and for DenseNet-161 mAP = 42.25% for the proposed algorithm. These and other similar experiments show that the choice of the underlying network has an influence on the productivity and accuracy of the re-identification algorithm. Metrics such as mAP, CMC, rank1, rank5 and rank10 are used to evaluate re-identification algorithms.

3. ReID models

There is no one-size-fits-all system that can effectively address and address all re-identification problems. Some problems are partially solved using dataset augmentation, which is used to re-train the backbone neural network, and some using special algorithms.

The simplest and low cost way to increase system resistance is to augment the dataset. The more variable the training dataset, the more reliable the trained system will be. The simplest ways to enlarge a dataset are to rotate, flip horizontally or vertically, resize, change the brightness, contrast of the image, and other similar manipulations. It is used by most re-identification systems and can increase the system's resistance to changes in the person position relative to a CCTV camera, to a difference in the quality of the images obtained and to a difference in illumination.

To increase resistance to occlusions, the "random erasing" method is used - an arbitrary fragment is randomly removed from the image and filled with null or random values. The application of this method gave good value of the increase in mAP, for example, for Market-1501 using ResNet50 as the basic network, the mAP increased from 65.60 to 71.31 [4]. Due to its good performance and ease of productivity, the method has become widespread.

The occlusion problem is considered by researchers in [5], and the authors propose to consider the signs of individual parts of the body. First, key points are determined with using CNN, then local features are extracted for each point, i.e. a person is considered not as a whole, but in parts. Each key point is considered as a node in the graph, and the relationship between the nodes is determined. The final step is matching the topological information with local features and predicting the similarity between the two images. Consideration of each body part separately also allows to improve the system's resistance to pose variations taken by a person.

In [6], the image is also considered in parts, however, strict horizontal separation (PCB) [1] is used and the Pose-guided Visible Part Matching (PVPM) method is proposed. The algorithm consists of two main components: pose-guided attention (PGA) and pose-guided visibility predictor (PVP). PVP - evaluates the corresponding parts characteristics in positive image pairs and generates pseudo-labels for the invisible parts. And the PGA module is used to obtain differential features for each image part.

Attention schemes are widely used in re-identification algorithms to improve feature learning. For example, in [7], the RGA (Relation aware global attention) module is proposed, which combines the local and global attention methods and allows compactly covering structural information for the image as a whole and local information about a person's appearance. In [8], a video-based re-identification method is proposed, which also uses attention scheme. The neural network extracts features, and the attention module is used to compute a weighted sum between several consecutive frames. Схемы внимания довольно широко применяются в алгоритмах повторной идентификации для улучшения изучения признаков.

An effective solution to increasing the dataset and improving the model learning ability is to use the Generative Adversarial network (GAN). A neural network is used to generate syntetic images based on existing ones [9]. There are many different uses for the GAN. For example, in [10], a re-identification algorithm is proposed, which implies application in real scenarios, which are complicated by various factors that degrade the image quality. And to train the network to extract reliable features, GAN is used to generate images with varying degrees and degradation types. This allows the system to be more resistant to changes in weather conditions, lighting and other factors that degrade image quality. Researchers in [11] propose using GANs to generate person images assuming different pose variations.

In [12], instead of generating images to augment the dataset, it is proposed to share the re-identification and data generation learning process throughout the learning process. The algorithm consists of two modules, generative (for generating images) and discriminative (for training). Two image comparisons are introduced: self-identification (i.e. generated by an image with a similar appearance of a person) and cross-identification (i.e., an image is generated, i.e. based on photographs of people with different appearance) and generated images are entered online in training, where features are extracted and analyzed in detail. This allows for more efficient use of the generated data.

In [13], a variant of solving the difference in illumination problem is proposed, and the use of a synthetic set 100 virtual people consisting, presented with different illumination degrees is proposed.

Some researchers suggest using auxiliary information to improve the re-identification quality. In [2], to improve the re-identification accuracy, a two-stream system is proposed, which, in addition to visual features, also uses spatial-temporal information. That is, the surveillance cameras location, the distance between them is taken into account, and the time it takes to get the frames is estimated. Visual features are extracted using CNN, and spatio-temporal information is provided with each image in the form of data about the camera number and the frame time. After receiving metrics two types, the metrics are combined and analyzed, after which a decision is made. Since a person takes some time to overcome the distance, it is possible to exclude unlikely options, even if there is visual similarity.

In [14], a two-stage re-identification learning algorithm is proposed - intra-camera and inter-camera similarity calculations. First, similarity metrics are computed based on the extracted features for the images taken from each camera separately. Different cameras create different pseudo-labels. At the second stage, each sample is considered as a new feature vector, which eliminates the mismatch in the distribution between cameras and creates more reliable pseudo-labels.

Table 1 shows the mAP / rank1 values for some state-of-the-art re-identification algorithms for different datasets.

Table 1. – Comparison results of several state-of-the-art algorithms for person re-identification

Algorithm	mAP / rank1			
	Market1501	DukeMTMC-ReID	CUHK03	MSMT17
stReID [2]	86.7 / 97.2	82.8 / 94	-	-
PTL [3]	87.34 / -	79.16 / -	-	-
RGA[7]	74.5 / 79.6	-	77.4 / 81.1	57.5 / 80.3
DG-Net[12]	83.0 / 94.8	74.8 / 86.6	61.1 / 65.6	52.3 / 77.2
IICS [14]	73.9 / 90.1	66.2 / 80.8	-	31.9 / 62.6

As can be seen from Table 1, the algorithm accuracy is influenced not only by the selected algorithm, but also by the dataset that was used for training and testing.

For research purposes, when developing algorithms for person re-identification, prepared marked and annotated data sets are most often used. To test re-identification algorithms, datasets such as Market-1501, Duke MTMC-ReID, MSMT17, CUHK03 are often used - containing bounding boxes with persons images, where each person can be represented from different angles, obtained from different video cameras. The dataset can also be represented by a video sequence, for example, datasets PRID-2011, MARS.

Market-1501 dataset for person re-identification was collected in front of a supermarket at Tsinghua University. Images were taken from 5 high-resolution video cameras and one low-resolution video camera. The dataset includes 32,668 handcrafted bounding boxes for 1501 individuals. The training uses 12,936 bounding boxes for 751 identity, and 19,732 images in the gallery for 750 people to test the re-identification algorithm.

The Duke MTMC-ReID dataset is an extension of the Duke MTMC dataset acquired in March 2014 from the Duke University campus. The images were taken from 8 cameras located between the buildings, and include 36,411 bounding boxes. 16,522 images for 702 identity are used to train the re-identification algorithm. The remaining 17,661 bounding boxes for 702 people are used for testing.

MSMT17 is a large re-identification dataset from 12 outdoor and 3 indoor video cameras located on campus. The survey was conducted on different days and at different times of the day, and includes images for 4 days with different weather conditions, in the morning, noon, and afternoon. Total dataset contains 126,441 bounding boxes for 4,101 people.

CUHK03 - the dataset consists of 13,164 images for 1,360 pedestrians from 6 video surveillance cameras at Chinese University Hong Kong. During the formation of this dataset, part of the data was handcraft annotated, while the other part was generated using an automatic detector.

Data sets such as PRID-2011, MARS can be used to test person re-identification algorithms based on video sequence analysis:

MARS (Motion Analysis and Re-identification set) is the Market-1501 dataset extension, and is also obtained on the Tsinghua University campus from six CCTV cameras. The dataset includes 20,715 tracklets for 1261 person, and 3,248 distractor tracklets. Tracklets are sequences of images for each of the pedestrians captured by at least 2 different cameras. There are 1,191,003 images in total, of which 509,914 bounding boxes for 625 identity are used for training, and 681,089 bounding boxes for 636 people are used for testing (12,180 tracklets).

The PRID (Person ReID) dataset was created at the Austrian Institute of Technology. 2 video cameras were used to form the dataset. Cameras was located on different sides of the building. Images from different cameras have different degrees of illumination and viewing angles. The dataset consist 475 tracklets for 385 person captured by the first camera and 856 tracklets with 749 person's images captured by the second camera. The first 200 tracklets contain pedestrians who are in the field of view of both cameras, the rest are recorded either only by the first or only by the second camera.

Conclusion. The investigation showed that in order to develop an effective re-identification system, attention should be paid to the choice of the image database, the neural network used and the re-identification model. The more diverse and large the dataset, the more robust the system being developed will be. The accuracy and speed

of re-identification is also influenced by the backbone neural network choice. However, the key moment that determines the re-identification system itself is the choice of methods and approaches that improve the study of the objects features. Modern systems use various combinations of such approaches, multi-stage ReID models, auxiliary information. It seems promising to use GAN, attention schemes, and additional data, such as spatial-temporal information, which is provided with each frame. The use of various methods for expanding the dataset can increase the model's resistance to occlusions, changes in lighting, changes in the person pose in the frame. Further research will help to select the most promising methods for developing an effective system for person re-identification.

REFERENCES

1. Yifan Sun, Liang Zheng, Yi Yang, Qi Tian, Shengjin Wang, "Beyond Part Models: Person Retrieval with Refined Part Pooling (and A Strong Convolutional Baseline)", in Proceedings of the European Conference on Computer Vision (ECCV), 2018, pp. 480-496.
2. Wang, G., Lai, J., Huang, P., Xie, X, "Spatial-Temporal Person Re-identification", 2019. URL: <https://arxiv.org/pdf/1812.03282v1.pdf>.
3. Yu, Zhengxu [et al.], "Progressive Transfer Learning for Person Re-identification", 2019. URL: <https://arxiv.org/pdf/1908.02492v1.pdf>.
4. Zhong, Zhun, L. Zheng, Guoliang Kang, Shaozi Li and Y. Yang. "Random Erasing Data Augmentation.", 2020. URL: <https://arxiv.org/pdf/1708.04896.pdf>.
5. Guan'an Wang [et al.], "High-Order Information Matters: Learning Relation and Topology for Occluded Person Re-Identification", Proceedings of the IEEE/CVF Conference on Computer Vision and Pattern Recognition (CVPR), 2020, pp. 6449-6458.
6. Shang Gao, Jingya Wang, Huchuan Lu, Zimo Liu, "Pose-Guided Visible Part Matching for Occluded Person ReID" Proceedings of the IEEE/CVF Conference on Computer Vision and Pattern Recognition (CVPR), 2020, pp. 11744-11752.
7. Zhizheng Zhang, [et al.], "Relation-Aware Global Attention for Person Re-Identification", Proceedings of the IEEE/CVF Conference on Computer Vision and Pattern Recognition (CVPR), 2020, pp. 3186-3195.
8. Pathak, P., Amir Erfan Eshratifar and M. Gormish. "Video Person Re-ID: Fantastic Techniques and Where to Find Them.", 2020. URL: <https://arxiv.org/pdf/1912.05295v1.pdf>.
9. Zheng, Zhedong [et al.], "Unlabeled Samples Generated by GAN Improve the Person Re-identification Baseline in Vitro.", *IEEE International Conference on Computer Vision (ICCV)*, 2017, pp. 3774-3782.
10. Yukun Huang, Zheng-Jun Zha, Xueyang Fu, Richang Hong, Liang Li, "Real-World Person Re-Identification via Degradation Invariance Learning" Proceedings of the IEEE/CVF Conference on Computer Vision and Pattern Recognition (CVPR), 2020, pp. 14084-14094.
11. Qian, X. [et al.], "Pose-Normalized Image Generation for Person Re-identification", 2018. URL: <https://arxiv.org/pdf/1712.02225v4.pdf>.
12. Zheng, Zhedong [et al.], "Joint Discriminative and Generative Learning for Person Re-Identification.", *IEEE/CVF Conference on Computer Vision and Pattern Recognition (CVPR)*, 2019, pp. 2133-2142.
13. Slawomir Bak, Peter Carr, Jean-Francois Lalonde, "Domain Adaptation through Synthesis for Unsupervised Person Re-identification" Proceedings of the European Conference on Computer Vision (ECCV), 2018, pp. 189-205.
14. Xuan, Shiyu and Shiliang Zhang. "Intra-Inter Camera Similarity for Unsupervised Person Re-Identification.", URL: <https://arxiv.org/pdf/2103.11658.pdf>.

CONTENTS

ARCHITECTURE AND CIVIL ENGINEERING

<i>Siniauskaya L., Koltunov A.</i> Non-destructive testing (NDT) of concrete strength: methods, particular qualities	3
<i>Zheng Zhixu, Yuan Jinbin, Yagubkin A.</i> Continuous monitoring of the operating temperature of wood concrete using a smart-system	7
<i>Zmitrovich D., Zhukau D.</i> Improvement of interior light environment in apartments of large-panel buildings of old typical series	10
<i>Tarasava M., Tarasava T., Tourichev L.</i> The history of architecture development, forms of building constructions and the establishment of computing methods in the first half of the 20 th century	13
<i>Khvatynets V., Parfenova L.</i> Methods for testing formulations for a construction 3D printer	16
<i>Podobed O., Khvatynets U.</i> Fiber concrete is a modern building material	18
<i>Borodeyko I., Khvatynets U.</i> Modular construction during a pandemic	20
<i>Shaleika Y., Khvatynets U.</i> Analysis of the development level of fiber concrete and its prospects	22
<i>Kurganov E., Shaniukevich I.</i> Applications of smart building technologies in the COVID-19 environment	24
<i>Zhavoronok D., Zhan Xinxin, Parfenova L.</i> Development of "green" construction in Belarus and China	26
<i>Yakauleva V., Dorofeev E., Niyakouski A.</i> Investigation of the influence of a specified water flow rate in the hot water supply systems of multi-apartment residential buildings on the material characteristic of a pipeline network	30

TECHNOLOGY, MACHINE-BUILDING

<i>Eliseeva A., Valeeva S., Ermak A.</i> Properties and thermo-oxidative stability of the dewaxed residual product of the vacuum gas oil hydrocracking process	32
<i>Fedorenkova D., Buraya I.</i> Reduction of losses of hydrocarbons in the tank farm of the filling station «Solnechnogorskaya» PAO «Transneft» (Russia) (overview)	36
<i>Talibli F., Nasirov M.</i> Research on chemical preservation of timber of historical monuments from external influences	40
<i>Qasimli F., Nasirov M.</i> Wood fire protection mechanisms	42
<i>Kashchonak A., Chigrinova N.</i> Application of the method electro-spark deposition with additional ultrasonic impact to extend the life of the metalworking tool	44
<i>Nasirov M.</i> Research of mould contamination on wooden surfaces of historical monuments with modern devices	48
<i>Guliyeva M., Nasirov M.</i> Performance of the technological process of printing with printing equipment	50
<i>Savelyeva V., Ovcharov E., Varonin A.</i> Overview of theoretical prospective methods to reduce hydraulic losses in a pipeline system	53
<i>Sarela D., Varonin A.</i> About the possibility of perspective application of hydrophobic and superhydrophobic modified internal coatings of pipelines in pipeline transport	56
<i>Zadorova K., Lukin D., Kosenko O.</i> Research of methods and algorithms for solving production planning problems	59
<i>Haikova V., Filimonova K., Lapkovskaya P.</i> Digital twins as a transport logistics tool	61
<i>Tikhon E., Popok N.</i> Production manufacturability assessment of the product design	64
<i>Studenkova M., Varonin A.</i> On the possible application of microbubble cavitation in pipeline transport	67
<i>Bogdanovich N., Spiridonok L.</i> Restoring regulatory depth of trunk pipelines	70
<i>Artemiev V., Nevzorova A.</i> Comparison of operation of physical and simulation model of proportional distributor	73
<i>Huang Nan, Adamovich A.</i> Charge electric vehicles	76
<i>Annayev G., Yakubouski S., Bulauka Y.</i> Waste of the agroindustrial complex of Turkmenistan as a raw material base for obtaining oil sorbents	78

Khmialnitskaya I., Popok N. Features of determining labor intensity of the design and technological cutting tools production preparation	81
Sytova N., Yanushkevich V. Communication 5 generation.....	83
Bulauka Y., Yakubouski S., Vashkova N. Rational refining of heavier cut of pyrolysis gas oil	85
Litvin A., Kovalenko I., Pugachev M., Safronova E. Analysis of the possibilities of using petroleum coke in various industries	88
Maksimenko D., Portyanko A., Popok N., Portyanko S. Simulating the influence of thermal exposure on the main elements of a cutting tool in SolidWorks	90
Dmitriev R., Matveenkov D., Popok N., Portyanko S. Modeling the operation of end mills in the cinema 4D program	93
Abragimovich D., Issa Abakar Ahmad Ilyass, Popok N., Portyanko S. Airflow simulation in SolidWorks FlowSimulation.....	98
Maksimenko D., Kudryakova V., Popok N., Portyanko S. Comparative analysis of 3D printers based on FDM and SLA technologies	102
Tachilo A., Tarashkevich D., Molodechkina T. Analysis of the dielectric characteristics of composite materials based on a polymer matrix	106
Biryukova D., Antonovich D. Comparative analysis of software for simulation of electronic - optical systems	109

ICT, ELECTRONICS, PROGRAMMING, GEODESY

Soldatenko P., Golubev Y. Methods of forming charged particle beams of large cross section	111
Gaychukov E., Livinskaya V. Research of current market needs using modern methods of data analysis	114
Zaitsev I., Zalivaka S. Analysis of the NAND Flash device garbage collection algorithms under lack of memory conditions.....	116
Moroz A., Yanushkevich V. Amplitude-type sensors in fiber-optic devices.....	120
Mtayrek M., Nevzorova A. Prospects for the development of oil fields in Lebanon.....	122
Budko D., Yanushkevich V. Fiber-optic communication line receivers	125
Makridin I., Yanushkevich V. Fiber-optic communication line amplifiers.....	127
Vasilyeva D., Glukhov D. Comparative analysis of models and forecasting methods	130
Zhou Hengyu, Dauhiala D. Research and application of feeder automation system in distribution network.....	134
Besetskaya A., Bohush R. Metallographic studies	137
Khodosevich A., Bogusch R. The server part of the online parking booking system.....	140
Kasimov D., Zargaryan Y. Control and measuring devices for controlling the temperature regime of the cooking cabinet.....	143
Ponaskova K., Zargaryan E. Analysis of the principles of belt conveyors.....	145
Dulepova A., Demidenko G. Robust stability in the problem of motion of an inverted pendulum with a vibrating suspension point.....	147
Ivanova E., Podoksenov M. Autoisometries of the four-dimensional Lie algebra of IV Bianci type.....	150
Shafarenko A., Glukhov D. Developing a system for automating the project-based didactic method of active learning in the educational process	155
Chernyavskii A., Yanushkevich V. The device for determining the direction of the infrared radio waves arrival from a brightly contrasting object	158
Dashko V., Ivanova P., Livinskaya V. ROC analysis as a binary classification tool	160
Liu Zhengming Present situation and development of photovoltaic power generation	163
Shnipova N., Yanushkevich V. Optical processors.....	166
Baklan U., Burachonak I. The concept of developing a communication service for students, administration and potential employers.....	168
Zheng Jiebin, Chertkov V. Redundant control method for yaw overload protection of wind turbine	171
Dolhi P. Lineament analysis of free space images in LEFA software	174
Lazerko A., Chertkov V. Robotic sorting for the main types of solid household waste	178
Kulik V., Valoshyna M. Modern methods of remote sensing of the Earth	182
Jichang Shang, Chertkov V. Improving the efficiency of using remote monitoring system of smart grid.....	184

<i>Kovalevsky V., Yanushkevich V.</i> Solar collector control system	188
<i>Smirnova N., Burachonak I.</i> Goaldiary time management platform.....	190
<i>Papkovich M., Skoromnik O.</i> The solution of the one multidimensional integral Abel type equation with the hyperbolic sine function in the kernel over pyramidal domain	193
<i>Rahouski S., Tanana V., Vabishchevich S.</i> Using computer vision to find outlines of objects	195
<i>Lan Shiyu, Dauhiala D.</i> Analysis and reduction of energy loss in power grid of industrial enterprise	198
<i>Dovgulevich D.</i> Artificial neural networks as a tool for simulating physical processes	200
<i>Garist E., Sinyak P., Golubeva O.</i> Application of virtual reality technologies for practicing human behavior skills in emergency situations	202
<i>Ihnatsyeva S., Bohush R.</i> Analysis person re-identification methods	204